The role of eEF1A-2 in the pathogenesis of Motor Neuron Disease

Helen Newbery

Thesis submitted for the degree of

Doctor of Philosophy

The University of Edinburgh

2003

Contents

List of Figures

List of Tables

Declaration

I declare that this thesis has been composed by myself, and that all the work is my own unless otherwise clearly stated.

Helen Newbery.

Acknowledgements

A lot of people have helped me over the last three years, and I am indebted to all of them. My apologies go to anyone I have not mentioned by name. First and foremost, I would like to thank Dr. Cathy Abbott for her support and guidance over the last three years. I would not have got to this point without her. I have also been fortunate to have the support of two second supervisors from the Department of Neuropathology, Drs. Stephen Wharton and Colin Smith. I would like to thank both of them for their input, and hope that Dr. Wharton is enjoying life down in Sheffield. I would also like to thank Professor Jeanne Bell in Neuropathology for her support. A huge thank you also to Frances Brannan, also in Neuropathology, for her support, both technical and personal, and for taking me up Ben Lawers!

I would also like to thank everyone in the Medical Genetics Section who has helped me. I would particularly like to thank the other members of the Abbott Group, past and present, for keeping me sane(ish!) and for putting up with me, especially Dr. Lorna McClaren – thanks for all the coffees! So, thanks (in no particular order) to Doreen for getting me started, Jean, Dawn, Julia, Katie, Danny, (wherever you are), Karen, Permphan, Romina and Vangelis. I wish the last three luck as they start their PhDs. I would also like to thank the other students, Rachel, Sarah, Simon, Wendy and Stephane for making me laugh. Thanks also to Ann Doherty for teaching me cell culture, Dr. Isabel Hanson and Rachel James various antibody techniques, Dr. Ben Pickard and Pat Malloy the ways of the microscope, Dr. Caroline Hayward, SSCP analysis, Stewart Morris for computer back up, Angie Fawkes and Alison Condie for sequencing, and Heather, Susan, Helen, Lorna and Rosemary for their admin support. Again, I'm sorry if I've forgotten anyone.

I would also like to thank Professor Veronica van Heyningen at the MRC for access to the DHPLC machine, and Dr. Kathy Williamson for her expertise and for helping me analyse my samples. Thanks also go to Lisa McKie, also at the MRC, for helping me in the mouse house. I would also like to thank the staff at the Western General

Hospital Library. Karen Wilson and Romina Aron-Badin did some experiments, on SMA and *Slc1a4*, respectively, which have been described in the main text.

Several people also supplied reagents. Professor Adrian Bird at the University of Edinburgh provided adult *X. laevis* – thanks too to Dr. Helle Færk Jørgensen for helping with the dissection. Dr. Josh Brickman, also at the University of Edinburgh, kindly supplied the gastrula-stage embryo. Dr. George Janssen of the Universiteit Leiden provided the *A. salina* EF1A antibody; Paolo Bigini of the Instituto di Recerche Farmacologiche Mario Negri, Milan, *wr* mouse brains. DNA samples were provided by Dr. Caroline Hayward, from patients recruited by Shuna Colville and Dr. Robert Swingler of the Department of Neurology at Ninewells Hospital, Dundee. Helen Munn from the Molecular Medicine Centre and Rachel James from the Medical Genetics Section supplied cell lines. I would also like to thank Dr. Maggie Chambers at Diagnostics Scotland for her help and advice with antibody generation. The work was funded by the Scottish Motor Neurone Disease Association.

Last but definitely not least I would like to thank Wilf for putting up with me.

Abstract

Motor neuron disease, or amyotrophic lateral sclerosis (ALS), is a disorder characterised by progressive weakness and atrophy of skeletal muscles, caused by the selective loss of motor neurons. It occurs in both familial and sporadic forms. Although the genetic basis of the disease in a minority of cases has been identified, the precise molecular mechanism underlying the disease remains to be elucidated. There is a range of mouse mutants which model the disease. These mouse models, both classical and transgenic, have been particularly valuable in providing clues to the pathogenesis of the disease. One such mutant is wasted, in which the mice develop a progressive neuromuscular phenotype from 21 days of age. They deteriorate quickly, and die by 28 days. The genetic defect responsible for wasted is a 15kb deletion which leads to the abolition of the expression of eukaryotic elongation factor 1A-2 (eEF1A-2). This is a tissue-specific isoform, apparently unique to mammals, of the more widely expressed eEF1A-1. In this PhD thesis I describe the further characterisation of wasted as a model for ALS, using immunohistochemistry to evaluate the similarities between the phenotype of wasted mice and that of ALS patients. I have also screened the human gene, *EEF1A2*, for mutations in both familial and sporadic patients. Although there were polymorphisms within the gene which were also present in healthy controls, there were no mutations. It is thus unlikely that mutations in *EEF1A2* are responsible for anything other than rare cases of ALS. I have designed and generated anti-peptide antibodies against eEF1A-1 and eEF1A-2 which I have shown to be isoform-specific. These were used to study the expression of the two isoforms in mouse tissues. I have also shown that the African clawed frog, *Xenopus laevis*, has a developmentally-regulated, tissue-specific isoform homologous to eEF1A-2.

Abbreviations and Symbols

ALS	amyotrophic lateral sclerosis
AMPS	ammonium persulphate
AMV	avian myeloblastosis virus
APOE	apolipoprotein E
β-gal	β-galactosidase
BIRC1	baculoviral IAP repeat-containing protein 1
bp	base pair
BSA	bovine serum albumin
CCS	copper chaperone for SOD1
Cln8	ceroid-lipofuscinosis, neuronal 8
CNS	central nervous system
DAB	diaminobenzidene
DABCO	1,4-Diazabicyclo[2.2.2]octane
DAPI	4',6-Diamino-2-phenylindole dihydrochloride
DEPC	diethyl pyrocarbonate
DHPLC	denaturing high performance liquid chromatography
DMEM	Dulbecco's Modified Eagle Medium
DMSO	dimethyl sulphoxide
dNTPs	deoxynucleotide triphosphates
DNA	deoxyribonucleic acid
dpc	days post coitus
ECL	enhanced chemiluminesence
EDTA	ethylenediamenetetraacetic acid
Eef1a2	eukaryotic elongation factor 1A2 (mouse gene)
EEF1A2	eukaryotic elongation factor 1A2 (human gene)
eEF1A-2	eukaryotic elongation factor 1A2 (protein)
EGF	epidermal growth factor
eIF2B	eukaryotic initiation factor 2B
ELISA	enzyme-linked immunosorbent assay
ENU	*N*-ethyl-*N*-nitrosourea
ES cell	embryonic stem cell
EPMR	progressive epilepsy with mental retardation
EST	expressed sequence tag
gad	gracile axonal dystrophy
Gapdh	glyceraldehyde-3-phosphate dehydrogenase
GDP	guanosine diphosphate
GEF	guanine exchange factor
GFAP	glial fibrillary acidic protein
GTP	guanosine triphosphate
H&E	haematoxylin and eosin
HGMP	Human Genome Mapping Project
HRP	horse radish peroxidase
HSP	hereditary spastic paraplegia
kb	kilobase pair
kD	kilodaltons
KLH	keyhole limpet hemocyanin

lacZ	β-galactosidase gene
Loa	Legs at odd angles
LIF	leukaemia inhibitory factor
mAChR	muscarinic acetylcholine receptor
MAGI	Multiple Alignment General Interface
MAP2	microtubule-associated protein 2
MAPT	microtubule-associated protein tau
MBT	midblastula transition
MND	motor neuron(e) disease
mnd	motor neuron degeneration
mneu	motor neurone disease
mRNA	messenger ribonucleic acid
NAIP	neuronal apoptosis inhibitory protein
NaN_3	sodium azide
NCBI	National Center for Biotechnology Information
ND	not determined
NEF3	neurofilament (medium chain) (human gene)
NEFH	neurofilament (heavy chain)
NEFL	neurofilament (light chain)
NFH	neurofilament (heavy chain) (protein)
NFL	neurofilament (light chain)
NFM	neurofilament (medium chain)
NGF	nerve growth factor
NIH	National Institutes of Health
nmd	neuromuscular degeneration
OPD	o-phenylenediamine dihydrochloride
P1	post-natal day 1
PBS	phosphate-buffered saline
PCR	polymerase chain reaction
PDB	Protein Data Bank
pmn	progressive motor neuronopathy
(J)PLS	(Juvenile-onset) primary lateral sclerosis
PMA	progressive muscular atrophy
PVDF	polyvinylidene difluoride
Rab1	member RAS (rat sarcoma) oncogene family
RISC	RNA-induced silencing complex
rpm	revolutions per minute
RPMI	Roswell Park Memorial Institute
RT	reverse transcriptase
SD	standard deviation
SDS	sodium dodecyl sulphate
Slc1a2	solute carrier family 1, member 2
SMA	spinal muscular atrophy
SMN	survival motor neuron
SOD1	superoxide dismutase
SSCP	single strand conformation polymorphism
Taq	*Thermus aquaticus*
TBE	tris-borate-EDTA

TBS	tris buffered saline
TEAA	triethylammonium acetate
TEMED	N,N,N',N'-tetramethylethylenediamine
TIGR	The Institute for Genome Research
TMACl	tetramethylammonium chloride
Uchl1	ubiquitin carboxy-terminal hydrolase isozyme 1
UTR	untranslated region
VWM	vanishing white matter
wr	wobbler
wst	wasted
ZPR1	zinc finger protein 1

1 Chapter 1 – Introduction

1.1 Introduction

This introduction will outline the current knowledge of motor neuron disease, and its genetics and pathogenesis. There are a number of mouse mutants which have been used to model the human disease. These are described, along with any insights into the pathogenesis of human motor neuron disease that they have provided. This PhD has focused on the mutant wasted. The genetic defect responsible for wasted has been identified as a deletion which abolishes the expression of eukaryotic elongation factor 1A2 (*Eef1a2*). This is a tissue-specific isoform of the more widely expressed *Eef1a1*. The biology of the proteins encoded by the two genes is discussed, focusing on the question of why a second isoform with a restricted expression pattern should be required.

1.2 Motor Neuron Disease

1.2.1 Introduction

Motor neuron (or neurone) disease is an umbrella term which refers to a group of neurodegenerative disorders characterised by progressive weakness and atrophy of skeletal muscles, caused by the selective loss of motor neurons. The most common adult form of the disease, amyotrophic lateral sclerosis or ALS (usually known as motor neuron disease or MND in the UK) usually affects those in middle age, with an average age of onset of 56 years of age for sporadic and 45.1 years for familial cases (Tandan and Bradley, 1985). The symptoms vary from patient to patient, but typically involve muscle cramping and fasiculations in the initial stages, followed by a progressive paralysis, shortness of breath and difficulty in breathing and swallowing. Most patients die between 2 and 5 years after diagnosis, and there is as yet no cure. The disease been identified in all populations investigated, with an incidence of between 0.4 and 1.8 per 100,000, depending on the particular population (Tandan and Bradley, 1985). It has been reported that this incidence is rising (Kurtzke, 1991; Lilienfield *et al.*, 1989), although this could be due to the continuing

increase in the life expectancy of the general population, improved disease ascertainment, or a combination of the two (Annegers *et al.*, 1991). There are also well-characterised geographical foci of the disease, for example, on the western Pacific island of Guam, where it is often associated with parkonsinism-dementia (Morris *et al.*, 2001).

1.2.2 Pathology

The main histological feature of ALS is the loss of motor neurons of the anterior horn region of the spinal cord, the brain stem and motor cortex (Graham and Lantos, 1997). A diagram of a motor neuron is given in figure 1-1. This is accompanied by reactive gliosis, in which microglia are activated and astrocytes accumulate and upregulate the expression of glial fibrillary acidic protein, GFAP (Fujita *et al.*, 1998; Nagy *et al.*, 1994). Inclusion bodies containing ubiquitin are seen in the surviving motor neurons of almost all cases (Leigh *et al.*, 1988; Leigh *et al.*, 1991). Accumulations of phosphorylated neurofilaments are also seen (Manetto *et al.*, 1988; Munoz *et al.*, 1988; Sobue *et al.*, 1990). In the muscles of affected patients, there are neurogenic changes involving the atrophy of muscle fibres, along with denervation and renervation (Graham and Lantos, 1997).

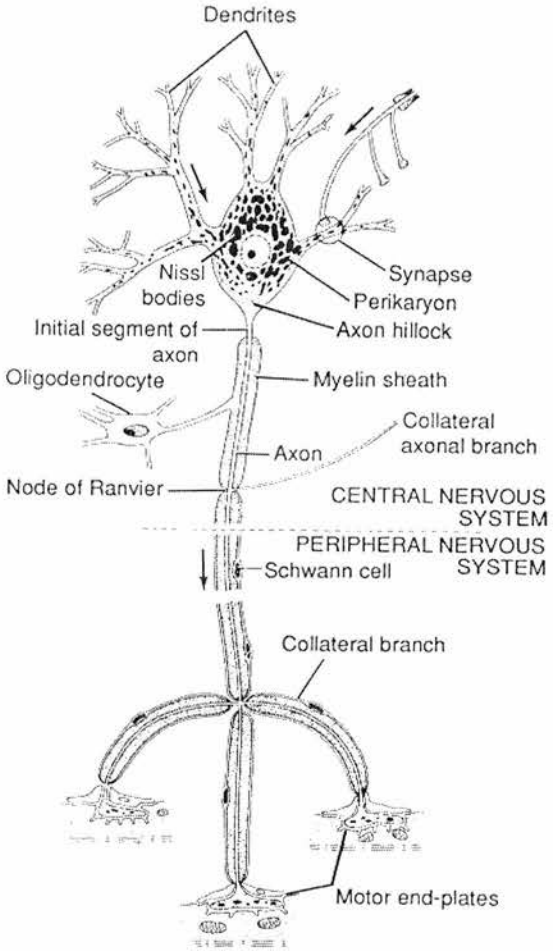

Figure 1-1 Diagram of motor neuron (from Junqueira *et al.*, 1995).

1.2.3 Genetics

The vast majority of ALS cases occur without any family history – only 10-20% of cases are familial. In these cases, the pattern of inheritance is usually autosomal dominant, but there are also rarer recessive forms with a juvenile onset. There is locus heterogeneity in both forms of the disease. Approximately 10-20% of the familial cases are linked to chromosome 21q22.1 (Siddique *et al.*, 1991). This locus is designated ALS1. The mutated gene has been identified as Cu/Zn superoxide dismutase (*SOD1*) (Rosen *et al.*, 1993). Over 100 different mutations have now been identified (Parton *et al.*, 2002). They are uniformly distributed through the protein, with no obvious clustering. The vast majority of mutations are dominant, but the

D90A mutation can be either dominant or recessive, leading to the suggestion that in the latter case there is a linked protective factor (Al-Chalabi *et al.*, 1998; Parton *et al.*, 2002). *SOD1* mutations have also been reported in a small number of sporadic cases (Jones *et al.*, 1993). It is still not clear why mutations in superoxide dismutase cause disease. The findings from *SOD1* knockout mice (see below), along with the autosomal dominant inheritance pattern and the fact that some of the mutant enzymes have normal dismutase activity (Ratovitski *et al.*, 1999), has led to the hypothesis that toxicity is caused by the gain of some novel, toxic function. The precise nature of this toxic function has not been characterised. Although novel protein interactions have been reported for two ALS-causing mutations, G85R and G93A (Kunst *et al.*, 1997), it is not clear how this could be extrapolated to other regions of the protein, in which there are mutations which lead to the same phenotype.

ALS2 is a juvenile-onset recessive form of the disease, shown to be linked to chromosome 2q33 (Hentati *et al.*, 1994). The genetic basis of the disease at this locus has recently been identified as a novel gene, alsin (Hadano *et al.*, 2001; Yang *et al.*, 2001). Three different mutations have been found in three ALS2 families, which all lead to a frameshift and production of a truncated protein product. Although they could therefore represent gain-of-function mutations, it is perhaps more likely that they result in a loss of function, given the recessive mode of inheritance of this form of the disease. It is currently not clear how mutations in alsin lead to ALS, especially as, like SOD1, it is expressed in a wide range of tissues. The gene has homology with guanine exchange factors, and may modulate microtubule assembly, membrane organisation and cell trafficking (Hadano *et al.*, 2001). Mutations in alsin also cause a juvenile-onset form of primary lateral sclerosis, JPLS (Yang *et al.*, 2001). The JPLS- causing mutations lie in exon 9, which is only present in one of two differently sized transcripts of alsin. The shorter transcript remains intact, which may explain why this mutation causes a milder phenotype. Where the mutations affect both transcripts, the resulting phenotype is the more clinically severe ALS. Alsin mutations have also recently been identified in patients with infantile-onset hereditary spastic paraplegia (HSP) (Eymard-Pierre *et al.*, 2002).

Other ALS loci for which chromosomal locations have been identified are ALS3 at 18q21 (Hand *et al.*, 2002), ALS4 at 9q34 (Blair *et al.*, 2000), and ALS5 at 15q15.1-q21.1 (Hentati *et al.*, 1998). All three are juvenile forms of the disease; ALS3 and ALS5 are autosomal recessive, whereas ALS4 is dominantly inherited. There is also an X-linked form of the disease at Xp11-q12 (Hong *et al.*, 1998). There are other loci which remain to be found, as there are families which do not show linkage to any of the identified loci. Due to this genetic heterogeneity, and the fact that ALS is a late-onset disease with a short disease duration, it is often difficult to identify loci using linkage analysis. Association studies and candidate gene approaches have therefore often been used in an attempt to identify other causative disease genes.

There are several genes in which mutations have been described in a small proportion of patients. These include the neurofilament heavy chain gene, in which mutations and deletions have been reported in a small number of patients (Al-Chalabi *et al.*, 1999; Figlewicz *et al.*, 1994; Tomkins *et al.*, 1998). Mutations have also been found in apurinic/apyrimidinic endonuclease (APEX nuclease; AP endonuclease) (Olkowstu, 1998) and in cytochrome c oxidase subunit 1 (Comi *et al.*, 1998). A mutation has also been reported in the leukaemia inhibitory gene, *LIF*, which was present in 4 of 104 ALS patients but was not present in 388 controls (Giess *et al.*, 2000). The manganese superoxide dismutase gene, *SOD2*, has been screened for mutations in ALS patients, although no mutations have been found (Tomkins *et al.*, 2001).

It is possible that along with causative mutations, there are susceptibility genes which predispose an individual to the disease in the presence of other genotypes or environmental triggers. For example, a polymorphism in the APEX nuclease gene differs in alleleic frequency different between ALS cases and controls (Hayward *et al.*, 1999). Survival motor neuron 1 (*SMN1*) is mutated in spinal muscular atrophy (SMA); both the gene and the disease are discussed in more detail in section 1.2.3.1, below. Although abnormal copy number of *SMN1* has also been identified as a susceptibility factor for ALS (Corcia *et al.*, 2002), the numbers involved in this study were not very large, and the findings are probably artefactual (Crawford and

Scholasky, 2002). The finding that a presenilin-1 polymorphism was associated with ALS may also be due to the relatively small number of patients involved, especially as the 95% confidence interval was only 1.06, with a p-value <0.03 (Panas *et al.*, 2000). The microtubule-associated protein tau (MAPT) has been implicated in a number of neurodegenerative diseases (reviewed in Lee *et al.*, 2001). A polymorphism in the *MAPT* gene has been identified as a susceptibility factor for the ALS-Parkinsonism Dementia Complex of Guam (Poorkaj *et al.*, 2001).

There may also be genotypes which affect the course of ALS in an individual, for example, the rate of progression of the disease or the age of its onset, rather than the overall susceptibility to the disorder. For example, the apolipoprotein E (*APOE*) ε4 allele has been associated with decreased survival times in ALS patients (Drory *et al.*, 2001). Monoamine oxidase B alleles have been found to be associated with the age of disease onset, but this finding may be artefactual, given the small numbers involved in the study (Orru *et al.*, 1999).

1.2.3.1 Spinal Muscular Atrophy

Spinal muscular atrophy is the second most common lethal autosomal recessive disease in Caucasian populations (after cystic fibrosis) (DiDonato *et al.*, 1994), with an incidence of 1 in 10,000 live births and a carrier frequency of 1 in 50 (Emery, 1991). Classification of the disease (reviewed in Hausmanowa-Petrusewicz, 1991) is based on age of onset. Where this is during infancy, the disease is classified as Werdnig-Hoffmann disease, and is invariably fatal by the age of 2 years. Types II and III are less severe, but still present in childhood. The much rarer Types IV and V are adult-onset forms of the disease. All three of the childhood forms are usually recessively inherited, although there are some rare cases of dominant inheritance. They are linked to chromosome 5q12.2-q13.3, and are caused by deletions or mutations in the survival motor neuron 1 (*SMN1*) gene (Brahe *et al.*, 1995; Brussaglia *et al.*, 1995; Burglen *et al.*, 1995; Gambardella *et al.*, 1998; Lefebvre *et al.*, 1995; Rodrigues *et al.*, 1995). At this locus there is a 500kb inverted repeat. The resulting (more centromeric) duplicated copy of *SMN1*, *SMN2,* differs from *SMN1* at only 5 nucleotide positions. However, it is only expressed at very low levels

due to an altered splicing pattern resulting in the loss of exon 7 (Lorson *et al.*, 1999; Monani *et al.*, 1999). There is also evidence that gene conversion from *SMN1* to *SMN2* can occur at this locus, and cause disease (Campbell *et al.*, 1997). A correlation has been reported between the amount of SMN protein and the severity of the spinal muscular atrophy phenotype (Lefebvre *et al.*, 1997). There is also some correlation between the copy number of *SMN2* and the disease, with a higher number of *SMN2* copies acting as a protective factor (Harada *et al.*, 2002). *SMN2* could thus be acting as a modifying factor in the disease (Frugier *et al.*, 2002). Other candidate modifying factors include baculoviral IAP repeat-containing protein 1, *BIRC1* (previously known as neuronal apoptosis inhibitory protein, *NAIP*), in which deletions in SMA patients have been reported (Roy *et al.*, 1995), and *SERFA4* (previously known as *H4F5*) (Scharf *et al.*, 1998), both in the *SMN* region. The structure of the gene locus is shown in figure 1-2.

Figure 1-2 Diagram (not to scale) of *SMN* gene locus on Chromosome 5q. Arrows indicate the direction of transcription. *SMN1* is the survival motor neuron 1 gene, *SMN2* is its duplicated copy, *BIRC1* encodes baculoviral IAP repeat-containing protein 1, and *ψBIRC1*, the *BIRC1* pseudogene.

Unlike the human *SMN* gene, the mouse gene is not duplicated, and knocking out *Smn* results in early embryonic lethality (Schrank *et al.*, 1997). Expressing the human *SMN2* gene in these mice results in a phenotype similar to SMA, with the *SMN2* transgene suppressing the phenotype to a degree dependent on the transgene copy number (Hsieh-Li *et al.*, 2000). Transgenic mice have also been produced in which an *SMN* gene containing SMA-associated mutations has been expressed in either

neuronal (Frugier *et al.*, 2000) or muscle cells (Cifuentes-Diaz *et al.*, 2001). In both cases, a phenotype similar to SMA was seen in the affected tissues, which suggests that both muscular and neuronal involvement is required for the disease.

1.2.4 Pathogenesis

Despite the identification of *SOD1* mutations almost 10 years ago, the precise cause of ALS remains unknown at a molecular level. There are several competing theories of pathogenesis, although it is likely that disease is caused by more than one mechanism. Theories currently include oxidative stress, neurofilament accumulation, excitotoxicity and mitochondrial dysfunction. A central question which remains to be answered is why motor neurons are selectively affected, when both SOD1 and alsin are ubiquitously expressed. Motor neurons are extremely large cells, with a somatic diameter of 50-60μM in man and long axonal processes. It is possible that their large size, with concomitant high energy demands and high metabolic rate, renders them particularly sensitive (Shaw and Eggett, 2000). Alternatively, the cells may be particularly susceptible to alterations in the cytoskeleton. Motor neurons are also uniquely vulnerable to exposure outside the CNS at the neuromuscular junction, where the axon termini are not protected by the blood-brain barrier. They may be affected by deleterious factors at this site, and may also require the retrograde transport of trophic factors and signalling molecules from muscle (Shaw and Eggett, 2000).

1.2.4.1 The Oxidative Stress hypothesis

SOD1 catalyses the reaction:

$$2O_2^{\cdot -} + 2H^+ \rightarrow O_2 + H_2O_2$$

The role of SOD1 in the metabolism of reactive oxygen led to the theory that pathogenesis was caused in some way by oxidative stress. Indeed, enhanced oxygen radical production is seen in transgenic mice carrying mutant human *SOD1* genes (Liu *et al.*, 1998). One hypothesis is that toxicity is caused by the copper-mediated metabolism of aberrant products. One candidate is peroxynitrite, and increased 3-nitrotyrosine, a marker for damage mediated by peroxynitrite, has been reported in

the motor neurons of both sporadic and familial ALS cases (Beal *et al.*, 1997). The delivery of copper to SOD1 is mediated through a soluble factor identified as the copper chaperone for SOD1 (CCS), which interacts directly with SOD1 (Leah *et al.*, 1998). However, knocking out CCS in mice carrying mutant *SOD1* genes did not affect the disease course, suggesting against an involvement for the aberrant copper mediated activity of mutant SOD1 in the pathogenesis of ALS (Subramaniam *et al.*, 2002).

1.2.4.2 Neurofilament Accumulation

Neurofilaments are intermediate filament proteins, and form the major component of the neuronal cytoskeleton (Julien and Mushynski, 1998). There are three neurofilament subunits, light, medium and heavy chain (NFL, NFM and NFH; encoded by the genes *NEFL*, *NEF3* and *NEFH* in humans and *Nefl*, *Nef3* and *Nefh* in mouse). All three contain two coiled-coiled domains, which are involved in the dimerisation of two neurofilament subunits. They are obligate heteropolymers, requiring the NFL subunit together with either the NFM or NFH subunit for polymerisation. NFM and NFH also have tail regions which contain multiple copies of the Lys-Ser-Pro (KSP) sequence motif. Mutations in these KSP regions have been found in a small minority of ALS patients (see section 1.2.3, above). These two subunits are highly phosphorylated, but are more highly phosphorylated in the axon than in the perikaryon. Neuronal accumulations of phosphorylated neurofilaments are found in 70% of ALS cases (Manetto *et al.*, 1988; Munoz *et al.*, 1988; Sobue *et al.*, 1990). This is not, however, due to any alteration in the physiochemical properties of the protein, but represents the mislocalisation of normally phosphorylated neurofilaments (Strong *et al.*, 2001). Paradoxically, *NEFL* mRNA levels are decreased in the motor neurons of ALS patients (Bergerton *et al.*, 1994). It was assumed that the accumulation of neurofilaments was pathogenic, either due to the strangulation of axonal transport or the entrapment of cellular organelles (Tu *et al.*, 1997). However, more recent work involving transgenic mice, outlined in section 1.2.5.2, below, has suggested that the perikaryal accumulation of neurofilaments may actually represent a protective mechanism.

1.2.4.3 Glutamate Excitotoxicity

Glutamate is an excitatory transmitter in the central nervous system, but it is harmful in excess. Rapid removal of glutamate is therefore required, and is carried out by excitatory amino acid transporters. In humans, there are five such transporters. The most abundant is *SLC1A2*, previously known as *EAAT2*. The mouse orthologue is *Slc1a2* (previously known as *GLT1*). Mice in which *Slc1a2* has been knocked out suffer epilepsy (Tanaka *et al.*, 1997). There have been a number of factors implicating glutamate transporters in the pathogenesis of ALS, suggesting that a lack of functional *SLC1A2* in ALS leads to the failure of glutamate clearance, resulting in prolonged neuronal excitation and motor neuron degeneration (Rothstein *et al.*, 1995).

Reduced levels of glutamate transport have been reported in the brain and spinal cord of ALS patients (Rothstein *et al.*, 1992). Reduced levels of *SLC1A2* in ALS cases have also been reported in the motor cortex and spinal cord of ALS patients (Fray *et al.*, 1998; Rothstein *et al.*, 1995). Similarly, in transgenic mice and rats that carry extra copies of a mutated *SOD1* gene, both increased levels of glutamate and reduced levels of *Slc1a2* have been found (Alexander *et al.*, 2000; Howland *et al.*, 2002). Mutations in *SLC1A2* have been found in one sporadic and two familial patients, although these were from the same family (Aoki *et al.*, 1998). Aberrant *SLC1A2* mRNA transcripts, involving either the retention of intron 7 or the skipping of exon 9, have also been found in the motor cortex of ALS patients but not of controls (Lin *et al.*, 1998). However, not only has a later study failed to replicate these findings (Flowers *et al.*, 2001), but aberrant transcripts have also been reported in control individuals (Honig *et al.*, 2000; Meyer *et al.*, 1999; Nagai *et al.*, 1998).

1.2.4.4 Mitochondrial Dysfunction

The skeletal muscles of ALS patients have mitochondrial respiratory chain defects, with reduced levels of NADH:cytochrome *c* oxidoreductase and cytochrome c oxidase and also reduced levels of manganese-superoxide dismutase. They also have reduced levels of mtDNA (Borthwick *et al.*, 1999; Vielhaber *et al.*, 2000). As with

all the pathological findings, it is difficult to separate out primary and resulting secondary changes – mitochondrial changes may reflect secondary changes, especially as they are only seen in a proportion of patients.

1.2.4.5 Environmental Agents

A number of environmental agents have been investigated as potential causes of ALS, reviewed by Mitchell (2000). These include occupational exposure, physical fitness, smoking, aluminium and heavy metals, with no clear frontrunners. The plant *Cycas circinalis* has been implicated in ALS-Parkinsonism-Dementia complex on Guam. The seeds, from which the islanders produce flour, contain the neurotoxins beta-N-methylamino-L alanine (BMAA) and methylazomethanol β-D-glucoside (Spencer *et al.*, 1987). The discovery of enterovirus DNA sequences in the spinal cord of ALS patients has led to the hypothesis that ALS is caused by latent viral infection (Berger *et al.*, 2000; Woodall *et al.*, 1994), although a later study failed to replicate these findings (Walker *et al.*, 2001). ALS can also occur secondary to HIV infection (Graham and Lantos, 1997).

1.2.5 Animal models of motor neuron disorders

Animal models are becoming increasingly valuable in the study of disease pathogenesis. Mice are particularly useful due to their short generation times and ease of breeding. With the advent of transgenic techniques, different mutant mice can be crossed to test or develop new theories about disease. In the case of motor neuron disease, they are of great value as material such as spinal cord can be accessed which would not be possible from living patients. They also allow the study of both presymptomatic animals and those at different, defined stages of the disease process, as the disease course is both known and predetermined. They can also, of course, be used to assess new treatments – for example, it was found that the administration of creatine to a transgenic model of ALS significantly increased survival (Klivenyi *et al.*, 1999). There are two kinds of mouse models – the "classical" models which have arisen either spontaneously or through mutagenesis programmes, for which the underlying genetic lesions are gradually becoming known, and those which have

been intentionally generated using transgenic or knockout technology. There are also other animals which have been used as models for ALS, which lie outside the scope of this thesis and are reviewed elsewhere (Doble and Kennel, 2000). It is interesting, however, to note that a transgenic rat model has recently been described (Nagai *et al.*, 2001).

1.2.5.1 Classical Models

Wasted, *wst*

Wasted is an autosomal recessive mutation which arose spontaneously in the Jackson laboratory in 1972 (Shultz *et al.*, 1982). Homozygous *wst/wst* mice are normal until weaning (approximately 21 days old), but then deteriorate rapidly and die by 28 days. This timecourse is unaffected either by the genetic background of the mice, or by any environmental influences to which they have been exposed. They develop a neuromuscular phenotype, which begins with tremoring and gait abnormalities, is followed by rapid weight loss and culminates in paralysis. The phenotype also has immunological features, which include atrophy of the spleen and thymus and a defective response of lymphoid-derived cells to radiation damage (Goldowitz *et al.*, 1985; Woloschak *et al.*, 1987). This immunological aspect of the phenotype originally led wasted mice to be considered as a model for ataxia telangiectasia (Shultz *et al.*, 1982). However, the neurological features of the phenotype, and, in particular, the specific loss of motor neurons of the anterior spinal cord, have led to the mice being considered as a model for motor neurone disease (Lutsep and Rodriguez, 1989).

The genetic defect responsible was identified in 1998 as a 15 kb deletion on mouse chromosome 2 (Chambers *et al.*, 1998). The deleted region includes the promoter region and first exon of the gene eukaryotic elongation factor 1a2, *Eef1a2*, which leads to the abolition of its expression. The protein which it encodes, eEF1A-2, is a tissue-specific isoform of the more widely expressed eEF1A-1. The two isoforms are discussed in more detail in section 1.3, below. There is no evidence, either experimental or *in silico*, for any other genes within the wasted deletion. The closest

gene is a novel gene, 10kb downstream of the deletion, and is currently being investigated in our laboratory.

Wobbler, *wr*

Wobbler (*wr*) is another autosomal recessive mutation. The mice are normal at birth, but develop neuromuscular features by their third week. These include tremoring, a wobbling gait and progressive weakness and wasting of the muscles of the head, neck and forelimbs. The mice usually die after three or four months, although in some cases the disease can "plateau" and in these cases the mice can live for over a year (Duchen *et al.*, 1968). They also have defects in spermatogenesis, caused by the failure of the acrosome to form properly and attach to the sperm nucleus (Heimann *et al.*, 1991; Leetsma and Sepsenwol, 1980). Histologically, they show vacuolisation of the cervical motor neurons, a decrease in the number of α-motor neurons in the anterior horn region of the cervical spinal cord, demyelination of nerve fibres and neurofilament accumulation (Baulac *et al.*, 1983; Pernas-Alsono *et al.*, 1996). The wobbler gene has been mapped to the proximal region of chromosome 11 (Kaupmann *et al.*, 1992), between D11Mit79 and D11Mit19 (Resch *et al.*, 1998), recently narrowed to the region between *147N22rev* and *Murr1* (Fuchs *et al.*, 2002). The *wr* locus is in a region of conserved synteny with human Chromosome 2p14 (Wedemeyer *et al.*, 1996). The genetic defect responsible for the wobbler phenotype remains unknown, although several genes, including the spectrin isoform *Spnb-2*, decarboxylase *Ddc* (Lengeling *et al.*, 1994) and *Rab1* have been excluded as candidates (Wedemeyer *et al.*, 1996). A genetic modifier, which aggravates the disease, has been identified on Chromosome 14, between D14MIT154 and D14MIT105 (Ulbrich *et al.*, 2002).

Neuromuscular degeneration, *nmd*

Neuromuscular degeneration is another spontaneous autosomal recessive mutation. The mice suffer a loss of motor neurons and skeletal muscle atrophy, become progressively more paralysed and die within four weeks of age. The causative genetic defect, previously mapped to chromosome 19 (Cook *et al.*, 1995), is in

immunoglobulin mu binding protein 2 (*ighmbp2*), a putative transcriptional activator and DNA helicase (Cox *et al.*, 1998). There are two alleles, the nmd^{2J} allele being caused by a splice site mutation, and the nmd^{J} allele by a single amino acid substitution. The authors also identified a modifier locus, *Mnm,* on chromosome 13. As with *SOD1* and alsin in human ALS, it is unclear why there is a specific neuronal phenotype as the gene is ubiquitously expressed. Mutations in *IGHMBP2*, the human orthologue of the mouse gene, have been identified as the causative mutation in spinal muscular atrophy with respiratory distress (SMARD) (Grohmann *et al.*, 2001).

Progressive motor neuronopathy, *pmn*

Progressive motor neuronopathy has been considered as a model for SMA. Homozygous mice show degeneration of their motor axons, and die from two to six weeks after birth (Schmalbruch *et al.*, 1991). The genetic defect underlying this model has recently been identified as an amino acid substitution in the tubulin-specific chaperone e (TBCE) protein (Martin *et al.*, 2002). Mutations in the human orthologue have been found to cause hypoparathyroidism-retardation-dysmorphism and autosomal recessive Kenny-Caffey syndrome (Consortium, 2002). In this case, there are thus clear differences between the human and mouse phenotypes caused by mutations in the same gene. This may be due to fundamental differences between humans and mice, but there may actually be unlooked-for similarities in other tissues.

Other classical models

Unlike the mutants described above, legs at odd angles (*Loa*) is an autosomal dominant mutation. It arose as a result of the ENU mutagenesis programme. The mice have a progressive loss of function of their hindlimbs and a normal lifespan (Nicholson *et al.*, 2000; Rogers *et al.*, 2001). The mutation maps to distal chromosome 12 (Witherden *et al.*, 2002). There are other models in which there is some motor neuron involvement, but they have been considered as better models for other diseases. For example, motor neuron degeneration, *mnd,* has been cloned as ceroid-lipofuscinosis, neuronal 8 (*Cln8*) (Ranta *et al.*, 1999). Mutations in the human

gene cause progressive epilepsy with mental retardation (EPMR) (Ranta *et al.*, 1999). Gracile axonal dystrophy (*gad*) shows sensory ataxia at an early stage, followed by motor ataxia at a later stage. It is caused by a deletion in *UchI1*, which encodes the ubiquitin carboxy-terminal hydrolase isozyme, involved in the de-ubiquitination pathway (Saigoh *et al.*, 1999). Dysfunction of *UchI1* in *gad* mice disturbs the re-use of free ubiquitin, and causes the accumulation of abnormal proteins. The chromosomal location of motor neuron disease, *mneu*, is unknown (Miyata, 1983).

1.2.5.2 Transgenic and knockout models

SOD1

The value of using transgenic mice in motor neuron research was demonstrated by the finding that SOD 1 knockout mice do not develop clinical features comparable with ALS, although they do show an increase in cell death after axonal injury (Raume *et al.*, 1996) and a late-onset neuromuscular pathology (Flood *et al.*, 1999). This led to the hypothesis that pathogenesis in human ALS is not caused by a loss of function of SOD1, but is more likely to occur due to a gain of some novel toxic function. Transgenic mice have been generated which carry several copies of human *SOD1* genes with the ALS mutations G37R (Wong *et al.*, 1995a), G85R (Bruijn *et al.*, 1997), G93A (Gurney *et al.*, 1994; Tu *et al.*, 1996) and G39R (Friedlander *et al.*, 1997), along with the mutated mouse gene G86R (Morrison *et al.*, 2000; Ripps *et al.*, 1995). They recapitulate features of the human disease, including abnormal neurofilament accumulation, and aggregations of mutant SOD1 (Johnston *et al.*, 2000), with an age of onset dependent on the transgene copy number. The G85R mice show a particularly aggressive disease progression.

These transgenic mice have been an extremely valuable research tool in studies on the pathogenesis of ALS, not least because they can be crossed with animals which are knockout or transgenic for other genes. For example, the earlier onset of disease in G93A mice which are also *CNTF* deficient suggest the latter is a modifier gene (Giess *et al.*, 2002). Similar results were reported for *SOD2*, but this has

subsequently been found not to be mutated in the disease (Andreassen *et al.*, 2000). A modifier locus on mouse chromosome 13, between *D13Mit36* and *D13Mit76*, has also been identified (Kunst *et al.*, 2000). This region includes *SMN*, which may provide a further link between the two diseases.

Transgenic techniques have also been used to restrict the expression of genes to particular cell types. For example, restricting the expression of the mutant SOD1 to astrocytes did not result in motor neuron degeneration (Gong *et al.*, 2000). However, it is difficult to understand why restricting the expression to neurons does not lead to a phenotype (Pramatarova *et al.*, 2001).

Overexpressing the non-mutated human gene in mice does not lead to clinical features of disease, although the mice do have subtle motor neuron pathology and abnormalities in the neuromuscular junctions of their tongues (Avraham *et al.*, 1988; Canto and Gurney, 1995; Epstein *et al.*, 1987). Aged mice of 2 years also show an impaired motor performance (Jaarsma *et al.*, 2000). It is interesting to note that the early studies on the *SOD1* overexpressing mice were done in the context of research on Down syndrome, before *SOD1* was identified as being mutated in ALS.

Neurofilaments

Mice in which the neurofilament genes have been knocked out individually either show no phenotype or a very mild one, despite a reduction in axonal calibre (diameter), and a loss of large motor axons. *Nefl* knockout mice have a delayed axonal regeneration after injury (Zhu *et al.*, 1997), *Nef3* knockouts have decreased NFL levels and increased NFH levels (Elder *et al.*, 1998a), and *Nefh* is required for the development of large calibre axons (Elder *et al.*, 1998b; Kriz *et al.*, 2000; Rao *et al.*, 1998; Zhu *et al.*, 1998). Mice in which both *Nef3* and *Nefh* have been knocked out show axonal atrophy and hindlimb paralysis at two years of age (Elder *et al.*, 1999a). These mice also demonstrated that NFL is essential for polymerisation (Elder *et al.*, 1999b).

Mice have also been generated which overexpress the neurofilament genes. The overexpression of wild-type mouse *Nefh* at up to 4.5 times the normal level does not give rise to a clinical phenotype (Marszalek *et al.*, 1996). However, overexpressing human *NEFH* does cause an ALS-like phenotype, with neurological defects, muscle atrophy and neurofilament accumulation (Cote *et al.*, 1993), which can be relieved by also overexpressing human *NEFL* (Beaulieu *et al.*, 2000; Meier *et al.*, 1999). This suggests that human *NEFH* acts in a dominant negative manner. Increasing mouse *Nef3* did not result in an overt phenotype, although neurofilamentous swellings were often seen in the perikarya and proximal axons of motor neurons (Wong *et al.*, 1995b), and there were changes in axonal transport (Xu and Tung, 2000). Overexpressing *Nefl* results in an ALS-like pathology which resolves on the cessation of transgene expression (Xu *et al.*, 1993). Mice in which the type III intermediate filament protein peripherin is overexpressed develop motor dysfunction and the loss of motor neurons at two years of age (Beaulieu *et al.*, 1999). This is exacerbated by a loss of *Nefl* (Beaulieu *et al.*, 2000). Mice were also generated which expressed an NFHLACZ transgene, in which a truncated NFH protein was fused to β-galactosidase (Eyer and Peterson, 1994; Tu *et al.*, 1997). The fusion protein accumulated in the perikarya, and the axons which developed had small calibres. The mice did not develop a phenotype, although they did lose Purkinje cells in old age. Transgenic mice in which a point mutation in the *Nefl* gene has been introduced have massive motor neuron degeneration and neurogenic atrophy of their skeletal muscles (Lee *et al.*, 1994). However, it is likely that this is due to defective RNA processing caused by a *c-myc* tag in the 3'UTR (Canete-Soler *et al.*, 1999), rather than the point mutation.

Combining neurofilament and *SOD1* transgenic mice has given some interesting insights into the role of neurofilaments in the disease process. Crossing mice transgenic for *SOD1* with those overexpressing human *NEFH* delayed the onset of disease by an average of 6 months (Couillard-Despres *et al.*, 1998). The delay was dependent on the degree of perikaryal neurofilament accumulation – the greater the accumulation, the later the disease onset. This effect may be because the accumulated neurofilaments form a phosphorylation "sink" and are phosphorylated

in preference to other proteins which would be more detrimental to the cell in a phosphorylated form (Nguyen *et al.*, 2001). Crossing *SOD1* mice with those carrying extra copies of mouse *Nefl* or *Nefh* also extended lifespan (Kong and Xu, 2000).

Perhaps counterintuitively, the calibre of the axons is not important in the pathogenesis of the disease. For example, as described above, mice with the *Nefh* or *Nef3* genes knocked out have a reduced axonal calibre and no phenotype. When mice hemizygous for all three neurofilament genes were crossed to *SOD1* transgenic mice their axonal caliber was reduced without affecting neurofilament stoichiometry, but the disease course remained unaltered (Nguyen *et al.*, 2000). Similarly, overexpressing *Nefl* led to a 50% increase in neurofilament density without affecting the disease course (Couillard-Despres *et al.*, 2000).

Vegf

Mice have been generated which lack the hypoxia-response element in the promoter region of the vascular endothelial growth factor (*Vegf*) gene (Oosthuyse *et al.*, 2001). They have a phenotype which is striking in its similarity with human ALS, with muscle weakness from 5-7 months of age due to the degeneration of lower motor neurons. Neuronal death may be caused by a reduction in perfusion under conditions of low oxygen, as the mice have reduced baseline and hypoxic levels of VEGF. Alternatively, the loss of VEGF may be directly neurotoxic, as VEGF seems to have a neuroprotective function.

Other transgenic models of motor neuron loss

Mice lacking the ciliary neurotrophic factor (CNTF) gene have a subtle phenotype in adulthood (Masu *et al.*, 1993). However, mice in which the receptor for CNTF has been knocked out die perinatally and show severe motor neuron defects (DeChiara *et al.*, 1995). Transgenic mice which overexpress interleukin 3 develop motor neuron degeneration from approximately 7 months of age. This is associated with an autoimmune reaction, and the mice have been proposed as a model for progressive muscular atrophy, PMA, rather than ALS (Chavany *et al.*, 1998).

1.3 Eukaryotic elongation factor 1 alpha

1.3.1 eEF1A

The translation of mature mRNA into protein occurs at the ribosome, and is composed of three stages: initiation, elongation and termination. The elongation stage involves the sequential addition of amino acids to the growing polypeptide chain by the translation elongation complex eEF1H. This complex is comprised of eEF1A and eEF1B. The role of eEF1A is to transport aminoacyl tRNAs to the ribosomal A-site in a GTP-dependent fashion (Hershey, 1996). On correct codon-anticodon recognition, GTP is hydrolysed to GDP. The continued addition of amino acids requires the exchange of bound GDP for GTP, which is performed by eEF1B. The process is illustrated in figure 1-3. eEF1B is comprised of three subunits, eEF1Bα, eEF1Bβ and eEF1Bγ. A guide to the current and past nomenclature of the translation elongation factors eEF1A and eEF1B is given in table 1-1.

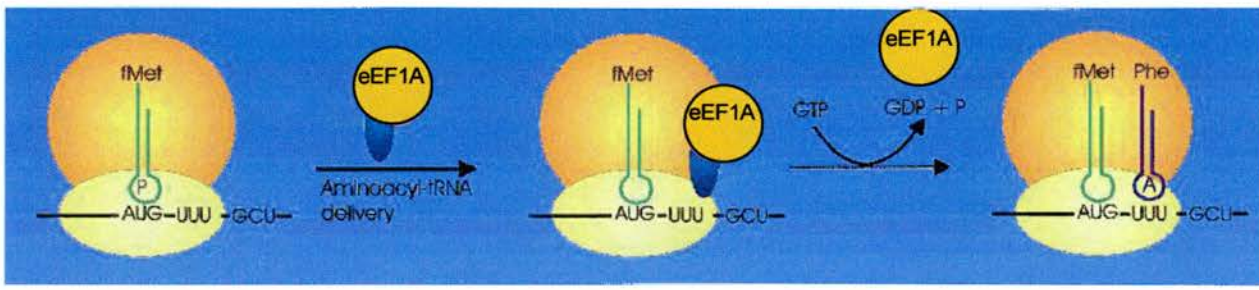

Figure 1-3 Diagram showing translation elongation (adapted from Stark *et al.*)

Gene name, human	Gene name, mouse	Protein	Aliases
EEF1A1	*Eef1a1*	eEF1A-1	EF-1α; EF1αEF1A; EEF1A
EEF1A2	*Eef1a2*	eEF1A-2	EF-1α2; S1
EEF1B2	*Eef1b2*	eEF1Bα	EF-1β; EF1β
EEF1D	*Eef1d*	eEF1Bβ	EF-1δ; EF1δ
EEF1G	*Eef1g**	eEF1Bγ	EF-1γ; EF1γ

Table 1-1 Nomenclature of eEF1A and eEF1B isoforms.
Eef1g is starred because it has not yet been assigned a gene symbol.

1.3.2 eEF1A-2

eEF1A-2 was initially isolated in the rat by Ann *et al.* on the basis of its antigenic similarity to statin, leading to its early designation as S1 (Ann *et al.*, 1991). In humans, eEF1A-1 and eEF1A-2 are 92% identical at the amino acid level (Knudsen *et al.*, 1993). There is also a high degree of similarity between the isoforms of different mammalian species, with only one amino acid difference between human and mouse eEF1A-2 proteins (Lee *et al.*, 1994). In humans, the protein consists of 463 amino acids with a predicted isoelectric point of 9.72 (Knudsen *et al.*, 1993). The mouse protein also has 463 amino acids. The eEF1A-1 proteins of both species have 462 amino acids. A line-up of the protein sequences demonstrates the similarity between the two isoforms, and is shown in figure 1-4. The human gene *EEF1A1* is located on chromosome 6, at 6p14, and *EEF1A2* is on chromosome 20, at 20q13.3 (Lund *et al.*, 1996). Although *EEF1A1* has numerous pseudogenes (Madsen *et al.*, 1990), *EEF1A2* appears to be single copy (Lund *et al.*, 1996).

The fact that there is only 20% homology between *Eef1a1* and *Eef1a2* in the 5' (and 3') untranslated regions led to initial speculation that the two genes are differentially regulated (Ann *et al.*, 1991). This was quickly borne out by the finding that the two isoforms have different expression patterns. Using Northern and RNase protection analyses, *Eef1a2* was shown to be expressed in brain, heart and skeletal muscle in rats (Lee *et al.*, 1992), rabbits (Kahns *et al.*, 1998) and humans (Knudsen *et al.*, 1993). At the protein level, eEF1A-2 was shown to be expressed in the brain, heart and skeletal muscle of rats, humans and mice, but not in the smooth muscle of the gut or bladder (Khalyfa *et al.*, 2001). Within the brain, only differentiated neurons express eEF1A-2, whereas proliferating neurogenic cells express only eEF1A-1 (Lee *et al.*, 1995). This, along with the fact that in mouse fibroblasts, *Eef1a2* is most abundant in G_0 phase, but is reduced in G_1 and S phase (Ann *et al.*, 1991), suggested expression is limited to terminally differentiated cells which cannot re-enter the cell cycle.

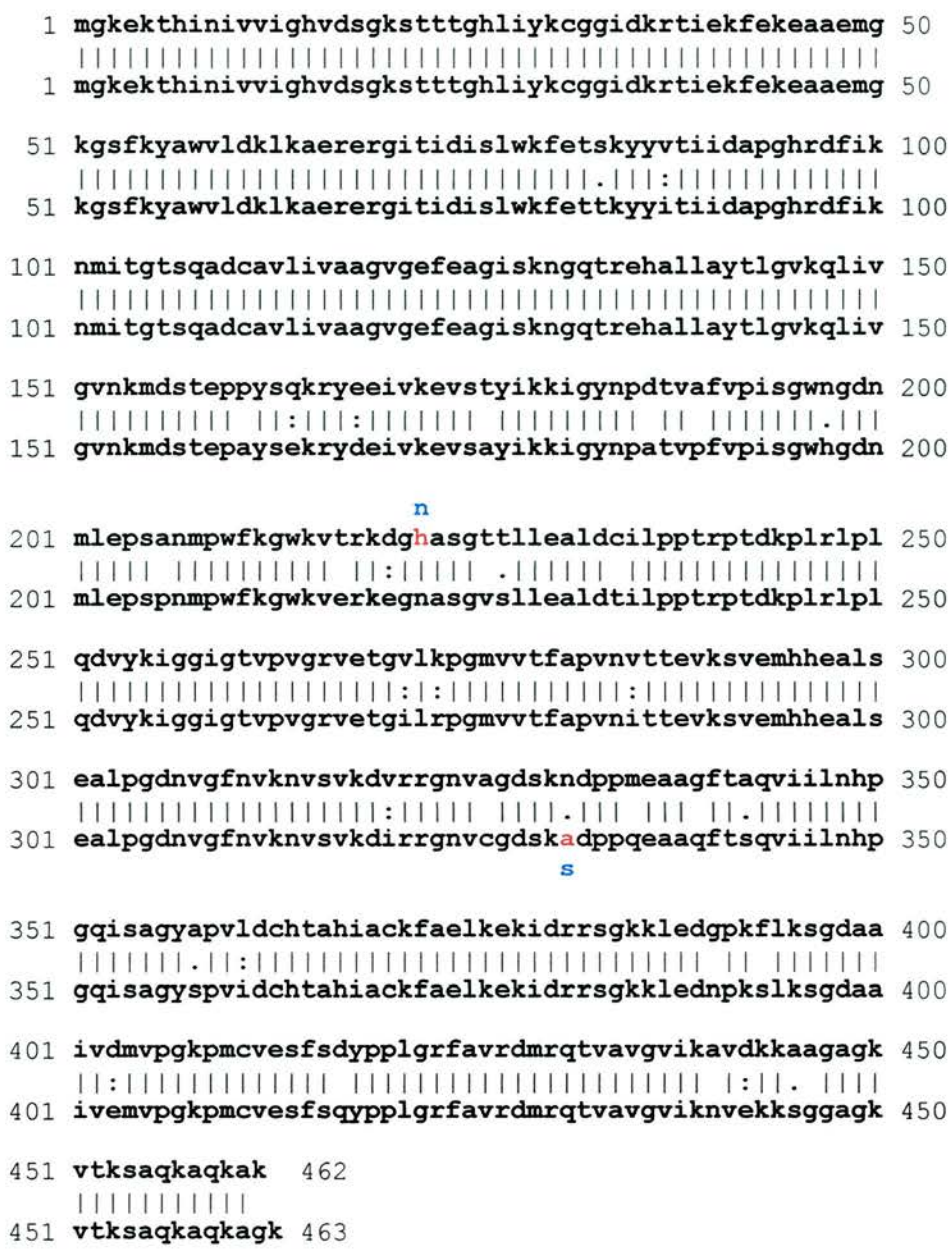

Figure 1-4 Line-up of mouse eEF1A-1 (top) and eEF1A-2 (bottom), showing the high degree of similarity between the two proteins. Identity between two amino acids is indicated by a vertical line, conservative amino acid substitutions by two dots and semi-conservative substitutions by one dot. Where there is no agreement between two amino acids, there is no symbol between them. The amino acids of eEF1A-1 and eEF1A-2 which differ between the mouse and human proteins are highlighted in **red**, with the equivalent human residues at these positions in **blue**.

1.3.2.1 Isoform switch

In those tissues in which eEF1A-2 is expressed, there is a switch in expression between the two isoforms (Lee *et al.*, 1995). In rat brains, *Eef1a2* mRNA levels increase steadily during late embryogenesis, and reach a plateau soon after birth. During this period, there is a slight drop in *Eef1a1* mRNA levels. (Lee *et al.*, 1993a). In muscle and heart, the increase in *Eef1a2* mRNA levels occurs after birth, and is accompanied by a much more precipitous drop in *Eef1a1* levels. A cartoon of the situation in muscle is shown in figure 1-5, below. This isoform switch explains the onset of wasted at 21 days, as it is at this point that *Eef1a1* levels have declined, but in wasted mice there is no *Eef1a2* to carry out translation.

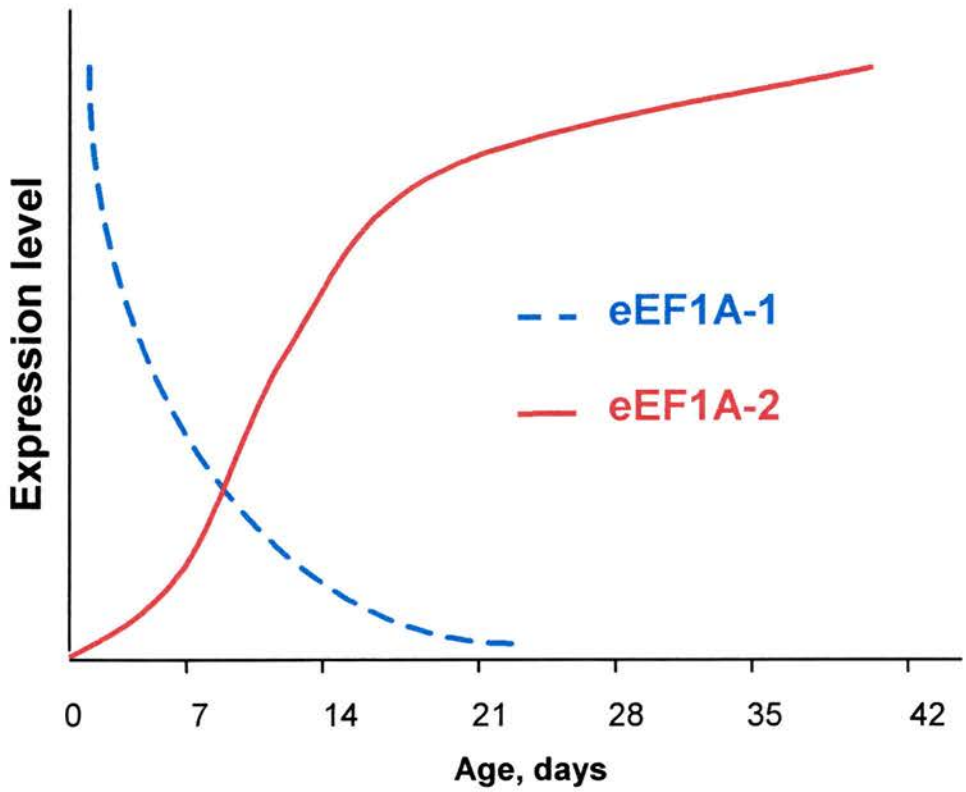

Figure 1-5 Cartoon of isoform switching in rat muscle

At the protein level, levels of eEF1A-2 appear to rise, and of eEF1A-1 to drop, from around postnatal day 1 (P1) in mouse brain and P7 in skeletal muscle. The switch appears to be much more gradual in mouse heart, with the switch occurring through late embryogenesis and early postnatal life (Khalyfa *et al.*, 2001). Although it has been reported that levels of eEF1A-2 in muscle remain stable through adulthood, the antibody used in this case probably recognises both isoforms (Welle *et al.*, 1997). In muscle, after injury induced by the toxin Marcaine, there is also a switch back to the embryonic expression pattern where eEF1A-1 levels are high compared to eEF1A-2 (Khalyfa *et al.*, 1999). Regenerating muscle cells could therefore represent a return to embryonic forms. Increased eEF1A-1 mRNA levels have also been reported in diabetic skeletal muscle (Reynet and Kahn, 2001). However, in this case it is not clear whether it is actually eEF1A-1 which was increased, as the identified clone was only partially sequenced, and reported as being 99% similar to eEF1A-1. It could, therefore, represent one of the eEF1A-1 pseudogenes which has been expressed.

1.3.2.2 Why are two isoforms needed?

It is not clear why two eEF1A isoforms are required. eEF1A-2 acts as a translation elongation factor with equal activity to eEF1A-1, although there are differences in the relative affinities for GTP and GDP between the two isoforms (Kahns *et al.*, 1998). One possible difference is that eEF1A-2, in contrast to eEF1A-1, has not been shown to interact with any of the components of the exchange factor eEF1Bα (Mansilla *et al.*, 2002). However, if this is the case, it is difficult to understand how GDP-GTP exchange can occur, as there do not appear to be tissue-specific isoforms of eEF1Bα (Chambers *et al.*, 2001). Yeast strains with mutations in eEF1Bα have a reduced translation and increased translational fidelity (Carr-Schmid *et al.*, 1999).

Aside from its role in translation, eEF1A-1 is also implicated in many other processes, including actin binding and bundling (Liu *et al.*, 2002; Yang *et al.*, 1990), the severing of microtubules (Shiina *et al.*, 1994), apoptosis (Chen *et al.*, 2000; Duttaroy *et al.*, 1998) and tumourigenesis (Tatsuka *et al.*, 1992). eEF1A is abundantly expressed, forming from 3 – 5% of the total cellular protein content (Lee

et al., 1993a). It is present at 7-35 times the amount of the other eEF1H components, which supports the idea that eEF1A-1 has important functions beyond its role in translation (Condeelis, 1995). It is possible that there are key differences between the two isoforms in one or more of these non-canonical functions.

1.3.2.3 Translation in neurons

One key distinguishing feature of neurons is their large size. It is therefore possible that eEF1A-2 is required in these cells due to an involvement in cytoskeletal modelling or transport. Overexpression of eEF1A-1 affects the organisation and function of the cytoskeleton in yeast (Munshi *et al.*, 2001). Alternatively, eEF1A-2 may be required for synaptic translation. In neurons, where the synapse may be some distance from the cell body, there is evidence that translation occurs locally in the dendrites (Job and Eberwine, 2001a; Job and Eberwine, 2001b). This spatial regulation of translation would allow the synthesis of proteins, such as receptors, at optimal distances from the stimulated membrane for synapse formation during development and for synaptic plasticity in mature neurons.

It is also possible that specific mRNAs are required to be translated specifically at the synapse. Although components of the translation machinery, such as ribosomes (Job and Eberwine, 2001b), and translational activity have been located at the distal regions of the dendrites, there have been no studies localising eEF1A-2 in neurons. Although eEF1A has been reported in dendrites, it is not clear whether this is specific for eEF1A-1 or eEF1A-2 (Job and Eberwine, 2001b). Immunofluoresent analysis of the subcellular localisation of eEF1A-1 has shown that it localises to both the cytoplasm and the nucleus (Sanders *et al.*, 1996). This is in contrast to the rest of the eEF1H components, which localise to the endoplasmic reticulum. However, the subcellular localisation of eEF1A-2 has not been clearly characterised, although this was investigated by Khalyfa *et al.* (Khalyfa *et al.*, 2001). A recent study claimed a cytoplasmic localisation in PC-12 cells, however, in this case an antibody to eEF1A-1 was used (McClatchy *et al.*, 2002).

There may also be important protein interactions which are specific for eEF1A-2. For example, the CNS-specific muscarinic acetylcholine receptor subtype M_4 has recently been shown to interact with eEF1A-2 (McClatchy *et al.*, 2002). Muscarinic activation is known to increase dendritic translation (Feig and Lipton, 1993). Dysfunction in mAChR signalling has also been implicated in disorders including Parkinsons and Alzheimers Disease (Hellstrom-Lindahl, 2000). Although eEF1A-1 binds to actin (Liu *et al.*, 2002; Yang *et al.*, 1990), it is not known whether eEF1A-2 also interacts. Data from yeast mutants has shown that although actin is not required for translation, it is important in translational fidelity (Kandl *et al.*, 2002).

1.3.2.4 eEF1A and cancer

There is evidence to implicate both eEF1A isoforms in cancer. eEF1A-1 renders cells susceptible to transformation (Tatsuka *et al.*, 1992), and is overexpressed in metastatic rat mammary adenocarcinoma, possibly through alterations in the cytoskeleton (Edmonds *et al.*, 1996). The PTI-1 oncogene is expressed in human prostatic carcinomas. It is a fusion between 630 bp of a *Mycoplasma* ribosomal RNA gene and 1493 bp of sequence representing a truncated and mutated pseudogene of *EEF1A1* (Shen *et al.*, 1995). *EEF1A2* has recently been identified as a putative oncogene in ovarian cancer (Anand *et al.*, 2002). It was found to be amplified in 25% of primary ovarian tumours and 4 of 12 ovarian tumour cell lines. The expression of *EEF1A2* also rendered NIH3T3 cells tumorigenic, and increased the growth of ovarian carcinoma cells xenografted into nude mice.

1.3.3 eEF1A and ZPR1 – a link with SMN?

The *SMN* gene encodes a ubiquitously expressed 294 amino acid protein with a molecular weight of 38 kD and no obvious sequence identity with any other proteins. It is currently unknown how mutations in *SMN* change the function of the protein and lead to disease. SMN has been implicated in the processing of small nuclear riboproteins (snRNAs) (Carvalho *et al.*, 1999), pre-mRNA splicing (Pellizzoni *et al.*, 1998), and transcription (Pellizzoni *et al.*, 2001). Cells in which the SMNΔN27 mutant protein is expressed show a reduction in transcription (Pellizzoni *et al.*,

2001). The SMN protein is expressed in both the cytoplasm and within nuclear bodies known as gems (gemini of coiled, or Cajal bodies) (Liu and Dreyfuss, 1996).

The zinc finger protein, ZPR1, has been identified as necessary for the nuclear translocation of SMN to the nucleus (Gangwani *et al.*, 2001). In the fibroblasts of patients with the SMNΔexon7 deletion, the interactions between SMN and ZPR1 are disrupted, probably because the missing C-terminus of SMN is required for the interaction with ZPR1, and neither protein translocates correctly. Mutant SMN proteins caused by the 472del5 frameshift mutation associated with cases of spinal muscular atrophy mislocalise to the nucleoplasm and nucleolus (Lefebvre *et al.*, 2002). Evidence from transgenic mice expressing a mutated *SMN* in which exon 7 has been deleted suggests that it is this disruption of the nuclear targeting of SMN which is responsible for the disease (Pellizzoni *et al.*, 2001).

ZPR1 also interacts with eEF1A-1. After stimulation by serum, mitogens, or epidermal growth factor, ZPR1 and eEF1A-1 translocate to the nucleus (Gangwani *et al.*, 1998). It is thus tempting to speculate that ZPR1, SMN and eEF1A-1 all form part of the same complex, although there is no direct evidence for this. There is similarly no indication of whether ZPR1 also interacts with eEF1A-2.

1.3.4 eEF1A isoforms through evolution

eEF1A has been conserved through evolution, indeed, it has been used for phylogenetic analysis (Roger *et al.*, 1999). In mice, rats, rabbits and humans, only the two previously described eEF1A isoforms, eEF1A-1 and eEF1A-2, have been characterised. The similarities between the same isoforms of different species are greater than those between the two isoforms of a single species. In chickens, only one eEF1A gene has been described (Wang *et al.*, 1994). In the African clawed frog *Xenopus laevis* there are two adult isoforms which are similar to the mammalian eEF1A, one oocyte-specific and one somatic (Abdallah *et al.*, 1991a; Dje *et al.*, 1990). There is a third form which is less similar to the mammalian genes, and is only expressed in immature oocytes and pre-meiotic germ cells. The *X. laevis*

isoforms are described in more detail in Chapter 6, section 6.1.2. In *Drosophila melanogaster*, there are two stage-specific genes, F1 and F2 (Hoveman *et al.*, 1988; Walldorf *et al.*, 1985). *Saccharomyces cerevisiae* have two genes, TEF1 and TEF2 (Schirmaier and Philippsen, 1984), whereas *S. pombe* have three genes, with differential regulation (Mita *et al.*, 1997). In *Escherichia coli* there are two identical EF-Tu genes. The presence of two tissue-specific isoforms of eEF1A, in which one is expressed in the CNS, heart and skeletal muscle of adult animals, thus appears to be specific to mammals.

1.4 Project Aims

The overall aim of this project was to investigate the potential involvement of eEF1A-2 in the pathogenesis of motor neuron disease. Within this broad theme there were four main aims. Firstly, to further characterise wasted mice, in order to evaluate them as a model for motor neuron disease. Secondly, to determine whether there is a direct involvement of *EEF1A2* in the disease, by mutation screening the gene in patients. Thirdly, to develop and characterise specific antibodies against eEF1A-2 and eEF1A-1 in order to analyse the expression of the two isoforms. Finally, to investigate the expression of the two isoforms in a non-mammalian species, *Xenopus laevis*.

2 Chapter 2 – Materials and Methods

2.1 General Materials and Solutions

Unless otherwise indicated, general laboratory chemicals were obtained from Sigma. All PCR primers were obtained from Sigma-Genosys. Cell culture media were obtained from Invitrogen.

PBS

Phosphate buffered saline was made by dissolving 1 PBS tablet (Sigma) in 200ml H_2O, and autoclaving.

2.2 General Equipment

Again, unless otherwise indicated, centrifugation was performed on an eppendorf 5415C microfuge. The vortex used was a Jencons MS1 minishaker. Absorbances at 260 and 280 nm were read on a Pharmacia Biotech Ultrospec 3000 spectrophotometer. Mice were weighed on an Avery-Berkel FB411. Their organs were weighed on a Sartorius BP150.

2.3 Genotyping of wasted mice

2.3.1 Mouse husbandry

Mice were housed at the Biomedical Research Facility at the Western General Hospital, a semi-barrier facility. They were fed a standard chow diet.

2.3.2 Extraction of genomic DNA from ear notches

For the purposes of identification and genotyping, mice were ear notched. The ear notches were boiled in 0.6 ml 50 mM NaOH for 10 minutes, vortexed, neutralised with 50µl TrisHCl pH 8.0 and centrifuged for 6 minutes. The supernatant was removed and 1µl was used in the genotyping PCR.

2.3.3 Genotyping

Two PCRs were used to genotype mice. One amplified the wild type allele, if present, and one amplified the wasted allele. In heterozygous mice, therefore, both alleles were amplified. The primers used are given in table 2-1. Primers P2F and P2R, originally designed by Khalyfa *et al.* (Khalyfa *et al.*, 2001), were used to amplify the wild-type allele, and gave a product of 452bp. Primers wstspanF and wstspanR, designed by Dawn Loh in our laboratory, were used to amplify the *wst* allele, and gave a product of 200bp. In each reaction mix were 5mM each primer, 0.05 mM dNTPs, 1 x Sigma Taq Buffer, 0.5U *Taq* polymerase and, for the wasted PCR, 1.485M betaine. The total reaction volume was 25µl. PCR conditions were 95^0C for 3 minutes, followed by 30 cycles of 94^0C for 30 seconds, 54^0C for 30 seconds and 72^0C for 30 seconds. They were then held at 72^0C for 10 minutes. An MJ Gradient Cycler was used. Products were analysed on a 2% w/v agarose gel.

Primer	Sequence
P2F	tag tgg ctc ctt gga aca g
P2R	cta ctc tcc ctg aat gcc tt
wstspanF	ata agc tcc cca atg gta gag aa
wstspanR	cgc gcc att ctt gta ttg tt

Table 2-1. Primer sequences used in wasted genotyping.

2.4 Immunohistochemistry

2.4.1 Paraffin embedding and sectioning

Dissection and paraffin embedding was carried out in collaboration with Dr. J. Peters at the MRC Mammalian Genetics Unit, Harwell. After dissection, mouse brain and spinal cords were embedded in paraffin. The processing schedule is described in table 2-2. Safeclear (Chemix) is a xylene alternative. Sections were then cut on a Rachert-Jung 2030 microtome with a thickness of 4 µm.

Chemical	Time, hours
70% Ethanol	3
90% Ethanol	2
100% Ethanol	2
100% Ethanol	1
100% Ethanol	1
Safeclear	3
Safeclear	2
Safeclear	2
Paraffin Wax	2
Paraffin Wax	1
Paraffin Wax (under vacuum)	1

Table 2-2 Processing schedule for sections

2.4.2 H & E Staining

Sections were hydrated by submersion for 5 minutes in 100% ethanol, followed by 5 minutes in 70% v/v ethanol and then 5 minutes in H_2O. Nuclei were then stained in haematoxylin (Surgipath) for 5-10 minutes, washed briefly in H_2O and differentiated in acid alcohol (0.5% w/v HCl in 70% v/v ethanol). They were again washed in H_2O and then stained in saturated aqueous lithium carbonate. They were washed in H_2O and then the cytoplasm and connective tissue were stained with eosin (Surgipath) for 5 minutes. The slides were finally washed in H_2O, dehydrated by submersion in 70% v/v ethanol, followed by 100% ethanol, and then two changes of xylene. Slides were mounted in pertex (CellPath).

2.4.3 Immunohistochemistry

The sections were rehydrated through a graded series of ethanols, with 5 minutes in two changes of 100% ethanol and 5 minutes in two changes of 70% v/v ethanol. They were then submerged in picric acid for 15 minutes and washed in H_20 for 5 minutes. Where antigen retrieval proved necessary (shown in table 2-3), slides were immersed in 0.01M citric acid (pH 6.0) and microwaved at full power for 15 minutes. They were allowed to cool and then washed in H_20 for 5 minutes before proceeding. All slides were then treated in 3% v/v hydrogen peroxide, to block

endogenous peroxidases. They were again washed in H_20 for 5 minutes, transferred to a Sequenza (Shandon) and then washed in TBS (25mM TrisEDTA; 137mM NaCl; 27mM KCl; pH 7.4) for 5 minutes. Non-specific binding of the secondary antibody was then blocked by incubating the slides in 100 µl sera (diluted 1 in 5 in TBS) from the animal in which the secondary antibody was raised. Sera were obtained from Diagnostics Scotland. The primary antibody (100µl) was then applied, diluted to an appropriate concentration in TBS, and the slides incubated for 30 minutes. They were then washed twice in TBS, and then incubated for 30 minutes in 100µl biotinylated secondary antibody (Dako), diluted 1 in 200 in TBS. They were then washed once in TBS and incubated in 3 drops (approximately 135µl) StreptABC (Dako) for 30 minutes. They were again washed in TBS, removed from the sequenza and treated in diaminobenzidene (DAB) for approximately 2 minutes. Excess DAB was removed by washing in H_20. The slides were counterstained in haematoxylin solution (Surgipath), rinsed in H_20 and differentiated in saturated lithium carbonate. They were washed once more in H_20, dehydrated through 70% v/v ethanol and then 100% ethanol to xylene and, finally, mounted in pertex (CellPath).

Primary Antibody	Source	Dilution	Antigen Retrieval	Blocking Serum	Secondary Antibody
GFAP	Dako; rabbit polyclonal	1:2000	None	Swine	Swine anti-rabbit
NF (P)	Dako; mouse monoclonal	1:80	Citric acid	Swine	Swine anti-rabbit
NF (de-P)	Zymed; mouse monoclonal	Undiluted	Citric acid	Rabbit	Rabbit anti-mouse
MAP2	Dako; mouse monoclonal	1:500	Citric acid	Rabbit	Rabbit anti-mouse
Ubiquitin	Dako; rabbit polyclonal	1:500	None	Swine	Swine anti-rabbit
EEF1A-2	Goat polyclonal	1:50	Citric acid	Rabbit	Rabbit anti-goat

Table 2-3 Experimental details for immunohistochemistry experiments

2.5 RT-PCR

2.5.1 Extraction of RNA from tissues

2.5.1.1 Extraction from mouse brain

The mouse brains were kept at -70^0C on receipt. Approximately half a mouse brain was homogenised in 1ml RNAzol (Biogenesis) and incubated at 4^0C for 5 minutes. 100µl chloroform was added, the samples were vortexed for 15 seconds, and incubated for 5 minutes at 4^0C. They were then centrifuged for 15 minutes at 12 000 rpm on a Beckman Coulter Avanti J-201 at 4^0C and the upper phase was removed. An equal volume of isopropanol was added and the samples were mixed by inversion, incubated further for 15 minutes at 4^0C and centrifuged at 12 000 rpm for 15 minutes at 4^0C. The supernatant was discarded and the pellet was washed with 75% v/v ethanol (made with DEPC H_20), centrifuged for 15 minutes at 12 000 rpm, and air dried. The RNA was resuspended in 50µl H_20 and stored at -70^0C.

2.5.1.2 Extraction from *X. laevis* tissue

The RNeasy® Midi kit (Qiagen) was used to extract RNA from 150mg *Xenopus* muscle, as per the manufacturer's instructions. The recommended modifications for extracting RNA from muscle were observed, namely homogenisation using a PowerGen 125 (Fisher), followed by Proteinase K incubation. The RNA was eluted in 300µl RNase-free water.

2.5.2 cDNA synthesis

The extracted RNA was quantified by measuring the absorbance at 260nm. 4µg RNA was treated with 1µl DNaseI (Roche) and 1.6µl DNase buffer in a total reaction volume of 16µl. This was then incubated at room temperature for 15 minutes. The DNase was inactivated by adding EDTA to a final concentration of 12.5mM and incubating at 65^0C for 10 minutes. Samples were then divided into two aliquots. In one (RT), the RNA was transcribed, whereas in the other, control sample, no reverse transcriptase was added. To both aliquots were added 2µl random hexamer primers, 1µl RNase inhibitor, dNTPs at 1.0mM, $MgCl_2$ at 5mM, 1 x Reaction Buffer, and

either 0.8µl AMT Reverse Transcriptase or H_20. All reagents were from the First Strand cDNA Synthesis kit (Roche). Samples were held at room temperature for 10 minutes, 42^{0}C for one hour and 99^{0}C for 5 minutes. The cDNA obtained was either placed on ice and used immediately for PCR, or stored at –20^{0}C until use.

2.5.3 RT-PCR

Each PCR contained 5mM forward and reverse primers, 0.05mM dNTPs, 1xPCR buffer (Sigma), 1.485M betaine and 1µl of either the reverse-transcribed or no-RT control RNA mixes, in a total volume of 50µl. Primer sequences are given in table 2-4. For the *Slc1a4* RT-PCR, cycling conditions were 95^{0}C for 3 minutes, 30 cycles of 94^{0}C for 1 minute, 50^{0}C for 1 minute and 72^{0}C for 1 minute, and 72^{0}C for 10 minutes, on a Hybaid Omnigene. Amplification of *Gapdh* was used as a control reaction to enable comparison between samples, using the same cycling conditions as for the RT-PCR. For the *X. laevis* RT-PCR, conditions were 95^{0}C for 3 minutes, followed by 40 cycles of 94^{0}C for 30 seconds, 55^{0}C for 30 seconds and 72^{0}C for 30 seconds, followed by 10 minutes at 72^{0}C, on an MJ Gradient Cycler.

Primer	Sequence
Slc1a4 5F2	atg aag gac atc gtc atg ct
Slc1a4 6R	cac ttc atc ata gac gga agg
Slc1a4 5F	aac ccg ttc acg ttc ctc ct
Slc1a4 7R	tcc aac act gga tgc cgt g
GAPDHF	cat cac cat ctt cca gga gc
GAPDHR	atg acc ttg ccc aca gcc tt
Xen1A2F2	tga gag gga gcg agg aat c
Xen1A2R1	gct tta gaa tgc cgg tc

Table 2-4 Primer sequences used in RT-PCR.

2.6 Mutation screening

2.6.1 Extraction of genomic DNA from mouse brains

Tissues were stored at –70^{0}C after receipt. Approximately half a brain was homogenised in a sterile Treff homogeniser in 3 ml TNE buffer (10mM Tris; 400mM NaCl; 2mM EDTA). Proteins were broken down by the addition of 100µg/ml Proteinase K (Sigma) and incubation overnight at 55^{0}C. To this was added 3ml 2.6 M NaCl, and the cell debris was pelleted by centrifugation at 14 000 rpm. An equal volume of ethanol was added to the supernatant to precipitate the DNA. It was then washed twice in 70% v/v ethanol, and resuspended in 200 µl sterile H_2O.

2.6.2 PCR

For the amplification of *EEF1A2*, each reaction contained forward and reverse primers at 5mM, dNTPs at 0.05mM each, either glycerol at 10% v/v, betaine at 1.485M, TMACl at 1.0mM or DMSO at 60mM, 0.5µl *Taq*, 1xPCR Buffer (Sigma) and 1µl DNA in a total reaction volume of 50µl. The PCR conditions used to amplify the exons of *EEF1A2* are given in table 2-5, and for the amplification of the introns and exons of *Slc1a4* in table 2-6. The primer sequences used to amplify *EEF1A2* are given in table 2-7. Some of the introns of *Slc1a4* were amplified using long-range PCR, described in section 2.6.2.1, below. Where a Hybaid Omnigene was used for amplification, cycling conditions were 95^{0}C for 3 minutes, 30 cycles of 94^{0}C for 1 minute, the appropriate annealing temperature for 1 minute and 72^{0}C for 1 minute, and 72^{0}C for 10 minutes. Where an MJ Gradient Cycler was used, the cycling conditions were 95^{0}C for 3 minutes, followed by 30 cycles of 94^{0}C for 30 seconds, the annealing temperature for 30 seconds and 72^{0}C for 30 seconds, and then 72^{0}C for 10 minutes.

Exon	Primers Used	Annealing temp, ^{0}C	Additive	PCR machine
2	2F & 2Rnew	54	Betaine	MJ
3	3F & 2R 3F1 & 2R1	60 53	Glycerol Glycerol	Hybaid Hybaid
4	4F & 4R2 4F2 & 4R4	58 59.5	Glycerol Glycerol	MJ MJ
5	5F2 & 5R2	55	Betaine	MJ
6	6F & 6R2	55	Glycerol	Hybaid
7	7F1 & 7R 7F & 7R1	55 55	Betaine Betaine	Hybaid MJ

Table 2-5. PCR conditions for amplification of *EEF1A2.*

Exon / Intron	Primers	Annealing temp, ^{0}C	Additive	PCR machine
Exon 1	1F & 1R 1F2 & 1R2	48 55	Glycerol Betaine	Hybaid Hybaid
Exon 2	2F5 & 2R2	49	Glycerol	Hybaid
Exon 3	3F3 & 3R4	47	TMACl	Hybaid
Exon 4	4F2 & 4R3	55	Glycerol	Hybaid
Exon 5	5F4 & 5R3	55	Glycerol	Hybaid
Exon 6	6F3 & 6R3	55	DMSO	Hybaid
Exon 7	7F3 & 7R2	50	DMSO	Hybaid
Exon 8	8F & 8R3	50	DMSO	Hybaid
Intron 2	2F & 3R	61	Betaine	MJ
Intron 3	3F & 4R	60	Long-range	MJ
Intron 4	4F & 5R	58	Long-range	MJ
Intron 5	5F & 6R	55	Betaine	MJ
Intron 6	6F & 7R	61	Betaine	MJ
Intron 7	7F2 & 8R2	62	Long-range	MJ

Table 2-6 PCR conditions for amplification of *Slc1a4.*

Primer	Sequence (5' → 3')
2F	Tgt gcc agg aca gtc tct gc
2Rnew	Gag atg cca agc ctg gcc ac
3F	Ctg taa caa gca gct cgc ac
2R	Ccc tgc tca cct ggg atg
3F1	Aca tca cca tca tcg atg cc
2R1	Cag agc act gga ttc atc ct
4F	Gga gag gcc tgg aag tga g
4R2	Ttc tcg ctg tag gcc ggc t
4F2	Cct aca cgc tgg gtg tga ag
4R4	Gga acc tgc att tcc cgg g
5F2	Agc agt act cct gga agc a
5R2	Tct agg gca ggc aga gct
6F	Gtc cca ggc ttt gtt ggt tt
6R2	Agt cct gct gct gtc cag cag
7F1	Gca gat tag cgc cgg cta c
7R	Ctg gat cag cca cag cct g
7F	Cct cca gtc agc act ccg g
7R1	Cca gct tct tgc cag agc g

Table 2-7 Primer sequences used to amplify *EEF1A2*

2.6.2.1 Long-range PCR

Introns 3,4 and 7 of *Slc1a4* were amplified using the Expand Long Template PCR System (Roche), according to the manufacturer's instructions. Briefly, two master mixes were made up. Mix one contained dNTPs, each at 350μM, forward and reverse primers at 300nM and 1μl DNA in a total reaction volume of 25μl per reaction. Mix two contained 1 x PCR buffer 1 and 0.75μl enzyme mix, also in a total volume of 25μl per reaction. The two were mixed immediately before cycling. Cycling was carried out on a Hybaid Omnigene. The cycling conditions were 92^0C for 1 minute, 10 cycles of 92^0C for 20 seconds, the annealing temperature for 1 minute, 68^0C for 8 minutes, 20 cycles of 92^0C for 20 seconds, annealing temperature for 1 minute, 68^0C for 8 minute (increasing by 20 seconds per cycle) and finally, 10 minutes at 68^0C. The annealing temperatures used were 60^0C for intron 3, 58^0C for intron 4 and 62^0C for intron 7.

2.6.3 SSCP

2.6.3.1 Ethanol precipitation of samples

Where the PCR additive betaine had been used, the PCR products were precipitated to remove it. Two volumes of ethanol and 0.1 volumes of 3M sodium acetate were added to each sample (usually 20µl) and the samples were kept at -20^0C for approximately 30 minutes. The precipitated DNA was pelleted by centrifugation at 14 000 rpm for 5 minutes, washed with 70% v/v ethanol and air dried. They were then resuspended in H_20 (usually 20µl) before SSCP analysis.

2.6.3.2 SSCP gels

PCR products (10µl) were mixed with 5µl loading buffer (95%v/v deionised formamide; 0.1%w/v bromophenol blue and 0.1%w/v xylene cyanol) and heated at 95^0C for 5 minutes to ensure they were single-stranded. They were then placed on ice, and maintained on ice during the loading of samples. All 15µl was then loaded onto a 10% polyacrylamide gel, containing 1 x TBE (0.1M tris; 0.1M boric acid; 2.5mM EDTA), 0.05% w/v AMPS and 0.06% v/v TEMED. Samples were run at 4^0C overnight at 10 mA per gel on a Hoefer PS 1500 power pack in 1 x TBE buffer.

Silver staining of gels

Gels were carefully removed from the apparatus, ensuring the minimum of handling to avoid inadvertent staining due to protein contamination. They were shaken in 500ml 10% v/v ethanol in a glass dish for 10 minutes, which was then removed by vacuum to avoid touching the gels. They were then soaked in 500ml 1% v/v nitric acid for 2 minutes, and then rinsed in deionised H_20. They were then shaken for 20 minutes in 500ml of a 500µg/l solution of silver nitrate. The silver nitrate was removed and excess silver was removed by adding approximately 200 ml developing solution (30g/l sodium carbonate and 0.05% v/v formaldehyde (Analar). This was removed as it changed colour. The gels were then shaken in 500ml developing solution, with one change of solution. Once the bands which appeared were of a sufficient intensity, the developing reaction was stopped by soaking the gels in 10%

v/v acetic acid for 10 minutes. The acetic acid was removed by soaking the gels twice in deionised water for 10 minutes. They were dried on a Bio-Rad 583 gel drier.

2.6.4 Sequencing

2.6.4.1 Manual Sequencing

Excess nucleotides and overhanging phosphate groups were removed by the addition of 10 units exonuclease I (USB) and 2 units shrimp alkaline phosphatase (USB) to 5µl PCR product. 1µl of this cleaned PCR product was added to a reaction mix containing 2.5pmoles primer, 4 units thermosequenase polymerase (USB) and 1 x reaction buffer in a total reaction volume of 10µl. This mix was divided between four tubes, each containing 1.25µl termination mix, comprising 0.25µl α^{33}P ddNTP and 1µl of each dNTP. Sequencing reactions were carried out on a Hybaid Omn-E, and comprised 50 cycles of 95^{0}C for 30 seconds, 55^{0}C for 30 seconds and 72^{0}C for one minute. They were then run on a 6% polyacrylamide gel at a constant temperature of 45^{0}C and 90Watts for 3-5 hours. Gels were dried on a Bio-Rad 583 gel drier. Autoradiography film was exposed to the gel from 16-48 hours and developed on a Hyper Processor (Amersham Life Science).

2.6.4.2 ABI Sequencing

PCR Clean up

Nucleotides and primers were removed by adding 1µl ExoSapIT (USB) to 5µl PCR product. They were then incubated at 37^{0}C for 15 minutes, followed by 80^{0}C for 15 minutes to inactivate the enzyme.

Sequencing Reactions

To the cleaned PCR products were added 2µl of either Rhodamine or Big Dye (ABgene) and 45ng primer in a total volume of 20µl. Cycling was carried out on an MJ Gradient Cycler, and comprised one cycle of 96^{0}C for 1 minute, followed by 24 cycles of 96^{0}C for 30 seconds, 50^{0}C for 15 seconds and 64^{0}C for 4 minutes.

Ethanol Precipitation

Samples were precipitated by adding 55µl 95% v/v ethanol, 2µl 3M sodium acetate (pH5.2) and 0.5µl pellet paint (Novachem). They were then kept at 4^0C for 30 minutes, centrifuged at 14 000 rpm for 30 minutes, washed in 70% v/v ethanol and air dried.

ABI Gels

Gels were run either by Angie Fawkes or Alison Condie an ABI 3100 capillary sequence analyser. The sequence traces obtained were analysed using the Chromas programme (Technelysium).

2.6.5 DHPLC

The PCR products were initially heteroduplexed. They were first heated to 95^0C for 5 minutes, the temperature was then decreased by 1.5^0C and held for one minute. This was then repeated 40 times. They were then subjected to high performance liquid chromatography on a WAVE® Nucleic Acid Fragment Analysis System (Transgenomic). The optimal denaturing temperature for use was determined by plotting the predicted helical fraction of the sample against the sequence at different temperatures, using the WAVE® System utility hardware. *EEF1A2* exon 2 products were run at 63^0C and 65^0C, and exon 5 products at 63^0C and 66^0C. The flow rate was 0.9 ml/min, and the buffer used was a combination of triethylammonium acetate (TEAA) and 25% acetonitrile (ACN) in TEAA, as outlined in tables 2-8 and 2-9.

Time, mins	% TEAA, 63^0C	% ACN in 25% TEAA, 63^0C	% TEAA, 65^0C	% ACN in 25% TEAA, 65^0C
0.0	49	51	51	49
0.1	44	56	46	54
4.6	35	65	37	63
4.7	0	100	0	100
5.2	0	100	0	100
5.3	49	51	51	49
7.3	49	51	51	49

Table 2-8 Buffer compositions used to analyse *EEF1A2* exon 2

Time, mins	% TEAA, 63°C	% ACN in 25% TEAA, 63°C	% TEAA, 66°C	% ACN in 25% TEAA, 66°C
0.0	51	49	53	47
0.1	46	54	48	52
4.6	37	63	39	41
4.7	0	100	0	100
5.2	0	100	0	100
5.3	51	49	53	47
7.3	51	49	53	47

Table 2-9. Buffer compositions used to analyse *EEF1A2* exon 5

2.7 Antibody Generation and Purification

2.7.1 Antibody Generation

Peptides were synthesised by Dr Graham Bloomberg at Bristol University (ordered through Zinsser Analytic), and conjugated to KLH. Four aliquots of 0.5mg were injected into a sheep by Diagnostics Scotland at monthly intervals. Serum was withdrawn one week after the second, third and fourth injections. The serum was stored at -70°C on receipt.

2.7.2 ELISA

Maxisorp plates (Nunc) were coated overnight at 4°C with different concentrations of peptide, from 5µg/ml to 1ng/ml, dissolved in 200µl coating buffer (15mM Na_2CO_3; 35mM $NaHCO_3$; 3.0mM NaN_3; pH 9.6). Blank wells in which coating buffer alone was added were included. The plates were then washed three times in wash buffer (0.14M NaCl; 1.5mM KH_2PO_4; 8.0mM Na_2HPO_4; 2.68M KCl; 0.05% v/v Tween 20; pH 7.4) and blocked in 1% w/v BSA (diluted in wash buffer) for 1 hour at room temperature. They were again washed three times in wash buffer, and then incubated for 1 hour at room temperature with 200µl of the appropriate serum diluted in wash buffer from 1 in 100 to 1 in 50 000. They were then incubated with HRP-conjugated anti-sheep/goat secondary antibody, diluted 1 in 1 000 in wash buffer, for 1 hour at room temperature. They were then washed three times and incubated for

approximately 15 minutes in 200µl o-phenylenediamine dihydrochloride substrate (OPD). This was prepared by adding 10mg OPD (Sigma) to 25ml OPD buffer (25mM citric acid; 0.1M Na_2HPO_4; pH 5.0) and adding 10µl 30% v/v H_20_2. The plates were then read at 450nm in an EL312e Microplate Bio-Kinetics plate reader (Bio-Techniques Instruments).

2.7.3 Antibody Purification

2.7.3.1 Ammonium sulphate precipitation

One volume (usually approximately 50ml) serum was centrifuged at 3 000xg for 30 minutes to remove any particulate matter. The supernatant was transferred to a beaker, and large protein aggregates along with proteins which precipitate at low concentrations of ammonium sulphate were removed. This was done by gradually adding 0.5 volumes saturated ammonium sulphate (made by adding 76.1g ammonium sulphate to 100ml H_20), whilst continuously stirring the mixture. It was then transferred to 4^0C, and stirred either for 6 hours or overnight. The mixture was then centrifuged at 3 000xg for 30 minutes, and the supernatant was removed.

The antibody component of the sera was then precipitated by the addition of another 0.5 volumes ammonium sulphate to the supernatant, bringing the final concentration of ammonium sulphate to 50% saturation, again whilst stirring continuously. It was then stirred overnight at 4^0C. The suspension was centrifuged at 3 000xg for 30 minutes, and the supernatant was discarded. The pellet was drained, and resuspended in 0.3 volumes (usually 15 ml) PBS. It was then dialysed against PBS at 4^0C for 24 hours, with three changes of PBS. The resulting antibody solution was further purified using immunoaffinity purification.

2.7.3.2 Immunoaffinity purification

The ammonium sulphate-precipitated antibody solution was immunoaffinity purified using a SulfoLink® Kit. A different kit was used for each antibody raised, with each peptide coupled to a different column.

Coupling of peptide to the column

The peptide against which the antibody was raised was coupled to the column through the terminal cysteine according to the manufacturer's instructions. Briefly, the column was drained and equilibrated with 12 ml SulfoLink® Coupling Buffer. Approximately 10mg peptide was dissolved in 2ml SulfoLink® Coupling Buffer and added to the column, and then incubated for approximately 1 hour at room temperature. The column was then drained and washed with 6ml Coupling Buffer. An approximation of the coupling efficiency was obtained by comparing the A_{280} of this wash buffer with the A_{280} of the starting peptide solution in coupling buffer. The A_{280} of the peptide solution was much higher than that of the wash solution, indicating that most of the peptide had been immobilised on the gel and had not been washed through the column. Nonspecific binding sites on the gel were blocked by adding 2ml of an 0.05M L-cysteine solution (provided in the kit) and incubated again for approximately 1 hour. The column was drained and washed four times with 4ml SulfoLink® Wash Buffer and then three times with 0.05% w/v sodium azide (NaN_3). The column was then either used immediately for affinity purification, or was stored in 0.05% w/v NaN_3 at 4^0C.

Affinity purification

The column was equilibrated with 6ml PBS. The antibody was then bound to the peptide which had been immobilised on the column. This was achieved by passing the ammonium sulphate-precipitated antibody solution (10-20ml) through the column. It was collected and recycled through the column approximately 5 times to maximise the amount of antibody bound. The column was then washed with 16ml PBS. The bound antibody was eluted by adding 8ml glycine buffer (100mM glycine, pH 2.5-3.0) to the column. Fractions (1ml) were collected and analysed for protein content by measuring the A_{280}. The fractions with the highest A_{280} (usually fractions 2, 3 and 4) were pooled and dialysed against PBS for 24 hours, with three changes of PBS. The column was regenerated by washing with 16ml PBS, and stored in degassed 0.05% w/v NaN_3.

2.8 Western Blotting

2.8.1 Protein extraction

Tissues were immediately frozen in liquid nitrogen after dissection and stored at -70^0C, if necessary, before extraction. Approximately 50mg tissue was ground to a powder using a pestle and mortar in liquid nitrogen. 0.5 ml protein extraction buffer was added (10 mM Tris.HCl pH 7.5, 2 ml 10 mM EDTA, 1 x Complete Antiprotease Cocktail, Roche). Samples were boiled for 5 minutes and centrifuged at 14 000 rpm for 5 minutes. Supernatants were quantified and loaded on an acrylamide gel.

2.8.2 Protein Gel

Protein concentrations were determined using the BioRad DC Protein Assay detection kit, based on the Bradford Assay, as per the manufacturer's instructions. Briefly, 5µl sample was mixed with 25µl Reagent A, 200µl Reagent B and then incubated for 15 minutes. The absorbance at 750 nm was read using an EL312e Microplate Bio-Kinetics Reader (Bio-Techniques Instruments). A standard curve was constructed by plotting absorbance values obtained from a range of bovine serum albumin (BSA) dilutions from 0-1.4 mg/ml, and was used to determine the concentration of samples.

A 15µg aliquot of protein lysate was mixed with Laemmli protein loading buffer (60 mM Tris.HCl pH 6.8; 2% w/v SDS; 0.1% w/v bromophenol blue; 10% v/v glycerol) and 1M dithiothreitol (DTT) and loaded onto a 10% SDS-polyacrylamide gel with 4.2% stacking gel. The Kaleidoscope or Broad Range Prestained ladders (BioRad) were used as markers. Gels were run using a Bio-Rad Protean III at 100-150 V for approximately 1-2 hours in Laemli running buffer (25mM Tris.EDTA; 192mM glycine; 0.1% w/v SDS; pH8.3). Proteins were electroeluted onto a polyvinylidene difluoride (PVDF) Hybond-P membrane (Amersham Pharmacia Biotech) in Bjerrum and Schafer-Neilsen transfer buffer (48mM Tris.EDTA; 39mM glycine, 20% v/v methanol, pH 9.2), using a BioRad Trans-Blot SD transfer cell at 15V for one hour.

2.8.3 Immunoblotting

Membranes were blocked overnight in blocking buffer containing 0.25% v/v Tween 20 and 5% w/v fat free powdered milk in PBS. Membranes were washed four times in PBS and then incubated in primary antibody at an appropriate dilution in blocking buffer for 2 hours. As the dilutions varied for different antibodies under different experimental conditions, they are given in the figure legends for each Western in chapters 5 and 6. They were again washed four times in PBS, before incubation with the secondary antibody (HRP-anti goat/sheep antibody for the sheep anti-eEF1A-1 and eEF1A-2 antibodies; HRP anti-rabbit for the rabbit anti-*A. salina* eEF1A-1 antibody; both at 1:500; Diagnostics Scotland). Membranes were again washed in PBS and detected using either diaminobenzidene (DAB; Sigma) or enhanced chemiluminesence (ECL; Amersham Biosciences) according to the manufacturer's instructions. When ECL detection was used, MACO-X-RAY HS90 medical film (Scientific Laboratory Supplies, SLS) was exposed and developed using a Hyper Processor (Amersham Life Science).

2.9 Immunofluoresence in cells

2.9.1 Cell Culture

PC-12 cells were a kind gift from Helen Munn. Cells were grown in 85% RPMI medium, 10% horse serum and 5% fetal calf serum, supplemented with penicillin at 100U/ml and streptomycin at 100μg/ml. Cells were differentiated by adding 50ng/ml human recombinant Nerve Growth Factor-β (Sigma) to the media, and maintained in this form by feeding them with the NGF-supplemented media every two days. SH-SY5Y cells were another gift, from Rachel James. They were grown in 44% DMEM, 44% Ham's F12 and 10% fetal calf serum, and supplemented with 1% non-essential amino acids, penicillin at 100U/ml and streptomycin at 100μg/ml. They were fed every two days and split 1:10 when they reached confluency.

2.9.2 Immunofluorescence

Cells were washed twice in PBS, then fixed in either 50:50 acetone:methanol, ice-cold methanol or paraformaldehyde for 5 minutes. If paraformaldehyde was used, they were then washed in 0.2% v/v Triton-X100. They were then washed twice in PBS, blocked for 30 minutes in 5% v/v donkey serum diluted in PBS, and washed in PBS containing 0.2% v/v Tween-20 (PBS-T). They were then incubated in the primary antibody, diluted in 1% v/v donkey serum and 0.2% v/v Tween-20 in PBS, for 45 minutes. They were washed three times in PBS-T and incubated for 30 minutes in fluorescently labelled donkey anti-sheep secondary antibody (Alexofluor), diluted 1:1 000 in 1% v/v donkey serum in PBS-T. They were again washed three times in PBS-T, then incubated in DAPI for 5 minutes, washed three times in PBS and mounted in mowiol mount (7.5% w/v mowiol 40-88; 10% v/v glycerol; 1.75% DABCO; 0.1M Tris.HCl, pH 8.5).

Peptide preabsorption

Different concentrations of the peptide against which each antibody was raised were added to a 1:10 solution of that antibody in blocking buffer. The concentrations used were 0.01, 0.1 and 1.0 ng peptide per µl antibody solution. These antibody and peptide solutions were then mixed overnight on a Labinco LD 79 revolving wheel.

3 Chapter 3 – Pathological analysis of wasted

3.1 Introduction

The wasted mutation arose spontaneously at the Jackson laboratory in 1972 (Shultz *et al.*, 1982). Homozygous wasted mice show hypoplasia of the spleen and thymus, and a decrease in the wet weight of these organs, relative to their declining body weight (Goldowitz *et al.*, 1985; Kaiserlian *et al.*, 1986; Shultz *et al.*, 1982). They also have a defective response to radiation damage in their lymphoid-derived cells (Shultz *et al.*, 1982). On the basis of their immunological defects, wasted mice were initially considered to be models for ataxia telangiectasia (Shultz *et al.*, 1982) and severe combined immunodeficiency with adenosine deaminase deficiency (Abbott *et al.*, 1986). However, the vacuolar degeneration of the anterior horn cell motor neurons of the spinal cord has led to the mice more recently being considered as a model for ALS (Lutsep and Rodriguez, 1989).

I have therefore further analysed homozygous wasted mice in order to determine whether they are indeed a suitable model for the disease. I have analysed their weight loss in detail, and undertaken further neuropathological observations. I focused on the neurological, rather than the immunological aspects of the phenotype as these are more relevant to the study of motor neuron dysfunction in humans.

3.2 Results

3.2.1 Analysis of weight loss in wasted

3.2.1.1 Total body weights

To characterise the weight loss seen in wasted mice, I weighed several litters of wasted and littermate controls, both heterozygous and homozygous wild-type, during their development from approximately one week old to the age of death of the wasted mice. The actual number of mice varied from 4 to 20 on each day, with the exception of 27 day-old wasted homozygotes and 20 day-old controls, where only one animal was weighed, and 20 and 26 day-old wasted homozygotes, where two animals were weighed. I then constructed a growth curve for wasted and littermate animals, shown in figure 3-1. The actual weights of the animals at each age is shown in appendix 2. To determine whether the weight loss seen in wasted was due to the loss of muscle mass, the ratio of muscle weight to total body weight was calculated. This was also done for the spleen, in which there is a known loss of mass, and for the brain and heart, to determine whether there is any weight loss in these eEF1A-2 expressing organs. As a control organ, the relative weight of the kidney was also measured, as it does not express eEF1A-2, and therefore was not expected to decrease in wasted mice, and because it is easy to excise whole.

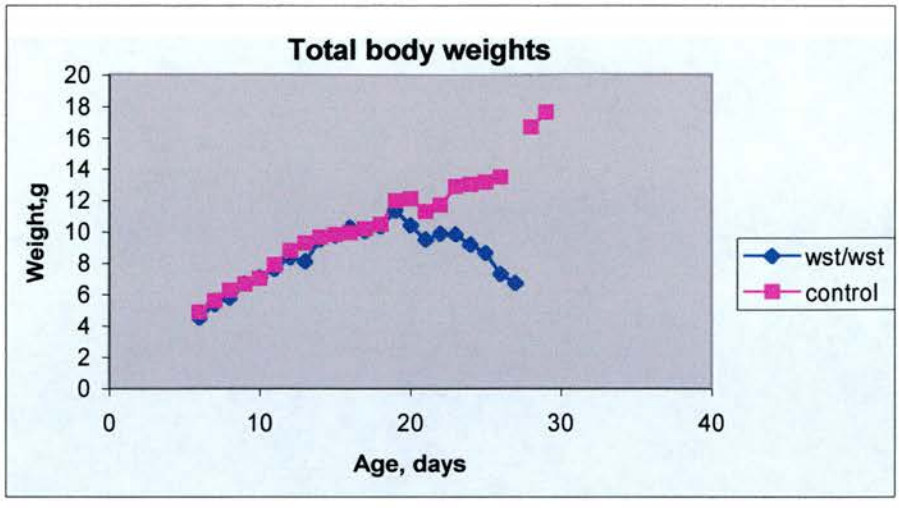

Figure 3-1 Graph showing total body weights of wasted and control (comprising heterozygous and wild type) mice

Age, days	*wst/wst* Weight, g	*wst/wst* Min, g	*wst/wst* Max, g	SD	Control Weight, g	Control Min,g	Control Max, g	SD
6	4.50	2.5	5.6	1.76	4.84	4.1	5.8	0.80
7	5.38	3.0	6.4	1.02	5.58	4.8	6.6	0.54
8	5.76	3.7	6.6	1.18	6.26	5.5	7.3	0.62
9	6.67	4.8	8.0	0.93	6.67	5.5	8.4	0.85
10	7.08	5.2	8.6	1.03	7.06	6.2	9.0	0.69
11	7.62	5.6	9.2	1.22	7.81	6.6	9.8	0.92
12	8.37	6.4	9.2	0.94	8.79	8.0	9.7	0.61
13	8.10	6.7	8.9	1.21	9.28	8.6	9.9	0.50
14	9.51	7.5	11.0	1.21	9.64	8.4	11.7	1.03
15	9.75	7.6	11.3	1.20	9.82	8.2	12.1	1.14
16	10.26	8.4	11.6	1.08	9.94	8.7	11.9	1.19
17	10.03	7.9	11.5	1.34	10.20	8.7	12.6	1.53
18	10.32	8.3	11.6	1.14	10.48	8.7	13.1	1.54
19	11.35	11.1	11.8	0.31	11.96	9.6	12.7	1.32
20	10.40	10.0	10.8	0.57	12.10	12.1	12.1	ND
21	9.49	7.7	11.0	1.04	11.26	10.4	14.1	1.14
22	9.88	7.4	11.3	1.40	11.65	10.0	13.9	1.21
23	9.82	7.3	11.0	1.13	12.89	11.6	14.8	1.17
24	9.17	7.0	10.3	1.06	12.98	11.2	15.1	1.11
25	8.75	7.8	9.7	0.67	13.17	11.2	16.0	1.22
26	7.30	7.1	7.5	0.28	13.47	12.9	13.9	0.45
27	6.70	6.7	6.7	ND	ND	ND	ND	ND
28	ND	ND	ND	ND	16.68	15.3	18.0	1.28
29	ND	ND	ND	ND	17.61	15.4	19.9	1.41

Table 3-1 Mean body weights of mice at different ages.
Maximum and minimum values, and standard deviations (SD), are also shown. No mice were weighed at the time points marked ND.

Figure 3-1 demonstrates that the weights of wasted and littermate controls are strikingly similar until 19 days, whereupon there is a sharp difference between the two. It is interesting to note that wild type mice also show a slight drop in average bodyweight at 20 days. It is probable that this is as a result of weaning, as the animals recover this weight within two days. The size difference between a wasted and a heterozygous animal can clearly be seen in figure 3-2, which shows two 24 day-old mice from the same litter, and also demonstrates a typically hunched posture.

Figure 3-2 wst/wst (left) and +/wst (right) mice, both from the same litter and 24 days old. The smaller size and hunched posture of the wasted homozygous mouse can clearly be seen.

3.2.1.2 Weights of different organs

Total organ weights

The spleen, brain, heart, kidney and a quadricep muscle were dissected from three wasted mice and three heterozygous littermates at 15, 19, 22 and 25 days of age. At 27 days, only one animal of each genotype was analysed, as homozygous wasted mice often died or were euthanised for welfare reasons before this point. The organs were then weighed, and the results are shown in figures 3-3 to 3-5 and table 3-2.

Relative organ weights

To calculate the muscle weight relative to the weight of the animal, the excised quadricep muscle was divided by the total bodyweight of the animal. This approach was also used to analyse the spleen, brain, heart and kidney. The results are shown in figures 3-6 to 3-10 and tables 3-3 to 3-7.

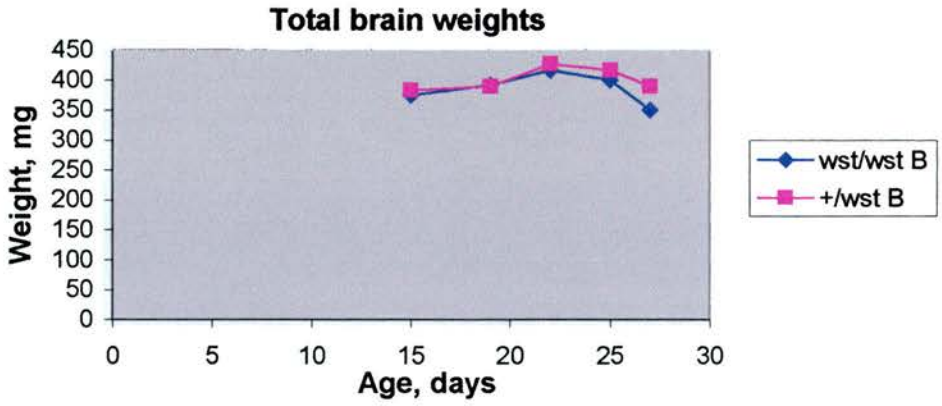

Figure 3-3 Graph showing mean total brain weights of homozygous wasted and heterozygous mice

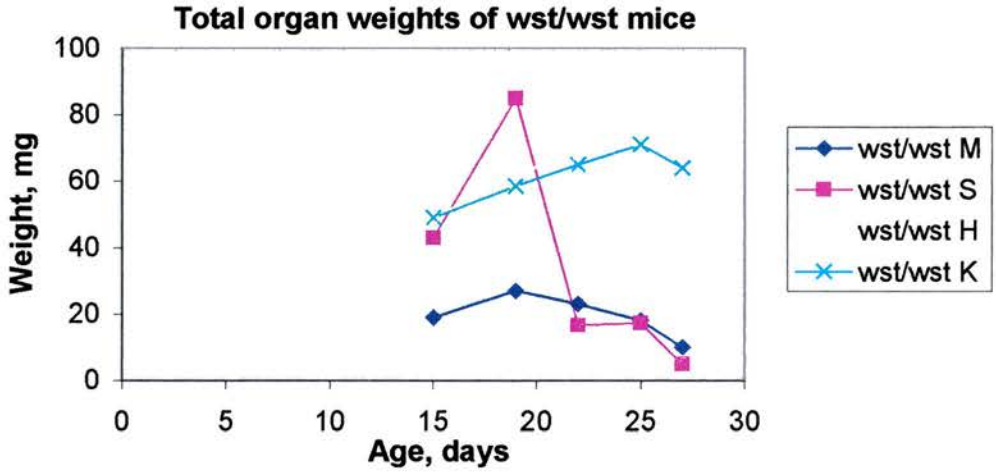

Figure 3-4 Graph showing mean total organ weights of homozygous wasted mice. M, muscle; S, spleen; H, heart; K, kidney.

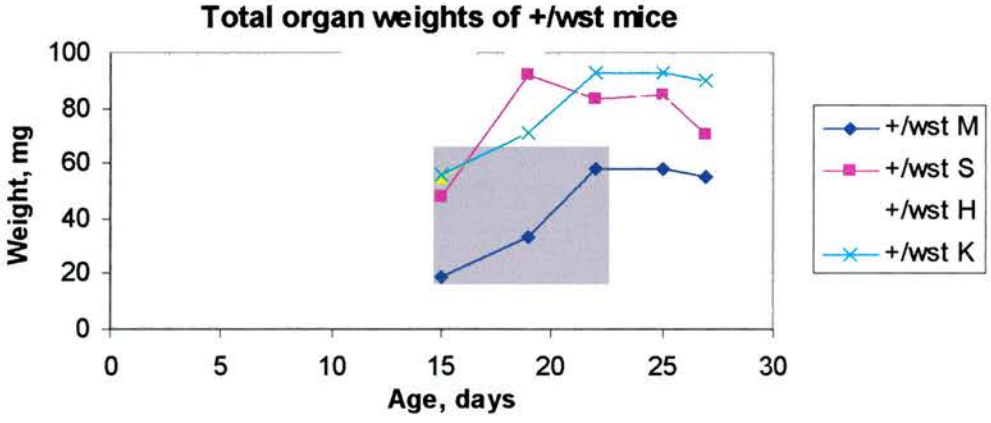

Figure 3-5 Graph showing mean total organ weights of heterozygous mice. M, muscle; S, spleen; H, heart; K, kidney.

Organ	Age, days	*wst/wst* Mean, mg	*wst/wst* Min, mg	*wst/wst* Max, mg	*+/wst* Mean, mg	*+/wst* Min, mg	*+/wst* Max, mg
Muscle	15	19	17	20	19	16	23
	19	27	22	32	33	29	40
	22	23	15	30	58	55	60
	25	17	16	20	58	50	70
	27	10	10	10	55	55	55
Spleen	15	43	38	47	48	46	50
	19	85	81	89	92	82	98
	22	17	10	30	83	60	100
	25	17	15	20	85	80	94
	27	5	5	5	70	70	70
Brain	15	375	354	414	383	361	402
	19	392	390	393	390	384	398
	22	417	400	440	427	410	450
	25	400	390	410	417	380	450
	27	350	350	350	390	390	390
Heart	15	50	44	55	55	50	62
	19	59	58	59	72	60	90
	22	77	70	90	90	80	110
	25	73	48	100	81	60	95
	27	70	70	70	90	90	90
Kidney	15	49	38	56	56	53	60
	19	59	57	61	71	70	71
	22	65	60	75	93	90	100
	25	71	60	90	93	90	95
	27	62	62	62	90	90	90

Table 3-2 Mean, maximum and minimum total organ weights

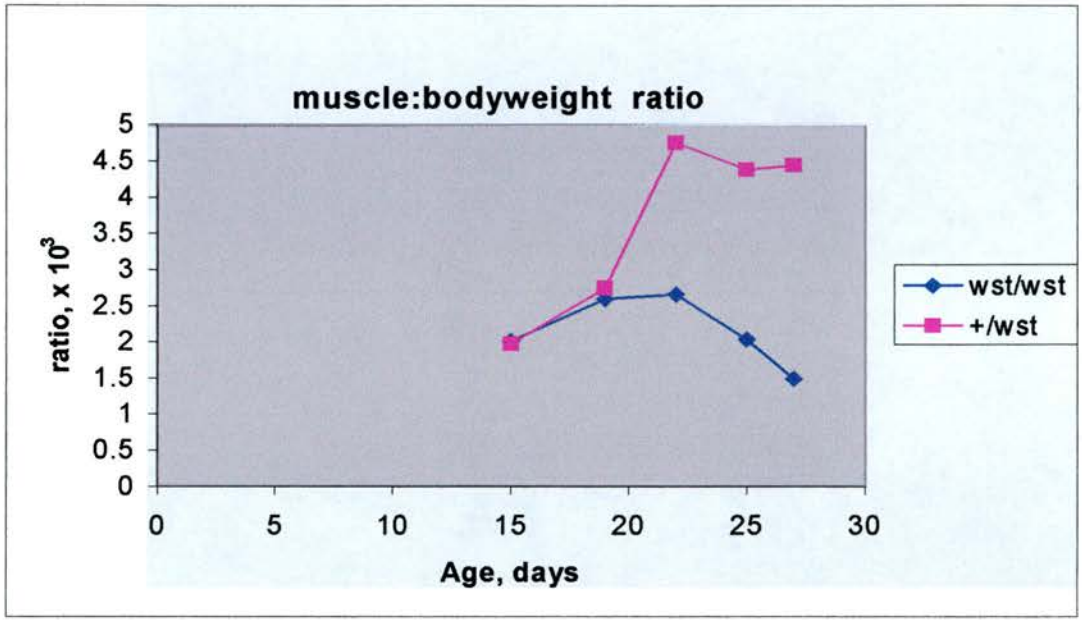

Figure 3-6 Graph showing relative muscle weights of homozygous wasted and heterozygous mice.

Age, days	*wst/wst* Mean ratio, x 10^3	Min	Max	*+/wst* Mean ratio, x 10^3	Min	Max
15	2.01	1.96	2.07	1.97	1.51	2.53
19	2.59	2.16	3.02	2.74	2.21	3.39
22	2.66	1.88	3.75	4.75	3.95	5.55
25	2.03	1.76	2.28	4.38	3.73	5.54
27	1.49	1.49	1.49	4.44	4.44	4.44

Table 3-3 Mean, minimum and maximum muscle:bodyweight ratios for homozygous wasted and heterozygous mice.

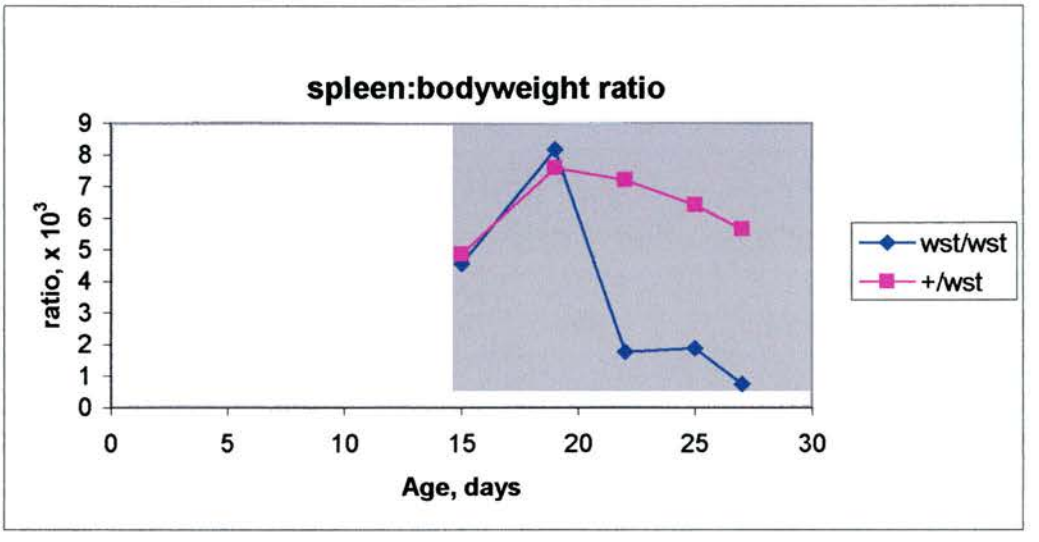

Figure 3-7 Graph showing relative spleen weights of homozygous wasted and heterozygous mice.

Age, days	*wst/wst* Mean ratio, x 10^3	Min	Max	*+/wst* Mean ratio, x 10^3	Min	Max
15	4.56	4.41	4.95	4.87	4.60	5.00
19	8.17	7.94	8.40	7.59	6.95	8.33
22	1.77	1.25	2.80	7.20	5.94	9.00
25	1.88	1.71	2.06	6.41	5.88	7.38
27	0.75	0.75	0.75	5.65	5.65	5.65

Table 3-4 Mean, minimum and maximum spleen:bodyweight ratios for homozygous wasted and heterozygous mice.

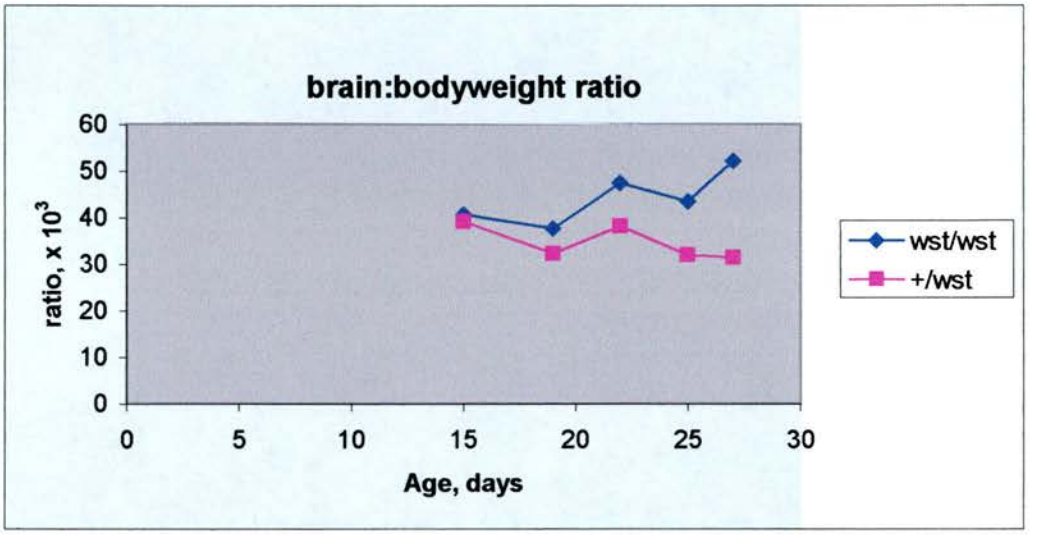

Figure 3-8 Graph showing relative brain weights of homozygous wasted and heterozygous mice.

Age, days	*wst/wst* Mean ratio, x 10^3	Min	Max	*+/wst* Mean ratio, x 10^3	Min	Max
15	40.7	34.7	43.7	39.2	36.5	48.5
19	37.7	36.8	38.5	32.3	30.4	34.0
22	47.5	41.1	51.3	38.2	30.0	43.6
25	43.5	40.0	46.8	32.0	26.9	41.5
27	52.2	52.2	52.2	31.5	31.5	31.5

Table 3-5 Mean, minimum and maximum brain:bodyweight ratios for homozygous wasted and heterozygous mice.

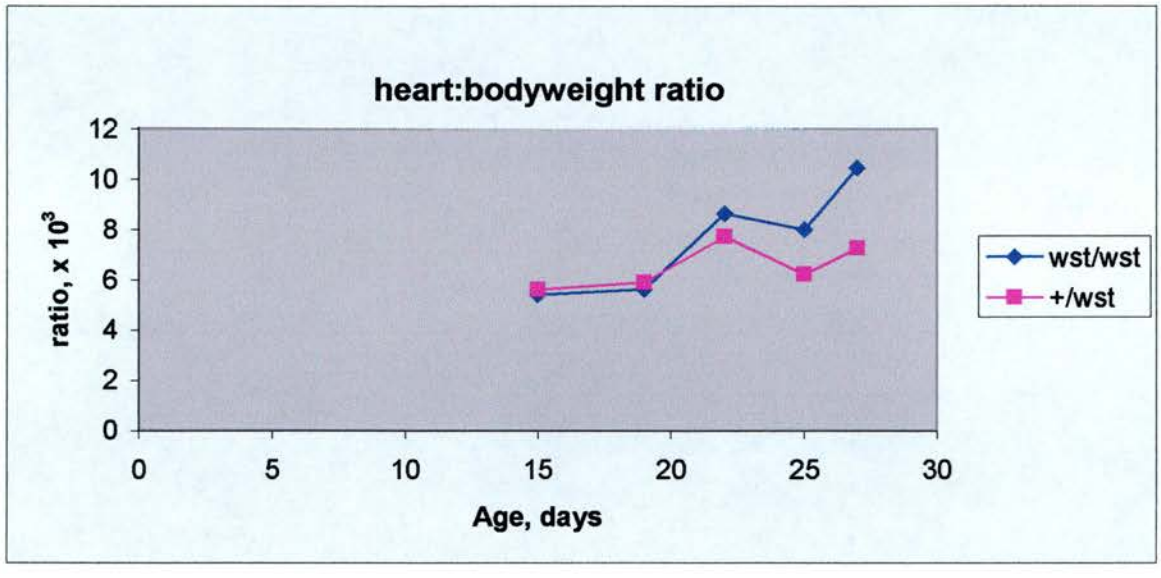

Figure 3-9 Graph of relative heart weights of homozygous wasted and heterozygous mice.

Age, days	*wst/wst* Mean ratio, x 10^3	Min	Max	*+/wst* Mean ratio, x 10^3	Min	Max
15	5.41	5.36	5.47	5.61	4.72	6.39
19	5.63	5.57	5.69	5.91	5.08	6.87
22	8.63	8.40	8.75	7.72	7.24	8.00
25	8.00	5.27	11.40	6.22	4.60	8.76
27	10.45	10.45	10.45	7.26	7.26	7.26

Table 3-6 Mean, minimum and maximum heart:bodyweight ratios for homozygous wasted and heterozygous mice.

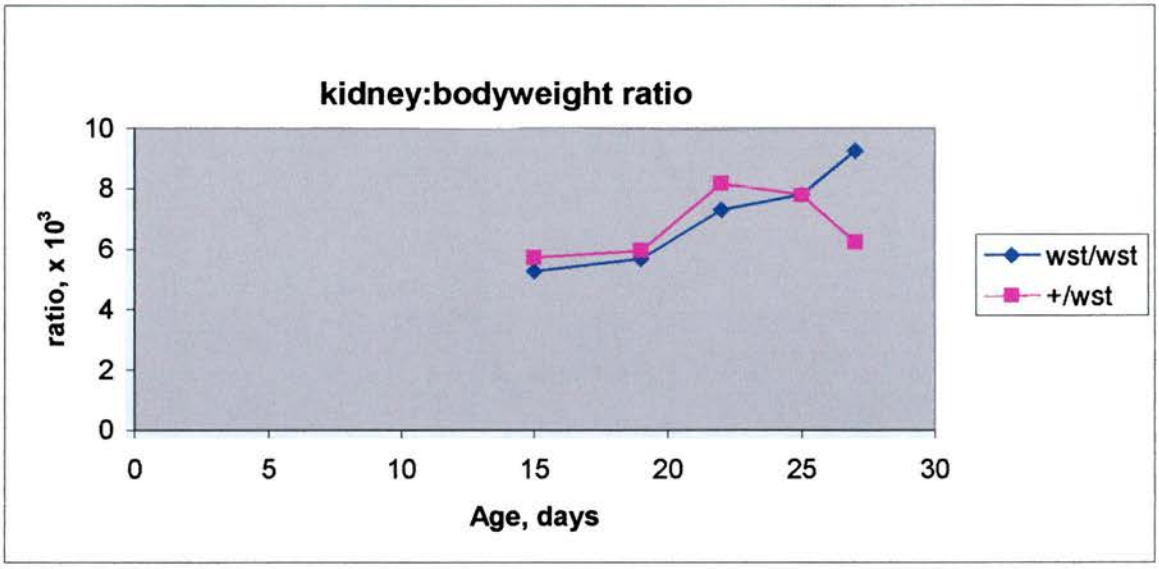

Figure 3-10 Graph showing relative kidney weights of homozygous wasted and heterozygous mice.

Age, days	*wst/wst* Mean ratio, x 10^3	Min	Max	*+/wst* Mean ratio, x 10^3	Min	Max
15	5.27	4.63	5.89	5.72	5.66	5.82
19	5.68	5.38	5.98	5.95	5.46	6.23
22	7.30	7.00	7.50	8.17	6.60	9.00
25	7.80	6.19	10.30	7.79	5.81	9.28
27	9.25	9.25	9.25	6.22	6.22	6.22

Table 3-7 Mean, minimum and maximum kidney:bodyweight ratios for homozygous wasted and heterozygous mice.

It can be seen from the graphs that the greatest drop in the organ:bodyweight ratio of wasted mice is seen in the spleen. There is a precipitous drop in the ratio from 19 days. There is also a drop in the ratio in muscle. Although this drop is relatively slight, in comparison, there is a rise in the ratio of muscle:bodyweight in heterozygous animals at this time, so that there is a large difference between the two sets of mice. By 27 days, for example, the ratio of muscle:bodyweight in homozygous wasted mice is one-third that of heterozygous controls. The rise in the muscle:bodyweight ratio for heterozygous animals probably reflects the drop in the total body weight of the animals at this time, as the increase in the total muscle weight, as shown in figure 3-5, is more modest. The fact that there is such a marked difference in the muscle weight:bodyweight ratio between wasted and heterozygous mice suggests that the dramatic weight loss seen in wasted is due to a loss of muscle mass.

As eEF1A-2 is also expressed in the brain and heart, it was interesting to determine whether these organs also show a loss of weight in wasted homozygotes. In contrast to the situation in muscle, the brain and heart do not show a decrease in the ratio of organ weight:total bodyweight. Indeed, the ratios actually increase after 19 days, which probably again reflects the fact that the mice are losing weight. The brain and heart are probably too essential to sustain life in a reduced size. The kidney was selected as a control organ which was not expected to vary greatly in size, and was easily removed intact. It, too, showed an increase in the organ:bodyweight ratio compared to heterozygous controls, but this was not as marked as in heart and brain.

3.2.2 Neuropathology

Sections were made from the paraffin-embedded spinal cords of wasted mice and heterozygous littermates. The spinal cords were originally dissected and embedded in collaboration with Dr. J. Peters at the MRC Mammalian Genetics Unit, Harwell. They were taken at the following ages: 19 days (4 *wst/wst* mice; 1 *+/wst* mice), 24 days (1 *wst/wst*; 1 *+/wst*), 28 days (3 *wst/wst*; 1 *+/wst*) and 29 days (1 *wst/wst*; 1 *+/wst*).

3.2.2.1 H&E Staining

H&E analysis showed vacuolisation of the anterior horn cells of the spinal cord and brain. An example is shown in figure 3-11. In all 28 day mice examined, vacuolation of the anterior horn cells of the cervical spinal cord were seen, similar to that described by Lutsep and Rodruigez (Lutsep and Rodriguez, 1989). Although this was not quantified, the neuronal loss would appear to be in line with the 4% reported (Lutsep and Rodriguez, 1989). The 29 day-old mouse was similarly affected. One 28 day-old mouse also appeared to have vacuolation of the thoracic spinal cord neurons. No vacuolation was seen in the lumbar regions, or in sections from 19 or 24 day-old mice. It is probable that only late-stage vacuolation is seen at 28 days, and that the neurons are in fact starting to undergo vacuolation prior to this.

Control cervical spinal cord:

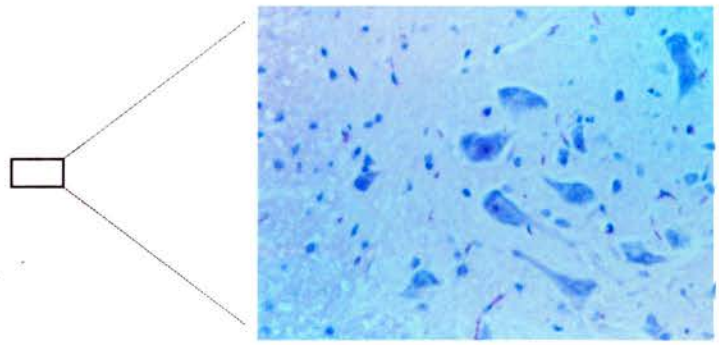

Whole spinal cord, X 25 Anterior horn region, X 100

Wasted spinal cord:

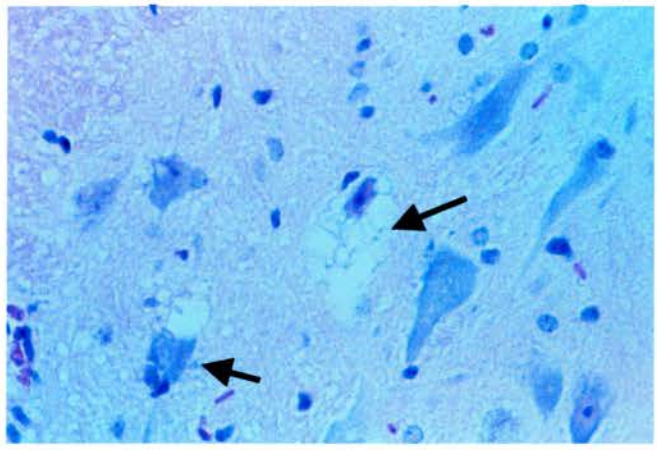

28 day wasted anterior horn, ×100

Figure 3-11 Sections through cervical spinal cord, after staining with haematoxylin and eosin. The top pictures are of a control animal, a heterozygous littermate of the wasted animal sectioned in the bottom picture. The vacuolated neurons are arrowed.

3.2.2.2 Glial fibrillary acidic protein

Reactive gliosis is a general response to neurological injury and disease, in which microglia are activated and astrocytes accumulate and upregulate the expression of glial fibrillary acidic protein, GFAP (Siegel *et al.*, 1999). GFAP has therefore been used as a marker for gliosis, and increased immunostaining for this protein has been reported in the brain and spinal cord of ALS patients (Fujita *et al.*, 1998; Nagy *et al.*, 1994). I therefore stained sections from homozygous wasted mice and their heterozygous littermates with an antibody against GFAP. Homozygous wasted mice showed a characteristic staining pattern, comprising strong foci of staining throughout the grey matter of the spinal cord. An example is shown in figure 3-12. These were only very rarely seen in heterozygous littermates. This increased GFAP staining in wasted homozygotes was then quantified by counting the number of GFAP-positive foci in the grey matter of the spinal cord. The results are shown in table 3-8.

Age	Region	*wst/wst*	*+/wst*
19 days	Cervical	48.0	2.0
	Thoracic	27.0	2.5
	Lumbar	7.0	3.5
24 days	Cervical	43.0	6.5
	Thoracic	37.0	1.5
	Lumbar	22.0	0.0
28 days	Cervical	37.0	0.0
	Thoracic	31.0	0.0
	Lumbar	4.0	0.0
29 days	Cervical	148.0	0.0
	Thoracic	52.0	2.5
	Lumbar	16.0	0.0

Table 3-8 Mean number of GFAP-positive cells in the grey matter of the spinal cord.

There was an increase in the number of GFAP-positive foci in all wasted animals examined. Interestingly, the number of foci appears to be higher at the cervical level of the spinal cord than at the thoracic level, which in turn appears to be higher than at the lumbar level. There therefore appears to be a gradient in gliosis from the cervical through to the lumbar region. This would correspond with the results from the H&E staining, in which there also appeared to be a gradient in vacuolation from the cervical through to the lumbar region.

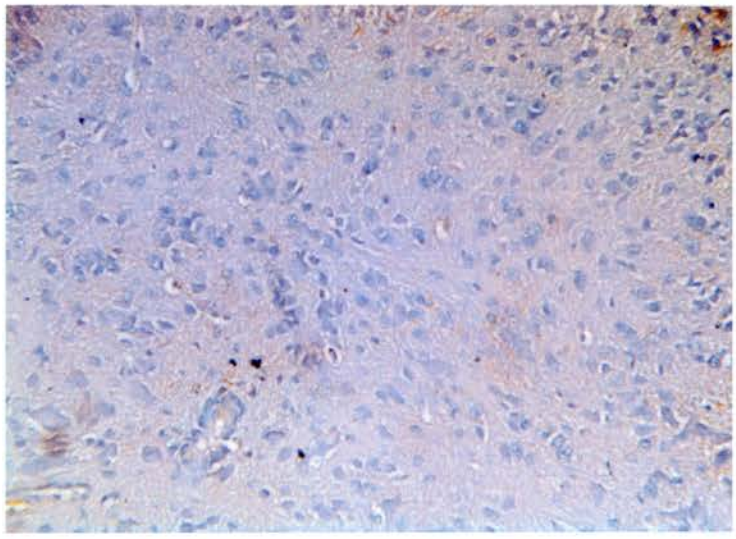

+/*wst* cervical spinal cord, x 16

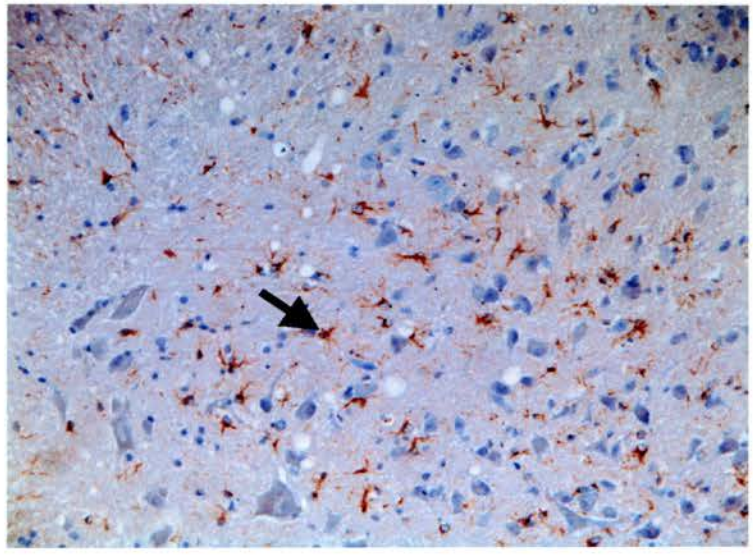

wst/wst cervical spinal cord, x 16

Figure 3-12 Sections stained with an antibody recognising glial fibrillary acidic protein, GFAP. Both sections are from the cervical spinal cord of 28 day-old mice. A central portion of the grey matter is shown. The section from the homozygous wasted mouse, bottom, shows characteristic staining throughout the grey matter of the spinal cord. An example is arrowed. This staining is absent in the section from the heterozygous animal.

3.2.2.3 Neurofilaments

Phosphorylated Neurofilaments

Using an antibody which recognised the light and heavy chain neurofilament proteins in their phosphorylated form, it was noted that there was increased staining in the cytoplasm of the neurons of wasted homozygotes, compared with heterozygous controls. An example is shown in figure 3-13. This increase in neurofilament staining was quantified by calculating the percentage of anterior horn neurons which stained with the antibody. The results are presented in table 3-9, below.

Age	Region	*wst/wst* (%)	*+/wst* (%)
19 days	Cervical	64	0
	Thoracic	80	13
	Lumbar	94	20
24 days	Cervical	ND	0
	Thoracic	75	25
	Lumbar	100	ND
28 days	Cervical	89	0
	Thoracic	75	0
	Lumbar	92	14
29 days	Cervical	ND	0
	Thoracic	77	0
	Lumbar	75	17

Table 3-9 Percentage of anterior horn motor neurons staining for phosphorylated neurofilaments. Where ND is given, the section did not have the correct orientation for a comparison to be made with the other sections.

There is a clear difference between the wasted homozygotes and their heterozygous littermates in the percentage of neurons staining positively for phosphorylated neurofilaments. However, there is no obvious correlation between the percentage of neurons staining positive for phosphorylated neurofilaments and either the age of the mice or the level of the spinal cord from which the sections were taken. This is in contrast to the GFAP results, in which there appeared to be a gradient from the cervical through to the lumbar regions of the spinal cord. However, although there

was no apparent variation in the percentage of neurons which stained for neurofilaments, this approach would not have quantified any differences in the intensity of antibody-staining between different sections.

It is interesting to note that, as with the GFAP results, there are changes in the homozygous wasted mice from 19 days of age onwards, that is, before the mice are demonstrating an overt neurological phenotype. This investigation extends previous work, which only investigated mice at 28 days of age (Lutsep and Rodriguez, 1989). Although I used an antibody which recognised both the light and heavy chain phosphorylated neurofilaments, the work of Lutsep and Rodriguez (1989) would also suggest that it was the 200kD heavy chain which was responsible for the increased staining. This is also consistent with the NFH overexpression seen in ALS patients (Munoz *et al.*, 1988; Sobue *et al.*, 1990). It is also the heavy chain subunit in which neurofilament mutations have been reported in a small proportion of ALS cases (Al-Chalabi *et al.*, 1999; Figlewicz *et al.*, 1994; Tomkins *et al.*, 1998).

Non-phosphorylated Neurofilaments

No differences were seen between wasted homozygous and heterozygous littermate control animals, using an antibody which recognised medium and heavy chain non-phosphorylated neurofilaments. Examples are shown in figure 3-14. The fact that cytoplasmic accumulation of phosphorylated neurofilaments, rather then the non-phosphorylated form, is seen in homozygous wasted mice is consistent with the fact that neurofilaments are more stable in their phosphorylated form. This is in contrast to other intermediate filament proteins, such as vimentin and laminin, which depolymerise on phosphorylation (Cooper, 2000).

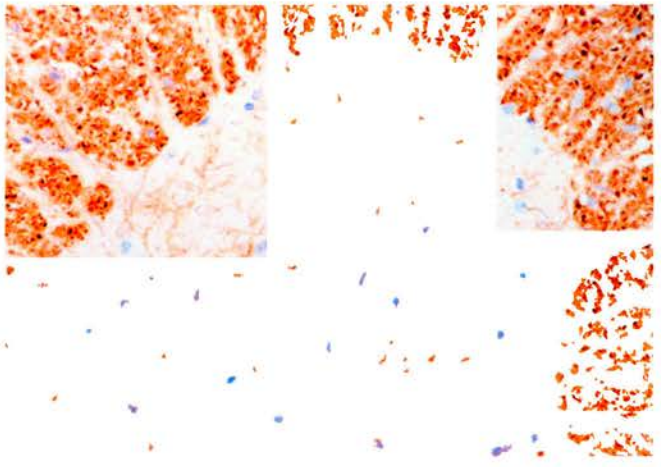

28 day control cervical spinal cord (×100)

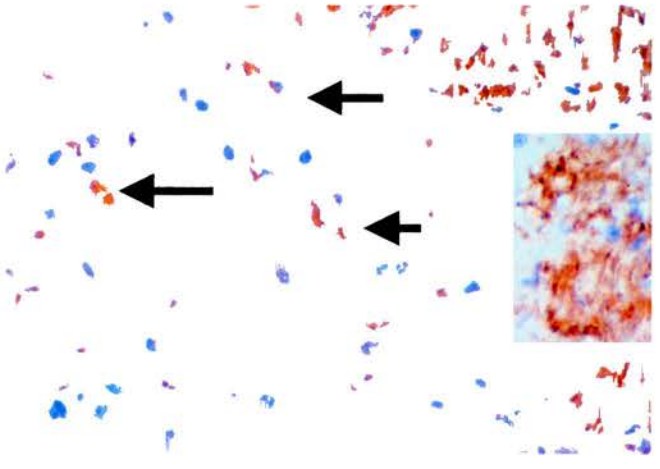

28 day wasted cervical spinal cord (× 150)

Figure 3-13 Sections stained with an antibody recognising phosphorylated neurofilaments. The sections are through the cervical spinal cord showing the anterior horn region, after staining with an antibody which recognises the light and heavy chain phosphorylated neurofilaments. The top section is through the spinal cord of a heterozygous mouse. The bottom section is from a homozygous wasted mouse, and shows cytoplasmic neuronal staining (arrowed).

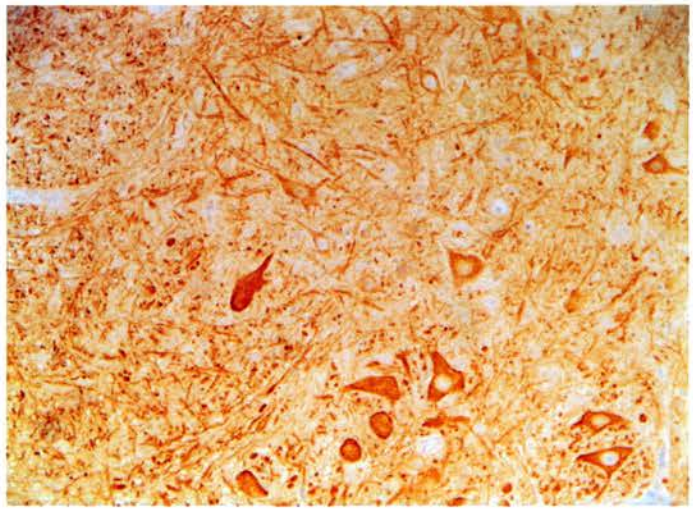

+/*wst* cervical spinal cord, x 16

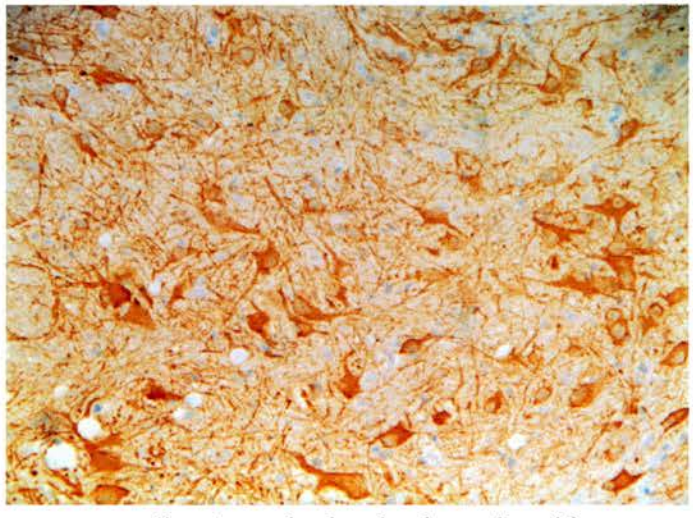

wst/*wst* cervical spinal cord, x 16

Figure 3-14 Sections stained with an antibody recognising the medium and heavy chain non-phosphorylated neurofilaments. Both sections are from the cervical spinal cord of a 28 day-old mouse, the top section, from a heterozygous mouse, and the bottom section, a homozygous wasted mouse.

3.2.2.4 Ubiquitin

Disruption of the ubiquitin-proteasome pathway is a feature of many neurodegenerative diseases (Sherman and Goldberg, 2001), and ubiquitinated inclusions are seen in the brain and spinal cords of ALS patients (Leigh *et al.*, 1988; Leigh *et al.*, 1991). I therefore investigated whether these were present in homozygous wasted mice, using an anti-ubiquitin antibody. No staining was observed in either wasted or heterozygous animals. A positive control from a human patient was included, and did show the expected ubiquitinated inclusions.

3.2.2.5 MAP2

Microtubule-associated proteins are involved in the assembly and stabilisation of microtubules. MAP2 is found specifically in the neuronal cell bodies and dendrites of the central nervous system, and promotes the polymerisation of tubulin into microtubules. There are three isoforms of the protein: MAP2A, MAP2B and MAP2C. Levels of MAP2 are reduced in the spinal cord of ALS patients (Kikuchi *et al.*, 1997). I therefore examined, using immunohistochemistry, whether there were differences in MAP2 expression between homozygous wasted mice and heterozygous control animals. No differences were seen between wasted and heterozygous animals in the staining pattern using an antibody which recognises all three MAP2 isoforms. In both cases, there was intense staining throughout the gray matter, with limited white matter staining. Typical sections are shown in figure 3-15.

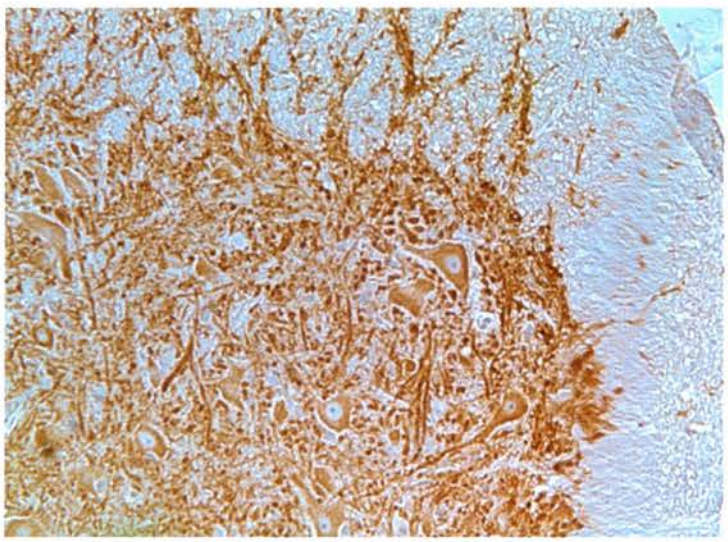

+/*wst* cervical spinal cord, x 16

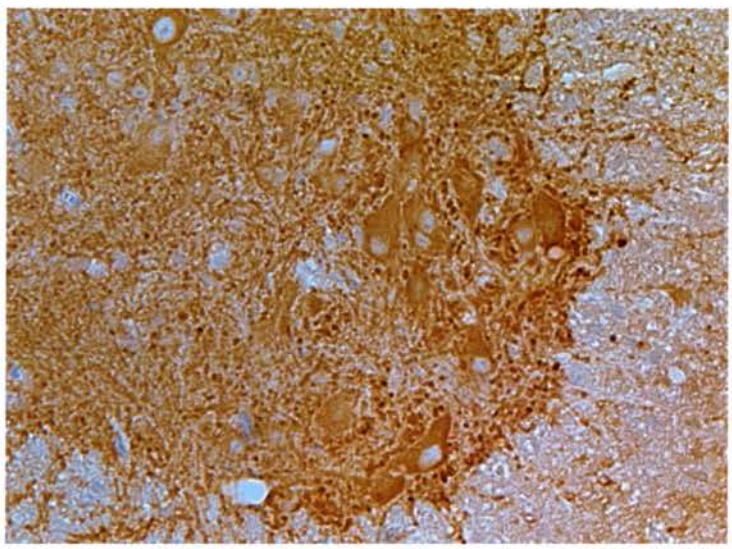

wst/*wst* cervical spinal cord, x 16

Figure 3-15 Sections stained with an antibody recognising MAP2. Both sections are from the cervical spinal cords of 28 day-old mice: top, +/*wst*; bottom, *wst*/*wst*.

3.3 Discussion

The reduction in total body weights which I have described in this thesis is in broad agreement with that previously reported, although in the study by Goldowitz *et al.* the wasted mice appear to lose weight relative to their heterozygous littermates slightly earlier, from 17 days of age (Goldowitz *et al.*, 1985). This study does not, however, record at what age the mice were weaned. In a further, less detailed, study, the difference between the two sets of mice appears to occur from 21 days onwards (Kaiserlian *et al.*, 1986).

I have demonstrated that there is a marked difference in the muscle weight:bodyweight ratio between homozygous wasted mice and heterozygous animals. This suggests that the weight loss seen in homozygous wasted mice is due to a loss of muscle mass. The only other organ in which there was such a difference between the two groups of mice was in the spleen, which would not affect the total body weight of the mice. There is actually an increase in the relative weights of the brain, heart and kidney in both homozygous wasted and heterozygous animals after 19 days, although this was more marked in homozygous wasted animals. This reflects the fact that both sets of animals lost weight around the period of weaning, a process which was continued and exacerbated in the homozygous wasted animals.

I have also extended the previous neuropathological findings in wasted mice, showing that there is vacuolation of the neurons of the cervical spinal cord from 28 days. I have also demonstrated that there is an increase in antibody staining for GFAP and phosphorylated neurofilaments in homozygous animals, when compared with their heterozygous littermates. However, these results were based on a limited number of mice, and clearly should be confirmed in a larger number of mice, particularly at 24 days of age. It would also be of interest to determine from what age these changes occur.

There are therefore a number of neuropathological similarities between wasted mice and ALS. These include the specific loss of anterior horn cell motor neurons, and accumulations of phosphorylated neurofilaments. One key hallmark of ALS that is not seen in wasted mice is the presence of ubiquitinated inclusions. It is possible, however, that this is due to the fact that the time course of the wasted phenotype is extremely rapid. If it were possible to extend the lifespan of the mice, perhaps by transgenic approaches, then it is possible that inclusions would be seen. It is usually only end-stage material which is reported in human ALS, so it is difficult to assess at what stage the inclusions arise. There were also no differences observed between homozygous wasted mice and heterozygous animals in MAP2-staining.

Another key difference is that the wasted phenotype begins at around 19 days, which, in mice, is approximately the time of weaning. Although there is no definitive correlation between different mouse and human ages, it is clear that a disease which afflicts mice from the time of weaning is affecting mice at a different stage of life from one which generally occurs in humans in middle or old age. It is therefore possible that wasted represents a better model of SMA, which usually has a much earlier age of onset than ALS. The mouse mutant neuromuscular degeneration, described in Chapter 1, section 1.2.5.1, was initially considered to be a model either of ALS, or of SMA (Cook *et al.*, 1995). The time course of the phenotype is similar to that of wasted mice, with impaired movement from 2 weeks of age, and death by four weeks. Furthermore, mutations in *IGHMBP2*, the human orthologue of the mutated mouse gene, have been identified as the causative mutation in spinal muscular atrophy with respiratory distress (SMARD) (Grohmann *et al.*, 2001).

One further difference between wasted and ALS is that the wasted phenotype has an immunological component. Although ALS does not have an overt immunological phenotype, reduced DNA repair has been reported in amyotrophic lateral sclerosis brain tissue (Kisby *et al.*, 1997). In wasted mice the reduced response to DNA damage has only been recorded in cells of a lymphoid origin, although it should be noted that this has not been investigated in the brain.

4 Chapter 4 - Mutation Analysis of ALS candidate genes

4.1 Screening of *EEF1A2* in ALS patients

4.1.1 Introduction

As both previous reports and the results I have presented in Chapter 3 are consistent with wasted being a model for motor neuron disease, and that the genetic lesion responsible for this mutant has been identified as the loss of *Eef1a2*, the human gene is a potential candidate for involvement in the disease. To test this hypothesis, *EEF1A2* was screened for mutations in DNA samples from patients with both familial and sporadic amyotrophic lateral sclerosis.

4.1.2 Study subjects

DNA samples were kindly provided by Dr. C. Hayward, previously at the Medical Genetics Section. The patients were originally recruited through the Scottish MND register by Shuna Colville and Dr. R. Swingler of the Department of Neurology at Ninewells Hospital, Dundee, and were screened for *SOD1* mutations. The DNA from 40 familial and 64 sporadic patients was analysed. DNA samples from 60 anonymous healthy Scottish adults were also examined as controls.

4.1.3 Strategy

EEF1A2 was screened on an exon-by exon basis. For most exons, single strand conformational polymorphism (SSCP) was used. In this method, the exon is first amplified using PCR, denatured and run on an acrylamide gel. The migration of the DNA through the gel is dependent on the sequence. Mutations cause a conformational change in the single stranded DNA which results in a shift in position of one or more of the bands seen on the gel (a band-shift) (Nataraj *et al.*, 1999). Exon 5, however, did not produce a reproducible pattern using SSCP analysis, and was therefore analysed using DHPLC. Exon 2 was also analysed using this method. DHPLC involves subjecting PCR products to ion-pair reverse-phase liquid

chromatography through a column (Liu *et al.*, 1998). The products are first denatured by heating and then cooled down slowly so that duplexes are formed. They are then run through a column containing alkylated non-porous particles in an acetonitrile gradient at a temperature which allows the partial denaturation of the samples. Heteroduplexes, formed by the reannealing of one mutant and one wild type strand, pass through the DHPLC column more quickly than the homoduplexes formed by the reannealing of two wild type strands. The elution profile also usually has an altered shape.

During the course of this project, the *EEF1A2* region of chromosome 20 was sequenced (Bischoff *et al.*, 2000)(accession number AF163763), which allowed the design of primers for the amplification of all the exons. Exons 3, 4 and 7 were amplified in two overlapping segments, either to obtain amplicons of a suitable size for analysis, or because the whole exon would not PCR-amplify. The strategy used for mutation analysis is described in table 4-1 and figure 4-1. Neither exon 1 (which does not encode protein) nor exon 8 were analysed as they were unamplifiable using a range of PCR conditions. Amplification was attempted using five different forward and reverse primers (in all possible combinations) at a range of annealing temperatures, and with a number of different *Taq* polymerases. The failure of these regions to amplify is probably due to the extremely GC-rich nature of these parts of the sequence. This is supported by the fact that when the WAVE® System utility hardware was used to plot the predicted helical fraction of the sample against the sequence of these exons, it was not possible to select a suitable annealing temperature.

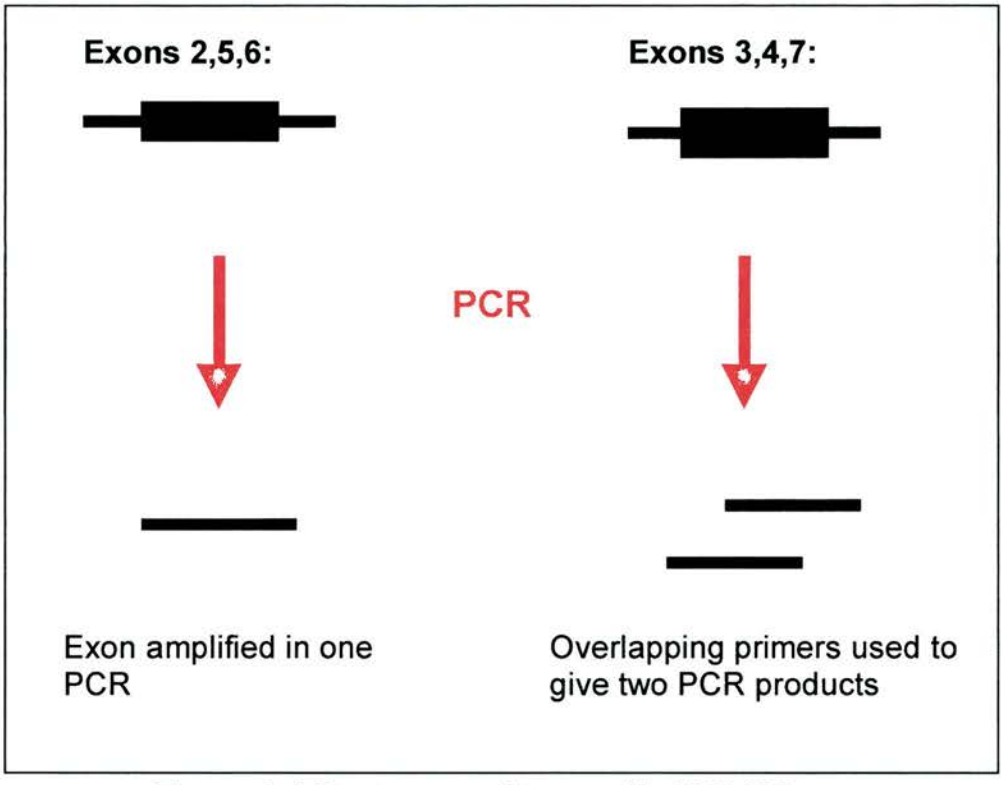

Figure 4-1 Strategy used to amplify *EEF1A2 exons*

Exon	Primers Used	Product Size, bp	Detection Method
2	2F & 2Rnew	369	SSCP & DHPLC
3	3F & 2R 3F1 & 2R1	268 255	SSCP
4	4F & 4R2 4F2 & 4R4	258 322	SSCP
5	5F2 & 5R2	297	DHPLC
6	6F & 6R2	409	SSCP & direct sequencing
7	7F1 & 7R 7F & 7R1	264 264	SSCP

Table 4-1 Strategy used to mutation screen *EEF1A2*

4.1.4 Results

4.1.4.1 Exon 2

Exon 2 was initially analysed using DHPLC at two different temperatures. No samples showed changed retention times at 63^0C. However, at 65^0C the trace obtained was difficult to interpret. Example traces at the two temperatures are shown in figure 4-2. The samples were therefore also analysed using SSCP analysis. No band shifts were seen. A typical gel is shown in figure 4-3.

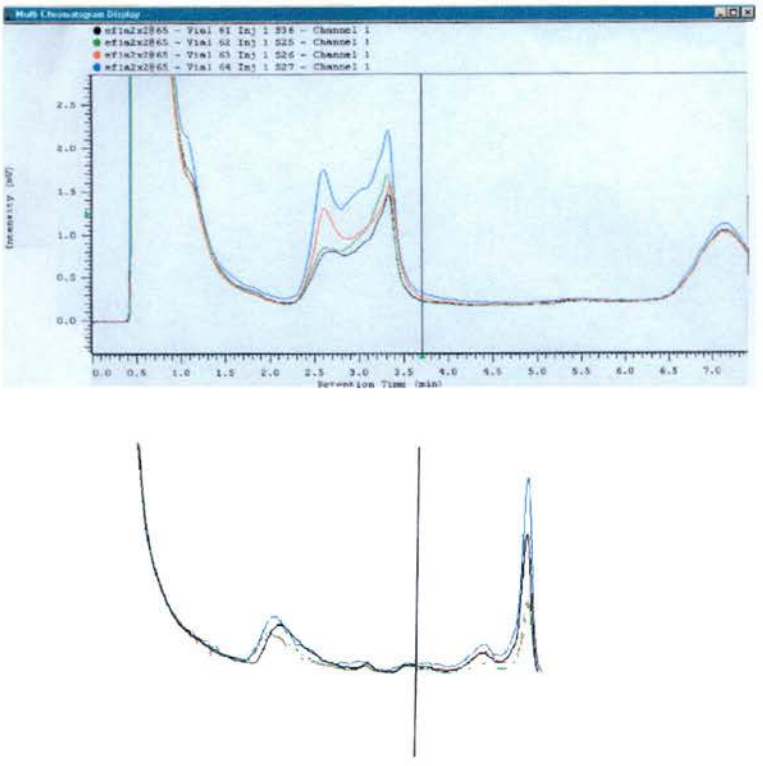

Figure 4-2 Typical traces obtained after DHPLC analysis of exon 2. The top trace shows samples run at 65^{0}C, and the bottom trace at 63^{0}C.

Figure 4-3 Typical exon 2 SSCP gel

4.1.4.2 Exon 3

Primers 3F and 2R were used to amplify 268 bp comprising most of exon 3. On SSCP analysis, a specific, reproducible band shift was noted. A typical gel is shown in figure 4-4. The amplicon producing the SSCP bandshift was manually sequenced, and revealed that those individuals showing the band shift were heterozygous for a C → T transition at nucleotide position 62 of the exon. The sequence is shown in figure 4-5.

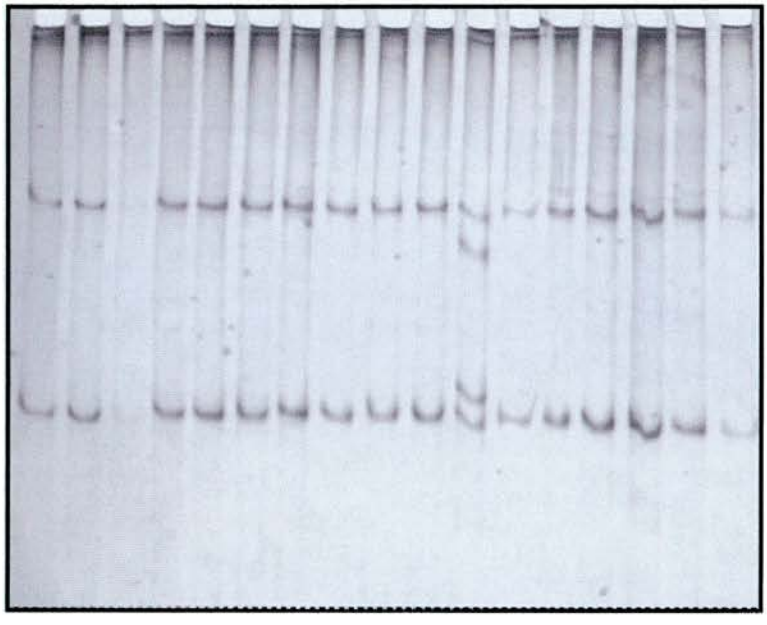

Figure 4-4 A typical SSCP gel, run after amplification using primers 3F and 2R. The sample in the 11th lane shows a band shift due to the individual being heterozygous for a C→A transversion.

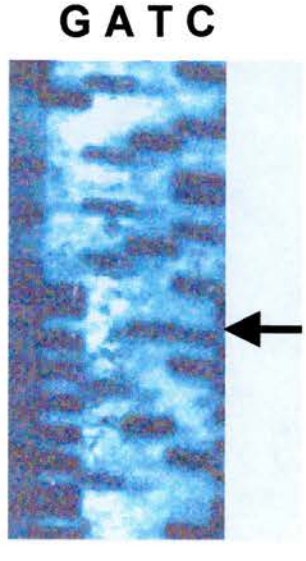

Figure 4-5 Part of exon 3 sequencing gel.
This individual is heterozygous for the nucleotide change at the position indicated by the arrow. The sequence around this point reads gga gcg tga gcg c/tgg cat cac cat cga c.

This change does not result in an amino acid change at the protein level. This would argue against a functional consequence of the nucleic acid change. However, as this change was noted in 5 of 64 sporadic ALS patients but in only 1 of 53 healthy controls, I analysed further patients and controls to determine whether there was a significant difference between the two groups. This could indicate a role for the polymorphism in disease susceptibility through being in linkage disequilibrium with a functionally important polymorphism. The results are shown in table 4-2.

Group	CT	CC	Total (N)
Familial ALS	0	40	40
Sporadic ALS	16	189	205
Healthy Controls	15	225	240

Table 4-2 Genotypes of enlarged study group.

Chi-square analysis gives a p-value ≤ 0.181 ($X^2 = 3.42$; 3×2 table, d.f=2). There are therefore no significant differences between sample groups. It is interesting that none of the familial ALS patients carried the polymorphism, whereas the allele frequency is 0.039 in sporadic patients and 0.031 in healthy controls. This difference is not, however, significant, with a p-value of 0.068 for familial vs. sporadic patients and 0.104 for familial vs controls.

Primers 3F1 and 2R1 were used to amplify the 3' end of exon 3 and the first part of intron 3. No SSCP band shifts were seen in the latter part of the exon (data not shown).

4.1.4.3 Exon 4

Primers 4F and 4R2 were used to amplify the first part of exon 4. SSCP analysis did not reveal any band shifts. A typical gel is shown in figure 4-6. No band shifts were noted in the second part of the exon, amplified using primers 4F2 and 4R4, and shown in figure 4-7.

Figure 4-6 TypicalSSCP gel after PCR amplification using primers 4F and 4R2.

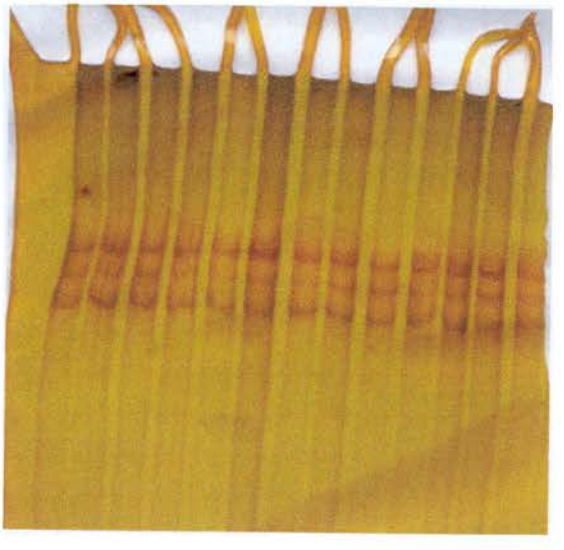

Figure 4-7 Typical SSCP gel after PCR amplification using primers 4F2 and 4R4.

4.1.4.4 Exon 5

Exon 5 amplicons did not give clear, reproducible bands on an SSCP gel. They were therefore analysed using DHPLC at two different annealing temperatures: 63^0C and 66^0C. At 63^0C, three different patterns caused by shifts in the peaks were noted in the amplicons from a small number of subjects, both ALS patients and controls, and are shown in figure 4-8.

The first pattern was seen in one sporadic patient and one healthy control. Manual sequencing showed it to be a C → A transversion at position 31 of intron 5. It therefore does not affect the translated protein. The second pattern was only seen in one familial patient. Sequencing on an ABI 3100 showed it to be a G → T transversion at position 39 of intron 5. The third pattern was found in three familial and four sporadic patients, along with seven controls. Sequencing on an ABI 3100 showed that these individuals carried both polymorphisms, at positions 31 and 39 of intron 5. The location of the polymorphisms I have found in *EEF1A2* and their frequencies in the control population are summarised in table 4-3 and illustrated in figure 4-9.

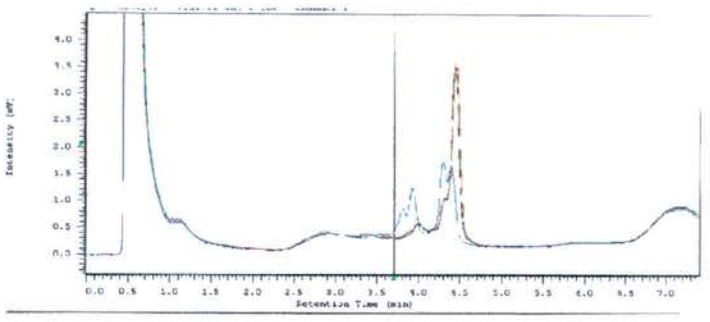

Pattern 1:
0/40 familial
1/64 sporadic
1/60 control

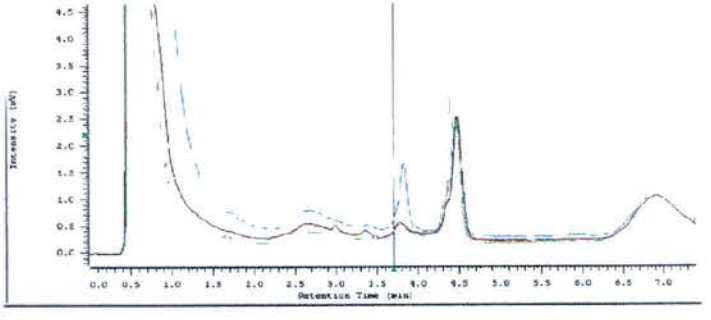

Pattern 2:
1/40 familial
0/64 sporadic
0/60 control

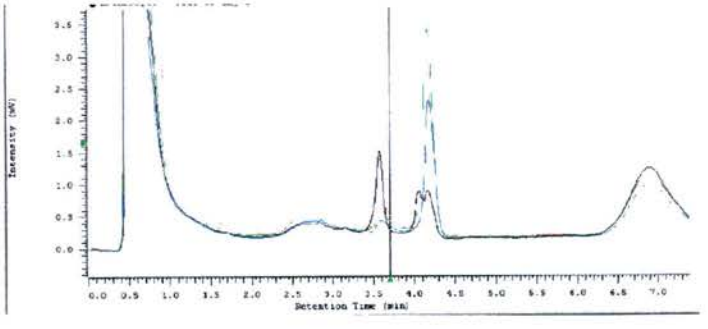

Pattern 3:
3/40 familial
4/64 sporadic
7/60 control

Figure 4-8 Typical traces obtained after DHPLC analysis of exon 5.

Position	Polymorphism	Allele frequency
Exon 3, position 62	C → T	0.031
Intron 5, position 31	C → A	0.033
Intron 5, position 39	G → T	0.058

Table 4-3 Summary of polymorphisms in *EEF1A2*.
The allele frequencies shown are for the control subjects.

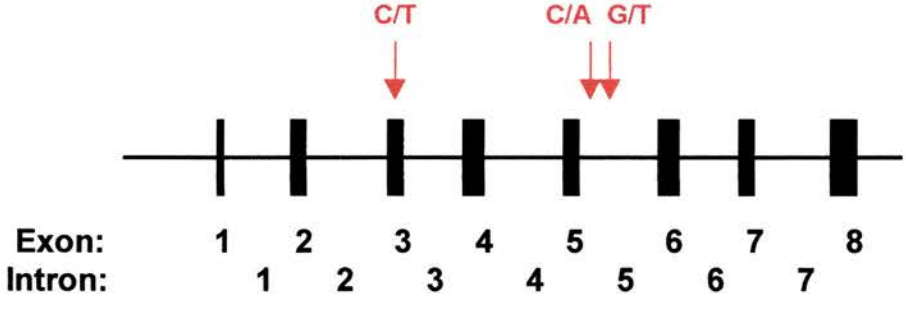

Figure 4-9 *EEF1A2* gene structure (not to scale), showing locations of polymorphisms (red arrows).

4.1.4.5 Exon 6

A combination of SSCP analysis and direct sequencing was performed by Doreen Chambers to screen exon 6. No mutations were found.

4.1.4.6 Exon 7

Exon 7 was amplified using two overlapping primer sets, 7F and 7R1, and 7F1 and 7R. SSCP analysis did not show any band shifts in ALS patients or control subjects. Representative gels are shown in figures 4-10 and 4-11.

Figure 4-10 Typical SSCP gel after amplification using primers 7F1 and 7R.

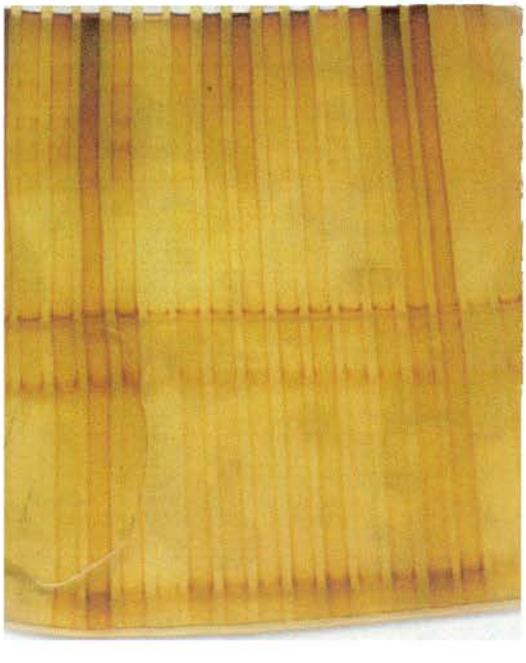

Figure 4-11 Typical SSCP gel after amplification using primers 7F and 7R1.

4.2 Screening of a candidate gene for wobbler

4.2.1 Introduction

As described in Chapter 1, section 1.2.5.1, wobbler is another mouse mutant which has been described as a model for ALS and SMA. Although the genetic basis has yet to be identified, it has been mapped to Chromosome 11 (Kaupmann *et al.*, 1992). The wobbler gene is closely linked to *Rab1* (Wichman *et al.*, 1992), although the latter has already been excluded as a candidate for *wr* (Wedemeyer *et al.*, 1996). In the region of human Chromosome 2 which shows conserved synteny with the *wr* locus on Chromosome 11, *RAB1* is close to member 4 of the solute carrier family 1 *SLC1A4,* at 2p15-13 (Hofmann *et al.*, 1994). *SLC1A4* is ubiquitously expressed, with the strongest expression in the brain, muscle and pancreas (Arriza *et al.*, 1993; Shafqat *et al.*, 1993). The expression pattern within the brain is uniform.

SLC1A4 is a neutral amino acid transporter with structural and sequence similarity to the glutamate transporter family (Arriza *et al.*, 1993; Shafqat *et al.*, 1993). Although its main substrates are alanine, serine and cysteine (which led to its previous name of *ASCT1*, an acronym for alanine, serine and cysteine transporter) (Zerangue and Kavanaugh, 1996), it will also transport glutamate at pH<7.4 (Makowske and Christensen, 1982; Tamarappoo *et al.*, 1996). Its most important substrate is cysteine, which acts as a neurotoxin with a pathology indistinguishable from that produced by glutamate (Karlsen *et al.*, 1981; Olney and Ho, 1970; Olney *et al.*, 1972; Olney *et al.*, 1990). The human gene has previously been mutation screened as a candidate gene for involvement in schizophrenia (Bennet *et al.*, 2000). The mouse gene, *Slc1a4*, encodes a protein of 532 amino acids with 89% identity with the human gene.

Thus, as well as potentially transporting glutamate under some conditions, the main substrate of *Slc1a4*, cysteine, is a neurotoxin. As glutamate excitotoxicity has been postulated as a mechanism of the pathogenesis of ALS, and *Slc1a4* maps to the region of the human genome with conserved synteny with the *wr* locus, I screened

the *Slc1a4* gene for mutations in DNA extracted from the brains of *wr/wr* and control littermates.

4.2.2 Strategy

Initially, only exonic sequence from *Slc1a4* was available. Therefore, designing primers to amplify and sequence the whole coding sequence necessitated obtaining intronic sequences which flanked the exons. Exons were identified by aligning the human and mouse mRNA sequences. As the intron-exon structure of the human gene had been elucidated, the high degree of nucleotide similarity between the two orthologues allowed the locations of the exon boundaries to be determined. Primers were designed from the exonic sequence to amplify each intron, which was then sequenced. Intron 1 failed to amplify, but during the lifetime of this project, sequence from this region became available at the NCBI trace archive. This was identified by blasting the 3' region of exon 1 against the archive. The largest contiguous sequence available was 7kb. This did not include any of exon 2, which suggests that intron 1 is at least 7 kb in size. Although a long-range PCR kit was used, it may be that it is just too large to amplify. The 3' region of intron 1 also became available, which was used to design the 5' primer used to amplify and sequence exon 2. The sequences used are all given in tables 4-4 and 4-5.

Intron	Primers Used	Sequence, 5' → 3'	Product Size, kb
1			> 7
2	2F & 3R	ttg tgg ttg ccg cat tca ct tgg gtc acc act gtg taa tc	1.4
3	3F & 4R	ggg aac gtg acc aaa gag aa cct tcc aca tct gtt aca ac	4.5
4	4F & 5R	cac aat ggt gct ggt gtc at ttg ctt ccg atc agg aac at	6 .0
5	5F & 6R	aac ccg ttc acg ttc ctc ct cac ttc atc ata gac gga agg	0.4
6	6F & 7R	acc tga acg cag gac aga tt tcc aac act gga tgc cgt g	1.4
7	7F2 & 8R2	ttg gag gcc att gga ttg cc ctt gta gct cct gct aca ct	2.0

Table 4-4 Primers used to amplify *Slc1a4* introns

Exon	Primers Used	Sequence, 5' → 3'	Product Size, bp
1	1F 1F2 1R2	tga tcc att cat tcg aaa cc atg ctg cgc atg atc atc ct gtt aag ggc caa cag taa ct	676 352
2	2F5 2R2	taa cat tgt ctc tgc tac ac tcc ctc ttt cct gta ctt ta	247
3	3F3 3R4	acg aat agt agc agc agt ag cag taa gta aca ggc aca tg	231
4	4F2 4R3	ttt cag aca ctg cac aga tc ttg tac cat gac aag cta tg	311
5	5F4 5R3	ctc agt acc tcc cag tct ca ctc acc tca ctc tgt acc ca	367
6	6F3 6R3	ata ccg atg tgt tct ggt g tta agc cag gcc taa caa tg	286
7	7F3 7R2	atg cat gat gta att ccc tg tgg agc atc aag tac tca ga	254
8	8F 8R3	acc agc ctg ctt gtg ata g cag tgt atg agg gcc atg c	399

Table 4-5 Primers used to amplify *Slc1a4* exons

4.2.3 Results

4.2.3.1 Sequencing of *Slc1a4*

Genomic DNA was extracted from the brains of homozygous wobbler mice and littermate control animals, both very kindly provided by Paolo Bigini of the Instituto di Recerche Farmacologiche Mario Negri, Milan. Introns 3-7 were successfully amplified and sufficient sequence information was obtained to design primers to amplify each exon. Each exon was successfully amplified and sequenced from both *wr/wr* and control animals. No mutations were found in any of the exons. A typical sequencing trace is shown in figure 4-12.

4.2.3.2 Expression analysis

RNA was extracted from both *wr/wr* and control brains. Karen Wilson (a summer student under my supervision) used RT-PCR to determine whether there were any differences in the expression levels of *Slc1a4* between *wr/wr* and control brains. Two sets of primers used: 5F2 & 6R, which gave a PCR product of 215bp, and 5F & 7R, giving a product of 238bp. A control PCR used to compare the relative levels of mRNA in samples amplified glyceraldehyde-3-phosphate dehydrogenase, *Gapdh*. Levels of *Slc1a4* were similar in both cases, as determined by the intensity of the band on agarose gel electrophoresis and shown in figure 4-13. This was not quantitative, but as no mutations had been found, it was judged to be sufficient evidence that *Slc1a4* was unlikely to be implicated in the wobbler phenotype.

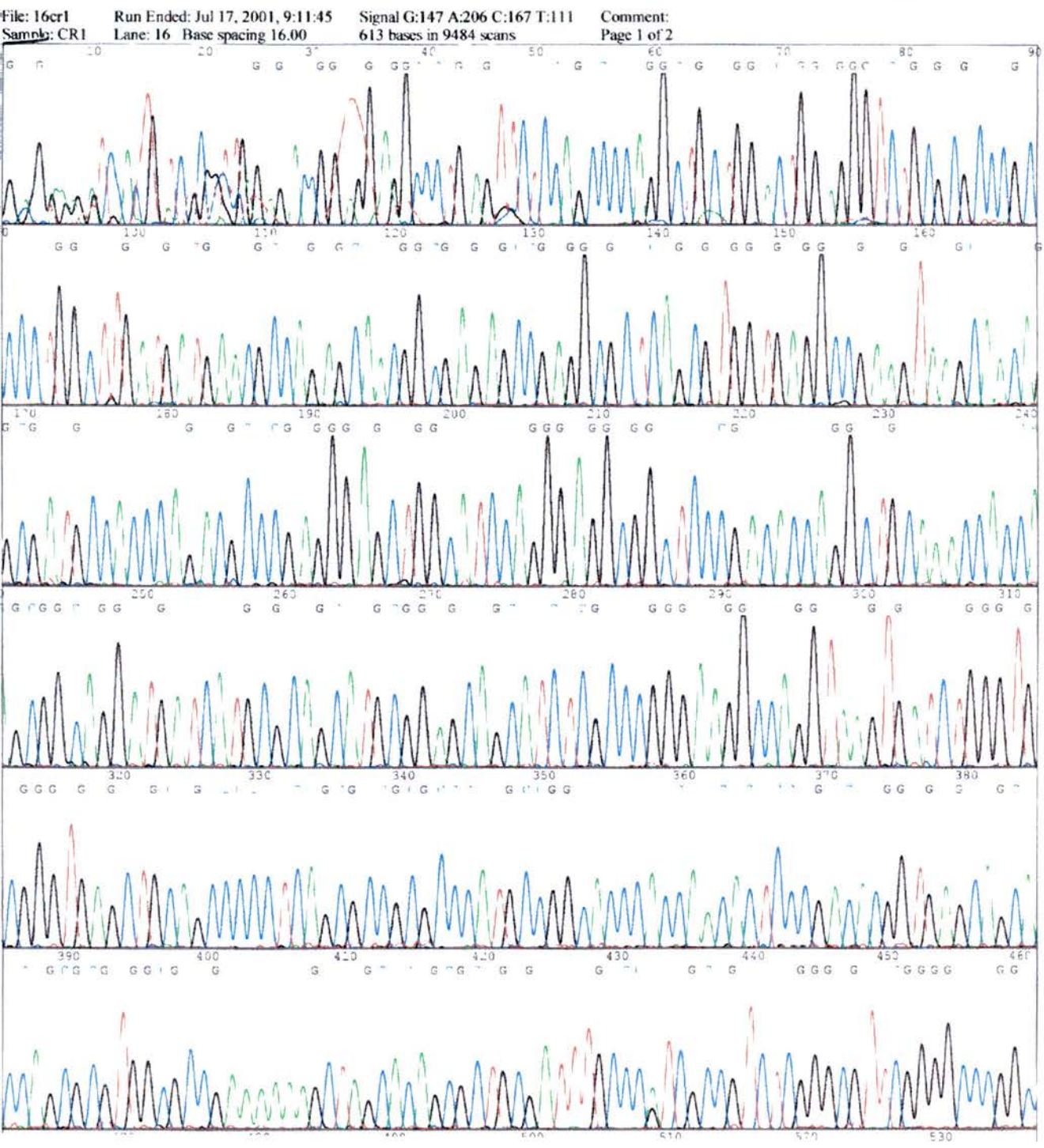

Figure 4-12 Typical sequence trace from *wr/wr* animal, showing exon 1 of *Slc1a4*.

Figure 4-13 Agarose gel (2%), showing results of the RT-PCR analysis of *Slc1a4*. The first eight lanes show the products obtained using primers 5F2 and 6R, giving a PCR product of 215bp, and the next eight using primers 5F and 7R, giving a product of 238bp. The GAPDH primers used gave a PCR product of 450bp. Lanes marked RT had reverse transcriptase added,and those marked No RT were control reactions with no reverse transcriptase. The lanes marked W and C stand for *wr* and littermate control samples, B for mouse brains used as an RNA extraction control, and – as a PCR control with no RNA added.

4.3 Discussion

No mutations were found in most of the protein-encoding region of *EEF1A2*. It is thus unlikely that mutations in *EEF1A2* are responsible for anything other than rare cases of motor neurone disease. There were, however, polymorphisms in the gene which were also present in healthy controls. These included a silent polymorphism in exon 3. It is unlikely that this polymorphism has a functional effect as it does not affect the amino acid sequence. There were also two polymorphisms in intron 5. As these polymorphisms are all SNPs, they could be useful in the mapping of other disease genes.

It was not possible, however, to screen the whole coding region, as exon 8, the first part of which forms part of the translated protein, was unamplifiable using PCR. This is probably due to the extremely GC-rich nature of this part of the sequence. PCR was attempted using five different forward and reverse primers (in all possible combinations) at a range of annealing temperatures, and with a number of different *Taq* polymerases. Thus, if mutations in exon 8 do underlie cases of ALS, I would not have detected them. Exon 1 was similarly refractory to analysis, using a range of primer sequences and conditions. Although this exon was not protein-encoding, it is possible that mutations could cause disease through, for example, affecting mRNA stability. It is also possible that mutations in the promoter region, which was not analysed, could also be important by, for example, affecting levels of the protein. Indeed, mutations in the promoter region of *Vegf* have been identified as underlying a mouse model of ALS (Oosthuyse *et al.*, 2001). There are also, for example, known regulatory sites in the first intron of *EEF1A2* (Bischoff *et al.*, 2000). However, as with any mutation screening programme, a balance needs to be struck between the comprehensive analysis of a gene and the resources in terms of both time and cost of doing so.

The other key question is whether the sensitivities of the techniques used were sufficient to detect mutations. The method I most often used was SSCP, which is a technologically straightforward way to analyse a relatively large number of samples.

Estimates of the sensitivity of this technique vary from 50% to 100%, with the sensitivity decreasing with increasing size of PCR product (Hayashi and Yandell, 1993). However, the sensitivity can be improved by running the gels under more than one set of conditions, for example, by running them at room temperature and at 4^0C, and with and without the addition of 5-10% glycerol. Again, there is a balance to be struck between maximising the chances of detecting a mutation and time considerations. One potential drawback to the technique is that the precise change in mobility caused by a particular mutation cannot be predicted, but depends on the surrounding sequence (Glavac and Dean, 1993; Nataraj *et al.*, 1999). An advantage of DHPLC is that it is less sequence-dependent, and can also be used for larger fragments (up to 1.5kb) (Liu *et al.*, 1998). The sensitivity appears to be in excess of 90% (Colosimo *et al.*, 2002; Liu *et al.*, 1998; Matyas *et al.*, 2002; Takashima *et al.*, 2001). It is also relatively straightforward to screen a large number of samples for mutations in the same gene. However, conditions do need to be optimised for each PCR product, so it is probably less suited to analysing a wider range of genes in a smaller number of samples.

EEF1A2 was also screened in SMA patients heterozygous for *SMN1* or *SMN2* mutations by Romina Aron-Badin as part of her MRes project (Aron-Badin, 2002). Subject to the same caveats that apply to the *EEF1A2* screening, no mutations were found. This suggests that *EEF1A2* is not implicated in SMA. As outlined in section 1.3.3, it is possible that SMN, eEF1A and ZPR1 are part of the same complex. It may be worthwhile, therefore, to screen *ZPR1* in either SMA cases in which SMA mutations have not been found, or in ALS cases.

It was hoped to investigate the expression of eEF1A-2 in human ALS spinal cords, using our specific antibodies, and compare this to healthy controls. Although neither of the eEF1A-2 antibodies have been tested on human tissue, it is anticipated that both would work – there are no amino acid differences between the human and mouse sequences in the regions of the protein where the peptides were selected. Any differences between these two groups would suggest a role for eEF1A-2 in the pathogenesis of ALS. If large differences in protein expression levels were noted,

analysis of, for example, the promoter region may have been justified. Such archival spinal cord material is available at the Western General Hospital. Unfortunately it proved impossible to access it within the timescale of this project due to the length of time needed to obtain ethical permission, in the wake of the Alderhay and other inquiries.

Slc1a4 has also been ruled out as the gene which is mutated in wobbler mice, as there were no mutations in any of the exons of the gene. If a change had been noted in the gene in *wr/wr* animals, the analysis of more mice would be necessary, to determine whether this change was the causative mutation or a polymorphism, as the mice have a mixed genetic background. RT-PCR analysis performed by Karen Wilson showed that mRNA levels were similar in *wr/wr* and littermate controls. This demonstrates one of the advantages of investigating mouse mutants, as no such material would be available from human patients.

Since this work was carried out, *Slc1a4* has been excluded from the *wr* critical region (Fuchs *et al.*, 2002). This has been refined to the region between *Murr1* and *147N22rev*. All eight genes within the region have been sequenced, but no mutations have been found in the coding regions or in the parts of the 3' and 5' UTRs that have been sequenced. The possibility remains that the wobbler phenotype is caused either by a mutation in an undiscovered gene in the region, or in an as yet unknown regulatory region. Comparative genomics may be of value to define these potential regulatory regions, as there is conservation of synteny between mouse proximal Chromosome 11 and human Chromosome 2p13-14. It is possible that identification of the genetic modifier locus on Chromosome 14 will aid in the identification of the causative gene (Ulbrich *et al.*, 2002).

During the course of this project, sequence information became available as a result of the mouse sequencing project which allowed the design of primers to amplify the whole of *Slc1a4* exon1, without having to sequence intron 1. Subsequently, the whole genomic sequence of the *Slc1a4* gene has been released on a large contig (accession number NW_000035, released October 2002). The mouse sequence has

recently been released (Mouse Gene Sequence Consortium, 2002), so that in future it will not be necessary for similar projects to sequence introns as all the information will be available.

5 Chapter 5 - Expression analysis of eEF1A-1 and eEF1A-2

5.1 Introduction

In order to study the expression of eEF1A-2 and eEF1A-1, and to answer basic biological questions about the two isoforms, I designed and characterised antibodies which were specific for eEF1A-2 and eEF1A-1.

5.2 Design, generation and characterisation of antibodies

5.2.1 Antibody design

Due to the high degree of similarity between eEF1A-1 and eEF1A-2, anti-peptide antibodies were generated to specifically recognise each isoform. Two peptide sequences were selected to generate antibodies, one comprising residues 439-452, at the C-terminus of the protein (hereafter designated eEF1A-2C or eEF1A-1C), and one comprising residues 161-176 (hereafter designated eEF1A-2M or eEF1A-1M). These sequences were selected on the basis of maximising differences between the two isoforms. Their location, and the difficulties in finding sequences with differences between the two proteins, are illustrated in figure 5-1. Their lengths, of 14 and 16 residues respectively, represented a compromise between maximising both the number of residues and the proportion of residues which differed between the two isoforms, and reducing costs. In order to use the antibodies for analysis of both human and mouse proteins, peptides were selected with no amino acid differences between the isoforms of the different species. A terminal cysteine was added to each peptide, to allow for conjugation to keyhole limpet hemocyanin, and also to allow the conjugation of the peptide to a SulfoLink® column for subsequent immunoaffinity purification. The cysteine was added to the C-termini of eEF1A-1C and eEF1A-2C, and to the N-termini of eEF1A-1M and eEF1A-2M.

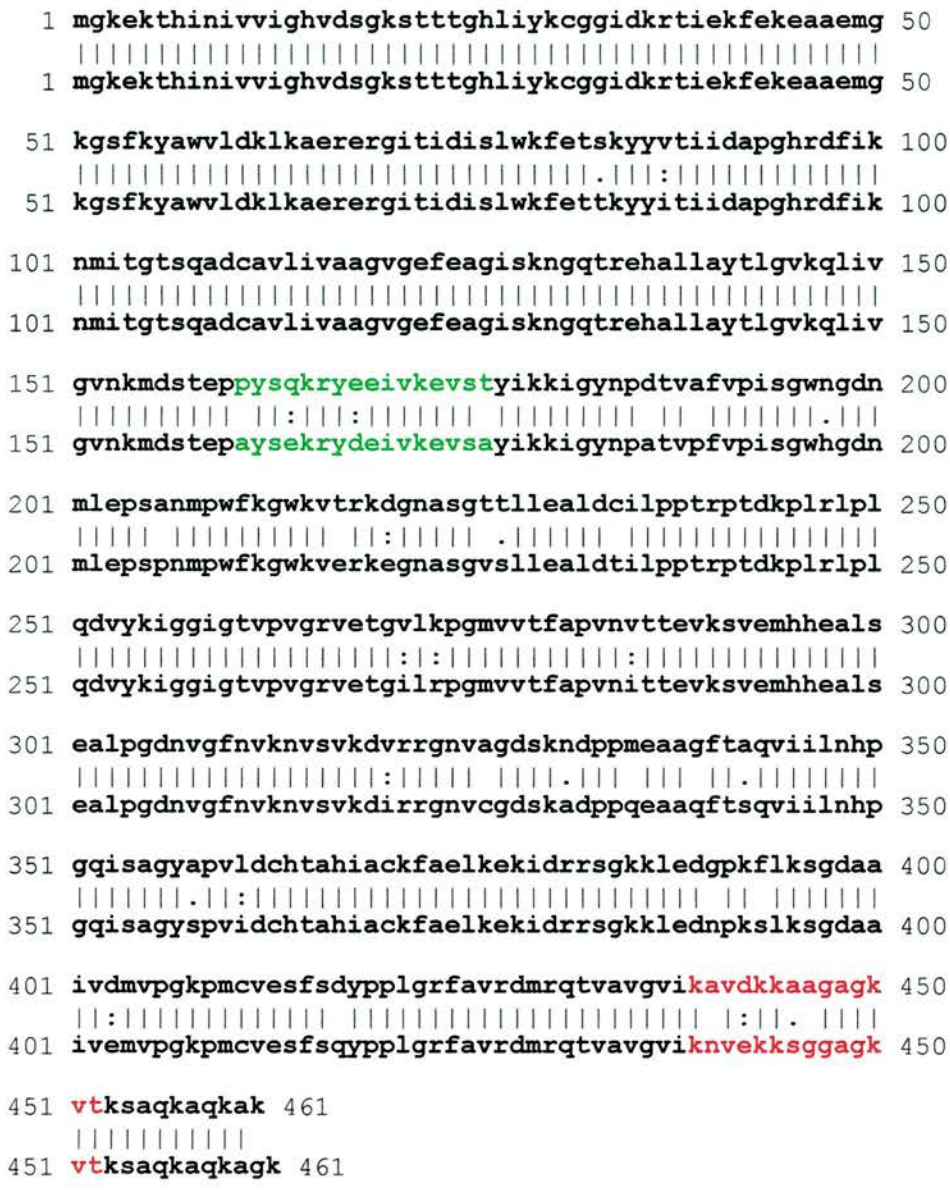

Figure 5-1 Peptide sequence of eEF1A-1 (top) and eEF1A-2 (bottom). The regions of the proteins to which antisera were raised are shown in **green** for eEF1A-1M and eEF1A-2M and in **red** for eEF1A-1C and eEF1A-2C.

There were other considerations in designing the peptides against which the antibodies were raised. For example, access of the antigen by the antibody is required in immunohistochemistry. Although the precise three-dimensional structure of mouse or human eEF1A-1 or eEF1A-2 had not been characterised at the time the peptides were designed, the structure of the bacterial protein EF-Tu had been resolved using X-ray crystallography (Song *et al.*, 1999). The amino acid sequence of eEF1A-2 was aligned with the bacterial EF-Tu sequence. Residues 161-176 (forming peptides eEF1A-1M and eEF1A-2M) correspond with residues 143-159 of the bacterial protein. Examining the protein structure at the Protein Data Bank (PDB), accessed through HGMP (www.hgmp.mrc.ac.uk), these residues appear to form an α-helical loop on the exterior of the protein. This is demonstrated in figure 5-2. Residues 439-452 (forming peptides eEF1A-1C and eEF1A-2C) are not homologous to any region of the bacterial protein, which terminates 20 residues short of the C-terminus of the eEF1A-2 protein. However, as these peptides are very close to the C-terminus of the protein, it is likely that they are also relatively exposed to the surface.

The antigenicity of the selected peptides was also assessed using the Antigenic programme of the PIX protein identification suite, also available through the HGMP. An antigenic peptide is more likely to provoke an immune response in the sheep. The majority of the residues of eEF1A-1M, and the last 9 amino acids of eEF1A-2M, were predicted to be antigenic. The first five residues of eEF1A-1C, and the first three of eEF1A-2C, also showed expected antigenicity.

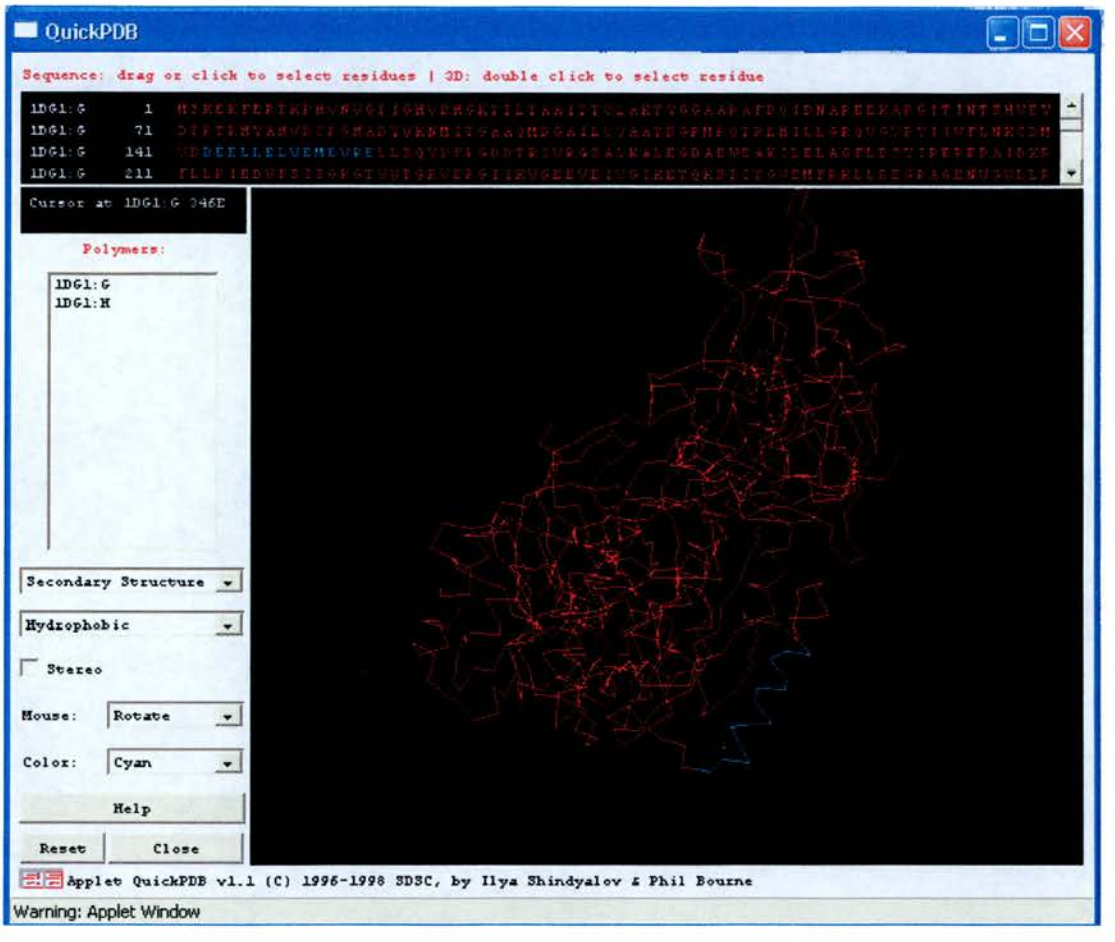

Figure 5-2 Structure of *E. Coli* EF-Tu.
Residues 143-159 are highlighted in **cyan**. These residues form an exposed α-helix.

5.2.2 Antibody Generation and Characterisation

The synthesised peptides were then linked to keyhole limpet hemocyanin, KLH, to improve the immunogenicity of the peptide and therefore the immune response in the sheep. The KLH-conjugated peptide was then injected into a sheep as described in Chapter 2, section 2.7.1, and the sera from three bleeds was obtained for each peptide. The sera were then characterised and purified for use in experiments.

The serum from each bleed was initially tested to determine whether it recognised the peptide using an ELISA (enzyme-linked immunosorbent assay). Different concentrations of sera, from 1:100 to1:100 000, were tested against different peptide concentrations, from 5μg/ml to 1ng/ml. Preimmune serum, obtained from the same animal into which the peptide was injected prior to immunisation, was used as a control. The preimmune serum from the animal into which the eEF1A-2M peptide was injected was not investigated, as the serum from this, and from eEF1A-1M, was initially tested on a Western blot, as outlined in section 5.2.2.1, below. As the eEF1A-2M antibody appeared to be specific on a Western blot, it was not considered necessary to test the pre-immune serum. As the eEF1A-1M antibody did not recognise a band of the correct size on a Western blot, the recognition of the antibody for the peptide against it was raised was tested using ELISA, and compared with that of the preimmune serum. The ELISA results are displayed graphically in figures 5-3 through 5-6.

In all cases investigated, the response of the serum raised against the peptide was greater than that of the preimmune serum. Whereas the absorbance at 450nm was typically at least 1.0, that of the preimmune sera was typically around 0.1-0.2. There was also a relationship between the concentration of the peptide and the ELISA response of the antibody-containing sera, with the absorbance at 450 nm increasing with increasing peptide concentration for each serum concentration. For the preimmune sera, there was no such relationship, with the graph of absorbance at 450nm versus peptide concentration at different serum concentrations resembling random noise.

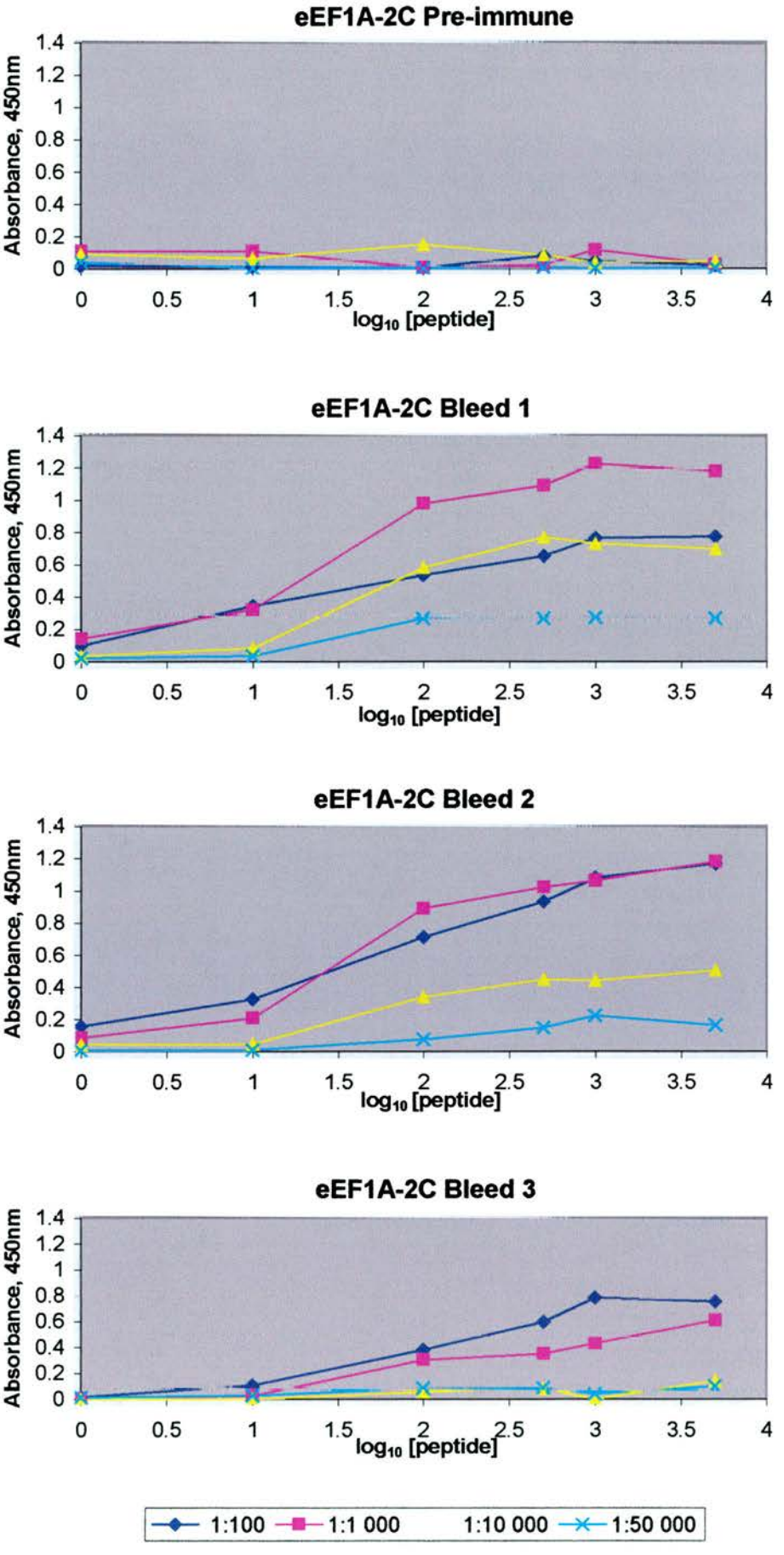

Figure 5-3 ELISA results from eEF1A-2C sera

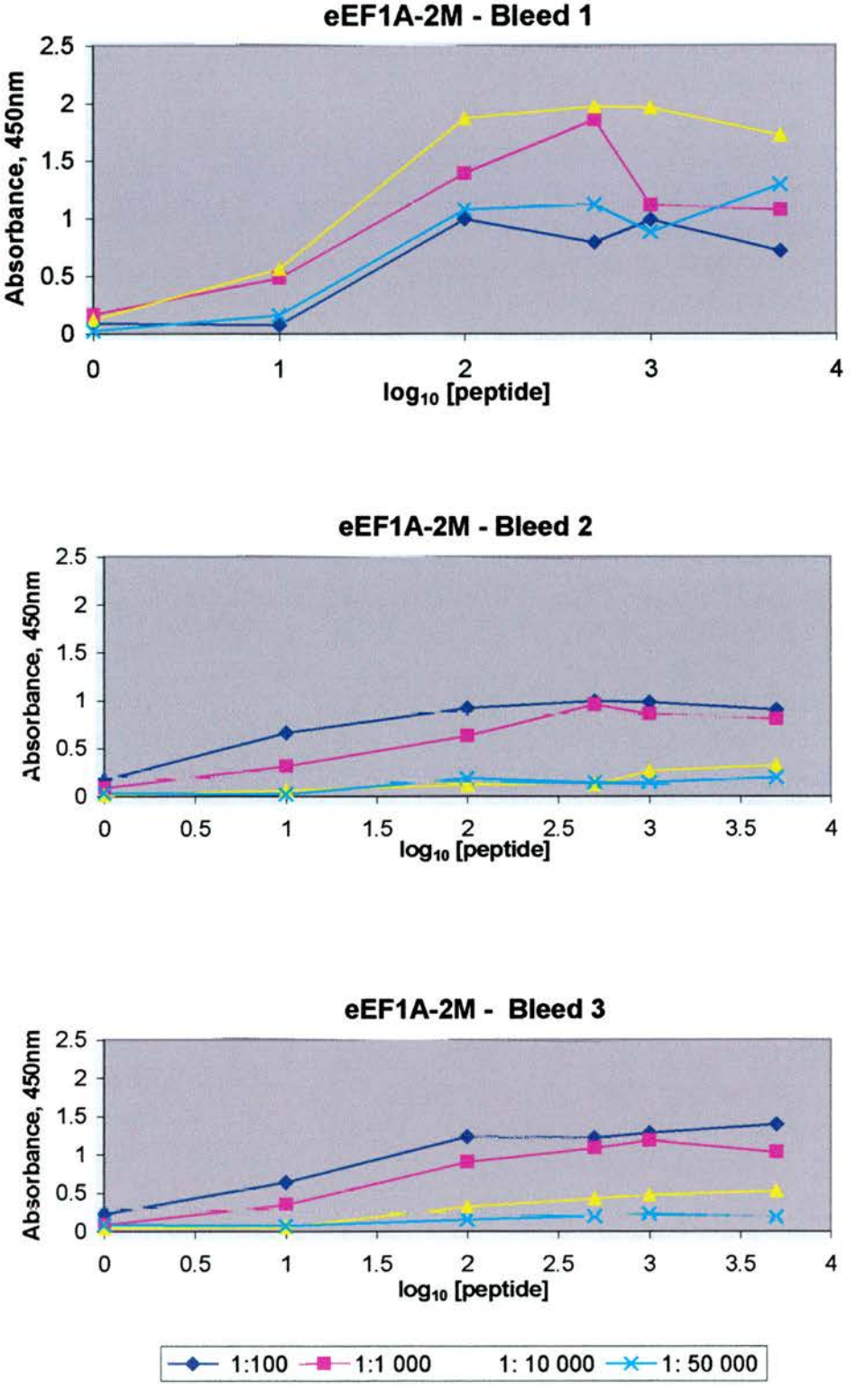

Figure 5-4 ELISA results from eEF1A-2M sera

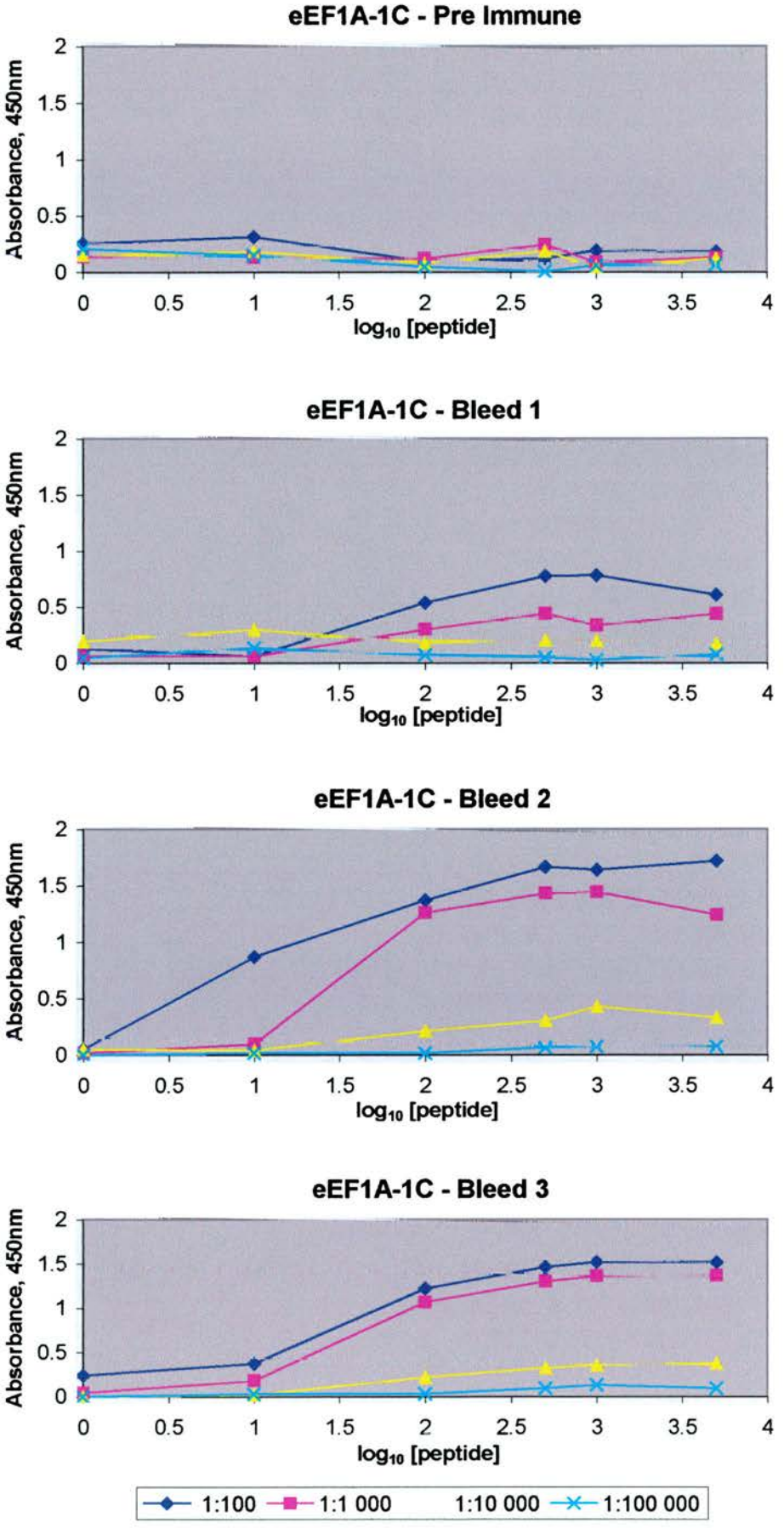

Figure 5-5 ELISA results from eEF1A-1C sera.

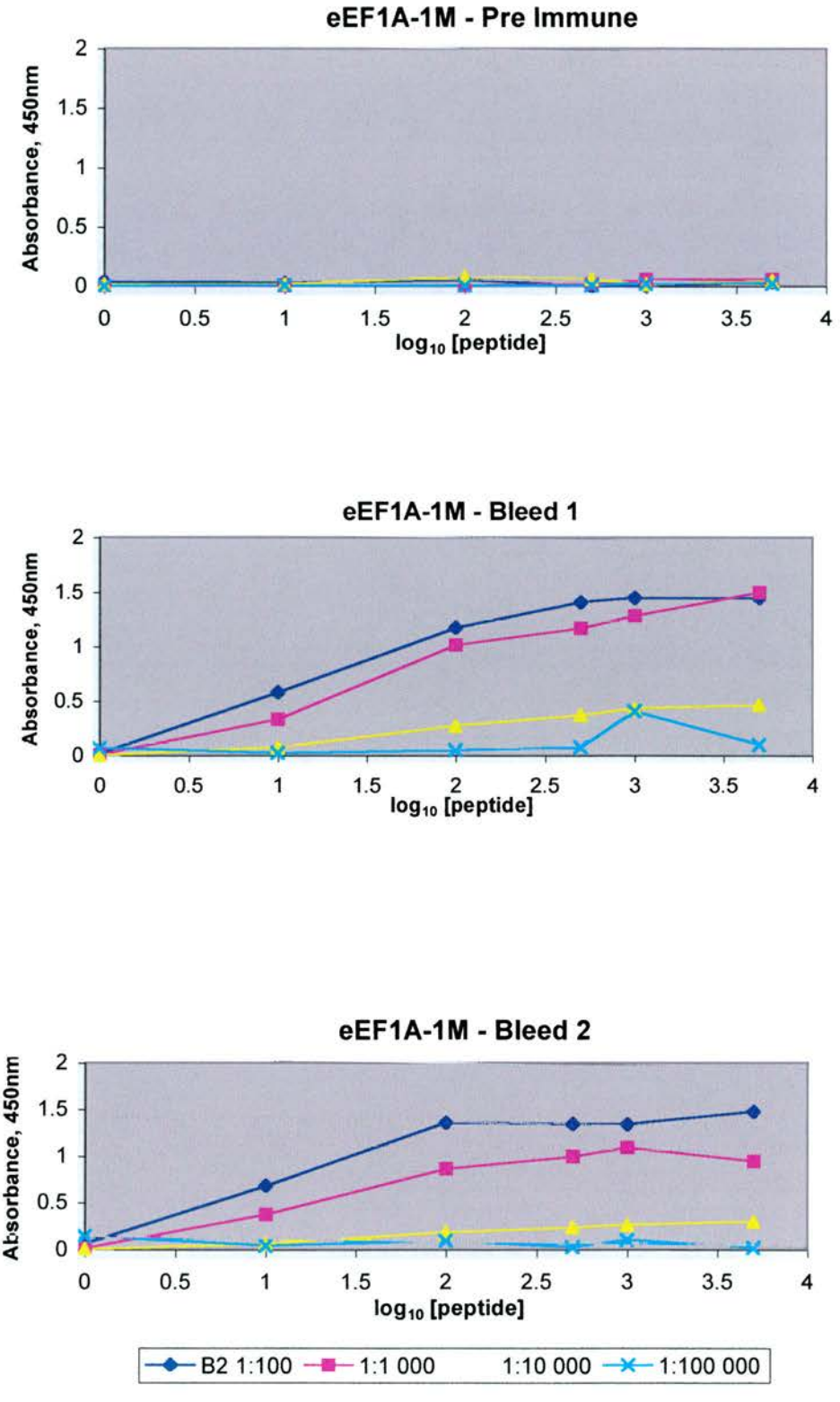

Figure 5-6 ELISA results from eEF1A-1M sera.

5.2.2.1 Antibody specificity

The specificity of the eEF1A-2 antibodies was determined using western blotting. Protein extracts from mouse brain were used, as it had previously been shown that the mRNA of both isoforms is expressed in the brain (Lee *et al.*, 1993b). Both anti-eEF1A-2 antibodies recognised a band of approximately 50kD in the brains of wild type mice. No band was recognised in tissue extracts made from the brains of wasted animals. In heterozygous mice, which carry one functional eEF1A-2 allele and would therefore be expected to express half the amount of eEF1A-2 protein, there was a band of approximately half the intensity of that seen in wild type animals. The fact that no band was seen in wasted animals demonstrated that the antibody is specific for eEF1A-2, and does not recognise eEF1A-1, as wasted mice are still expected to express eEF1A-1 at wild-type levels. An illustrative Western blot is shown in figure 5-7. The specificity of the antibodies was further confirmed by investigating the expression pattern of eEF1A-2 in a range of tissues. This is discussed further in section 5.3.1, below.

The specificity of the eEF1A-1 antibodies was also investigated using Western blotting. Unlike the situation with eEF1A-2, there is no deletion control as there are no eEF1A-1 knockout mice. However, the known eEF1A-1 tissue specificity allowed a negative control, as eEF1A-1 is known not to be expressed in muscle after 25 days at the RNA level (Chambers *et al.*, 1998). The eEF1A-1C antibody recognised a band of approximately 50kD in all adult tissues examined with the exception of adult muscle. The results are presented and discussed further in section 5.3.1, below. Although the eEF1A-1M antisera did recognise the peptide against it was raised, it did not recognise any bands of the correct size using Western blotting, either before or after purification. It was therefore not further investigated.

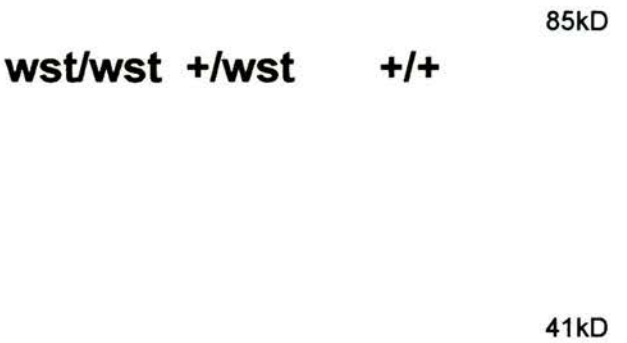

Figure 5-7 Western blot of protein extracts from mouse brains of different genotypes: w/w, wasted; +/w, heterozygotes; +/+, wild-type animals. 15μg total protein extract was loaded. The antibody used was the unpurified eEF1A-2C antibody at a concentration of 1:50. Similar results (data not shown) were obtained for the eEF1A-2M antibody. No band is seen in the extracts from wasted animals, and a much weaker band is seen in the heterozygous animals than in the wild type animals. This reflects the fact that they only have half the amount of eEF1A-2 protein of the wild type animals.

5.2.3 Antibody Purification

The specificity of the antibodies was improved by purification, as illustrated in figure 5-8. Antibodies were initially purified using ammonium sulphate precipitation, which separates the immunoglobulin component of the sera from the other components. This resulted in a decrease in the intensity of non-specific bands on a Western blot. The precipitated antibodies were further purified using immunoaffinity purification, in which the antibody is purified against the initial peptide. After such purification, only antibodies specific for the peptide in question should be present. This resulted in the removal of all non-specific bands on a Western blot.

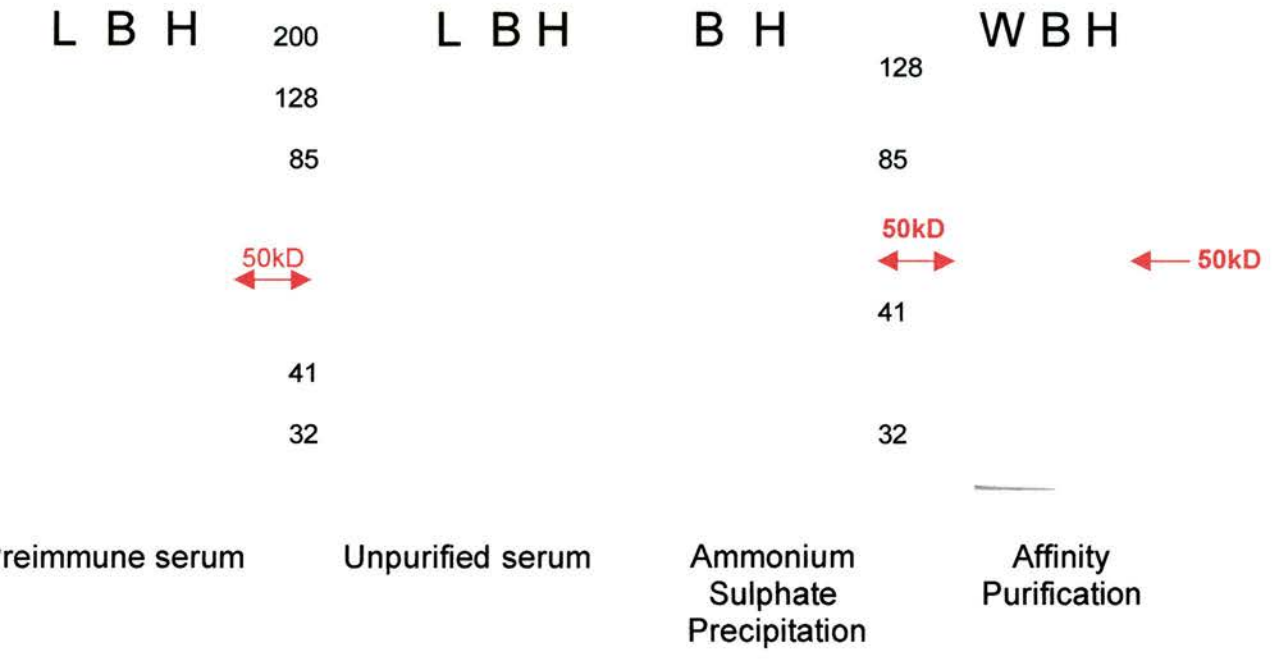

Figure 5-9 Immunoblots of Westerns after different stages of antibody purification. The first blot has been immunoblotted with pre-immune sera from the same sheep into which the eEF1A-2C peptide was subsequently injected, the second, sera before purification, the third, after ammonium sulphate precipitation and fourthly, after immunoaffinity purification. Protein extracts were made from mouse tissues: B, brain; H, heart; L, liver; W, brain from a wasted mouse. The preimmune and unpurified sera were used at 1:100 in blocking buffer, and the ammonium sulphate and affinity-purified eEF1A-2 antibodies were used at 1:50 in blocking buffer. The number of bands recognised progressively decreases until a specific band of 50kD is recognised. Note that eEF1A-2 is not expressed in liver; the L and W tracks therefore act as negative controls, demonstrating a lack of cross-reactivity with eEF1A-1. The numbers next to the blots represent the size, in kilodaltons, of the bands of the prestained ladder.

5.3 Expression analysis

5.3.1 Analysis in mouse tissues

The eEF1A-2C and eEF1A-1C antibodies were used in Western blotting in a range of adult mouse tissues. The resulting blots are shown in figures 5-9 and 5-10. These confirm previous findings at the RNA level that eEF1A-2 expression in the adult mouse is confined to the brain, spinal cord, heart and skeletal muscle. No signal was detected in any of the other tissues examined, namely the kidney, spleen, thymus, liver or lung. The eEF1A-1 antibody recognised a band in all tissues studied, with the exception of adult muscle. These results also confirm the specificity of the two antibodies for their respective eEF1A isoforms.

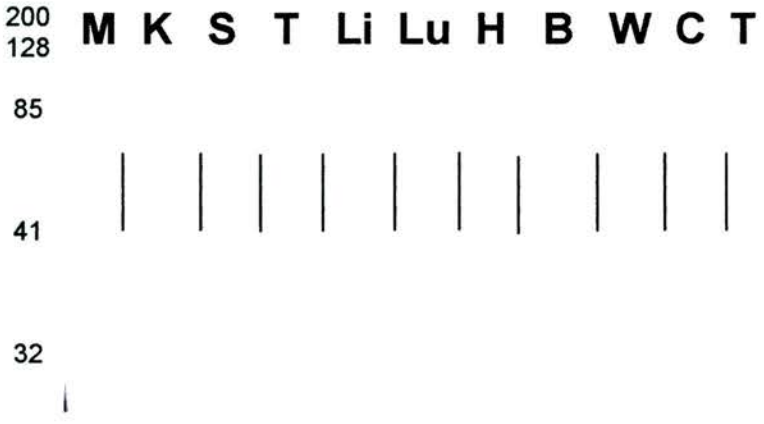

Figure 5-9 Western blot showing eEF1A-2 expression in protein extracts from a range of adult mouse tissues. M, muscle; K, kidney; S, spleen; T, thymus, Li, liver; Lu, lung; H, heart; B, brain; W, wasted brain; C, cervical spinal cord; T, thoracic spinal cord. The antibody used was the affinity-purified eEF1A-2C at a concentration of 1:50. The numbers to the left of this blot, and the blot below, represent the sizes, in kilodaltons, of the prestained ladders.

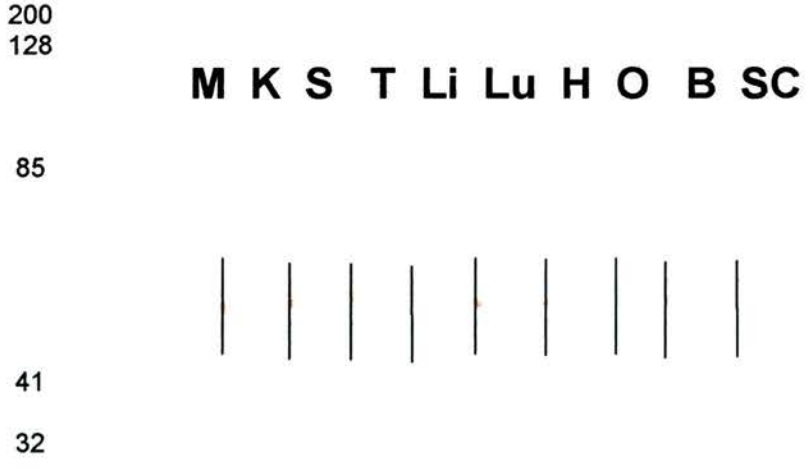

Figure 5-10 Western blot of a range of mouse tissues (as figure 5-9, with the exception that SC represents spinal cord and O, an overspill lane), blotted with the eEF1A-1C antibody at a concentration of 1:50.

Although at the start of this project the timing of the isoform switch in the central nervous system in mouse was unknown, work by Khalyfa *et al.* has subsequently shown that eEF1A-2 is present at post natal day 1 (P1) in the brain (2001). I therefore decided to investigate whether eEF1A-2 was present in the developing embryo. Western analysis on tissue extracts from 13.5 and 14.5 dpc heads showed that eEF1A-2 was indeed present in mouse embryos at those ages. The blots are shown in figure 5-11. Although it was not possible within the timescale of this project, it will therefore be of great interest to investigate the expression pattern in the embryo using *in situ* immunohistochemistry.

As the expression pattern of the two isoforms in the eye had not been investigated, I examined their expression in protein extracts made from adult eyes. This demonstrated that, at the level of whole tissue extracts, eEF1A-2, and not eEF1A-1, is expressed in mouse eyes. This is shown in figure 5-12. It is clearly possible, however, that a subset of cells within the eye are expressing eEF1A-1.

As outlined in Chapter 3, there appeared to be a gradient in the severity of the pathology seen in the spinal cord, from the cervical through the thoracic to the lumbar region. The timing of the wasted phenotype is presumably coincident with the loss of eEF1A-1. It is possible that the gradient in the pathology seen within the spinal cord is caused by a gradient in the loss of expression of eEF1A-1. It was hoped to determine the switch between eEF1A-1 and eEF1A-2 at different levels of the spinal cord. However, it was not possible to do this using Western blotting, as there are cell types other than motor neurons within the spinal cord which express eEF1A-1, so that at best a decrease in eEF1A-1 levels would be seen. A more appropriate method would therefore have been to use immunohistochemistry on spinal cord sections on mice from a number of ages. However, this was not possible as neither eEF1A-1 antibody worked in immunohistochemical experiments under a range of conditions, on either paraffin-embedded or frozen cryostat sections.

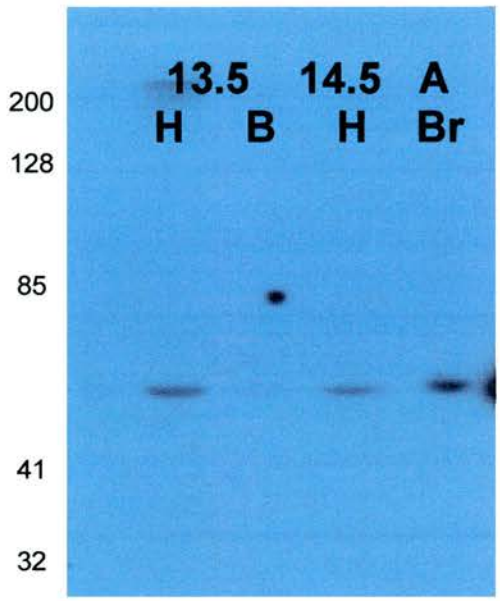

Figure 5-11 Western blot of mouse embryo tissue extracts.
The antibody used was eEF1A-2M at a concentration of 1:200.The ages of the embryos were E13.5 and E14.5 dpc. The extract from an adult brain, A Br, was used as a positive control. H, embryonic head; B, embryonic body.

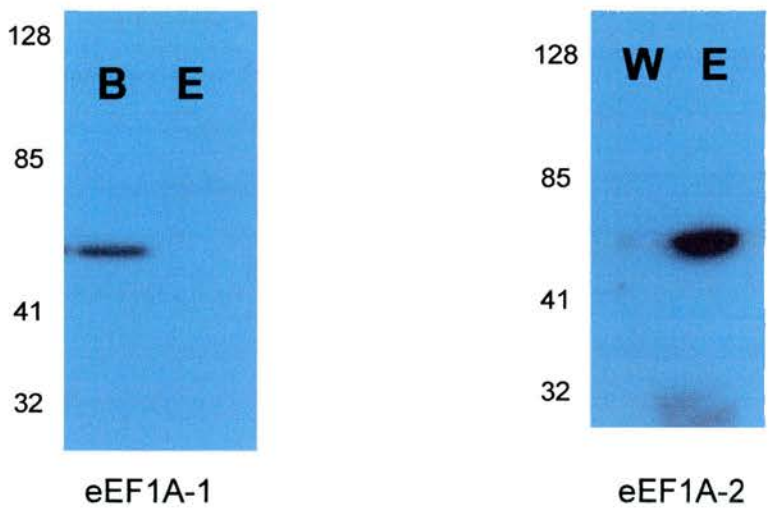

Figure 5-12 Western blots of mouse eye extracts.
The blot on the left has been probed with the eEF1A-1C antibody, at a concentration of 1:50. That on the right has been probed with the eEF1A-2C antibody, at a concentration of 1:200. E, adult eye; B, brain eEF1A-1 positive control; W, wasted brain eEF1A-2 negative control. The numbers to the left of the blots in figures 5-11 and 5-12 are the sizes, in kilodaltons, of the prestained ladders.

To try to determine the subcellular localisation of eEF1A-2, I analysed its expression in wild type mouse spinal cords using immunohistochemistry. This is shown in figure 5-13. Expression was observed in the neuronal cytoplasm. However, it was not possible to determine whether eEF1A-2 was also expressed in the dendrites. In order to do this, it was deemed necessary to perform immunofluorescent expression analysis in cultured cells.

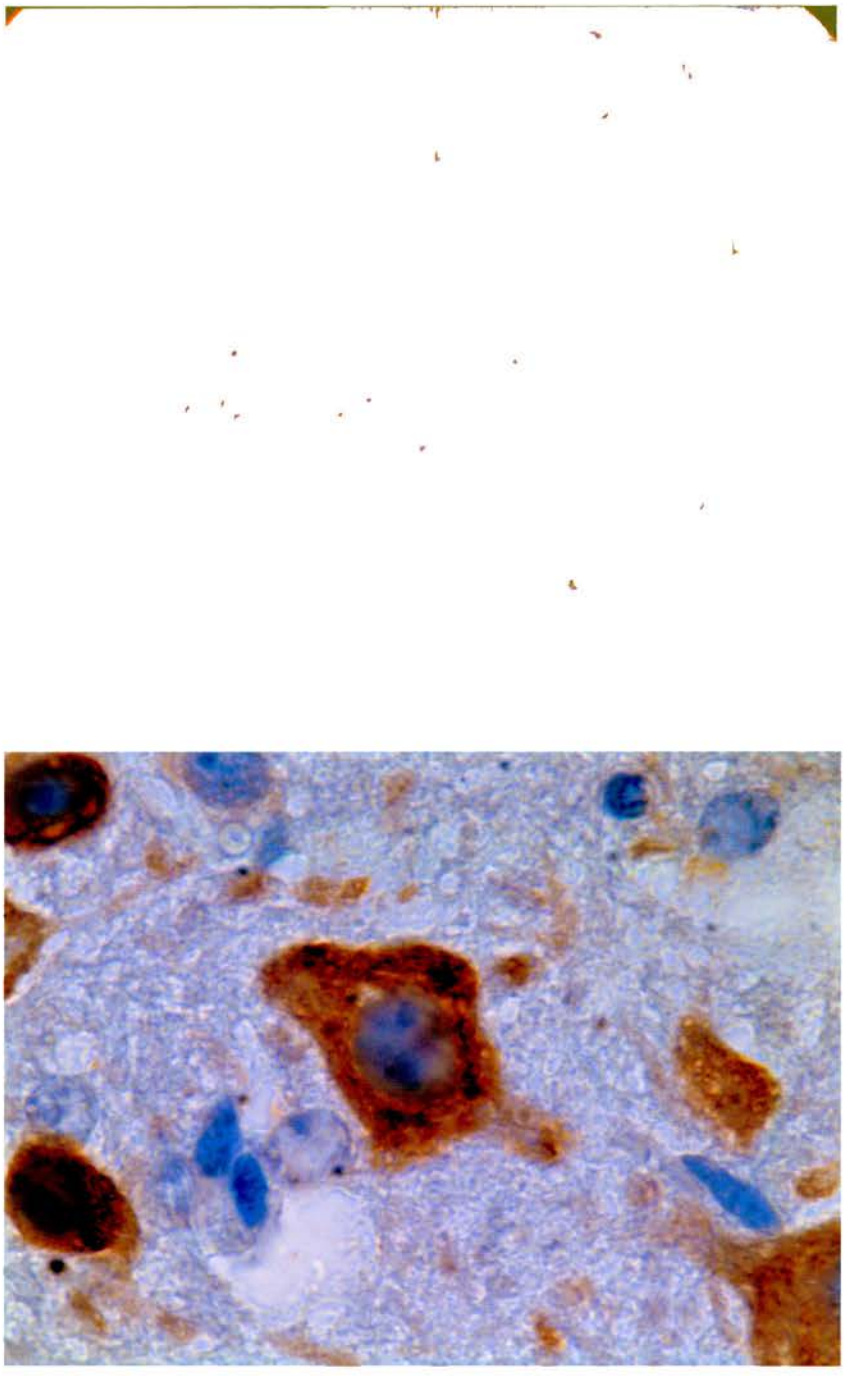

Figure 5-13 Immunohistochemistry on sections through spinal cord of 28-day +/*wst* mouse, using the eEF1A-2C antibody at a concentration of 1:10, showing cytoplasmic neuronal staining. The top slide shows the whole spinal cord, at a magnification of 1:10, and the bottom slide a close-up of the anterior horn region, at a magnification at 1:100.

5.3.2 Analysis in cells

5.3.2.1 Establishing a cell culture system

It still not known why two elongation factor isoforms are required in neurons. It may be that one (or more) of the non-canonical functions of eEF1A-2 is (or are) important. For example, eEF1A-2 may be necessary for an as yet unidentified cytoskeletal function which is particularly important for neurons, with their large cytoplasmic volumes and long axons. An alternative hypothesis is that neurons have both forms because they function slightly differently in translation. Neurons have an unusual property in that translation occurs both at the cell body and at the synapse (Job and Eberwine, 2001a; Job and Eberwine, 2001b). It is therefore conceivable that eEF1A-2 is required for synaptic translation, particularly as the peak expression of eEF1A-2 coincides with the completion of synaptogenesis. A key experiment is therefore to determine the relative subcellular localisation of the two isoforms in neurons, which, as outlined in Chapter 1, section 1.3.2.3, has not been definitively characterised.

To this end I investigated a cell system for study. The PC-12 cell line was originally derived from a rat pheochromocytoma (Greene and Tischler, 1976). On exposure to nerve growth factor-β (NGF-β), they differentiate, growing processes so that they resemble neurons. I investigated the expression of the two eEF1A isoforms in PC-12 cells. Using Western blotting, I showed that that they were expressing both eEF1A-1 and eEF1A-2, both before and after differentiation (figure 5-14). Petroulakis *et al.* subsequently confirmed this result (Petroulakis and Wang, 2002). I also investigated the expression of eEF1A-1 and eEF1A-2 in the human cell line SH-SY5Y, originally derived from a neuroblastoma (Biedler *et al.*, 1978). This cell line was also found to express both isoforms. Westerns are also shown in figure 5-14.

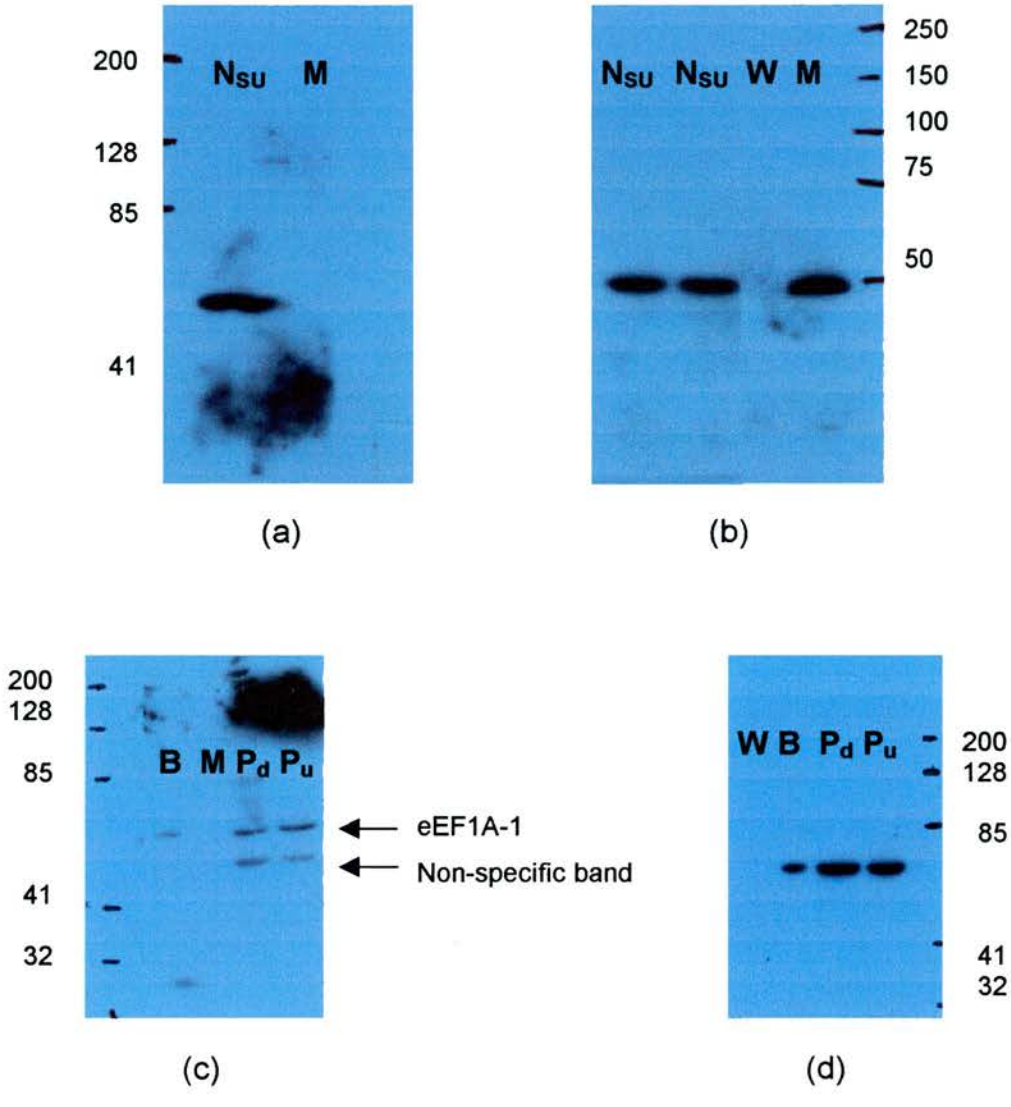

Figure 5-14 Expression of eEF1A isoforms in cell lines.
(a) shows the expression of eEF1A-1 in the neuroblastoma cell line SU-SY5Y, (b); eEF1A-2 in SU-SY5Y cells, (c); eEF1A-1 in PC-12 cells , (d); eEF1A-2 in PC-12 cells. Abbreviations are as follows: N_{SU}, SU-SY5Y cell extracts; M, wild type muscle; W, wasted brain; B, wild type brain; P_d, differentiated PC-12 cells; P_u, undifferentiated PC-12 cells. Muscle is an eEF1A-1 negative control; Wasted brain, an eEF1A-2 negative control, and wild-type brain a positive control for both isoforms. The eEF1A-1 antibody was used at a concentration of 1:50, and the eEF1A-2 antibody at a concentration of 1:200. 15μg total protein extract was loaded on the gel. The numbers next to the autoradiograms represent the sizes, in kilodaltons, of the prestained ladders.

5.3.2.2 Subcellular localisation experiments

Unfortunately, it was not possible to obtain a specific signal using immunofluorescent detection on either cell line, using either of the eEF1A-2 antibodies. Different fixation methods, namely 50:50 acetone:methanol, ice-cold methanol and paraformaldehyde were used. Primary antibody concentrations from 1:10 to 1:1 000 were also tried. However, in all cases the signal obtained resembled that obtained with the preimmune serum, as shown in figure 5-15. This signal was not decreased on preabsorption of the primary antibody with different concentrations from 0.01 to 1.0 ng/µl antibody solution, of the peptide against which the antibody was raised, confirming that the signal obtained was not specific.

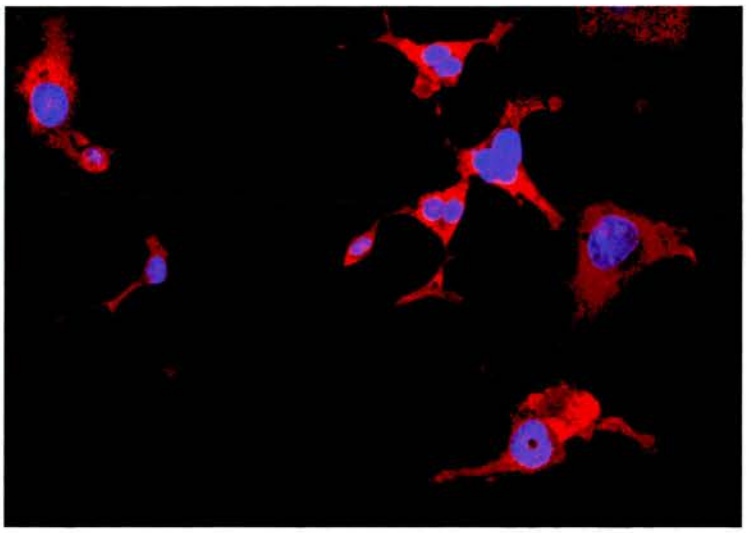

eEF1A-2C, x 16

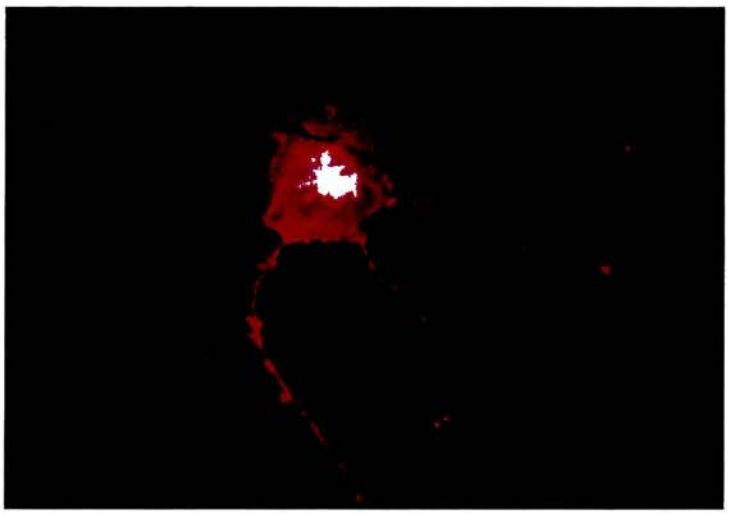

Preimmune serum, x100

Figure 5-15 Immunofluorescence analysis in PC-12 cells.
The top figure is of cells stained with eEF1A-2C at a concentration of 1:100, and the bottom figure, with pre-immune serum from the same animal, also at a concentration of 1:100. Although the signal obtained with the eEF1A-2C antibody appears to show cytoplasmic staining, a similar signal is obtained using the pre-immune serum.

5.4 Discussion

5.4.1 Specificity of antibodies

During this PhD I have produced antibodies which are completely specific for the two eEF1A isoforms, that is, two antibodies which recognise eEF1A-2 and not eEF1A-1, and one antibody which labels eEF1A-1 and not eEF1A-2. Although an early eEF1A-2 antibody, raised against the whole protein, has been described, no evidence of its specificity was provided (Liu *et al.*, 1993). Moreover, the more recently reported eEF1A-1 antibody described by Khalyfa *et al.* recognises a band in muscle, in which there is no evidence of eEF1A-1 expression (Khalyfa *et al.*, 2001). Their antibodies to both isoforms also recognise a number of non-specific bands. Other studies have inferred the localisation of eEF1A-2 using an antibody which actually recognises eEF1A-1 (McClatchy *et al.*, 2002). My antibodies will therefore be useful for the further expression analysis of eEF1A-1 and eEF1A-2, both on tissues and in cells.

5.4.2 Expression in tissues

The results hereby confirm the expression results obtained at the RNA level. It also confirms the limited findings of Khalyfa *et al.* (Khalyfa *et al.*, 2001), who demonstrated that the eEF1A-2 protein is expressed in the brain, heart and skeletal muscle. However, in order to do so, they immunoprecipitated both isoforms from the respective tissues, using an antibody which recognised both eEF1A-1 and eEF1A-2, and then blotted them with the isoform-specific antibodies. In contrast, I have investigated the expression of both isoforms directly on a Western blot from tissue extracts.

I have demonstrated that eEF1A-2 is expressed at least as early as E13.5 in embryonic development. As expression at this embryonic stage is quite strong, it is probably expressed at an even earlier stage. It would therefore be interesting to track the expression of eEF1A-2 during embryonic development. Given that it is expressed in the eyes of adult mice, it would also be interesting to track its expression during

the embryonic development of the eye. It would also be worthwhile to investigate the expression in the eyes of adult mice using immunohistochemistry, to identify the cell types which express eEF1A-2. Cell types which might be expected to express eEF1A-2 include photoreceptor cells, which have an elongated cytoplasm reminiscent of neurons and might therefore share their requirement for eEF1A-2, muscle cells and neuronal cells such as bipolar cells.

5.4.3 Expression in cells

It was hoped to analyse the subcellular localisation of eEF1A-2. Although this has been described in mouse brains, the resolution in this case was not sufficient to be able to tell, for example, whether eEF1A-2 is expressed at the synapse (Khalyfa *et al.*, 2001). It is interesting to speculate that the second eEF1A isoform is required for synaptic translation. Unfortunately, it was not possible to obtain a specific signal for eEF1A-2 in PC-12 or neuroblastoma cells. Although a signal was obtained using DAB staining on paraffin-embedded sections, this method did not give sufficient resolution. It is possible, therefore, that it would be necessary to transfect a tagged *Eef1a2* cDNA into the cells and analyse the expression pattern obtained. However, this approach does risk obtaining an expression pattern which does not accurately reflect the *in vivo* situation.

6 Chapter 6 - eEF1A isoforms in *Xenopus Laevis*

6.1 Introduction

6.1.1 *Xenopus laevis*

There are seven recognised species of *Xenopus*, of which the aquatic *X. laevis*, the African Clawed Frog, is the most common. They are members of the family *Pipidae*. At spawning, between 300 and 1000 eggs are released. Within 3 days, the larvae hatch, and reach metamorphosis in around two months in conditions of plentiful food. They can breed from about 18 months of age onwards. Females can live for up to 15 years in captivity, and grow continuously. Males, however, stop growing at between two and four years of age (Deuchar, 1975).

X. laevis have been used in science for many years – an early use was in pregnancy testing. However, they are better known as a model system in developmental biology, due to the large size, transparency and external development of their embryos. These are also robust, as each egg carries its own power source in the form of its yolk, so that they can be transplanted. Genetic techniques have been developed which have given great insights into genes involved in embryogenesis. However, a major drawback to the use of *X. laevis* as a model system is that they are allotetraploid, that is, they have double the usual number of chromosomes. Although in this case it is relatively straightforward to add genes, it becomes much harder to subtract them, as four copies of a gene may need to be inactivated. In addition, many genes are represented by extra copies which may or may not be functional. The animals also take a long time to reach sexual maturity, resulting in a long generation time which is not amenable to multi-generation experiments. Because of these factors, attention has become focused on *Xenopus tropicalis* (see Amaya *et al.* and related links). Indeed, the genome of *X. tropicalis* is currently being sequenced. A summary of some of the important differences between the two species is given in table 6-1.

Species	*X. laevis*	*X. tropicalis*
Ploidy	Allotetraploid	Diploid
Chromosomes	36	20
Genome Size	3.1×10^9	1.7×10^9
Optimal Temp.	16-22^{0}C	25-30^{0}C
Adult Size	10 cm	4-5 cm
Egg Size	1.0-1.3 mm	0.7-0.8 mm
Eggs/Spawn	300-1000	1000-3000
Generation time	1-2 years	< 5 months

Table 6-1. Comparison of *X. laevis* and *X. tropicalis* (from Amaya *et al.*).

6.1.2 eEF1A isoforms in *X. Laevis*

Two main isoforms of eEF1A have been described in *X. laevis*. Although the early literature describes these as EF-1αO and EF-1αS, I will subsequently refer to these as eEF1A-O and eEF1A-S respectively, to maintain consistency of nomenclature. eEF1A-O is expressed in mature oocytes, spermatogonia and primary spermatocytes and, transiently, in early embryos (Abdallah *et al.*, 1991a; Dje *et al.*, 1990). The somatically expressed eEF1A-S is expressed in adult liver (Dje *et al.*, 1990) and in a small region of the oocyte cytoplasm known as the mitochondrial mass or Balbiani body (Viel *et al.*, 1990). It is also expressed in the germ cells of the gonad prior to metamorphosis (Abdallah *et al.*, 1996). At metamorphosis there is a switch from the somatic to the oocyte-specific form in the germ cells. At the amino acid level, the eEF1A-O and eEF1A-S proteins are 91% identical.

eEF1A-S is a major transcript from the midblastula transition (MBT) onwards in early embryogenesis, representing up to 40% of the total polyadenylated transcripts (Krieg *et al.*, 1989). It is at the midblastula transition that embryonic sequences begin to be transcribed into mRNA. Up until this point, only maternal sequences from the oocyte are transcribed. The high levels of eEF1A-S may be required by the early embryo in order to accumulate large amounts of translational machinery, or may reflect the requirement for some other, uncharacterised, function. In gastrula-stage embryos, two alternative cDNAs have been identified which differ from each other at 3.5% of nucleotide positions, but have no resulting amino acid differences in the encoded proteins (Potting *et al.*, 1990). One of these differs from the eEF1A-S

sequence obtained by Krieg *et al.* (Krieg *et al.*, 1989) at only three nucleotide positions, but all three changes lead to amino acid substitutions, one of them non-conservative. These alternative cDNAs probably represent expressed retropseudogenes, as several have been identified (Abdallah *et al.*, 1991a), including one with similarity to one of the cDNAs identified by Potting *et al.* (Potting *et al.*, 1990). They may, however, represent functional genes which have been duplicated as a result of the allotetraploidy of the *X. laevis* genome.

There is a third eEF1A isoform, described as 42Sp50, 42Sp48 or thesaurin a, which is expressed in immature oocytes and pre-meiotic germ cells (oogonia) (Abdallah *et al.*, 1991b; Dje *et al.*, 1990; Viel *et al.*, 1987). It appears to be encoded by two different genes (Coppard *et al.*, 1991). With 69% identity at the amino acid level with eEF1A-O and eEF1A-S, this isoform is much more diverged, especially at the C- and N-termini (Dje *et al.*, 1990). However, although it is structurally similar to both eEF1A-1 and the bacterial EF-Tu (Viel *et al.*, 1991), it appears to be used mainly in the storage of tRNAs (Morales *et al.*, 1993).

X. laevis eEF1A-S is 96% identical to human eEF1A-1 (Potting *et al.*, 1990). There are no reports in the literature of an equivalent of the mammalian eEF1A-2, that is, an isoform of eEF1A which is expressed only in the CNS, heart and skeletal muscle. This is perhaps surprising, given that amphibians also have a central nervous system. It is difficult to reconcile a need for an isoform switch to eEF1A-2 in neurons with the lack of an eEF1A-2 orthologue in *X. laevis*. On searching the *X. laevis* EST database at NCBI with the mouse *Eef1a2* sequence, Dr. C. Abbott noted ESTs generated from brain, eye and heart libraries which, once translated, were more like eEF1A-2 than any of the known *X. laevis* EEF1A isoforms. It is therefore possible that there is an eEF1A-2 orthologue in *X. laevis*. I investigated this possibility using expression analysis and sequencing.

6.2 Results

6.2.1 Expression analysis of eEF1A isoforms in *X. laevis*

In order to test the hypothesis that an orthologue of eEF1A-2 exists in *X. laevis*, and, as in mammals, is expressed in a tissue-specific and developmentally-regulated manner, I used anti-eEF1A-1 and anti-eEF1A-2 antibodies on a range of tissue extracts from an adult female frog and also on a late gastrula-stage embryo. I used both our sheep anti-eEF1A-2 antibodies and an antibody raised in rabbit against the eEF1A protein from the brine shrimp, *Artemia salina* (Sanders *et al.*, 1996). As described in Chapter 5 (section 5.2.1), the eEF1A-2M antibody was raised against a peptide in the centre of the mouse protein, whereas eEF1A-2C recognises a peptide near its C-terminus.

6.2.1.1 eEF1A expression is tissue-specific

The eEF1A-2M antibody recognised a single band of approximately 50kD (and the same size as the band in a positive control mouse brain sample) on a Western blot of a range of adult tissues from *X. laevis*. This is shown in figure 6-1. A band was present in the extracts from brain, spinal cord, optic ganglion and muscle. A weaker band was also seen in heart. No signal was observed in liver, gall bladder, lung, kidney, spleen or oocyte. Neither of the sheep anti-eEF1A-1 antibodies which I generated recognised a specific band in tissue extracts from *X. laevis* (data not shown). However, the antibody raised against the *A. salina* eEF1A protein recognised a protein of approximately 50kD present in spleen, kidney, lung, liver, gall bladder, heart, spinal cord and brain (figure 6-1). No signal was observed in muscle, optic ganglion or oocyte.

These data are compatible with the idea that there is an additional, tissue-specific eEF1A isoform. This *X. laevis* orthologue of eEF1A-2 is expressed in the same tissues as those of the previously studied mammalian species (rat, mouse and human); namely the central nervous system, skeletal muscle and heart. For clarity, this novel isoform will subsequently be described as XeEF1A-2. The other isoform is

expressed in the same tissues as the mammalian eEF1A-1. It is probable that this isoform is the previously described eEF1A-S. The two isoforms are distinct from the oocyte-specific eEF1A-O, as neither of the antibodies used recognised a band in oocyte tissue extracts.

eEF1A-1:

eEF1A-2:

Figure 6-1 Western blots of a range of adult *X. laevis* tissues.
The top filter was blotted using the anti-*A. salina* eEF1A antibody at a concentration of 1:50, and the bottom filter using our eEF1A-2M antibody at 1:20. The tissues used were as follows: OG, optic ganglion; B, brain; SC, spinal cord; M, muscle; H, heart; O, oocyte; Li; liver; GB, gall bladder; Lu, lung; K, kidney; S, spleen; C, control. The positive control sample in the last lane was a protein extract from a human neuroblastoma cell line which expresses both eEF1A-1 and eEF1A-2. The 50kD band corresponding to eEF1A-1 and eEF1A-2 is arrowed.

The eEF1A-2C antibody recognised bands of approximately 50kD in all adult tissues, with the exception of oocyte. A Western blot is shown in figure 6-2. However, the band in muscle and heart was slightly larger than in liver, lung and spleen. This suggests that the eEF1A-2C antibody recognises both eEF1A-S and XeEF1A-2, and that eEF1A-2 is slightly larger than eEF1A-S isoform. This is consistent with the situation in the rat, in which eEF1A-2 has been described as 0.5kD larger than eEF1A-1 (Petroulakis and Wang, 2002). As the two proteins differ in size by only one amino acid (of 462 or 463 residues), it is possible that that this difference is as a result of posttranslational modifications. However, although a number of modifications have been described for eEF1A-1, including phosphorylation (Keilbassa *et al.*, 1995; Venema *et al.*, 1991), the methylation of lysine residues (Dever *et al.*, 1989) and the addition of ethanolamine-phosphoglycerides (Rosenberry *et al.*, 1989; Whiteheart *et al.*, 1989) no such modifications have been described for eEF1A-2 in any species.

Figure 6-2 Western blot of a range of adult *X. laevis* tissues, using the eEF1A-2C antibody at a concentration of 1:20. Tissues used are: M, muscle, H, heart, Lu, lung, S, spleen. B represents a mouse brain extract used as a control.

6.2.1.2 XeEF1A-2 expression is developmentally regulated

As there appeared to be an orthologue of eEF1A-2 in *X. laevis*, I decided to determine whether this protein is developmentally regulated in these frogs, as it is in mammals.

The anti-*A. salina* eEF1A and eEF1A-2M antibodies were used in an immunoblot of protein extracts from a late gastrula stage embryo. Immunoblotting with the anti-*A. salina* eEF1A antibody resulted in a very strong 50kD band (figure 6-3). No band was observed using the eEF1A-2M antibody. Thus, whilst *X. laevis* adult tissues have two isoforms, antigenically similar to eEF1A-1 and eEF1A-2, early embryos have only one form, antigenically similar to eEF1A-1. In *X. laevis*, XeEF1A-2 is thus developmentally regulated. Further work, is, however, required to determine from which stage in *X. laevis* development this novel isoform is expressed.

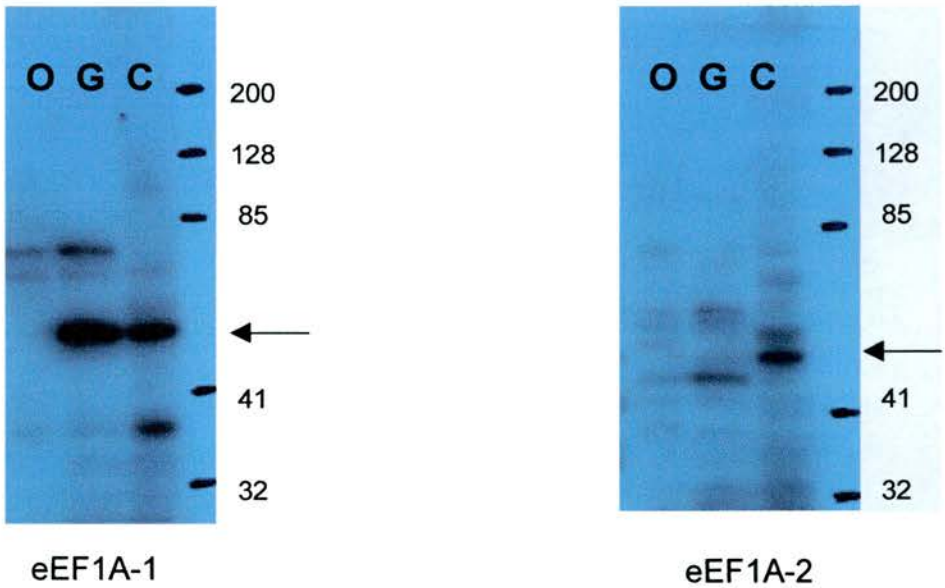

Figure 6-3 Western blots of gastrula-stage embryos.
The left-hand filter was blotted with the anti-*A. salina* eEF1A antibody at 1:50, and the right-hand filter with the eEF1A-2M antibody at 1:20. The samples used were: O, adult oocyte; G, gastrula and C, control, a cell extract from a human neuroblastoma cell line which expresses both eEF1A-1 and eEF1A-2. The band representing eEF1A-1 or eEF1A-2 is arrowed. Note that there are also some non-specific bands, particularly at just smaller than 50kD in gastrula, using eEF1A-2. The numbers to the right of the autoradiograms represent the sizes, in kilodaltons, of the prestained ladders.

6.2.2 Completing sequence of XeEF1A-2

In the available EST sequence of the XeEF1A-2, there was a gap which resulted in a break in the deduced amino acid sequence of 77 residues. This is demonstrated in figure 6-4. In order to generate full-length cDNA sequence and to confirm the identity of this as an eEF1A-2 orthologue, the mRNA was sequenced. RNA was extracted from muscle and reverse transcribed into cDNA. RT-PCR primers were designed from the EST sequence information to specifically amplify mRNA from XeEF1A-2. The location of the primers within the RNA is shown in figure 6-4. A product of 625bp, the expected size based on alignment with the mouse eEF1A-2 sequence, was successfully amplified from the cDNA generated from adult muscle. This was then sequenced in duplicate in both directions. An agarose gel showing the RT-PCR product obtained is shown in figure 6-5, and a typical sequence trace obtained is shown in figure 6-6. The completed nucleotide sequence obtained is shown in figure 6-7. It was translated into amino acids, and the protein sequence thus obtained is shown in figure 6-7. This was then aligned with the other known mouse eEF1A and *X. laevis* eEF1A protein sequences, using the multiple alignment general interface (MAGI). The alignment is shown in figure 6-8.

```
M1a2   GAGAGATAAAACCGCCGGCGCCGGGCCACCAGTCCTTCTGACTGAGTCCTCGGCTCTGGA
Xen1   ----------GCCGTCAATAGGTGGACCCCTCCCGGAGAAATAAAACTGCCTGATCCGGA

M1a2   GTTCCTGCCCAGCATATACCTCAACCCCAAACCAGAGCCCCCACAGTGCCAGCCCCTCCC
Xen1    GCCGCCAGCCCCTGC-TGTCTGAGAGCTCGGCTACAGACTTCCTTGCACTCACCGTAGTG

M1a2   TCACCCA-GGCAGAATGGGCAAGGAGAAGACACACATCAACATTGTGGTCATTGGCCACG
Xen1   TCACCCCCAGGAGGATGGGGAAAGAGAAGACACACATCAACATCGTGGTTATTGGCCACG
Pr                   M  G  K  E  K  T  H  I  N  I  V  V  I  G  H  V

M1a2   TGGACTCAGGCAAGTCCACCACGACAGGCCACCTCATCTACAAGTGTGGTGGCATCGACA
Xen1   TGGACTCTGGCAAGTCCACCACCACTGGCCACCTGATCTACAAGTGTGGAGGCATCGACA
Pr       D  S  G  K  S  T  T  T  G  H  L  I  Y  K  C  G  G  I  D  K

M1a2   AGCGGACCATCGAGAAGTTTGAGAAGGAGGCAGCAGAGATGGGGAAGGGCTCTTTTAAAT
Xen1   AAAGGACAATAGAGAAGTTTGAGAAGGAAGCACCTGACATGGGGAAAGGTTCCTTTAAAT
Pr       R  T  I  E  K  F  E  K  E  A  P  D  M  G  K  G  S  F  K  Y

M1a2   ATGCCTGGGTGCTGGACAAGCTGAAGGCCGAGCGGGAACGGGGCATCACCATCGACATCT
Xen1   ACGCTTGGGTTTTGGACAAACTGAAGGCTGAGAGGGAGCGAGGAATCACCATTGATATCC  Xen1A2F2
Pr       A  W  V  L  D  K  L  K  A  E  R  E  R  G  I  T  I  D  I  P

M1a2   CCCTCTGGAAGTTTGAGACCACCAAGTACTACATCACCATCATCGATGCTCCAGGACACC
Xen1   CCCTGTGGAAGTTTGACACAACCAAATATTATATCACCATCATTGATGCTCCATGACATC
Pr       L  W  K  F  D  T  T  K  Y  Y  I  T  I  I  D  A  P  *  H  R

M1a2   GAGACTTCATCAAGAATATGATTACAGGCACATCCCAGGCCGACTGTGCAGTACTGATCG
Xen1   GAGACTTTATCAAGAATATGATCACTGGAACCTCTCACGCAGACTGTTCATTGCTGATAG
Pr       D  F  I  K  N  M  I  T  G  T  S  H  A  D  C  S  L  L  I  V

M1a2   TCGCAGCCGGTGTGGGCGAGTTTGAGGCGGGCATCTCCAAGAACGGGCAAACCCGGGAAC
Xen1   TGGCACCCGGGGCGGGTGAGTTTGA----------------------------------
Pr       A  P  G  A  G  E  F

M1a2   ACGCACTCCTGGCCTACACTCTGGGTGTGAAGCAGCTCATTGTGGGTGTCAACAAGATGG
       ------------------------------------------------------------

M1a2   ACTCCACGGAACCAGCCTACAGCGAGAAGCGCTATGATGAGATTGTTAAGGAGGTCAGCG
       ------------------------------------------------------------

M1a2   CCTACATCAAGAAGATCGGCTACAACCCAGCCACGGTGCCCTTCGTGCCCATCTCGGGCT
Xen2   ----------------------------------------TTTGTACCCATTTCTGGCTG

M1a2   GCATGGTGACAACATGCTGGAGCCTTCACCTAATATGCCATGGTTCAAAGGCTGGAAAGT
Xen2   GCATGGGGATAACATGTTGGAGCCCTCTCCCAATATGCCATGGTTCAAGGGATGGAAAGT
Pr                   M  L  E  P  S  P  N  M  P  W  F  K  G  W  K  V

M1a2   AGAGCGTAAGGAAGGAAATGCAAGCGGCGTGTCCCTGCTGGAAGCCCTGGACACAATCCT
Xen2   GGAGAGGAAGGAAGGCAATGCAAATGGAGTTTCCCTGCTTGAGGCTTTGGACACCATCCT
Pr       E  R  K  E  G  N  A  N  G  V  S  L  L  E  A  L  D  T  I  L

M1a2   GCCCCCCACCCGCCCCACTGACAAGCCCCTTCGTCTGCCTCTGCAGGATGTGTACAAGAT
Xen2   CCCTCCATCTCGCCCAACAGACAAACCTCTCCGTCTTCCTCTGCAAGATGTCTATAAAAT
Pr       P  P  S  R  P  T  D  K  P  L  R  L  P  L  Q  D  V  Y  K  I

M1a2   TGGGGGCATTGGGACCGTGCCTGTGGGCCGAGTGGAGACCGGTATCCTCCGGCCTGGTAT
Xen2   TGGAGGAATCGGCACTGTTCCAGTAGGTCGAGTGGAGACCGGCATTCTAAAGCCAGGCAT  Xen1A2R1
Pr       G  G  I  G  T  V  P  V  G  R  V  E  T  G  I  L  K  P  G  M

M1a2   GGTGGTGACCTTTGCGCCAGTCAACATCACCACAGAGGTGAAGTCTGTGGAAATGCACCA
Xen2   GGTGGTGACCTTTGCTCCAGTCAATATCACAACTGAGGTAAAGTCTGTTGAGATGCATCA
Pr       V  V  T  F  A  P  V  N  I  T  T  E  V  K  S  V  E  M  H  E
```

Figure 6-4 Figure legend and continuation of sequences on following page.

```
M1a2   TGAGGCACTTAGCGAGGCCCTGCCTGGTGACAATG-TCGGGTTCAATGTGAAGAATGTGT
Xen2   TGAGGCTCTGAGTGAGGCTCTGCCTGGGGACAATGGTTGGCTTCAACGTCAAGAACGTGT
Pr      A  L  S  E  A  L  P  G  D  N  V  G  F  N  V  K  N  V  S  V

M1a2   CCGTTAAGGATATTCGCCGGGGCAATGTCTGCGGGGACAGCAAAGCTGACCCGCCTCAGG
Xen2   CAGTCAAGGACATTCGCAGAGGCAATGTTTGTGGTGACAGCAAGACTGACCCTCCCCAGG
Pr      K  D  I  R  R  G  N  V  C  G  D  T  K  T  D  P  P  Q  E  P

M1a2   AGGCTGCCCAGTTCACCTCTCAGGTTATCATCCTGAACCACCCTGGGCAAATCAGCGCTG
Xen2   AAGCCGCAGGTTTCACTGCTCAGGTGATCATCTTGAACCACCCTGGTCAGATCAGTGCTG
Pr      A  G  F  T  A  H  V  I  I  L  N  H  P  G  Q  I  S  A  G  Y

M1a2   GCTACTCGCCAGTCATCGACTGTCACACGGCCCACATTGCCTGCAAGTTTGCCGAGCTAA
Xen2   GATATTCCCCAGTTATTGACTGCCATACTGCACATATCGCCTGTAAGTTTGCAGAGCTAA
Pr      S  P  L  I  D  C  H  T  A  H  I  A  C  K  F  A  E  L  K  E

M1a2   AGGAGAAGATTGACCGTCGTTCTGGCAAGAAGCTGGAGGACAACCCCAAGTCCCTGAAGT
Xen2   AAGAAAAGATTGATCGCCGATCTGGCAAAAAGCTTGAGGACAACCCCAAGTCTCTGAAAT
Pr      K  I  D  R  R  S  G  K  K  L  E  D  N  P  K  S  L  K  S  G

M1a2   CTGGTGATGCAGCAATTGTAGAGATGGTCCCTGGAAAACCAATGTGTGTGGAGAGCTTCT
Xen2   CTGGAGATGCTGCCATTGTGGAGATGGTCCCTGGGAAGCCTATGTGTGTGGAGAGCTTCT
Pr      D  A  A  I  V  E  M  V  P  G  K  P  M  C  V  E  S  F  S  Q

M1a2   CACAGTACCCACCCCTCGGCCGCTTCGCCGTGCGAGACATGCGGCAGACTGTGGCCGTGG
Xen2   CCCAATACCCACCTCTTGGGCGCTTTGCTGTGAGAGACATGAGGCAGACTGTGGCCGTGG
Pr      Y  P  P  L  G  R  F  A  V  R  D  M  R  Q  T  V  A  V  G  V

M1a2   GCGTCATCAAGAACGTGGAGAAGAAGAGCGGCGGCGCCGGCAAGGTCACAAAATCCGCAC
Xen2   GAGTCATTAAGAACGTGGAGAAGAAAATCGGAGGAGCTGGCAAGGTGACAAAGTCCGCAC
Pr      I  K  N  V  E  K  K  I  G  G  A  G  K  V  T  K  S  A  Q  K

M1a2   AGAAGGCGCAGAAAGCGGGCAAGTGAACCGGCGCCCGGCGAGGCCCTGCGCGCCCCCAGC
Xen2   AGAAAGCCCAGAAGGCTGCAAAATGAATTGCCG----------------GTTCCCTTCGC
Pr      A  Q  K  A  A  K

M1a2   CCCGCCCCCGGCACTGGCCCCTGCCCCGCCCCAGCGCGGCCCCTCTGCCCCGACCCCCTG
Xen2   CTGGCACACAAGCCTTGTCCCT--------CTGAGAAGGTCCTTC--CCCTTACCTTTG-

M1a2   CCAGGCGCATGTCTGCACCTCCGCTTGTAAGAGGCTCTACGTCAGCGACTGGATGCTCGC
Xen2   --AGGTGCACGCGAGCCCATCTGCTTGTAAAAGCCTGTACGTCAACGACTGGATGCTCAC

M1a2   CATCAAAGTCCAGTGGAAATTCTTCAAGAGGAAAAGCGCCCCCAGGCTTCGCCAGCGCTC
Xen2   CATTAAAGTCCAGTGGAAGTTCTTTAAGAGGAAAAGCATGCTCCTGCTCTGTAATC----

M1a2   ACCACGCTCAGTGCCCGTTTTCCCAAT-AAACTGA-GCGAC-CCCA--------
Xen2   ------TTTAGTGTCCATTTTACCAATTAAACTGGTACAACATTCAAACAATAT
```

Figure 6-4 Line-up of mouse *Eef1a2* mRNA sequence (`M1a2`) with *X. laevis* EST sequences: `Xen1`, from BG814373, available through NCBI (http://www.ncbi.nlm.nih.gov); `Xen2`, from TC28037, available through TIGR (http://www.tigr.org/tdb/xgi) and `Pr`, deduced amino acid sequence of *X. laevis* ESTs. The sequences used for the RT-PCR primers are underlined. `Xen1` and `Xen2` represent either end of the predicted eEF1A-2 orthologue.

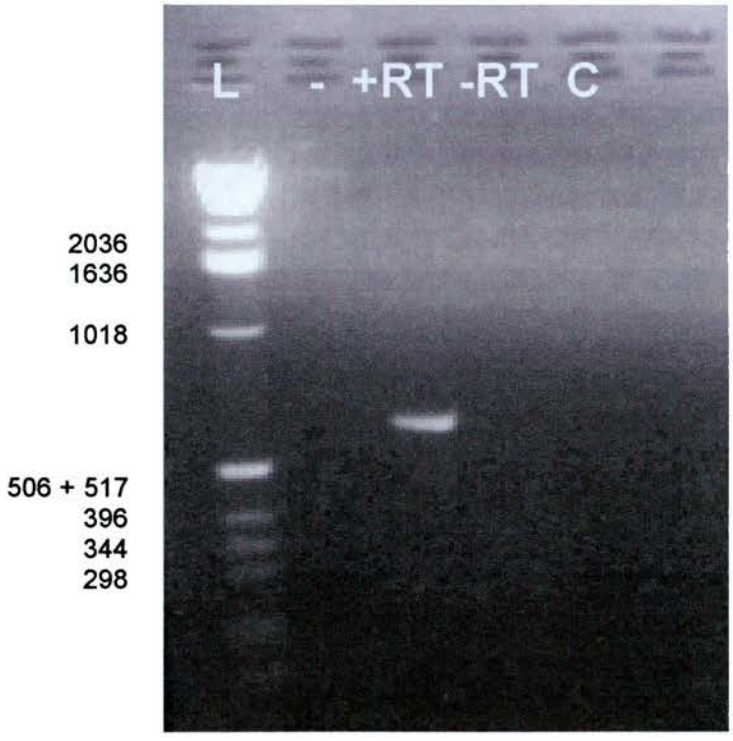

Figure 6-5 Agarose gel (2%) showing RT-PCR product obtained from *X. laevis* adult muscle. Lanes are: L, Gibco 1kb ladder; -, no sample; +RT, reverse transcriptase in cDNA synthesis reaction; -RT, no reverse transcriptase; C, PCR control with no DNA. The sizes of the bands in the 1kb ladder are given to the left of the gel picture. The expected size of the RT-PCR product, based on alignment with the mouse mRNA sequence, is 625bp.

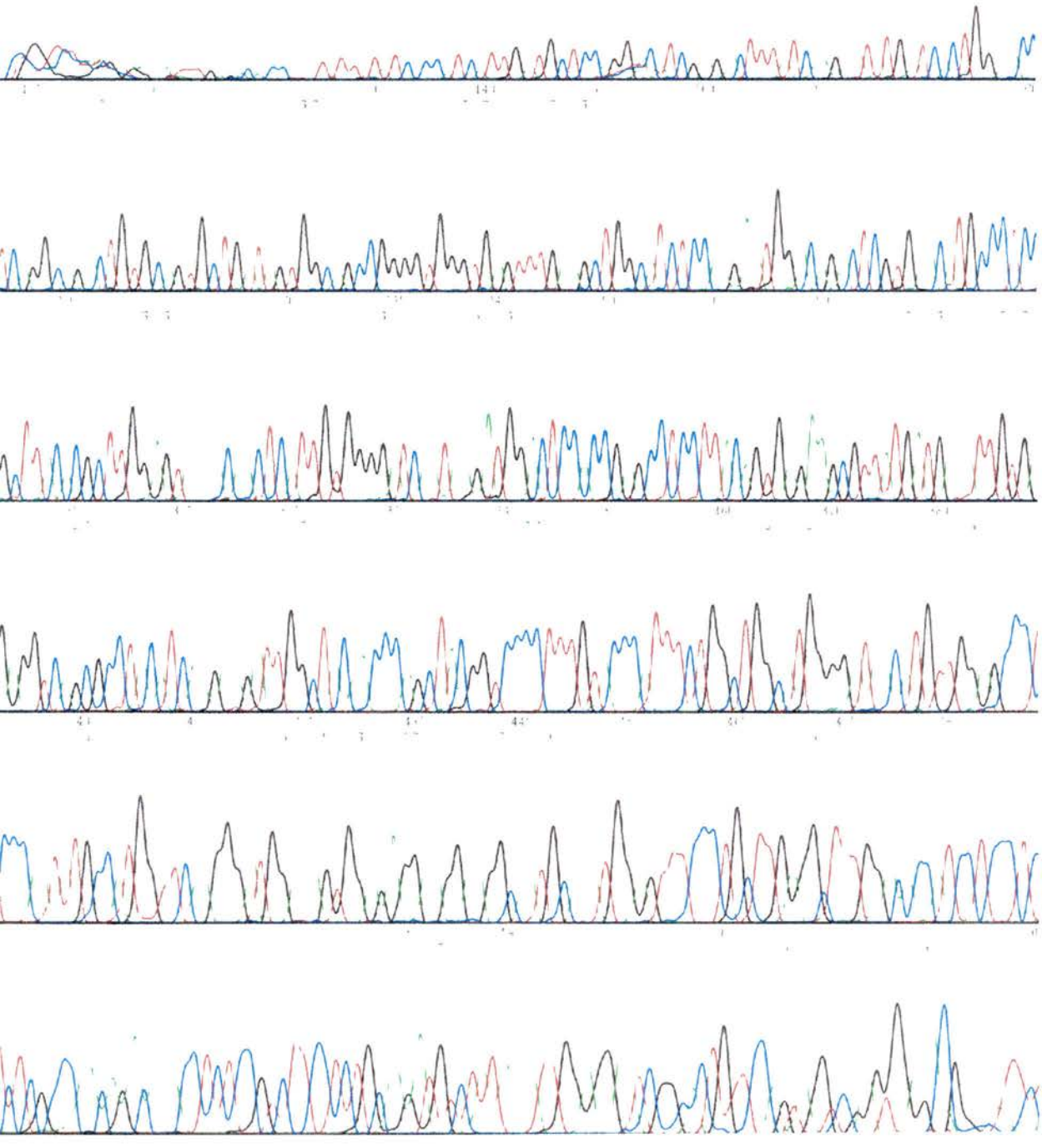

Figure 6-6 Typical sequence trace of *X. laevis* RT-PCR product.

```
GCCGTCAATAGGTGGACCCCTCCCGGAGAAATAAAACTGCCTGATCCGGAGCCGCCAGCC
CCTGCTGTCTGAGAGCTCGGCTACAGACTTCCTTGCACTCACCGTAGTGTCACCCCCAGG
AGGATGGGGAAAGAGAAGACACACATCAACATCGTGGTTATTGGCCACGTGGACTCTGGC
   M  G  K  E  K  T  H  I  N  I  V  V  I  G  H  V  D  S  G
AAGTCCACCACCACTGGCCACCTGATCTACAAGTGTGGAGGCATCGACAAAAGGACAATA
K  S  T  T  T  G  H  L  I  Y  K  C  G  G  I  D  K  R  T  I
GAGAAGTTTGAGAAGGAAGCACCTGACATGGGGAAAGGTTCCTTTAAATACGCTTGGGTT
E  K  F  E  K  E  A  P  D  M  G  K  G  S  F  K  Y  A  W  V
TTGGACAAACTGAAGGCTGAGAGGGAGCGAGGAATCACCATTGATATCCCCCTGTGGAAG
L  D  K  L  K  A  E  R  E  R  G  I  T  I  D  I  P  L  W  K
TTTGACACAACCAAATATTATATCACCATCATTGATGCTCCAGGACATCGAGACTTTATC
F  D  T  T  K  Y  Y  I  T  I  I  D  A  P  G  H  R  D  F  I
AAGAATATGATCACTGGAACCTCTCAGGCAGACTGTGCAGTGCTGATAGTGGCAGCCGGG
K  N  M  I  T  G  T  S  Q  A  D  C  A  V  L  I  V  A  A  G
GTGGGTGAGTTTGAAGCTGGCATCTCCAAGAATGGACAGACTCGTGAACATGCCCTCCTG
V  G  E  F  E  A  G  I  S  K  N  G  Q  T  R  E  H  A  L  L
GCTTACACGCTTGGAGTAAAACAACTCATTGTGGGGATCAATAAGATGGACTCCACCGAG
A  Y  T  L  G  V  K  Q  L  I  V  G  I  N  K  M  D  S  T  E
CCTCCTTACAGTGAGAAGCGTTATGATGAAATTGTGAAGGAGGTCAGCGCCTACATCAAG
P  P  Y  S  E  K  R  Y  D  E  I  V  K  E  V  S  A  Y  I  K
AAGATTGGCTACAACCCAGCTACGGTCCCCTTTGTACCCATTTCTGGCTGGCATGGGGAT
K  I  G  Y  N  P  A  T  V  P  F  V  P  I  S  G  W  H  G  D
AACATGTTGGAGCCCTCTCCCAATATGCCATGGTTCAAGGGATGGAAAGTGGAGAGGAAG
N  M  L  E  P  S  P  N  M  P  W  F  K  G  W  K  V  E  R  K
GAAGGCAATGCAAATGGAGTTTCCCTGCTTGAGGCTTTGGACACCATCCTCCCTCCATCT
E  G  N  A  N  G  V  S  L  L  E  A  L  D  T  I  L  P  P  S
CGCCCAACAGACAAACCTCTCCGTCTTCCTCTGCAAGATGTCTATAAAATTGGAGGAATC
R  P  T  D  K  P  L  R  L  P  L  Q  D  V  Y  K  I  G  G  I
GGCACTGTTCCAGTAGGTCGAGTGGAGACCGGCATTCTAAAGCCAGGCATGGTGGTGACC
G  T  V  P  V  G  R  V  E  T  G  I  L  K  P  G  M  V  V  T
TTTGCTCCAGTCAATATCACAACTGAGGTAAAGTCTGTTGAGATGCATCATGAGGCTCTG
F  A  P  V  N  I  T  T  E  V  K  S  V  E  M  H  H  E  A  L
AGTGAGGCTCTGCCTGGGGACAATGTTGGCTTCAACGTCAAGAACGTGTCAGTCAAGGAC
S  E  A  L  P  G  D  N  V  G  F  N  V  K  N  V  S  V  K  D
ATTCGCAGAGGCAATGTTTGTGGTGACAGCAAGACTGACCCTCCCCAGGAAGCCGCAGGT
I  R  R  G  N  V  C  G  D  S  K  T  D  P  P  Q  E  A  A  G
TTCACTGCTCAGGTGATCATCTTGAACCACCCTGGTCAGATCAGTGCTGGATATTCCCCA
F  T  A  Q  V  I  I  L  N  H  P  G  Q  I  S  A  G  Y  S  P
GTTATTGACTGCCATACTGCACATATCGCCTGTAAGTTTGCAGAGCTAAAAGAAAAGATT
V  I  D  C  H  T  A  H  I  A  C  K  F  A  E  L  K  E  K  I
GATCGCCGATCTGGCAAAAAGCTTGAGGACAACCCCAAGTCTCTGAAATCTGGAGATGCT
D  R  R  S  G  K  K  L  E  D  N  P  K  S  L  K  S  G  D  A
GCCATTGTGGAGATGGTCCCTGGGAAGCCTATGTGTGTGGAGAGCTTCTCCCAATACCCA
A  I  V  E  M  V  P  G  K  P  M  C  V  E  S  F  S  Q  Y  P
CCTCTTGGGCGCTTTGCTGTGAGAGACATGAGGCAGACTGTGGCCGTGGGAGTCATTAAG
P  L  G  R  F  A  V  R  D  M  R  Q  T  V  A  V  G  V  I  K
AACGTGGAGAAGAAAATCGGAGGAGCTGGCAAGGTGACAAAGTCCGCACAGAAAGCCCAG
N  V  E  K  K  I  G  G  A  G  K  V  T  K  S  A  Q  K  A  Q
AAGGCTGCAAAATGAATTGCCGGTTCCCTTCGCCTGGCACACAAGCCTTGTCCCTCTGAG
K  A  A  K
AAGGTCCTTCCCCTTACCTTTGAGGTGCACGCGAGCCCATCTGCTTGTAAAAGCCTGTAC
GTCAACGACTGGATGCTCACCATTAAAGTCCAGTGGAAGTTCTTTAAGAGGAAAAGCATG
CTCCTGCTCTGTAATCTTTAGTGTCCATTTTACCAATTAAACTGGTACAACATTCAAACA
ATAT
```

Figure 6-7 Completed nucleotide sequence and deduced amino acid sequence of *X. laevis* eEF1A-2 orthologue.

```
X1A-2  MGKEKTHINIVVIGHVDSGKSTTTGHLIYKCGGIDKRTIEKFEKEAAEMGKGSFKYAWVL
M1A-2  MGKEKTHINIVVIGHVDSGKSTTTGHLIYKCGGIDKRTIEKFEKEAAEMGKGSFKYAWVL
M1A-1  MGKEKTHINIVVIGHVDSGKSTTTGHLIYKCGGIDKRTIEKFEKEAAEMGKGSFKYAWVL
X1A-S  MGKEKTHINIVVIGHVDSGKSTTTGHLIYKCGGIDKRTIEKFEKEAAEMGKGSFKYAWVL
X1A-O  MGKEKIHINIVVIGHVDSGKSTTTGHLIYKCGGIDKRTIEKFEKEAAEMGKGSFKYAWVL

X1A-2  DKLKAERERGITIDISLWKFETTKYYITIIDAPGHRDFIKNMITGTSQADCAVLIVAAGV
M1A-2  DKLKAERERGITIDISLWKFETTKYYITIIDAPGHRDFIKNMITGTSQADCAVLIVAAGV
M1A-1  DKLKAERERGITIDISQRKFETSKYYVTIIESPGHRDFIKNMITGTSQADCAVLIVAAGV
X1A-S  DKLKAERERGITIDISLWKFETSKYYVTIIDAPGHRDFIKNMITGTSQADCAVLIVAAGV
X1A-O  DKLKAERERGITIDISLWKFETGKFYITIIDAPGHRDFIKNMITGTSQADCAVLIVAGGV

X1A-2  GEFEAGISKNGQTREHALLAYTLGVKQLIVGINKMDSTEPPYSEKRYDEIVKEVSAYIKK
M1A-2  GEFEAGISKNGQTREHALLAYTLGVKQLIVGVNKMDSTEPAYSEKRYDEIVKEVSAYIKK
M1A-1  GEFEAGISKNGQTREHALLAYTLGVKQLIVGVNKMDSTEPPYSQKRYEEIVKEVSTYIKK
X1A-S  GEFEAGISKNGQTREHALLAYTLGVKQLIVGINKMDSTEPPYSQKRYEEIVKEVSTYIKK
X1A-O  GEFEAGISKNGQTREHALLAFTLGVKQLIIGVNKMDSTEPPFSQKRFEEITKEVSAYIKK

X1A-2  IGYNPATVPFVPISGWHGDNMLEPSPNMPWFKGWKVERKEGNANGVSLLEALDTILPPTR
M1A-2  IGYNPATVPFVPISGWHGDNMLEPSPNMPWFKGWKVERKEGNASGVSLLEALDTILPPTR
M1A-1  IGYNPDTVAFVPISGWNGDNMLEPSANMPWFKGWKVTRKDGSAVAPTLLEALDCILPPTR
X1A-S  IGYNPDTVAFVPISGWNGDNMLEPSPNMPWFKGWKITRKEGSGSGTTLLEALDCILPPSR
X1A-O  IGYNPATVPFVPISGWHGDNMLEASTNMPWFKGWKIERKEGNASGVTLLEALDCIIPPQR

X1A-2  PTDKPLRLPLQDVYKIGGIGTVPVGRVETGILRPGMVVTFAPVNITTEVKSVEMHHEALS
M1A-2  PTDKPLRLPLQDVYKIGGIGTVPVGRVETGILRPGMVVTFAPVNITTEVKSVEMHHEALS
M1A-1  PTDKPLRLPLQDVYKIGGIGTVPVGRVETGVLKPGMVVTFAPVNVTTEVKSVEMHHEALS
X1A-S  PTDKPLRLPLQDVYKIGGIGTVPVGRVETGVIKPGMVVTFAPVNVTTEVKSVEMHHEALT
X1A-O  PTAKPLRLPLQDVYKIGGIGTVPVGRVETGVLKPGMIVTFAPSNVTTEVKSVEMHHEAVQ

X1A-2  EALPGDNVGFNVKNVSVKDIRRGNVCGDSKADPPQEAAQFTSQVIILNHPGQISAGYSPV
M1A-2  EALPGDNVGFNVKNVSVKDIRRGNVCGDSKADPPQEAAQFTSQVIILNHPGQISAGYSPV
M1A-1  EALPGDNVGFNVKNVSVKDVRRGNVAGDSKNDPPMEAAGFTAQVIILNHPGQISAGYAPV
X1A-S  EAVPGDNVGFNVKNVSVKDVRRGNVAGDSKNDPPMEAGSFTAQVIILNHPGQIGAGYAPV
X1A-O  EALPGDNVGFNVKNISVKDIRRGNVAGDSKNDPPMQAGSFTAQVIILNHPGQISAGYAPV

X1A-2  IDCHTAHIACKFAELKEKIDRRSGKKLEDNPKSLKSGDAAIVEMVPGKPMCVESFSQYPP
M1A-2  IDCHTAHIACKFAELKEKIDRRSGKKLEDNPKSLKSGDAAIVEMVPGKPMCVESFSQYPP
M1A-1  LDCHTAHIACKFAELKEKIDRRSGKKLEDGPKFLKSGDAAIVDMVPGKPMCVESFSDYPP
X1A-S  LDCHTAHIACKFAELKEKIDRRSGKKLEDNPKFLKSGDAAIVDMIPGKPMCVESFSDYPP
X1A-O  LDCHTAHIACKFAELKQKIDRRSGKKLEDDPKFLKSGDAAIVEMIPGKPMCVESFSDYPP

X1A-2  LGRFAVRDMRQTVAVGVIKNVEKKIGGAGKVTKSAQKAQKAAK
M1A-2  LGRFAVRDMRQTVAVGVIKNVEKKSGGAGKVTKSAQKAQKAGK
M1A-1  LGRFAVRDMRQTVAVGVIKAVDKKAAGAGKVTKSAQKAQKAK
X1A-S  LGRFAVRDMRQTVAVGVIKAVEKKAAGSGKVTKSAQKAAKTK
X1A-O  LGRFAVRDMRQTVALGVIKGVDKKAASSGKVTKSAVKAGKK
```

Figure 6-8 Line-up of deduced *X. laevis* eEF1A-2 orthologue (X1A-2) and eEF1A isoforms from mouse (M1A-2 and M1A-1) and *X. laevis* (X1A-S and X1A-O). The peptide sequences used in generating the antibodies are highlighted in **green** for eEF1A-2M and **red** for eEF1A-2C, as in Chapter 5, section 5.2.1. Differences between mouse eEF1A-2 and its *X. laevis* othologue are highlighted in **blue**.

6.3 Discussion

6.3.1 eEF1A isoforms in *X. laevis*

The available data from the literature suggested that the presence of a second, tissue-specific eEF1A isoform is mammalian specific. I have shown that there is an isoform of eEF1A in an amphibian species, *Xenopus laevis*, which is consistent with the situation in mammals in that it is expressed in the heart, skeletal muscle and cells of the central nervous system. This experimental finding is consistent with the *in silico* data, as the ESTs were isolated from the brain, eye and heart. An eEF1A isoform, presumably the previously described eEF1A-S, is expressed in all tissues examined, except muscle, oocyte and optic ganglion. XeEF1A-2 is also developmentally regulated, as this isoform is not present in a gastrula stage embryo. It would therefore be of great interest to determine at what stage in *X. laevis* the potential switch in expression between the two isoforms occurs. The very strong band observed using the eEF1A-1 antibody against gastrula tissue extracts is consistent with previous findings which found that eEF1A-S is a major transcript in developing embryos (Krieg *et al.*, 1989).

The RT-PCR result confirms the existence of XeEF1A-2 in muscle at the RNA level. The primers I designed could also be used to confirm the presence of the mRNA for this isoform in the heart and brain. Other tissues, for example the eye, could also be examined. Primers at the same position in the eEF1A-S transcript could be used to investigate its expression at the RNA level, and could also be used to sequence the isoform in, for example, liver, to confirm that the protein recognised by the anti-*A. salina* eEF1A antibody is, in fact, eEF1A-S.

The striking feature of XeEF1A-2 is the similarity of its amino acid sequence with the mouse eEF1A-2 protein. Like mouse eEF1A-2, it is 463 amino acids long, and there are only three differences between them. There is less similarity with the known *X. laevis* isoforms. The percentage identity between XeEF1A-2 and the known isoforms in mouse and *X. laevis* are shown in table 6-2. At the nucleotide

level, the coding regions of the mouse eEF1A-2 mRNA and its *X. laevis* orthologue are the most similar. As with eEF1A-1 and eEF1A-2 in mammals, there is much more divergence between the isoforms in the 3' and 5' UTRs than in the coding regions, which were not included in the analysis.

	mouse eEF1A-2	mouse eEF1A-1	eEF1A-S	eEF1A-O
Nucleotide	83.2%	77.4%	79.0%	78.2%
Amino acid	99.4%	93.3%	90.5%	88.6%

Table 6-2 Percentage identities between the coding regions of XeEF1A-2 and the known mouse and *X. laevis* isoforms. The identities between the nucleotide sequences are calculated from the coding regions of the genes.

6.3.2 Antibody Specificity

Both eEF1A-2 antibodies (eEF1A-2C and eEF1A-2M) recognised XeEF1A-2. This is despite the presence of one amino acid difference between each peptide and XeEF1A-2. Within the 16 amino acids of the peptide against which eEF1A-2M was raised, there are three which differ between eEF1A-S and the peptide. This was sufficient for the antibody to be specific for XeEF1A-2, and not recognise eEF1A-S. However, the eEF1A-2C antibody appeared to recognise both XeEF1A-2 and eEF1A-S, even though there were 4 (of 14) amino acid differences between XeEF1A-2 and eEF1A-S. It is therefore possible that there are differences in the secondary structure between the two peptides. It may be important that one of the differences between the peptide and eEF1A is at the C-terminus of the peptide, and may therefore be more exposed. It is also possible that eEF1A-2C is recognising another *X. laevis* eEF1A isoform. However, there is no evidence for another isoform in the EST databases. Given that 4 amino acid differences were sufficient for antibody specificity of both eEF1A-2 antibodies in mice, it is difficult to draw any general conclusions which would aid in the design of future anti-peptide antibodies.

It is also intriguing that the antibody raised against the *A. salina* eEF1A protein was apparently specific for eEF1A-S, unlike the two anti-eEF1A-1 antibodies which I raised. This antibody was raised against the whole protein, rather than a peptide.

There are 80 amino acid differences between the *A. salina* eEF1A and *X. laevis* eEF1A-S proteins (82.7% identity), whereas there are 85 differences between the *A. salina* protein and *X. laevis* eEF1A-2 orthologue (81.6% identity). It is difficult to account for why such a small difference in the overall percentage identity could affect antibody specificity so dramatically. It is possible that there are more differences between the *A. salina* eEF1A and *X. laevis* eEF1A-2 orthologue in the more exposed residues of the proteins, or that there are differences in posttranslational modification between them. Alternatively, this antibody may also recognise another, as yet uncharacterised, isoform of eEF1A, although again, there is no evidence for this from the EST databases.

7 Chapter 7 – General Discussion

7.1 Discussion

7.1.1 Project Aims

The genetic mutant wasted is caused by a deletion which results in the loss of eEF1A-2, a tissue-specific isoform of the more widely-expressed eEF1A-1. The main theme of this project has been the potential relationship between eEF1A-2 and the motor neuron diseases. Within this area of research there were four main aims. Firstly, to further characterise wasted mice, and evaluate whether they are a suitable model for ALS. Secondly, to determine whether there is a direct involvement of *EEF1A2* in ALS, by mutation screening the gene in patients. Thirdly, to develop and characterise specific antibodies which recognise the two isoforms of eEF1A, eEF1A-1 and eEF1A-2. Finally, to investigate whether eEF1A-2 is really confined to mammals, or whether there is evidence for its existence in other vertebrates.

7.1.2 Pathological analysis of wasted

In this thesis I have extended the previous pathological observations of wasted mice. I have shown that the weight loss seen in homozygous wasted mice is due to muscle atrophy. Vacuolation of their motor neurons is seen from 28 days, and not at 24 days, and therefore represents a later feature of the phenotype. Both astrogliosis and the accumulation of phosphorylated neurofilaments are present from at least as early as 19 days, which preceeds the onset of overt neuromuscular symptoms. There also appears to be a gradient in the severity of vacuolation and of gliosis from the cervical to the lumbar region. The features of the wasted phenotype are summarised and compared with those of ALS in table 7-1.

Feature	Wasted	ALS
Age of onset	19 days	55 years (mean for sporadic disease)
Muscle	Muscle atrophy	Muscle atrophy
H&E	Loss of anterior horn motor neurons	Loss of anterior horn motor neurons
GFAP	Increased staining	Increased staining
Neurofilaments	Cytoplasmic accumulation of phosphorylated neurofilaments	Cytoplasmic accumulation of phosphorylated neurofilaments
Ubiquitin	No increased staining	Ubiquitinated inclusions
MAP2	No decreased staining	Decreased staining

Table 7-1 Summary of neuropathological findings, and comparison with ALS.

There are thus several features in common between the phenotype of wasted mice and human ALS. Both are progressive neurodegenerative conditions in which there is increasing paralysis and a loss of muscle mass. On a microscopic level, both show the specific loss of anterior horn cell motor neurons, gliosis and the neuronal cytoplasmic accumulation of phosphorylated neurofilaments (Graham and Lantos, 1997; Manetto *et al.*, 1988; Munoz *et al.*, 1988; Sobue *et al.*, 1990). One difference between them is that wasted mice do not have ubiquitinated inclusions, which are a common feature of ALS. However, the time course of the wasted phenotype is extremely rapid. If it were possible to extend the lifespan of wasted homozygous mice, perhaps using transgenic approaches, then it is conceivable that ubiquitinated inclusions would then be seen. The presence of ubiquitinated inclusions may represent an end-point of the human disease, as it is usually only autopsy material which is available from ALS patients.

Another obvious difference between the phenotypes of wasted mice and the symptoms of human ALS sufferers is one of timing. The wasted phenotype has an

onset at 19 days, around the time of weaning, whereas ALS usually occurs in middle or old age in humans. Wasted mice may actually therefore provide a better model of SMA, or of one of the rarer forms of ALS with a juvenile onset, than of the more common, adult-onset form of ALS. There may indeed be some degree of overlap between ALS and SMA, as, for example, there are reports of families in which the two diseases coexist (reviewed in Orrell *et al.*, 1997). However, reports of an association between SMN gene copy number and ALS probably represent artefactual findings (Crawford and Scholasky, 2002).

One further key difference between the wasted phenotype and human ALS is that there is no overt immunological phenotype in ALS, whereas wasted mice show atrophy of the spleen and thymus, and a defective response to radiation-induced damage in lymphoid-derived cells. It is not known what potential long-term effects these defects would produce, but it is possible that they would include lymphoma. It has been suggested that ALS sufferers are more likely to also have lymphoproliferative disease than the general population (Gordon, 1997). However, there does not seem to have been a systematic evaluation of this, which would in any case be difficult given the relative rarity of the two diseases. The available data appears to be confined to case reports.

7.1.3 Mutation analysis of ALS candidate genes

Both my pathological observations, summarised above, and previous reports (Lutsep and Rodriguez, 1989; Woloschak *et al.*, 1987) are consistent with wasted being at least a partial model of human motor neuron disease. As the genetic lesion responsible for wasted abolishes the expression of the gene encoding eEF1A-2 (Chambers *et al.*, 1998), I screened the human *EEF1A2* gene for mutations in patients with both familial and sporadic ALS. No mutations were found, which argues against the gene having a major involvement in the disease. Although I found polymorphisms in exons 3 and 5 of the gene, these were not associated with disease susceptibility.

As eEF1A-2 is expressed during embryonic development from at least as early as13.5 dpc, and that the wasted phenotype has an early onset in homozygous mice, it is possible that *EEF1A2* is actually a better candidate for involvement in spinal muscular atrophy (SMA). The age of onset is during childhood for the more common types of SMA (Hausmanowa-Petrusewicz, 1991), whereas it is on average 45.1 years for familial ALS and 56 years for sporadic ALS (Tandan and Bradley, 1985). Romina Aron-Baden therefore screened a small cohort of SMA patients as part of her MSc project, but did not find any mutations (Aron-Badin, 2002).

Wobbler is another mouse mutant which has been described as a model for human motor neuron disorders (Duchen *et al.*, 1968; Mitsomoto and Bradley, 1982). On the basis of its location, apparently close to the *wr* interval, and function as an amino acid transporter, I investigated the mouse solute carrier family 1, member 4 gene, *Slc1A4*, for mutations in a *wr/wr* homozygous mouse and a littermate control. As no mutations were found, and the gene had similar expression levels in a wobbler and a littermate control mouse, I excluded *Slc1a4* as a candidate for *wr*. *Slc1a4* has subsequently been excluded from the *wr* critical interval (Fuchs *et al.*, 2002).

During the course of this project, several genes were identified which are mutated either in ALS or in the mouse models of the disease. These include *Alsin*, mutated in human ALS2 (Hadano *et al.*, 2001; Yang *et al.*, 1990), *Tbce*, mutated in the mouse mutant progressive motor neuropathy (*pmn*) (Martin *et al.*, 2002) and *Vegf* (Oosthuyse *et al.*, 2001), which has subsequently become a novel mouse model of the disease. As the genetic causes of other mouse models and of human forms of ALS are revealed they may resolve long-standing questions about the pathogenesis of the disease. However, the tenth anniversary of the discovery of mutations in *SOD1* in familial ALS is approaching, with no clear mechanism linking these mutations with the disease revealed.

One key question in ALS research is why motor neurons are selectively vulnerable to mutations in ubiquitous proteins such as SOD1. It is possible that SOD1 has one or more as yet unidentified alternative functions which are responsible for the

neuromuscular phenotype. It is also unclear why the different SOD1 mutations responsible for ALS cause the same phenotype, with no apparent genotype-phenotype correlation, when the mutated residues are scattered throughout the protein.

eEF1A-2 appears to be unusual amongst the genes mutated in human and animal motor neuron disorders in that it has a restricted expression pattern. It is interesting to note that mutations in another translation factor, the initiation factor *eIF2B*, have recently been identified as responsible for the rare neurological disorder leukoencephalopathy with vanishing white matter (VWM) (Leegwater *et al.*, 2001). However, in contrast to eEF1A-2, eIF2B is ubiquitously expressed.

There is a clear need to identify the other genes involved in the approximately 90% of familial ALS cases for which the genetic defect has not been identified. Moreover, most ALS cases are apparently sporadic, although it is possible they represent novel mutations in unknown genes. There may also be environmental triggers, although no obvious candidates have emerged (Mitchell, 2000). A recent study has intriguingly implicated physical fitness, although the criteria for identifying subjects as "varsity athletes" or "slim" were hardly rigorous (Scarmeas *et al.*, 2002).

The precise relationships between ALS and the other forms of motor neuron disease, particularly SMA, have yet to be determined. The fact that there are families in which the two diseases coexist suggests that the two may in fact be part of the same clinical spectrum (Orrell *et al.*, 1997). There have been many attempts at a rigorous classification of the motor neuron diseases (see, for example, Orrell *et al.*, 1997). However, ultimately the diseases will be classified according to the genetic lesions responsible, as these become known.

7.1.4 Expression analysis of eEF1A isoforms

eEF1A-2 is a tissue-specific isoform of the more ubiquitously expressed eEF1A-1. In those cells in which it is expressed, namely the brain, heart and skeletal muscle, there is a switch in isoform expression from eEF1A-1 to eEF1A-2. Understanding the functions of these two isoforms may help to elucidate why two isoforms are required in neurons, which may in turn give us fundamental information about the biology of motor neurons. A key experimental tool for the functional investigation of eEF1A-1 and eEF1A-2 are antibodies which specifically recognise the two isoforms. However, at the start of this project, such antibodies were unavailable. In this thesis I have described the design and characterisation of antibodies which are completely specific for the two isoforms of eEF1A. These were used to show that expression of the eEF1A-2 protein is confined to the brain, spinal cord and muscle of adult mice. This confirms the previously described results at the RNA level, and the results of Khalyfa *et al.* (2001). I have also shown that eEF1A-2 is expressed from at least as early as 13.5dpc.

It is still unclear, however, why there is a requirement for a second isoform in certain cells from a particular developmental stage. As eEF1A-1 has a known role in cytoskeletal remodelling, it is possible that eEF1A-2 has a subtly different role which means that it is required in neurons and other cells. This may form a link between eEF1A-2 and motor neuron dysfunction, as many of the genes which have been identified in motor neuron disease have links with the cytoskeleton. For example, alsin, mutations in which underlie ALS2, contains domains which are homologous to RhoGEF, which may be involved in the organisation of the cytoskeleton. In addition, the perturbation of neurofilament metabolism is a feature of both human ALS and animal models of the disease, and overexpression of human *NEFH* in mice recapitulates the disease (Cote *et al.*, 1993). Moreover, neurofilament gene mutations have been found in a small proportion of patients (Al-Chalabi *et al.*, 1999; Figlewicz *et al.*, 1994; Tomkins *et al.*, 1998).

Alternatively, there may be novel energy requirements in certain cells, which necessitate a second eEF1A isoform. One obvious feature of neurons is their large

size, with large cytoplasmic volumes and long axonal processes. It is conceivable that these have requirements for an enhanced energy supply or for novel metabolites. A second isoform may also be required in neurons for the translation of proteins at sites other than the endoplasmic reticulum. For example, there is evidence that, in neurons, translation occurs locally in the dendrites (Job and Eberwine, 2001a; Job and Eberwine, 2001b). This spatial regulation of translation may be important to allow the synthesis of proteins, such as receptors, at optimal distances from the stimulated membrane for synapse formation during development, and for synaptic plasticity in mature neurons.

Determining and comparing the subcellular localisation of eEF1A-1 and eEF1A-2 may therefore help to explain why two isoforms are required. If the two isoforms localise differently within the cell, this suggests that they function differently in translation. For example, if eEF1A-1 localises to the cell body alone, whereas eEF1A-2 also localises to the dendrites of neuronal cells, this would suggest that eEF1A-2 is required for translation at these sites. It may also explain why neurons require this second isoform.

There have not been any definitive studies which have investigated the relative localisation of the two isoforms. Immunofluoresent analysis of the subcellular localisation of eEF1A-1 in fibroblasts has shown that it localises to both the cytoplasm and the nucleus (Sanders *et al.*, 1996). This is in contrast to the rest of the eEF1H components, which localise to the endoplasmic reticulum. However, the subcellular localisation of eEF1A-2 has not been clearly characterised, although this has been investigated by Khalyfa *et al.* (Khalyfa *et al.*, 2001). One study has claimed that eEF1A-2 localises to the cytoplasm of PC-12 cells, but in this case an antibody to eEF1A-1 was used (McClatchy *et al.*, 2002). And although eEF1A has been reported in dendrites, it is not clear whether this is specific for eEF1A-1 or eEF1A-2 (Job and Eberwine, 2001b). There is thus a need for a comparative analysis of the subcellular localisation of the two isoforms to be made, using clearly specific antibodies. Unfortunately, I was unable to obtain a specific signal for either isoform, using immunofluorescent detection on differentiated PC-12 cells or glioblastoma SU-

SY5Y cells. The specific antibodies which I have raised will, however, be useful in continuing studies investigating the subcellular localisation of the two isoforms. This should, in turn, help to answer questions about their biological functions.

7.1.5 eEF1A isoforms in *X. laevis*

Given that eEF1A-2 is essential for neuronal survival, demonstrated by the fact that a loss of eEF1A-2 leads to the loss of motor neurons and the death of homozygous wasted mice, it seemed surprising that the data from the literature suggested that eEF1A-2 was restricted to mammals. I have shown that there is in fact an orthologue of eEF1A-2 in the frog *X. laevis*, which is expressed only in the brain, optic ganglia, muscle and heart of adult animals. This is consistent with the mammalian expression pattern. Like the mammalian eEF1A-2, this novel eEF1A-2 orthologue is also developmentally regulated. Moreover, its amino acid sequence is strikingly similar to the mouse amino acid sequence. This implies that the amino acid differences between eEF1A-1 and eEF1A-2 are functionally important, as they are conserved between mouse and *X. laevis*. It is not clear what functional effect the amino acid substitutions between eEF1A-1 and eEF1A-2 have. There are only two substitutions, one conservative and one semi-conservative, in the first 160 amino acids, and the remaining 33 substitutions appear to cluster slightly. Perhaps unsurprisingly, given the essential role of GTP hydrolysis in translation elongation, the three GTP binding sites are unaffected.

This thesis also demonstrates the value of using peptides to generate antibodies where it is necessary to distinguish between two very similar proteins. Both the short peptides selected had four differences between the two isoforms, out of 16 residues for eEF1A-2M and 14 for eEF1A-2C. However, the results from the *X. laevis* work have shown that it is difficult to deduce any firm rules about antibody specificity in designing peptides. The eEF1A-2M antibody was specific for the novel *X. laevis* eEF1A-2 isoform (XeEF1A-2), and did not recognise eEF1A-S, even though there were only 3 amino acid differences between XeEF1A-2 and eEF1A-S within the peptide. In contrast, the eEF1A-2C antibody appeared to recognise both, despite

there being four amino acid differences between XeEF1A-2 and eEF1A-S within this peptide. This reflects the fact that there is some inherent uncertainty in designing anti-peptide antibodies, as it is rarely possible to predict the exact *in vivo* conformation of the peptide. The protein in question may also have posttranslational modifications which would render the peptide antigenically different from the native protein.

7.2 Future work

7.2.1 The wasted phenotype

There are further experiments which would expand on the neuropathological findings presented in this thesis. Mice at a younger age could be analysed to determine from what age gliosis and neurofilament accumulation occurs in wasted mice. More mice could also be investigated, both for GFAP and for neurofilament staining, at the time points studied, particularly at 24 days, where only one homozygous wasted and one heterozygous animal were compared. The antibody I used to show the accumulation of phosphorylated neurofilaments in homozygous wasted mice was a pan-specific antibody which recognised both the light and heavy chain neurofilament proteins. This was selected to maximise any differences seen between wasted and control animals. Antibodies specifically raised against the light and heavy chains could be used to determine which of the two proteins was responsible for the increased antibody staining. Lutsep *et al.* showed that the increased staining they observed was due to the heavy chain neurofilament (Lutsep and Rodriguez, 1989). It is therefore likely that the increased neurofilament accumulation I observed was also due to the heavy chain protein, although as Lutsep *et al.* only investigated mice at 28 days, the possibility cannot be ruled out that there are differences in the other neurofilament proteins at 24 and 28 days.

It would also be interesting to determine whether the muscle atrophy seen in wasted mice is as a result of denervation atrophy or a primary myopathy. Experiments are currently being carried out in our laboratory to determine which process is

responsible. Conditional knockouts, in which the expression of *Eef1a2* is specifically eliminated from neurons and from muscle, could be a way to investigate this question. One further potential transgenic approach would be to produce mice with *Eef1a2* controlled by a muscle-specific promoter, and to cross these with wasted mice. This would confine the phenotype to its neurological (and immunological) components. It may also be possible to generate transgenic mice in which the immunological features of the phenotype are removed, which may then provide a better model of ALS.

The wasted mutation is recessive, and heterozygous animals are apparently normal. They do not show any weight loss or obvious neurological or immunological defects, and breed normally. As eEF1A-1 is known to be expressed at high levels, forming between 3 and 5% of the total cellular protein (Lee *et al.*, 1993a), it is expected that eEF1A-2 is also expressed at high levels. Heterozygotes express half the amount of eEF1A-2, which is presumably sufficient for normal cellular function. However, it is possible that heterozygous mice do show subtle defects, perhaps in old age, or in response to particular environmental stresses. It may therefore be worthwhile to examine aged wasted heterozygotes, by, for example, behavioural testing using the SHIRPA protocol (Rogers *et al.*, 2001). It would also be interesting to perform neuropathological analysis on old heterozygotes, to see if any of the features seen in wasted homozygotes are recapitulated. For example, spinal cord sections could be stained with H&E, to determine whether there is any neuronal vacuolation, and with the GFAP and neurofilament antibodies, to investigate whether there is any increase in their expression. This would help to determine whether wasted represents a true recessive phenotype.

Wasted and ALS/SMA

The timing of the eEF1A-1/eEF1A-2 switch in humans is still unknown, and clearly has a direct bearing on the relevance for an involvement of eEF1A-2 in human ALS. It would therefore be of interest to determine the relative levels of eEF1A-1 and eEF1A-2 in human brain and muscle at different ages. If the isoform switch occurs early in postnatal life, as in mice, then *EEF1A2* becomes a much less promising

candidate for involvement in the common, adult-onset form of ALS, and is more likely to be involved in either the rarer juvenile-onset forms, or in SMA. However, it is becoming increasingly difficult to obtain ethical permission to access human material.

7.2.2 Functions of eEF1A isoforms

It remains to be determined why two eEF1A isoforms are required. Do they have equivalent functions? As outlined above, determining whether the two proteins have the same subcellular localisation would help to answer this question. For example, eEF1A-2 may be required for synaptic translation.

Although I was not able to determine the subcellular localisation in cells using the native protein, it may be possible to achieve this by transfecting a tagged protein into cells. This was not possible within the timescale of this project. This approach has been undertaken with GFP-fusion proteins, in the human epithelial kidney cell line HEK293, and both isoforms localised to the cytoplasm (Danielewicz, 2002). However, as eEF1A-2 is not normally expressed in the kidney, this may not represent its normal localisation. Moreover, kidney cells do not possess dendrites. As there have been problems noted with the use of β-gal fusion proteins (Berns, 2000), this approach may also not accurately reflect the localisation of the native protein. Nevertheless, if differences between eEF1A-1 and eEF1A-2 were noted in their localisation, this is highly suggestive that the two isoforms do indeed have different functions.

Another cellular approach used in the understanding of gene function is the use of RNA interference, or RNAi. In this technique, (reviewed in McManus and Sharp, 2002), double-stranded RNA is introduced into a mammalian cell. It binds to the mRNA of the target gene, which is then degraded by the RNA-induced silencing complex (RISC), abolishing the expression of that gene. RNAi could be used in human and mouse cell lines to knockdown the expression of eEF1A-1 and eEF1A-2, and possibly illuminate their relative functions. For example, it would be interesting

to study the phenotype of neuronal cells such as SU-SY5Y, which I have shown to express both isoforms, after the abolition of eEF1A-1 or eEF1A-2 expression. This would demonstrate whether both isoforms are required for cell viability, and it would also be interesting to determine whether there were any cytoskeletal differences between the two knockdowns.

Many useful mutant mice have been generated by the ENU mutagenesis programme (Hrabe de Angelis *et al.,* 2000; Nolan *et al.,* 2000). In this programme, male mice are exposed to ethylnitrosourea, which leads to point mutations in the DNA of the premeiotic spermatogonial stem cells, with a specific locus mutation rate of 0.00108 (Coghill *et al.*, 2002). After a brief period of sterility, the mice are mated, and the F1 offspring examined for phenotypic abnormalities. The DNA of the F1 males has been stored, and can be screened for the presence of mutations in a particular gene of interest. The sperm of these mice is also stored, so that lines of mice which express the mutation can be generated. Screening the DNA of the F1 mice for mutations in *Eef1a1* and *Eef1a2* may uncover novel mutations in either or both of these genes. This would be particularly instructive for *Eef1a1*, in which there are no known mutations. Any such mutations would be expected to have a subtle effect on the protein, as *Eef1a1* null mutants would be expected to be early embryonic lethal, as the gene product has such a crucial role, and is almost ubiquitously expressed. If more than one allele was generated, it may be possible to construct an alleleic series, with different mutations having different severities of phenotype. It is possible that the mice generated could also be crossed to generate further alleles, with more subtle differences between them.

Gene trapping is based on the random integration of a reporter gene cassette into the genome of an embryonic stem (ES) cell. The reporter cassette comprises a reporter gene such as *lacZ* with a selection gene such as neomycin, and serves to both mutate and identify the locus into which it integrates. These ES cells are used in the generation of chimaeras, which are then used to produce mice which are usually effectively null for the integrated locus. Several reference libraries of such cell lines, with sequence information on the trapped genes, are now available, (for example, see

Wiles *et al.*, 2000). Gene traps could thus be a further way to generate mice carrying mutated alleles of *Eef1a1* and *Eef1a2*, and a further way to investigate the functions of eEF1A-1 and eEF1A-2. The fact that the trapped gene contains a *lacZ* reporter gene, under the control of the endogenous promoter, could be a further tool to investigate the expression of the two isoforms. There is the caveat that the signal obtained may not reflect that of the native protein, as problems have been noted with the use of a *lacZ* reporter gene (Berns, 2000). However, in this case the *lacZ* gene was located in the 3'UTR of the *Eef1a1* gene. It is possible that the location of the gene trap *lacZ* gene will not lead to such effects.

Transgenic approaches could also be used to investigate whether the two isoforms are functionally equivalent. One way to determine this would be to substitute eEF1A-1 for eEF1A-2. If eEF1A-1 were to be placed under the control of the eEF1A-2 promoter in transgenic mice, then eEF1A-1 would be expressed when and where eEF1A-2 is ordinarily expressed. If, when crossed to wasted mice, these transgenic mice correct the wasted phenotype, then the implication is that the two isoforms have identical functions.

The two isoforms may also have different interactions. eEF1A-1 is known to interact with components of the cytoskeleton, for example actin and microtubules (Liu *et al.*, 2002; Shiina *et al.*, 1994; Yang *et al.*, 1990). There may be differences between eEF1A-1 and eEF1A-2 in, for example, the affinity for these cytoskeletal components, leading to differences in cytoskeletal modelling capabilities between the two isoforms. The antibodies I have generated could be used to investigate such interactions using, for example, immunoprecipitation. This could also be used to investigate the ZPR1/SMN complex. Although eEF1A-1 is known to interact with ZPR1, it is not known whether eEF1A-2 also interacts. A direct interaction has not been demonstrated between either of the eEF1A isoforms and SMN. Intriguingly, an unidentified 50kD protein has been pulled-down in immunoprecipitation experiments using an anti-SMN antibody (Charroux *et al.*, 2000). It is therefore tempting to speculate that eEF1A-1, SMN and ZPR1 all form part of the same complex, and that eEF1A-2 also interacts.

As part of her MRes Project, Romina Aron-Badin investigated whether there was a difference in the expression of ZPR1 and SMN between homozygous wasted mice and their wild type littermates (Aron-Badin, 2002). There were no differences between the two groups of animals in ZPR1 mRNA levels, assessed using RT-PCR. However, using Western analysis, it was noted that the expression of SMN was reduced in the heart and muscle of homozygous wasted mice when compared with those of control animals. This was not, however, due to a general loss of translational capacity in homozygous wasted mice, as the levels of other proteins were unaffected. It would be interesting to determine whether this reduction in SMN is at the level of transcription or translation. RT-PCR analysis could therefore be used to compare SMN mRNA levels between homozygous wasted mice and controls. It is possible that the differences seen at the protein level were caused by the mislocalisation of SMN to the nucleus. Although Romina Aron-Badin performed immunohistochemical analysis on cryostat sections of muscle, brain and spinal cord, the morphology was not of a sufficient quality to resolve this question (Aron-Badin, 2002). It may therefore be useful to investigate SMN localisation in paraffin-embedded sections from homozygous wasted mice and controls.

7.2.3 eEF1A-2 expression in mice

Given that eEF1A-2 is strongly expressed in 13.5 and 14.5 dpc embryos, it would be very interesting to perform *in situ* hybridisation to determine the precise expression pattern of *Eef1a2* during embryonic development. If novel sites of expression were uncovered, it could hint at new potential functions of eEF1A-2. Given the finding that eEF1A-2 is also expressed in the eye, it would also be of interest to determine where within the eye it is expressed, and also to determine whether there is also an isoform switch in this organ. There are several cell types which might be expected to express eEF1A-2 on the basis of either their shape or function. These include neuronal cells such as bipolar cells, and muscle cells. The shape of photoreceptor cells, with their elongated cytoplasm, is somewhat similar to neurons, and may indicate that these cells also have a requirement for eEF1A-2. However, there are

many cells which would not be expected to express eEF1A-2, so the fact that there was no eEF1A-1 signal at the level of a Western blot was somewhat surprising. It would therefore be interesting to study the expression of both isoforms in the adult eye using immunohistochemistry.

Immunohistochemistry could also be used to study the expression of eEF1A-1 in the spinal cord. There appeared to be a gradient in the severity of the vacuolation and gliosis from the cervical through the thoracic to the lumbar spinal cord. It is conceivable that this phenotypic gradient is due to a gradient in the loss of eEF1A-1 expression. However, it was not possible to test this hypothesis using Western blotting, as there are also cells within the spinal cord which permanently express eEF1A-1, and do not switch to eEF1A-2 expression. This means that the decrease in eEF1A-1 levels is modest at the whole tissue level. Immunohistochemistry would therefore probably be the best method to investigate this question, as it would enable the reduction in eEF1A-1 levels to be visualised in different cells. However, I was unable to obtain a positive signal using either of our eEF1A-1 antibodies, so it is possible that this would necessitate the designing of another eEF1A-1 anti-peptide antibody.

7.2.4 eEF1A expression in non-mammalian species

I have shown that there is an eEF1A-2 orthologue in *X. laevis*, which has a restricted expression pattern in adults and is not expressed in gastrula-stage embryos. It would therefore be of interest to investigate the precise developmental stage at which this gene is first expressed. This could be done using both Western analysis and *in situ* hybridisation on developing embryos. The sites of expression determined using *in situ* analysis could be compared with those obtained in mouse embryos.

I have also confirmed the presence of XeEF1A-2 in muscle at the RNA level, using RT-PCR. Other tissues could also be tested, to confirm the Western results. As the primers were specific for XeEF1A-2, demonstrated by the unambiguous sequence obtained, primers at the equivalent locations in the gene encoding eEF1A-S could be

used to confirm the expression pattern of eEF1A-S at the RNA level. If the tissues in which eEF1A-S mRNA is expressed is consistent with those in which the protein is expressed, and the sequence is that of eEF1A-S, this would confirm the protein recognised by the anti-*A. salina* eEF1A antibody and eEF1A-2C as eEF1A-S.

It would also be interesting to determine whether there is an orthologue of eEF1A-2 in other non-mammalian vertebrates, for example, the zebrafish, another model organism. Establishing this timing may be useful in the construction of a developmental "clock" between different organisms. It is currently difficult to directly compare different developmental stages between different organisms. It may also be worthwhile to examine whether there is an eEF1A-2 orthologue in *X. tropicalis*, especially as this organism is both more amenable to genetic analysis, and, more practically, will have its genome sequenced.

The eEF1A isoforms therefore represent a very interesting system for study on several levels. As vertebrate-specific, evolutionarily conserved proteins, they can be used to study the relationships between organisms. Understanding why there is an isoform switch in, for example, neurons could improve the knowledge of their basic cell biology. There is even a link with human disease in the form of the wasted mouse, a spontaneously-occurring eEF1A-2 knockout.

References

Abbott, C M, *et al.* (1986). Deficiency of adenosine deaminase in the wasted mouse. *Proceedings of the National Academy of Sciences* **83**: 693-695.

Abbott, C, *et al.* (1994). Linkage Mapping around the Ragged (*Ra*) and Wasted (*wst*) Loci on Distal Chromosome 2. *Genomics* **20**: 94-98.

Abdallah, B, *et al.* (1991a). Germ cell-specific expression of a gene encoding eukaryotic translation elongation factor 1α (eEF-1α) and generation of eEF-1α retropseudogenes in *Xenopus laevis*. *Proceedings of the National Academy of Sciences* **88**: 9277-9281.

Abdallah, B, *et al.* (1991b). The genes encoding the major 42 S storage particle proteins are expressed in male and female germ cells of *Xenopus laevis*. *Development* **113**: 851-856.

Abdallah, B, *et al.* (1996). Thyroid hormone regulation of germ cell-specific EF-1α expression during metamorphosis of *Xenopus laevis*. *International Journal of Developmental Biology* **40**: 507-514.

Al-Chalabi, A, *et al.* (1998). Recessive amyotrophic lateral sclerosis families with the D90A SOD1 mutation share a common founder: evidence for a linked protective factor. *Human Molecular Genetics* **7**: 2045-2050.

Al-Chalabi, A, *et al.* (1999). Deletions of the heavy neurofilament subunit tail in amyotrophic lateral sclerosis. *Human Molecular Genetics* **8**: 157-164.

Alexander, G M, *et al.* (2000). Elevated Cortical Extracellular Fluid Glutamate in Transgenic Mice Expressing Human Mutant (G93A) Cu/Zn Superoxide Dismutase. *Journal of Neurochemistry* **74**: 1666-1673.

Amaya, E, Offield, M F and Grainger, R M
http://faculty.virginia.edu/xtropicalis/overview/amaya.html

Anand, N, *et al.* (2002) Protein elongation factor *EEF1A2* is a putative oncogene in ovarian cancer. *Nature Genetics*. **3**: 301-5.

Andreassen, O A, *et al.* (2000). Partial Deficiency of Manganese Superoxide Dismutase Exacerbates a Transgenic Mouse Model of Amyotrophic Lateral Sclerosis. *Annals of Neurology* **47**: 447-455.

Ann, D K, *et al.* (1991). Isolation and Characterisation of the Rat Chromosomal Gene for a Polypeptide (pS1) Antigenically Related to Statin. *The Journal of Biological Chemistry* **266**: 10429-10437.

Annegers, J F, *et al.* (1991). Amyotrophic Lateral Sclerosis Mortality Rates in Harris County, Texas. *Advances in Neurology* **56**: 239-243.

Aoki, M, *et al.* (1998). Mutations in the glutamate transporter EAAT2 gene do not cause abnormal EAAT2 transcripts in amyotrophic lateral sclerosis. *Annals of Neurology* **43**: 645-653.

Aron-Badin, R (2002). A possible role of eukaryotic translation elongation factor A2 (eEF1A-2) in spinal muscular atrophy. MRes thesis, University of Edinburgh.

Arriza, J L, *et al.* (1993). Cloning and expression of a human neutral amino acid transporter with structural similarity to the glutamate transporter gene family. *Journal of Biological Chemistry* **268**: 15329-15332.

Avraham, K B, *et al.* (1988). Down's Syndrome: Abnormal Neuromuscular Junction In Tongue of Transgenic Mice with Elevated Levels of Human Cu/Zn-Superoxide Dismutase. *Cell* **54**: 823-829.

Baulac, M, Rieger, F and Meininger, V (1983). The loss of motoneurons corresponding to specific muscles in the *wobbler* mutant mouse. *Neuroscience Letters* **37**: 99-104.

Beal, M F, *et al.* (1997). Increased 3-Nitrotyrosine in Both Sporadic and Familial Amyotrophic Lateral Sclerosis. *Annals of Neurology* **42**: 646-654.

Beaulieu, J-M, Jacomy, H and Julien, J-P (2000). Formation of Intermediate Filament Protein Aggregates with Disparate Effects in Two Transgenic Mouse Models Lacking the Neurofilament Light Subunit. *Journal of Neuroscience* **20**: 5321-5328.

Beaulieu, J-M, Nguyen, M D and Julien, J-P (1999). Late Onset Death of Motor Neurons in Mice Overexpressing Wild-Type Peripherin. *Journal of Cell Biology* **147**: 531-544.

Bennet, P L, *et al.* (2000). Mutation screening of a neutral amino acid transporter, ASCT1, and its potential role in schizophrenia. *Psychiatric Genetics* **10**: 79-82.

Berger, M M, *et al.* (2000). Detection and cellular localization of enterovirus RNA sequences in spinal cord of patients with ALS. *Neurology* **54**: 20-25.

Bergerton, C, *et al.* (1994). Neurofilament Light and Polyadenylated mRNA Levels are Decreased in Amyotrophic Lateral Sclerosis Motor Neurons. *Journal of Neuropathology and Experimental Neurology* **53**: 221-230.

Berns, A (2000). Personal Communication.

Biedler, J L, *et al.* (1978). Multiple neurotransmitter synthesis by human neuroblastoma cell lines and clones. *Cancer Research* **11**: 3751-3757.

Bischoff, C, *et al.* (2000). The Human Elongation Factor 1 A-2 Gene (*EEF1A2*): Complete Structure and Characterisation of Gene Structure and Promoter Activity. *Genomics* **68**: 63-70.

Blair, I P, *et al.* (2000). A gene for autosomal dominant juvenile amyotrophic lateral sclerosis (ALS4) localizes to a 500-kb interval on chromosome 9q34. *Neurogenetics* **3**: 1-6.

Borthwick, G M, *et al.* (1999). Mitochondrial Enzyme Activity in Amyotrophic Lateral Sclerosis: Implications for the Role of Mitochondria in Neuronal Cell Death. *Annals of Neurology* **46**: 787-790.

Brahe, C, *et al.* (1995). Genetic homogeneity between childhood-onset and adult-onset autosomal recessive spinal muscular atrophy. *Lancet* **346**: 741-742.

Bruijn, L I, *et al.* (1997). ALS-Linked SOD1 Mutant G85R Mediates Damage to Astrocytes and Promotes Rapidly Progressive Disease with SOD1-Containing Inclusions. *Neuron* **18**: 327-338.

Brussaglia, E, *et al.* (1995). A frame-shift deletion in the survival motor neuron gene in Spanish spinal muscular atrophy patients. *Nature Genetics* **11**: 335-337.

Burglen, L, *et al.* (1995). SMN gene deletion in variant of infantile spinal muscular atrophy. *Lancet* **346**: 316-317.

Campbell, L, *et al.* (1997). Genomic variation and gene conversion in spinal muscular atrophy: implications for disease process and clinical phenotype. *American Journal of Human Genetics* **61**: 40-50.

Canete-Soler, R, *et al.* (1999). Mutation in Neurofilament Transgene Implicates RNA Processing in the Pathogenesis of Neurodegenerative Disease. *Journal of Neuroscience* **19**: 1273-1283.

Canto, M C D and Gurney, M E (1995). Neuropathological changes in two lines of mice carrying a transgene for mutant human Cu,Zn SOD, and in mice overexpressing wild type human SOD: a model of familial amyotrophic lateral sclerosis (FALS). *Brain Research* **676**: 25-40.

Carr-Schmid, A, *et al.* (1999). Mutations in Elongation Factor 1β, a Guanine Nucleotide Exchange Factor, Enhance Translational Fidelity. *Molecular and Cellular Biology* **19**: 5257-5266.

Carvalho, T, *et al.* (1999). The spinal muscular atrophy disease gene product, SMN: a link between snRNP biogenesis and the Cajal (coiled) body. *Journal of Cell Biology* **147**: 715-727.

Chambers, D M, Peters, J and Abbott, C M (1998). The lethal mutation of the mouse wasted (*wst*) is a deletion that abolishes expression of a tissue-specific isoform of

translation elongation factor 1α, encoded by the *Eef1a2* gene. *Proceedings of the National Academy of Sciences* **95**: 4463-4468.

Chambers, D M, Rouleau, G A and Abbott, C M (2001). Comparative Genomic Analysis of Genes Encoding Translation Elongation Factor 1Bα in Human and Mouse Shows *EEF1B1* to Be a Recent Retrotransposition Event. *Genomics* **77**: 145-148.

Charroux, B, *et al.* (2000). Gemin4. A novel component of the SMN complex that is found in both gems and nucleoli. *Journal of Cell Biology* **148**: 1177-1186.

Chavany, C, *et al.* (1998). Transgenic mice for interleukin 3 develop motor neuron degeneration associated with autoimmune reaction against spinal cord motor neurons. *Proceedings of the National Academy of Sciences* **95**: 11354-11359.

Chen, E, *et al.* (2000). Rapid up-regulation of peptide elongation factor EF-1α protein levels is an immediate early event during oxidative stress-induced apoptosis. *Experimental Cell Research* **259**: 140-148.

Cifuentes-Diaz, C, *et al.* (2001). Deletion of murine *Smn* exon 7b directed to skeletal muscle leads to severe muscular dystrophy. *Journal of Cell Biology* **152**: 1107-1114.

Coghill, E L, *et al.* (2002). A gene-driven approach to the identification of ENU mutants in the mouse. *Nature Genetics* **30**: 255-256.

Colosimo, A, *et al.* (2002). Reliability of DHPLC in mutational screening of beta-globin (HBB) alleles. *Human Mutation* **19**: 287-295.

Comi, G P, *et al.* (1998). Cytochrome c oxidase subunit 1 microdeletion in a Patient with Motor Neurone Disease. *Annals of Neurology* **43**: 110-116.

Condeelis, J (1995). Elongation factor 1α, translation and the cytoskeleton. *Trends in Biological Science* **20**: 169-170.

Cook, S A, *et al.* (1995). Neuromuscular degeneration (*nmd*): a mutation on mouse Chromosome 19 that causes motor neuron degeneration. *Mammalian Genome* **6**: 187-191.

Cooper, G M (2000). The Cell - A Molecular Approach. 2nd Edition. Sinauer Associates Inc, Sunderland, MA

Coppard, N J, *et al.* (1991). 42Sp48 in Previtellogenic *Xenopus* Oocytes Is Structurally Homologous to EF-1α and May Be a Stage-specific Elongation Factor. *Journal of Cell Biology* **112**: 237-243.

Corcia, P, *et al.* (2002). Abnormal SMN1 Gene Copy Number Is a Susceptibility Factor for Amyotrophic Lateral Sclerosis. *Annals of Neurology* **51**: (243-246).

Cote, F, Collard, J-F and Julien, J-P (1993). Progressive Neuronopathy in Transgenic Mice Expressing the Human Neurofilament Heavy Gene: A Mouse Model of Amyotrophic Lateral Sclerosis. *Cell* **73**: 35-46.

Couillard-Despres, S, Meier, J and Julien, J-P (2000). Extra Axonal Neurofilaments Do Not Exacerbate Disease Caused by Mutant Cu,Zn Superoxide Dismutase. *Neurobiology of Disease* **7**: 462-470.

Couillard-Despres, S, *et al.* (1998). Protective effect of neurofilament heavy gene overexpression in motor neuron disease induced by mutant superoxide dismutase. *Proceedings of the National Academy of Sciences* **95**: 9626-9630.

Cox, G A, Mahaffey, C L and Frankel, W N (1998). Identification of the Mouse Neuromuscular Degeneration Gene and Mapping of a Second Site Suppressor Allele. *Neuron* **21**: 1327-1337.

Crawford, T O and Scholasky, R L (2002). The Relationship of *SMN* to Amyotrophic Lateral Sclerosis; and replies. *Annals of Neurology*: 857-861.

Danielewicz, A (2002). Expression of the Human Elongation Factor 1A Isoforms in Three Eukaryotic Systems: *Saccharomyces cerevisiae*, *Podospora anserina* and Human Cell Culture. PhD thesis, University of Arhus.

DeChiara, T M, *et al.* (1995). Mice Lacking the CNTF Receptor, Unlike Mice Lacking CNTF, Exhibit Profound Motor Neuron Deficits at Birth. *Cell* **83**: 313-322.

Deuchar, E M (1975). *XENOPUS*: The South African Clawed Frog. John Wiley & Sons, Ltd, London.

Dever, T E, *et al.* (1989). Location of seven post-translational modifications in rabbit elongation factor 1α including dimethyllysine, trimethyllysine, and glycerylphosphorylethanolamine. *Journal of Biological Chemistry* **264**: 20518-20525.

DiDonato, C J, *et al.* (1994). Association between Ag1-CA alleles and severity of autosomal recessive proximal spinal muscular atrophy. *American Journal of Human Genetics* **55**: 1218-1229.

Dje, M K, *et al.* (1990). Three genes under different developmental control encode elongation factor 1-α in *Xenopus laevis*. *Nucleic Acids Research* **18**: 3489-3493.

Doble, A and Kennel, P (2000). Animal models of amyotrophic lateral sclerosis. *ALS and other motor neuron disorders* **1**: 301-312.

Drory, V E, *et al.* (2001). Association of APOE ε4 allele with survival in amyotrophic lateral sclerosis. *Journal of the neurological Sciences* **190**: 17-20.

Duchen, L W, Strich, S J and Falconer, D S (1968). An hereditary motor neurone disease with progressive denervation of muscle in the mouse: the mutant "wobbler". *Journal of Neurology, Neurosurgery and Psychiatry* **31**: 535-542.

Duttaroy, A, *et al.* (1998). Apoptosis Rate Can Be Accelerated or Decelerated by Overexpression or Reduction of the Level of Elongation Factor-1α. *Experimental Cell Research* **238**: 168-176.

Edmonds, B T, *et al.* (1996). Elongation factor-1α is an overexpressed actin binding protein in metastatic rat mammary adenocarcinoma. *Journal of Cell Science* **109**: 2705-2714.

Elder, G A, *et al.* (1998a). Absence of the Mid-sized Neurofilament Subunit Increases Axonal Calibers, Levels of Light Neurofilament (NF-L), and Neurofilament Content. *Journal of Cell Biology* **141**: 727-739.

Elder, G A, *et al.* (1998b). Requirement of Heavy Neurofilament Subunit in the Development of Axons with Large Calibers. *Journal of Cell Biology* **143**: 195-205.

Elder, G A, *et al.* (1999a). Age-related Atrophy of Motor Axons in Mice Deficient in the Mid-sized Neurofilament Subunit. *Journal of Cell Biology* **146**: 181-192.

Elder, G A, *et al.* (1999b). Mice With Disrupted Midsized and Heavy Neurofilament Genes Lack Axonal Neurofilaments but Have Unaltered Numbers of Axonal Microtubules. *Journal of Neuroscience Research* **57**: 23-32.

Emery, A E (1991). Population frequencies of inherited neuromuscular diseases - a world survey. *Neuromuscular Disorders* **1**: 19-29.

Epstein, C J, *et al.* (1987). Transgenic mice with increased Cu/Zn-superoxide dismutase activity: Animal model of dosage effects in Down syndrome. *Proceedings of the National Academy of Sciences* **84**: 8044-8048.

Eyer, J and Peterson, A (1994). Neurofilament-Deficient Axons and perikaryal Aggregates in Viable Transgenic Mice Expressing a Neurofilament-B-Galactosidase Fusion Protein. *Neuron* **12**: 389-405.

Eymard-Pierre, E, *et al.* (2002). Infantile-onset ascending hereditary spastic paralysis is associated with mutations in the alsin gene. *American Journal of Human Genetics* **71**: 518-527.

Feig, S and Lipton, P (1993). Pairing the cholinergic agonist carbachol with patterned Schaffer collateral stimulation initiates protein synthesis in hippocampal CA1 pyramidal cell dendrites via a muscarinic, NMDA-dependent mechanism. *Journal of Neuroscience* **13**: 1010-1021.

Figlewicz, D A, *et al.* (1994). Variants of the heavy neurofilament subunit are associated with the development of amyotrophic lateral sclerosis. *Human Molecular Genetics* **3**: 1757-1761.

Flood, D G, *et al.* (1999). Hindlimb Motor Neurons Require Cu/Zn Superoxide Dismutase for Maintenance of Neuromuscular Junctions. *American Journal of Pathology* **155**: 663-672.

Flowers, J M, *et al.* (2001). Intron 7 Retention and Exon Skipping EAAT2 mRNA Variants Are Not Associated with Amyotrophic Lateral Sclerosis. *Annals of Neurology* **49**: 643-649.

Fray, A E, *et al.* (1998). The expression of the glial glutamate transporter protein EAAT2 in motor neuron disease: an immunohistochemical study. *European Journal of Neuroscience* **10**: 2481-2489.

Friedlander, R M, *et al.* (1997). Inhibition of ICE slows ALS in mice. *Nature* **388**: 31.

Frugier, T, *et al.* (2000). Nuclear targeting deficit of SMN lacking the C-terminus in a mouse model of spinal muscular atrophy. *Human Molecular Genetics* **9**: 849-858.

Frugier, T, *et al.* (2002). The molecular bases of spinal muscular atrophy. *Current Opinion in Genetics and Development* **12**: 294-298.

Fuchs, S, *et al.* (2002). Comparative transcription map of the *wobbler* critical region on mouse chromosome 11 and the homologous region on human chromosome 2p13-14. *Biomed Central Genetics* **3**: 14.

Fujita, K, *et al.* (1998). Increases in fragmented glial fibrillary acidic protein levels in the spinal cords of patients with amyotrophic lateral sclerosis. *Neurochemical Research* **23**: 169-174.

Gambardella, A, *et al.* (1998). Spinal Muscular Atrophy due to an Isolated Deletion of Exon 8 of the Telomeric Survival Motor Neuron Gene. *Annals of Neurology* **44**: 836-839.

Gangwani, L, *et al.* (1998). Interaction of ZPR1 with Translation Elongation Factor-1α in Proliferating Cells. *Journal of Cell Biology* **143**: 1471-1484.

Gangwani, L, *et al.* (2001). Spinal muscular atrophy disrupts the interaction of ZPR1 with the SMN protein. *Nature Cell Biology* **3**: 376-383.

Giess, R, *et al.* (2000). Potential role of *LIF* as a modifier gene in the pathogenesis of amyotrophic lateral sclerosis. *Neurology* **54**: 1003-1005.

Giess, R, *et al.* (2002). Early Onset of Severe Familial Amyotrophic Lateral Sclerosis with a SOD-1 mutation: Potential Impact of CNTF as a Candidate Modifier Gene. *American Journal of Human Genetics* **70**: 1277-1286.

Glavac, D and Dean, M (1993). Optimization of the Single-Strand Conformation Polymorphism (SSCP) Technique for Detection of Point Mutations. *Human Mutation* **2**: 404-414.

Goldowitz, D, *et al.* (1985). Longitudinal Assessment of Immunologic Abnormalities of Mice with the autosomal recessive mutation, "wasted". *Journal of Immunology* **135**: 1806-1812.

Gong, Y H, *et al.* (2000). Restricted Expression of G86R Cu/Zn Superoxide Dismutase in Astrocytes Results in Astrocytosis But Does Not Cause Motoneuron Degeneration. *Journal of Neuroscience* **20**: 660-665.

Gordon, P H (1997). Lymphoproliferative disorders and motor neuron disease: an update. *Neurology* **48**: 1671-1678.

Graham, D I and Lantos, P L, Eds. (1997). Greenfield's Neuropathology, 6th Edition. Arnold, London

Greene, L A and Tischler, A S (1976). Establishment of a noradrenergic clonal line of rat adrenal pheochromocytoma cells which respond to nerve growth factor. *Proceedings of the National Academy of Sciences* **73**: 2424-2428.

Grohmann, K, *et al.* (2001). Mutations in the gene encoding immunoglobulin mu-binding protein 2 cause spinal muscular atrophy with respiratory distress type 1. *Nature Genetics* **29**: 75-77.

Gurney, M E, *et al.* (1994). Motor Neuron Degeneration in Mice That Express a Human Cu,Zn Superoxide Dismutase Mutation. *Science* **264**: 1772-1774.

Hadano, S, *et al.* (2001). A gene encoding a putative GTPase regulator is mutated in familial amyotrophic lateral sclerosis 2. *Nature Genetics* **29**: 166-173.

Hand, C K, *et al.* (2002). A Novel Locus for Familial Amyotrophic Lateral Sclerosis, on Chromosome 18q. *American Journal of Human Genetics* **70**: 251-256.

Harada, Y, *et al.* (2002). Correlation between SMN2 copy number and clinical phenotype of spinal muscular atrophy: three SMN2 copies fail to rescue some patients from the disease severity. *Journal of Neurology* **249**: 1211-1219.

Hausmanowa-Petrusewicz, I (1991). Spinal Muscular Atrophies: How Many Types? *Advances in Neurology* **56**: 157-167.

Hayashi, K and Yandell, D W (1993). How Sensitive Is PCR-SSCP? *Human Mutation* **2**: 338-346.

Hayward, C, *et al.* (1999). Molecular genetic analysis of the APEX nuclease gene in amyotrophic lateral sclerosis. *Neurology* **52**: 1899-1901.

Heimann, P, Laage, S and Jockusch, H (1991). Defect of sperm assembly in a neurological mutant of the mouse, wobbler (WR). *Differentiation* **47**: 77-83.

Hellstrom-Lindahl, E (2000). Modulation of beta-amyloid precursor protein processing and tau phosphorylation by acetylcholine receptors. *European Journal of Pharmacology* **393**: 1-3.

Hentati, A, *et al.* (1994). Linkage of recessive familial amyotrophic lateral sclerosis to chromosome 2q33-q35. *Nature Genetics* **7**: 425-428.

Hentati, A, *et al.* (1998). Linkage of a commoner form of recessive amyotrophic lateral sclerosis to chromosome 15q15-q22 markers. *Neurogenetics* **2**: 55-60.

Hershey, J W (1996). Translational control in mammalian cells. *Annual Review of Biochemistry* **60**: 717-755.

Hofmann, K, *et al.* (1994). Human neutral amino acid transporter ASCT1: structure of the gene (SLC1A4) and localization to chromosome 2p13-p15. *Genomics* **24**: 20-26.

Hong, S, *et al.* (1998). X-linked dominant locus for late-onset familial amyotrophic lateral sclerosis. *Society of Neuroscience Abstracts* **24**: 478.

Honig, L S, *et al.* (2000). Glutamate transporter EAAT2 splice variants occur not only in ALS, but also in AD and controls. *Neurology* **55**: 1082-1088.

Hoveman, B, *et al.* (1988). Two genes encode related cytoplasmic elongation factors 1α (EF-1α) in *Drosophila melanogaster* with continuous and stage specific expression. *Nucleic Acids Research* **16**: 3175-3194.

Howland, D S, *et al.* (2002). Focal loss of the glutamate transporter EAAT2 in a transgenic rat model of SOD1 mutant-mediated amyotrophic lateral sclerosis (ALS). *Proceedings of the National Academy of Sciences* **99**: 1604-1609.

Hrabe de Angelis, M H, *et al.* (2000). Genome-wide, large scale production of mutant mice by ENU mutagenesis. *Nature Genetics* **4**: 444-447.

HRD / Autosomal Recessive Kenny-Caffey Syndrome Consortium (2002). Mutation of *TBCE* causes hypoparathyroidism-retardation-dysmorphism and autosomal recessive Kenny-Caffey syndrome. *Nature Genetics* **32**: 448-452.

Hsieh-Li, H M, *et al.* (2000). A mouse model for spinal muscular atrophy. *Nature Genetics* **66-70**.

Jaarsma, D, *et al.* (2000). Human Cu/Zn Superoxide Dismutase (SOD1) Overexpression in Mice Causes Mitochondrial Vacuolization, Axonal Degeneration, and Premature Motorneuron Death and Accelerates Motoneuron Disease in Mice Expressing a Familial Amyotrophic Lateral Sclerosis Mutant SOD1. *Neurobiology of Disease* **7**: 623-643.

Job, C and Eberwine, J (2001a). Identification of sites for exponential translation in living dendrites. *Proceedings of the National Academy of Sciences* **98**: 13037-13042.

Job, C and Eberwine, J (2001b). Localization and translation of mRNA in dendrites and axons. *Nature Reviews Neuroscience* **2**: 889-898.

Johnston, J A, *et al.* (2000). Formation of high molecular weight complexes of mutant Cu,Zn-superoxide dismutase in a mouse model for familial amyotrophic lateral sclerosis. *Proceedings of the National Academy of Sciences* **97**: 12571-12576.

Jones, C T, *et al.* (1993). Cu/Zn superoxide dismutase (SOD1) mutations and sporadic amyotrophic lateral sclerosis. *Lancet* **342**: 1050-1051.

Julien, J-P and Mushynski, W E (1998). Neurofilaments in Health and Disease. *Progress in Nucleic Acid Research and Molecular Biology* **61**: 1-23.

Junqueira, L C, Carneiro, J, Kelley, R O (1995). Basic Histology, 8th Edition. Prentice-Hall, London.

Kahns, S, *et al.* (1998). The elongation factor 1 A-2 isoform from rabbit: cloning of the cDNA and characterisation of the protein. *Nucleic Acids Research* **26**: 1884-1890.

Kaiserlian, D, *et al.* (1986). The wasted mutant mouse. II. Immunological abnormalities in a mouse described as a model of ataxia-telangiectasia. *Clinical Experimental Immunology* **63**: 562-569.

Kandl, K A, *et al.* (2002). Identification of a role for actin in translational fidelity in yeast. *Molecular Genetics and Genomics* **268**: 10-18.

Karlsen, R L, *et al.* (1981). Morphological Changes in Rat Brain Induced by L-Cysteine Injection in Newborn Animals. *Brain Research* **208**: 167-180.

Kaupmann, K, *et al.* (1992). Wobbler, a Mutation Affecting Motoneuron Survival and Gonadal Functions in the Mouse, Maps to Proximal Chromosome 11. *Genomics* **13**: 39-43.

Keilbassa, K, *et al.* (1995). Protein kinase C δ-specific phosphorylation of the elongation factor eEF-α and an eEF-1α peptide at threonine 431. *Journal of Biological Chemistry* **270**: 6156-6162.

Khalyfa, A, *et al.* (1999). Toxin Injury-Dependent Switched Expression Between EF-1α and Its Sister, S1, in Rat Skeletal Muscle. *Developmental Dynamics* **216**: 267-273.

Khalyfa, A, *et al.* (2001). Characterization of Elongation Factor-1A (eEF1A-1) and eEF1A-2/S1 Protein Expression in Normal and *wasted* Mice. *Journal of Biological Chemistry* **276**: 22915-22922.

Kikuchi, H, *et al.* (1997). Immunohistochemical analysis of spinal cord lesions in amyotrophic lateral sclerosis using microtubule-associated protein 2 (MAP2) antibodies. *Acta Neuropathologica* **97**: 13-21.

Kisby, G E, Milne, J and Sweatt, C (1997). Evidence of reduced DNA repair in amyotrophic lateral sclerosis brain tissue. *NeuroReport* **8**: 1337-1340.

Klivenyi, P, *et al.* (1999). Neuroprotective effect of creatine in a transgenic animal model of amyotrophic lateral sclerosis. *Nature Medicine* **5**: 347-350.

Knudsen, S M, *et al.* (1993). Tissue-dependent variation in the expression of elongation factor-1α isoforms: Isolation and characterisation of a cDNA encoding a novel variant of human elongation-factor 1α. *European Journal of Biochemistry* **215**: 549-554.

Kong, J and Xu, Z (2000). Overexpression of neurofilament subunit NF-L and NF-H extends survival of a mouse model for amyotrophic lateral sclerosis. *Neuroscience Letters* **281**: 72-74.

Krieg, P A, *et al.* (1989). The mRNA Encoding Elongation Factor 1-α (EF-1α) Is a Major Transcript at the Midblastula Transition in *Xenopus*. *Developmental Biology* **133**: 93-100.

Kriz, J, *et al.* (2000). Electrophysiological properties of axons in mice lacking neurofilament subunit genes: disparity between conduction velocity and axon diameter in absence of NF-H. *Brain Research* **885**: 32-44.

Kunst, C B, *et al.* (2000). Genetic Mapping of a Mouse Modifier Gene That Can Prevent ALS Onset. *Genomics* **70**: 181-189.

Kunst, C B, *et al.* (1997). Mutations in SOD1 associated with amyotrophic lateral sclerosis cause novel protein interactions. *Nature Genetics* **15**: 91-94.

Kurtzke, J F (1991). Risk Factors in Amyotrophic Lateral Sclerosis. *Advances in Neurology* **56**: 245-269.

Leah, R, *et al.* (1998). The Copper Chaperone CCS Directly Interacts with Copper/Zinc Superoxide Dismutase. *Journal of Biological Chemistry* **273**: 23625-23628.

Lee, M K, Marszalek, J R and Cleveland, D W (1994). A Mutant Neurofilament Subunit Causes Massive, Selective Motor Neuron Death: Implications for the Pathogenesis of Human Motor Neuron Disease. *Neuron* **13**: 975-988.

Lee, S, *et al.* (1992). Tissue-Specific Expression in Mammalian Brain, Heart and Muscle of S1, A Member of the Elongation Factor-1α Gene Family. *Journal of Biological Chemistry* **267**: 24064-24068.

Lee, S, Wolfraim, L A and Wang, E (1993a). Differential Expression of S1 and Elongation Factor-1α during Rat Development. *Journal of Biological Chemistry* **268**: 24453-24459.

Lee, S, Stollar, E and Wang, E (1993b). Localization of S1 and Elongation Factor-1α mRNA in Rat Brain and Liver by Non-radioactive In Situ Hybridization. *Journal of Histochemistry and Cytochemistry* **41**: 1093-1098.

Lee, S, Ann, D K and Wang, E (1994). Cloning of human and mouse brain cDNAs coding for S1, the second member of the mammalian elongation factor-1 alpha gene family:Analysis of a possible evolutionary pathway. *Biochemical and Biophysical Research Communications* **203**: 1371-1377.

Lee, S, *et al.* (1995). Terminal Differentiation-Dependent Alteration in the Expression of Translation Elongation Factor-1α and Its Sister Gene, S1, in Neurons. *Experimental Cell Research* **219**: 589-597.

Lee, V M, Goedert, M and Trojanowski, J Q (2001). Neurodegenerative tauopathies. *Annual Review of Neuroscience* **24**: 1121-1159.

Leegwater, P A J, *et al.* (2001). Subunits of the translation initiation factor eIF2B are mutant in leukoencephalopathy with vanishing white matter. *Nature Genetics* **29**: 1-6.

Leetsma, J E and Sepsenwol, S (1980). Sperm axoneme alterations in the wobbler mouse. *Journal of Reproduction and Fertility* **58**: 267-280.

Lefebvre, S, *et al.* (1995). Identification and characterization of a spinal muscular atrophy-determining gene. *Cell* **80**: 155-165.

Lefebvre, S, *et al.* (1997). Correlation between severity and SMN protein level in spinal muscular atrophy. *Nature Genetics* **16**: 265-269.

Lefebvre, S, *et al.* (2002). A novel nuclear structure containing the survival of motor neurons protein. *Human Molecular Genetics* **11**: 1017-1027.

Leigh, P N, *et al.* (1988). Ubiquitin deposits in anterior horn cells in motor neurone disease. *Neuroscience Letters* **93**: 197-203.

Leigh, P N, *et al.* (1991). Ubiquitin-immunoreactive intraneuronal inclusions in amyotrophic lateral sclerosis. *Brain* **114**: 775-788.

Lengeling, A, *et al.* (1994). Exclusion of two candidate genes, *Spnb-2* and *Ddc,* for the wobbler spinal muscular atrophy gene on proximal mouse Chromosome 11. *Mammalian Genome* **5**: 163-166.

Lilienfield, D E, *et al.* (1989). Rising mortality from motoneuron disease in the USA, 1962-84. *Lancet*: 711-713.

Lin, C-L G, *et al.* (1998). Aberrant RNA Processing in a Neurodegenerative Disease: the Cause for Absent EAAT2, a Glutamate Transporter, in Amyotrophic Lateral Sclerosis. *Neuron* **20**: 589-602.

Liu, C H L, Liu, S and Wang, E (1993). Expression of an EF-1α-like rat cDNA, S1, in *E. Coli* and production of a rabbit polyclonal antiserum to the recombinant protein. *Biochemical and Biophysical Research Communications* **195**: 1371-1378.

Liu, G, *et al.* (2002). Interactions of Elongation Factor 1α with F-Actin and β-Actin mRNA: Implications for Anchoring mRNA in Cell Protrusions. *Molecular Biology of the Cell* **13**: 579-592.

Liu, Q and Dreyfuss, G (1996). A novel nuclear structure containing the survival of motor neurons protein. *EMBO Journal* **15**: 3555-3565.

Liu, R, *et al.* (1998). Enhanced Oxygen Radical Production in a Transgenic Mouse Model of Familial Amyotrophic Lateral Sclerosis. *Annals of Neurology* **44**: 763-770.

Liu, W, *et al.* (1998). Denaturing high performance liquid chromatography (DHPLC) used in the detection of germline and somatic mutations. *Nucleic Acids Research* **26**: 1396-1400.

Lorson, C L, *et al.* (1999). A single nucleotide in the *SMN* gene regulates splicing and is responsible for spinal muscular atrophy. *Proceedings of the National Academy of Sciences* **96**: 6307-6311.

Lund, A, *et al.* (1996). Assignment of Human Elongation Factor 1α Genes: *EEF1A* Maps to Chromosome 6q14 and *EEF1A2* to 20q13.3. *Genomics* **36**: 359-361.

Lutsep, H L and Rodriguez, M (1989). Ultrastructural, Morphometric and Immunocytochemical Study of Anterior Horn Cells in Mice with "Wasted" Mutation. *Journal of Neuropathology and Experimental Neurology* **48**: 519-533.

Madsen, H O, *et al.* (1990). Retropseudogenes constitute the major part of the human elongation factor 1α gene family. *Nucleic Acids Research* **18**: 1513-1516.

Makowske, M and Christensen, H N (1982). Hepatic Transport System Interconverted by Protonation from Service for Neutral to Service for Anionic Amino Acids. *Journal of Biological Chemistry* **257**: 14635-14638.

Manetto, V, *et al.* (1988). Phosphorylation of Neurofilaments Is Altered in Amyotrophic Lateral Sclerosis. *Journal of Neuropathology and Experimental Neurology* **47**: 642-653.

Mansilla, F, *et al.* (2002). Mapping the human translation elongation factor eEF1H complex using the yeast two-hybrid system. *Biochemical Journal* **365**: 669-676.

Marszalek, J R, *et al.* (1996). Neurofilament subunit NF-H modulates axonal diameter by selectively slowing neurofilament transport. *Journal of Cell Biology* **135**: 711-724.

Martin, N, *et al.* (2002). A missense mutation in *Tbce* causes progressive motor neuronopathy in mice. *Nature Genetics* **32**: 443-447.

Masu, Y, *et al.* (1993). Disruption of the CNTF gene results in motor neuron degeneration. *Nature* **365**: 27-32.

Matyas, G, *et al.* (2002). Evaluation and application of denaturing HPLC for mutation detection in Marfan syndrome: Identification of 20 novel mutations and two novel polymorphisms in the FBN1 gene. *Human Mutation* **19**: 443-456.

McClatchy, D B, *et al.* (2002). Novel interaction between the M_4 muscarinic acetylcholine receptor and elongation factor 1A2. *Journal of Biological Chemistry* **277**: 29268-29274.

McManus, M T and Sharp, P A (2002). Gene Silencing in Mammals by Small Interfering RNAs. *Nature Reviews Genetics* **3**: 737-747.

Meier, J, *et al.* (1999). Extra Neurofilament NF-L Subunits Rescue Motor Neuron Disease Caused by Overexpression of the Human NF-H Gene in Mice. *Journal of Neuropathology and Experimental Neurology* **58**: 1099-1110.

Meyer, T, *et al.* (1999). The RNA of the glutamate transporter *EAAT2* is variably spliced in amyotrophic lateral sclerosis and normal individuals. *Journal of Neurological Science* **170**: 45-50.

Mita, K, *et al.* (1997). Comprehensive cloning of *Schizosaccharomyces pombe* genes encoding translation elongation factors. *Gene* **187**: 259-266.

Mitchell, J D (2000). Amyotrophic lateral slerosis:toxins and environment. *ALS and other motor neuron disorders* **1**: 235-250.

Mitsomoto, H and Bradley, W G (1982). Murine motor neuron disease (the wobbler mouse). Degeneration and regeneration of the lower motor neurons. *Brain* **105**: 811-834.

Miyata, Y (1983). A new mutant mouse with motor neuron disease. *Brain Research* **312**: 139-142.

Monani, U R, *et al.* (1999). A single nucleotide difference that alters splicing patterns distinguishes the DSMA gene *SMN1* from the copy gene *SMN2*. *Human Molecular Genetics* **8**: 1177-1183.

Morales, J, *et al.* (1993). Expression of Elongation Factor 1α (EF-1α) and 1βγ (EF-1βγ) Are Uncoupled in Early *Xenopus* Embryos. *Developmental Genetics* **14**: 440-448.

Morris, H R, *et al.* (2001). A clinical and pathological study of motor neurone disease on Guam. *Brain* **124**: 2215-2222.

Morrison, B M, *et al.* (2000). Early and Selective Pathology of Light Chain Neurofilament in the Spinal Cord and Sciatic Nerve of G86R Mutant Superoxide Dismutase Transgenic Mice. *Experimental Neurology* **165**: 207-220.

Mouse Genome Sequencing Consortium (2002). Initial sequencing and comparative analysis of the mouse genome. *Nature* **420**: 520-526.

Munoz, D G, *et al.* (1988). Accumulation of Phosphorylated Neurofilaments in Anterior Horn Motoneurons of Amyotrophic Lateral Sclerosis Patients. *Journal of Neuropathology and Experimental Neurology* **47**: 9-18.

Munshi, R, *et al.* (2001). Overexpression of translation Elongation Factor 1A Affects the Organisation and Function of the Actin Cytoskeleton in Yeast. *Genetics* **157**: 1425-1436.

Nagai, M, *et al.* (1998). Identification of alternative splicing forms of GLT-1 mRNA in the spinal cord of amyotrophic lateral sclerosis patients. *Neuroscience Letters* **244**: 165-168.

Nagai, M, *et al.* (2001). Rats Expressing Human Cytosolic Copper-Zinc Superoxide Dismutase Transgenes with Amyotrophic Lateral Sclerosis: Associated Mutations Develop Motor Neuron Disease. *Journal of Neuroscience* **2001**: 9246-9254.

Nagy, D, Kato, T and Kushner, P D (1994). Reactive astrocytes are widespread in the cortical gray matter of amyotrophic lateral sclerosis. *Journal of Neuroscience Research* **38**: 336-347.

Nataraj, A J, *et al.* (1999). Single-strand conformation polymorphism and heteroduplex analysis for gel-based mutation detection. *Electrophoresis* **20**: 1177-1185.

Nguyen, M D, Lariviere, R C and Julien, J-P (2000). Reduction of axonal caliber does not alleviate motor neuron disease caused by mutant superoxide dismutase 1. *Proceedings of the National Academy of Sciences* **97**: 12306-12311.

Nguyen, M D, Lariviere, R C and Julien, J-P (2001). Deregulation of Cdk5 in a Mouse Model of ALS: Toxicity Alleviated by Perikaryal Neurofilament Inclusions. *Neuron* **30**: 135-147.

Nicholson, S J, *et al.* (2000). Mice, the motor neuron system and human motor neuron pathology. *Mammalian Genome* **11**: 1041-1052.

Nolan, P M and al, e (2000). A systematic, genome-wide, phenotype-driven mutagenesis programme for gene function studies in the mouse. *Nature Genetics* **4**: 440-443.

Olkowstu, Z L (1998). Mutant AP endonuclease in patients with amyotrophic lateral sclerosis. *NeuroReport* **9**: 239-242.

Olney, J W and Ho, O-L (1970). Brain Damage in Infant Mice following Oral Intake of Glutamate, Aspartate or Cysteine. *Nature* **227**: 609-610.

Olney, J W, *et al.* (1972). Cysteine-induced brain damage in infant and fetal rodents. *Brain Research* **45**: 309-313.

Olney, J W, *et al.* (1990). L-Cysteine, a Bicarbonate-Sensitive Endogenous Excitotoxin. *Science* **248**: 596-599.

Oosthuyse, B, *et al.* (2001). Deletion of the hypoxia-response element in the vascular endothelial growth factor promoter causes motor neuron degeneration. *Nature Genetics* **28**: 131-138.

Orrell, R W, *et al.* (1997). The relationship of spinal muscular atrophy to motor neuron disease: Investigation of SMN and NAIP gene deletions in sporadic and familial ALS. *Journal of the Neurological Sciences* **145**: 55-61.

Orru, S, *et al.* (1999). Association of monoamine oxidase B alleles with age at onset in amyotrophic lateral sclerosis. *Neuromuscular Disorders* **9**: 593-597.

Panas, M, *et al.* (2000). Genotyping of presenilin-1 polymorphism in amyotrophic lateral sclerosis. *Journal of Neurology* **247**: 940-942.

Parton, M J, *et al.* (2002). D90A-*SOD1* Mediated Amyotrophic Lateral Sclerosis: A Single Founder for All Cases With Evidence for a *Cis*-acting Disease Modifier in the Recessive Haplotype. *Human Mutation* **20**: 473-481.

Pellizzoni, L, *et al.* (2001). A functional interaction between the survival motor neuron complex and RNA polymerase II. *Journal of Cell Biology* **152**: 75-95.

Pellizzoni, L, *et al.* (1998). A novel function for SMN, the spinal muscular atrophy disease gene product, in pre-mRNA splicing. *Cell* **95**: 615-624.

Pernas-Alsono, R, *et al.* (1996). Early upregulation of medium neurofilament gene expression in developing spinal cord of the wobbler mouse mutant. *Molecular Brain Research* **38**: 267-275.

Petroulakis, E and Wang, E (2002). Nerve growth factor specifically stimulates translation of eukaryotic elongation factor 1A-1 (eEF1A-1) mRNA by recruitment to polyribosomes in PC12 cells. *Journal of Biological Chemistry* **277**: 18718-18727.

Poorkaj, P, *et al.* (2001). TAU as a Susceptibility Gene for Amyotrophic Lateral Sclerosis-Parkinsonism Dementia Complex of Guam. *Archives of Neurology* **58**: 1871-1878.

Pötting, A, *et al.* (1990). Two different mRNAs coding for identical elongation factor 1α (EF-1α) polypeptides in *Xenopus laevis* embryos. *Differentiation* **44**: 103-110.

Pramatarova, A, *et al.* (2001). Neuron-Specific Expression of Mutant Superoxide Dismutase 1 in Transgenic Mice Does Not Lead to Motor Impairment. *Journal of Neuroscience* **21**: 3369-3374.

Ranta, S, *et al.* (1999). The neuronal ceroid lipofuscinoses in human EPMR and *mnd* mutant mice are associated with mutations in *CLN8*. *Nature Genetics* **23**: 233-236.

Rao, M V, *et al.* (1998). Neurofilament-dependent Radial Growth of Motor Axons and Axonal Organization of Neurofilaments Does Not Require the Neurofilament Heavy Subunit (NF-H) or Its Phosphorylation. *Journal of Cell Biology* **1998**: 171-181.

Ratovitski, T, *et al.* (1999). Variation in the biochemical/biophysical properties of mutant superoxide dismutase 1 enzymes and the rate of disease progression in familial amyotrophic lateral sclerosis kindreds. *Human Molecular Genetics* **8**: 1451-1460.

Raume, A G, *et al.* (1996). Motor neurons in Cu/Zn superoxide dismutase-deficient mice develop normally but exhibit enhance cell death after axonal injury. *Nature Genetics* **13**: 43-47.

Resch, K, *et al.* (1998). Homology between human Chromosome 2p13.3 and the wobbler critical region on mouse Chromosome 11: comparative high-resolution mapping of STS and EST loci on YAC/BAC contigs. *Mammalian Genome* **9**: 893-898.

Reynet, C and Kahn, C R (2001). Unbalanced expression of the different subunits of elongation factor 1 in diabetic skeletal muscle. *Proceedings of the National Academy of Sciences* **98**: 3422-3427.

Ripps, M E, *et al.* (1995). Transgenic mice expressing an altered murine superoxide dismutase gene provide an animal model of amyotrophic lateral sclerosis. *Proceedings of the National Academy of Sciences* **92**: 689-693.

Rodrigues, N R, *et al.* (1995). Deletions in the survival motor neuron gene on 5q13 in autosomal recessive spinal muscular atrophy. *Human Molecular Genetics* **4**: 631-634.

Roger, A J, *et al.* (1999). An evaluation of elongation factor 1α as a phylogenetic marker for eukaryotes. *Molecular Biology of Evolution* **16**: 218-233.

Rogers, D C, *et al.* (2001). SHIRPA, a protocol for behavioral assessment: validation for longitudinal study of neurological dysfunction in mice. *Neuroscience Letters* **306**: 89-92.

Rosen, D R, *et al.* (1993). Mutations in Cu/Zn superoxide dismutase are associated with familial amyotrophic lateral sclerosis. *Nature* **362**: 59-62.

Rosenberry, T L, *et al.* (1989). Biosynthetic incorporation of [3H]ethanolamine into protein synthesis elongation factor 1 alpha reveals a new post-translational protein modification. *Journal of Biological Chemistry* **264**: 7096-7099.

Rothstein, J D, Martin, L J and Kuncl, R W (1992). Decreased glutamate transport by the brain and spinal cord in amyotrophic lateral sclerosis. *New England Journal of Medicine* **326**: 1464-1468.

Rothstein, J D, *et al.* (1995). Selective loss of glial glutamate transporter GLT-1 in amyotrophic lateral sclerosis. *Annals of Neurology* **38**: 73-84.

Roy, N, *et al.* (1995). The gene for neuronal apoptosis inhibitory protein is partially deleted in individuals with spinal muscular atrophy. *Cell* **80**: 167-178.

Saigoh, K, *et al.* (1999). Intragenic deletion in the gene encoding ubiquitin carboxy-terminal hydrolase in *gad* mice. *Nature Genetics* **23**: 47-51.

Sanders, J, *et al.* (1996). Immunofluorescence studies of human fibroblasts demonstrate the presence of the complex of elongation factor-1βγδ in the endoplasmic reticulum. *Journal of Cell Science* **109**: 1113-1117.

Scarmeas, N, *et al.* (2002). Premorbid weight, body mass, and varsity athletics in ALS. *Neurology* **59**: 773-775.

Scharf, J M, *et al.* (1998). Identification of a candidate gene for spinal muscular atrophy by comparative genomics. *Nature Genetics* **20**: 83-87.

Schirmaier, F and Philippsen, P (1984). Identification of two genes coding for the translation elongation factor EF-1α of *S. cerevisiae*. *EMBO Journal* **3**: 3311-3315.

Schmalbruch, H, *et al.* (1991). A new mouse mutant with progressive motor neuronopathy. *Journal of Neuropathology and Experimental Neurology* **50**: 192-204.

Schrank, B, *et al.* (1997). Inactivation of the survival motor neuron gene, a candidate gene for human spinal muscular atrophy, leads to massive cell death in early mouse embryos. *Proceedings of the National Academy of Sciences* **94**: 9920-9925.

Shafqat, S, *et al.* (1993). Cloning and expression of a novel Na(+)-dependent neutral amino acid transporter structurally related to mammalian Na (+)/glutamate cotransporters. *Journal of Biological Chemistry* **268**: 15351-15355.

Shaw, P J and Eggett, C J (2000). Molecular factors underlying selective vulnerability of motor neurons to neurodegeneration in amyotrophic lateral sclerosis. *Journal of Neurology* **247 Suppl. 1**: I/17-I/27.

Shen, R, *et al.* (1995). Identification of the human prostatic carcinoma oncogene PTI-1 by rapid expression cloning and differential RNA display. *Proceedings of the National Academy of Sciences* **92**: 6778-6782.

Sherman, M Y and Goldberg, A L (2001). Cellular Defenses against Unfolded Proteins: A Cell Biologist Thinks about Neurodegenerative Diseases. *Neuron* **29**: 15-32.

Shiina, N, *et al.* (1994). Microtubule Severing by Elongation Factor 1α. *Science* **266**: 282-285.

Shultz, L D, *et al.* (1982). "*Wasted*", a new mutant of the mouse with abnormalities characteristic of ataxia telangiectasia. *Nature* **297**: 402-404.

Siddique, T, *et al.* (1991). Linkage of a gene causing familial amyotrophic lateral sclerosis to chromosome 21 and evidence of genetic locus heterogeneity. *New England Journal of Medicine* **324**: 1381-1384.

Siegel, G J, *et al.*, Eds. (1999). Basic Neurochemistry, 6th Edition. Lippincott, Williams and Wilkins, Philadelphia

Sobue, G, *et al.* (1990). phosphorylated high molecular weight neurofilament protein in lower motor neurons in amyotrophic lateral sclerosis and other neurodegenerative diseases involving ventral horn cells. *Acta Neuropathologica* **79**: 402-408.

Song, H, *et al.* (1999). Crystal Structure of Intact Elongation Factor EF-Tu from *Escherichia coli* in GDP Conformation at 2.05A Resolution. *Journal of Molecular Biology* **285**: 1245-1256.

Spencer, P S, *et al.* (1987). Guam Amyotrophic Lateral-Sclerosis-Parkinsonism-Dementia Linked to a Plant Excitant Neurotoxin. *Science* **237**: 517-522.

Stark , H *et al.*
http://www.mpibpc.gwdg.de/abteilungen/103/pics/Ribo/elongation.jpg

Strong, M J, *et al.* (2001). Phosphorylation state of the native high-molecular-weight neurofilament subunit protein from cervical spinal cord in sporadic amyotrophic lateral sclerosis. *Journal of Neurochemistry* **76**: 1315-1325.

Subramaniam, J R, *et al.* (2002). Mutant SOD1 causes motor neuron disease independent of copper chaperone-mediated copper loading. *Nature Neuroscience* **5**: 301-307.

Takashima, H, Boerkoel, C F and Lupski, J R (2001). Screening for mutations in a genetically heterogeneous disorder: DHPLC versus DNA sequence for mutation detection in multiple genes causing Charcot-Marie-Tooth neuropathy. *Genetic Medicine* **3**: 335-342.

Tamarappoo, B K, McDonald, K K and Kilberg, M S (1996). Expressed human hippocampal ASCT1 amino acid transporter exhibits a pH-dependent change in substrate specificity. *Biochimica et Biophysica Acta* **1279**: 131-136.

Tanaka, K, *et al.* (1997). Epilepsy and exacerbation of brain injury in mice lacking the glutamate transporter GLT-1. *Science* **276**: 1699-1702.

Tandan, R and Bradley, W G (1985). Amyotrophic Lateral Sclerosis: Part 1. Clinical Features, Pathology and Ethical Issues in Management. *Annals of Neurology* **18**: 271-280.

Tatsuka, M, *et al.* (1992). Elongation factor-1α gene determines susceptibility to transformation. *Nature* **359**: 333-336.

Tomkins, J, *et al.* (1998). Novel insertion in the KSP region of the neurofilament heavy gene in amyotrophic lateral sclerosis. *NeuroReport* **9**: 3967-3970.

Tomkins, J, *et al.* (2001). Mutation screening of manganese superoxide dismutase in amyotrophic lateral sclerosis. *NeuroReport* **12**: 2319-2322.

Tu, P-H, *et al.* (1996). Transgenic mice carrying a human mutant superoxide dismutase transgene develop neuronal cytoskeletal pathology resembling human amyotrophic lateral sclerosis lesions. *Proceedings of the National Academy of Sciences* **93**: 3155-3160.

Tu, P-H, *et al.* (1997). Selective Degeneration of Purkinje Cells with Lewy Body-Like Inclusions in Aged NFHLACZ Transgenic Mice. *Journal of Neuroscience* **17**: 1064-1074.

Ulbrich, M, *et al.* (2002). Genetic modifiers that aggravate the neurological phenotype of the wobbler mouse. *NeuroReport* **13**: 535-539.

Venema, R C, Peters, H I and Traugh, J A (1991). Phosphorylation of elongation factor 1 (EF-1) and Valyl-tRNA Synthetase by protein kinase C and Stimulation of eEF-1 activity. *Journal of Biological Chemistry* **266**: 12574-12580.

Viel, A, *et al.* (1987). Thesaurin a, the major protein of *Xenopus laevis* previtellogenic oocytes, present in the 42 S particles, is homologous to elongation factor EF-1α. *FEBS Letters* **223**: 232-236.

Viel, A, *et al.* (1990). Elongation factor 1 α (EF-1 α) is concentrated in the Balbini body and accumulates coordinately with the ribosomes during oogenesis of *Xenopus laevis*. *Developmental Biology* **141**: 270-278.

Viel, A, *et al.* (1991). Structural and Functional Properties of Thesaurin a (42Sp50), the Major Protein of the 42 S Particles Present in *Xenopus laevis* Previtellogenic Oocytes. *Journal of Biological Chemistry* **266**: 10392-10399.

Vielhaber, S, *et al.* (2000). Mitochondrial DNA abnormalities in skeletal muscle of patients with sporadic amyotrophic lateral sclerosis. *Brain* **123**: 1339-1248.

Walker, M P, *et al.* (2001). Absence of Echovirus Sequences in Brain and Spinal Cord of Amyotrophic Lateral Sclerosis Patients. *Annals of Neurology* **49**: 249-253.

Walldorf, U, Hoveman, B and Bautz, E K F (1985). F1 and F2: Two similar genes regulated differently during development of Drosophila melanogaster. *Proceedings of the National Academy of Sciences* **82**: 5795-5799.

Wang, H, Parent, M and Morais, R (1994). Cloning and characterization of a cDNA encoding elongation factor 1α from chicken cells devoid of mitochondrial DNA. *Gene* **140**: 155-161.

Wedemeyer, N, *et al.* (1996). YAC Contigs of the *Rab1* and wobbler (*wr*) Spinal Muscular Atrophy Gene Region on Proximal Mouse Chromosome 11 and of the homologous Region on Human Chromosome 2p. *Genomics* **32**: 447-454.

Welle, S, *et al.* (1997). Expression of Elongation Factor-1α and S1 in Young and Old Human Skeletal Muscle. *Journal of Gerontology* **52A**: B235-B239.

Whiteheart, S W, *et al.* (1989). Murine Elongation Factor 1α (EF-1α) Is Posttranslationally Modified by Novel Amide-linked Ethanolamine-phosphoglycerol Moieties. *Journal of Biological Chemistry* **264**: 14334-14341.

Wichman, H, *et al.* (1992). The mouse homolog to the *ras*-related yeast gene *YPT1* maps on Chromosome 11 close to the wobbler (*wr*) locus. *Mammalian Genome* **3**: 467-468.

Wiles, M V, *et al.* (2000). Establishment of a gene-trap sequence tag library to generate mutant mice from embryonic stem cells. *Nature Genetics* **24**: 13-14.

Witherden, A S, *et al.* (2002). An integrated genetic, radiation hybrid, physical and transcription map of a region of distal mouse chromosome 12, including an imprinted locus and the 'Legs at odd angles' (Loa) mutation. *Gene* **283**: 71-82.

Woloschak, G E, Rodriguez, M and Krco, C J (1987). Characterization of Immunologic and Neuropathologic Abnormalities in wasted mice. *Journal of Immunology* **138**: 2493-2499.

Wong, P C, *et al.* (1995a). An Adverse Property of a Familial ALS-Linked SOD1 Mutation Causes Motor Neuron Disease Characterized by Vacuolar Degeneration of Mitochondria. *Neuron* **14**: 1105-1116.

Wong, P C, *et al.* (1995b). Increasing Neurofilament Subunit NF-M Expression Reduces Axonal NF-H, Inhibits Radial Growth, and Results in Neurofilamentous Accumulation in Motor Neurons. *Journal of Cell Biology* **130**: 1413-1422.

Woodall, C J, *et al.* (1994). Sequences specific form enterovirus detected in spinal cord from patients with motor neurone disease. *British Journal of Medicine* **308**: 1541-1543.

Xu, Z, *et al.* (1993). Increased Expression of Neurofilament Subunit NF-L Produces Morphological Alterations That Resemble the Pathology of Human Motor Neuron Disease. *Cell* **73**: 23-33.

Xu, Z and Tung, V W-Y (2000). Overexpression of neurofilament subunit M accelerates axonal transport of neurofilaments. *Brain Research* **866**: 326-332.

Yang, F M, *et al.* (1990). Identification of an actin-binding protein from *Dictyostelium* as elongation factor 1α. *Nature* **347**: 494-496.

Yang, Y, *et al.* (2001). The gene encoding alsin, a protein with three guanine-nucleotide exchange factor domains, is mutated in a form of recessive amyotrophic lateral sclerosis. *Nature Genetics* **29**: 160-165.

Zerangue, N and Kavanaugh, M P (1996). ASCT-1 Is a Neutral Amino Acid Exchanger with Chloride Channel Activity. *Journal of Biological Chemistry* **271**: 27991-27994.

Zhu, Q, Couillard-Despres, S and Julien, J-P (1997). Delayed Maturation of Regenerating Myelinated Axons in Mice Lacking Neurofilaments. *Experimental Neurology* **148**: 299-316.

Zhu, Q, *et al.* (1998). Disruption of the NF-H Gene Increases Axonal Microtubule Content and Velocity of Neurofilament Transport: Relief of Axonopathy Resulting from the Toxin β,β'-Iminodipropionitrile. *Journal of Cell Biology* **143**: 183-193.

Appendix 1

Genetic background of wasted mice

The wasted mutation arose spontaneously in the inbred HRS/J colony at the Mouse Mutant Stocks Center of the Jackson Laboratory. The mutation was then crossed to a segregating C3HeB/FeJ × C57BL/6J background.

For the immunohistochemistry experiments described in Chapter 3, section 3.2.2, mice heterozygous for the wasted mutation were also heterozygous for the closely linked mutation ragged, *Ra* (Abbot *et al.,* 1994). This allowed the presymptomatic identification of homozygous *wst/wst* and *+/wst* animals, as *+/Ra* heterozygotes show visible coat defects. *Ra/Ra* homozygotes, which did not carry any wasted alleles, died soon after birth. The animals used in the weighing experiments, described in section 3.2.1, did not carry the ragged mutation, and were genotyped according to the method described in Chapter 2, section 2.3.3.

Appendix 2

Total body weights of *wst/wst* mice

Age, days	N	Weights, g
6	3	2.5; 5.5; 5.6
7	9	3.0; 5.1; 5.1; 5.2; 5.5; 5.8; 6.0; 6.3; 6.4
8	5	3.7; 5.9; 6.2; 6.4; 6.6
9	10	4.8; 6.0; 6.2; 6.3; 6.6; 6.8; 6.9; 7.4; 7.7; 8.0
10	9	5.2; 6.5; 6.6; 6.8; 6.9; 7.3; 7.4; 8.4; 8.6
11	9	5.6; 5.8; 7.2; 7.7; 8.0; 8.3; 8.3; 8.5; 9.2
12	7	6.4; 8.2; 8.4; 8.6; 8.7; 9.1; 9.2
13	3	6.7; 8.7; 8.9
14	10	7.5; 8.1; 8.4; 9.1; 9.4; 9.9; 10.4; 10.6; 10.7; 11.0
15	16	7.6; 8.0; 8.3; 8.5; 8.8; 9.5; 9.6; 9.7; 10.2; 10.2; 10.7; 10.7; 10.8; 11.0; 11.1; 11.3
16	8	8.4; 9.0; 10.1; 10.4; 10.6; 11.0; 11.0; 11.6
17	10	7.9; 8.3; 8.5; 9.6; 10.6; 10.8; 10.8; 11.0; 11.3; 11.5
18	12	8.3; 8.6; 9.2; 9.5; 10.2; 10.6; 11.1; 11.1; 11.2; 11.2; 11.2; 11.6
19	4	11.1; 11.2; 11.3; 11.8
20	2	10.0; 10.8
21	7	7.7; 8.9; 9.1; 9.8; 9.9; 10.0; 11.0
22	12	7.4; 8.0; 8.0; 9.4; 9.5; 10.3; 10.6; 10.9; 10.9; 10.9; 11.3; 11.3
23	9	7.3; 9.0; 9.6; 9.9; 10.0; 10.3; 10.4; 10.9; 11.0
24	9	7.0; 8.4; 8.6; 8.8; 9.6; 9.9; 9.9; 10.0; 10.3
25	6	7.8; 8.3; 8.6; 9.0; 9.1; 9.7
26	2	7.1; 7.5
27	1	6.7
28	0	
29	0	

Total body weights of control (+/*wst* and *wst/wst*) mice

Age, days	N	Weights, g
6	5	4.1; 4.2; 4.5; 5.6; 5.8
7	17	4.8; 4.9; 5.0; 5.2; 5.2; 5.3; 5.4; 5.4; 5.5; 5.5; 5.5; 5.5; 6.0; 6.2; 6.4; 6.4; 6.6
8	8	5.5; 5.5; 6.0; 6.2; 6.2; 6.7; 6.7; 7.3
9	16	5.5; 5.7; 5.8; 6.0; 6.2; 6.3; 6.3; 6.4; 6.5; 6.6; 6.7; 6.9; 7.3; 7.8; 8.2; 8.4
10	19	6.2; 6.4; 6.4; 6.5; 6.7; 6.7; 6.8; 6.9; 6.9; 7.0; 7.0; 7.0; 7.1; 7.2; 7.2; 7.3; 7.3; 8.6; 9.0
11	13	6.6; 6.8; 6.9; 7.0; 7.5; 7.7; 7.8; 7.9; 8.0; 8.0; 8.5; 9.1; 9.8
12	9	8.0; 8.2; 8.3; 8.3; 8.8; 9.1; 9.3; 9.4; 9.7
13	6	8.6; 8.9; 9.1; 9.5; 9.7; 9.9
14	20	8.4; 8.4; 8.4; 8.5; 8.6; 8.7; 8.9; 9.1; 9.4; 9.6; 9.8; 9.9; 10.0; 10.2; 10.2; 10.3; 10.4; 10.6; 11.7; 11.7
15	28	8.2; 8.5; 8.6; 8.6; 8.7; 8.7; 8.7; 8.7; 8.8; 8.9; 8.9; 9.1; 9.5; 9.7; 10.0; 10.1; 10.2; 10.4; 10.5; 10.6; 10.6; 10.7; 10.8; 10.9; 11.0; 11.5; 12.0; 12.1
16	11	8.7; 8.8; 9.0; 9.0; 9.1; 9.2; 9.3; 10.7; 11.2; 11.3; 11.9
17	15	8.7; 8.8; 8.8; 8.9; 8.9; 8.9; 8.9; 9.1; 11.0; 11.1; 11.2; 11.5; 12.3; 12.3; 12.6
18	20	8.7; 8.9; 9.0; 9.1; 9.1; 9.3; 9.3; 9.3; 9.4; 9.5; 9.5; 11.2; 11.4; 11.7; 11.8; 11.8; 12.0; 12.5; 13.0; 13.1
19	5	9.6; 12.4; 12.5; 12.6; 12.7
20	1	12.1
21	13	10.4; 10.5; 10.5; 10.5; 10.6; 10.6; 10.8; 10.9; 11.1; 11.2; 12.3; 12.9; 14.1
22	21	10.0; 10.1; 10.2; 10.3; 10.6; 10.8; 11.0; 11.0; 11.3; 11.3; 11.4; 11.7; 11.7; 12.1; 12.1; 12.3; 12.3; 13.1; 13.6; 13.9; 13.9
23	12	11.6; 11.6; 11.6; 12.1; 12.4; 12.5; 12.6; 13.1; 13.8; 13.9; 14.7; 14.8
24	21	11.2; 11.3; 11.9; 12.2; 12.2; 12.2; 12.2; 12.4; 12.5; 12.6; 12.8; 12.8; 13.3; 13.5; 13.5; 13.5; 13.8; 14.2; 14.4; 15.1; 15.1
25	15	11.2; 11.3; 12.1; 12.8; 12.8; 12.9; 13.0; 13.0; 13.0; 13.4; 13.4; 13.8; 14.1; 14.8; 16.0
26	6	12.9; 13.0; 13.3; 13.8; 13.9; 13.9
27	0	
28	5	15.3; 15.4; 16.9; 17.8; 18.0
29	8	15.4; 16.6; 16.8; 17.2; 17.8; 18.5; 18.7; 19.9

Appendix 3

Newbery, H J and Abbott, C M, (2002). "Of Mice, Men and Motor Neurons" *Trends in Molecular Medicine*. **8**: 88-92.

erner, L.J. and Jordan, V.C. (1990) Development antiestrogens and their use in breast cancer: ghth Cain memorial award lecture. *Cancer Res.*), 4177–4189
ordan, V.C. and Morrow, M. (1999) Tamoxifen, loxifene, and the prevention of breast cancer. *ndocr. Rev.* 20, 253–278
ordan, V.C. and Morrow, M. (1999) Raloxifene s a multifunctional medicine? Current trials ill show whether it is effective in both steoporosis and breast cancer. *Br. Med. J.* 19, 331–332
uiper, G.G. *et al.* (1996) Cloning of a novel ceptor expressed in rat prostate and ovary. *Proc. atl. Acad. Sci. U. S. A.* 93, 5925–5930
uiper, G.G. *et al.* (1997) Comparison of the gand binding specificity and transcript tissue istribution of estrogen receptors α and β. *ndocrinology* 138, 863–870
rzozowski, A.M. *et al.* (1997) Molecular basis of gonism and antagonism in the oestrogen ceptor. *Nature* 389, 753–758
/olf, D.M. and Jordan, V.C. (1994) The estrogen ceptor from a tamoxifen stimulated MCF-7 mor variant contains a point mutation in the gand binding domain. *Breast Cancer Res. Treat.* 1, 129–138
evenson, A.S. *et al.* (1997) Estrogenic activity is ncreased for an antiestrogen by a natural nutation of the estrogen receptor. *J. Steroid iochem. Mol. Biol.* 60, 261–268
lacGregor Schafer, J. *et al.* (2000) Allosteric ilencing of activating function 1 in the 4-hydroxytamoxifen estrogen receptor complex is induced by substituting glycine for aspartate at amino acid 351. *Cancer Res.* 60, 5097–5105
42 Bentrem, D. *et al.* (2001) Molecular mechanism of action at estrogen receptor α of a new clinically relevant antiestrogen (GW7604) related to tamoxifen. *Endocrinology* 142, 838–846
43 Liu, H. *et al.* (2001) Silencing and reactivation of the selective estrogen receptor modulator–estrogen receptor α complex. *Cancer Res.* 61, 3632–3639
44 McDonnell, D.P. (1999) The Molecular Pharmacology of SERMs. *Trends Endocrinol. Metab.* 10, 301–311
45 Paech, K. *et al.* (1997) Differential ligand activation of estrogen receptors ERα and ERβ at AP1 sites. *Science* 277, 1508–1510
46 Onate, S.A. *et al.* (1995) Sequence and characterization of a coactivator for the steroid hormone receptor superfamily. *Science* 270, 1354–1357
47 Spencer, T.E. *et al.* (1997) Steroid receptor coactivator-1 is a histone acetyltransferase. *Nature* 389, 194–198
48 Horlein, A.J. *et al.* (1995) Ligand-independent repression by the thyroid hormone receptor mediated by a nuclear receptor co-repressor. *Nature* 377, 397–404
49 Chen, J.D. and Evans, R.M. (1995) A transcriptional co-repressor that interacts with nuclear hormone receptors. *Nature* 377, 454–457
50 Biswas, D.K. *et al.* (2000) Epidermal growth factor-induced nuclear factor κB activation: A major pathway of cell-cycle progression in estrogen-receptor negative breast cancer cells. *Proc. Natl. Acad. Sci. U. S. A.* 97, 8542–8547
51 Stein, B. and Yang, M.X. (1995) Repression of the interleukin-6 promoter by estrogen receptor is mediated by NF-κB and C/EBP β. *Mol. Cell. Biol.* 15, 4971–4979
52 Munster, P.N. *et al.* (2001) Phase I study of a third-generation selective estrogen receptor modulator, LY353381.HCL, in metastatic breast cancer. *J. Clin. Oncol.* 19, 2002–2009
53 Labrie, F. *et al.* (1999) EM-652 (SCH 57068), a third generation SERM acting as pure antiestrogen in the mammary gland and endometrium. *J. Steroid Biochem. Mol. Biol.* 69, 51–84
54 Ke, H.Z. *et al.* (2001) Lasofoxifene (CP-336,156) protects against the age-related changes in bone mass, bone strength, and total serum cholesterol in intact aged male rats. *J. Bone Miner. Res.* 16, 765–773
55 Sun, J. *et al.* (1999) Novel ligands that function as selective estrogens or antiestrogens for estrogen receptor-α or estrogen receptor-β. *Endocrinology* 140, 800–804
56 Jordan, V.C. (2001) Selective estrogen receptor modulation: a personal perspective. *Cancer Res.* 61, 5683–5687
57 Sporn, M.B. *et al.* (2001) Prospects for prevention and treatment of cancer with selective PPARγ modulators (SPARMs). *Trends Mol. Med.* 7, 395–400

f mice, men and motor neurons

len J. Newbery and Catherine M. Abbott

use of mouse models has been of particular importance in studying the ogenesis of amyotrophic lateral sclerosis. Here, we describe both sgenic and classical mutants for which the genetic lesion is known. We attention, wherever possible, to pathological factors common to iple models.

J. Newbery and
rine M. Abbott*
al Genetics Section,
rsity of Edinburgh,
ular Medicine
e, Western General
tal, Edinburgh, UK
XU.
il: c.abbott@ed.ac.uk

The term 'motor neuron disease' encompasses a group of clinically distinct neurodegenerative conditions. The most common adult-onset form is known as either amyotrophic lateral sclerosis (ALS), Lou Gehrig's disease, or simply, motor neuron disease (MND). At any one time, ~30 000 individuals in the USA and ~5000 in the UK are affected by ALS. The specific loss of motor neurons in the spinal cord, brain stem and motor cortex leads to progressive paralysis and, usually, death within five years of diagnosis. This neuronal loss is also associated with astrocytosis and the presence of ubiquitinated inclusions. Approximately 10% of cases are familial. Of these, around 20% are caused by dominant mutations in the Cu/Zn superoxide dismutase gene, *SOD1* (Ref. [1]). The mean age of onset of the familial form is 46 years, about 10 years earlier than for sporadic ALS. There are also rare recessively inherited forms of ALS, which tend to have juvenile onset [1]. Spinal muscular atrophy, another motor neuron disease that predominantly affects young children, has an incidence of 1 in 6000 live births and is almost invariably caused by mutations in the survival motor neuron gene (*SMN1*; see OMIM reference #253300).

One of the central mysteries in MND research is why ubiquitously expressed genes such as *SOD1* should cause such devastation to motor neurons in the absence of pathology in other tissues. Another key question is why such different underlying causes (e.g. mutations in a metabolic enzyme, a translation elongation factor or a transcriptional activator) all lead to motor neuron degeneration. It is only by studying as many underlying causes as possible that we will gain some insight into the final cascade(s) of events in ALS, and how these might be prevented. For example, a number of common downstream events (such as neurofilament

 1471-4914/02/$ - see front matter PII: S1471-4914(01)02159-1

1. Mouse models of amyotrophic lateral sclerosis[a]

e 1	Mutation	Gene 2	Mutation	Phenotype/pathology	NF accumulation?	Refs
ant Cu/Zn eroxide nutase (SOD1) rexpressors	hG93A hG93R hG85R mG86R hG37R			Tremors and progressive paralysis, with age of onset from 3–14 months, depending on transgene copy number. Loss of spinal motor neurons; presence of phosphorylated NF inclusions and reactive astrogliosis.	Perikaryal NF inclusions, axonal spheroids	[4] (and references therein)
	hG37R	↑NF-H (mouse)		Delayed age of disease onset in those mice in which there is perikaryal NF accumulation. Delay is proportional to degree of accumulation. Overexpressing murine NF-H also extends lifespan of G93A mice.	Perikaryal NF inclusions	[16,17,28]
	hG93A	↑NF-L (mouse)		Extension of lifespan of SOD1 transgenic mice	n.r.	[28]
	hG37R	NF-L NF-M NF-H	+/– +/– +/– ↑NF-L (human)	Mice heterozygous for all three neurofilament genes have a reduced axonal caliber, but this does not affect the lifespan of G37R mice. Increasing NF density does not affect disease course.	TH mice have no NF accumulation	[18]
	hG85R hG37R	NF-L	–/–	Extension of lifespan, despite an increase in axonal loss.	Increased perikaryal NF-H accumulation	[17,29]
rofilaments , *Nfm*, *Nfh*	↑NF-H (human)			Correlation between severity of symptoms (tremors, weakness) and NF-H levels. Overexpression of NF-L rescues phenotype.	Perikarya and proximal axons, reduced by overexpressing NF-L	[13,30]
	↑NF-L (mouse)			Growth retardation and muscle atrophy. Recovery of mice that survive the third week, which could be attributed to decreased expression of transgene.	All neuronal cellular compartments have phosphorylated NF accumulation	[31]
pherin *ph1*	↑*Prph1*	NF-L	–/–	Decreased grasping time from six months, and motor dysfunction from eight months. Mice overexpressing peripherin alone show late-onset motor dysfunction at age two years.	Inclusions in perikarya and proximal axons containing peripherin, NF-M and NF-H	[32,33]
cular endothelial owth factor *Vegf*	Deletion in promoter			60% die at birth. From four months, survivors show muscle weakness and limb paresis, owing to neurogenic atrophy of muscle. Lower motor neuron degeneration.	Yes — intracellular localization not reported	[19]
aryotic elongation ctor 1A-2 *Eef1a2*	15.8 kb deletion			Spontaneous recessive mutant — wasted (wst). Tremors, ataxia and muscle wasting. from 21 days	Accumulation of phosphorylated NF in perikarya	[20]
nunoglobulin mu nding protein 2 *mbp2*	Two alleles			Spontaneous recessive mutant — neuromuscular regeneration (nmd). Impaired movement at two weeks	n.r.	[25]

ne symbols for the mouse genes are given. ↑ represents transgenic overexpression of a gene. Abbreviations: NF, neurofilaments (NF-H, heavy form; NF-M, medium form; ., light form); n.r., not reported; TH, triple heterozygote.

accumulation) can be identified, in spite of the great diversity of the gene products that are mutated in mouse and human ALS. Here, we will highlight similarities and potential links between apparently different models.

That mouse models are valuable in the study of human disease pathogenesis can be in no doubt, but there are specific disorders in which they are especially useful because of particular constraints on the study of human subjects. ALS provides a good example of this: pre-symptomatic stages of the disease can be studied in mice, and it is possible to access material, for example from the spinal cord, that cannot be obtained from living patients. Here, we will discuss some of the many mouse mutants (classical, knockout and transgenic) that undergo motor neuron degeneration, but we will confine the scope to those in which the underlying genetic lesion has been identified. Our main emphasis will be on mouse models of ALS, concentrating in particular on interactions between genotypes. The key mutants are described in Table 1. More comprehensive reviews that also describe mutants for which the genetic cause is unknown can be found elsewhere [2].

Transgenic models: SOD1

The identification of dominantly inherited point mutations in the *SOD1* gene in familial ALS in 1993 was rapidly followed by the generation of the first specific mouse models. A crucial early result was the finding that SOD1 null mice are essentially normal [3], which gave strong support to the idea that the

SOD1 mutations underlying ALS have caused the protein to acquire a new toxic function. Transgenic mice carrying several copies of human *SOD1* genes with ALS-causing mutations ($SOD1^{G37R}$, $SOD1^{G85R}$, $SOD1^{G93A}$, $SOD1^{G93R}$) develop a pathology resembling ALS, including abnormal neurofilament accumulation, with an age of onset dependent on transgene copy number [4]. These mice have been used extensively in ALS research and have led to a number of new insights into disease pathogenesis. Intercrosses with other transgenic mice have been particularly informative (Table 1). One of the most dramatic findings has come from crosses of $SOD1^{G37R}$ transgenic mice to mice overexpressing the human neurofilament heavy chain: the lifespan of these mice is a full six months longer than that of those carrying only the *SOD1* transgene. These intercrosses are discussed in more detail later in this review. Simpler, but invaluable results have also been obtained using *SOD1* transgenic mice. Oral administration of creatine, for example, was found to improve motor performance and extend survival in these mice, a result with obvious application to the human disease [5]. An interesting but baffling recent result is that mice overexpressing mutant $SOD1^{G37R}$ solely in neurons do not have any apparent motor deficits [6]. If the reverse is true, and expressing the same transgene in such a way that it is depleted specifically in neurons does give rise to MND, study in this field will be opened up enormously.

Neurofilaments and the role of the cytoskeleton

Neurofilament proteins represent the main intermediate filament component of the cytoskeleton of neurons. There are three forms of neurofilament: heavy (NF-H); medium (NF-M); and light (NF-L). There is considerable evidence to implicate the perturbation of neurofilament biology in the pathogenesis of ALS. Accumulations of phosphorylated neurofilaments are a feature of the disease [7]. Mutations in the KSP (Lys-Ser-Pro repeat) region have also been found in a small proportion of sporadic patients [1]. Fundamental insights into the role of neurofilaments and the cytoskeleton in ALS have been obtained by the study of transgenic mice.

Neurofilament knockouts

Mice in which any of the three neurofilament genes have been targeted are outwardly phenotypically normal, although they have a reduction of axonal caliber and show a loss of large motor neurons [8–12].

Neurofilament overexpression

Mice have been engineered to overexpress human [13] or mouse [14] NF-H. There is a surprising discrepancy in the results of these studies. Twofold overexpression of human NF-H (compared with endogenous NF-H) gives rise to mice with neurological defects, muscle atrophy and abnormal accumulation of neurofilaments, a phenotype strikingly similar to ALS. By contrast, overexpression of mouse NF-H at 4.5-times the normal level gives rise to no clinical phenotype and no notable neuronal loss even in the presence of abnormal perikaryal NF accumulation (the perikaryon is the cytoplasm of the cell body of the neuron). These results suggest that human NF-H acts as an aberrant subunit in a dominant negative manner.

Neurofilament–SOD1 interactions

Perikaryal accumulation of phosphorylated neurofilaments is a hallmark of ALS. This has been suggested as one of the possible causes of the disease, either through the strangulation of axonal transport or the entrapment of cellular organelles [15]. It was therefore expected that crossing mutant *SOD1*-bearing mice to NF-H overexpressing transgenic mice might exacerbate disease progression. Surprisingly, however, it was found that mice overexpressing both $SOD1^{G37R}$ and human NF-H had a delayed age of onset of disease, by up to six months [16]. This delay appeared to be dependent on the degree of perikaryal neurofilament accumulation – the greater the accumulation, the later the disease onset. It was postulated that this accumulation protects neurons by forming a 'phosphorylation sink': these neurofilaments are phosphorylated in preference to other neuronal proteins that would be detrimental to the cell in a phosphorylated form [17]. In view of the very different phenotypes of mice overexpressing mouse and human NF-H, it would be interesting to establish the effect of 'humanizing' all NF genes in mouse simultaneously, and to examine interactions of mutant *SOD1* transgenes with this genotype.

Efficient intracellular transport is clearly crucial for cells such as motor neurons, which in humans can be over a meter long. However, the caliber, or thickness, of the axons is not a factor in disease pathogenesis (as noted above, mice null for either NF-H or NF-M have a reduced axonal caliber and no phenotype). In an elegant experiment by Nguyen *et al.* [18], mice were produced that were hemizygous for all three NF genes, which resulted in a reduction of axonal caliber without affecting neurofilament stoichiometry. Crossing these to $SOD1^{G37R}$ transgenics did not affect either the age of disease onset or the lifespan of the mice. The disease course was also unaltered when mice overexpressing NF-L, which have a 50% increase in neurofilament density, were crossed to *SOD1* transgenics.

Vascular endothelial growth factor

Recently, mice carrying a targeted deletion of the hypoxia response element (HRE) within the vascular endothelial growth factor (VEGF) promoter were described [19]. These mice have a phenotype that is

strikingly similar to that of *SOD1* mutant mice and human ALS. From 5–7 months of age, they show muscle weakness owing to the degeneration of lower motor neurons, and again display abnormal accumulation of neurofilaments. Their neurons have reduced baseline and hypoxic levels of VEGF, which could cause motor neuron death by reducing perfusion under low oxygen conditions. Alternatively, the lack of VEGF might be actively neurotoxic – there is evidence to suggest that, at least *in vitro*, VEGF has a direct neuroprotective effect. Of course, motor neuron death could result from a combination of these (and indeed other) mechanisms.

Classical models

Although there are many 'classical' (non-targeted) models of ALS, only two have so far been characterized at a molecular level – *wst* and *nmd*. As many other mutants are the subject of intensive positional cloning efforts, it is probable that significant progress will be made in this area within the next few years.

Wasted

The spontaneous mutation *wst* is a 15.8 kb deletion that removes the promoter region and first exon of the gene encoding translation elongation factor 1A-2 (eEF1A-2), abolishing its expression [20]. Homozygous *wst/wst* mice die at about four weeks. They suffer from immunological abnormalities, possibly caused by the effect of the deletion on a neighboring gene, and muscle atrophy. The only defect within the central nervous system (CNS) of these mice is loss of motor neurons within the spinal cord; although they were reported in early studies to have cerebellar defects this is not in fact the case (Ref. [21] and our own unpublished results). This clearly makes them a better model for ALS than previously thought. As in ALS patients and *SOD1* transgenics, *wst/wst* mice have abnormal accumulations of phosphorylated NF-H in the perikarya of motor neurons [21]. Unlike eEF1A-1, with which it shares 92% identity, eEF1A-2 is only expressed in terminally differentiated cells of the CNS, heart and skeletal muscle. eEF1A-1 has a number of functions in addition to its role in protein synthesis. Interestingly, it has been shown to interact with the transcription factor ZPR1 [22], which also interacts with SMN1 [23]. In both cases, binding to ZPR1 is required for translocation of the proteins from cytoplasm to nucleus. It is therefore possible that all three proteins are part of a complex. SMN is deleted or mutated in >95% of cases in spinal muscular atrophy (SMA). If eEF1A-2 also interacts with this complex, this would provide a molecular link between *wst* mice and SMA. In addition, eEF1A-1 is a known cytoskeletal interacting protein: it can bind and bundle actin and sever microtubules [24]. If eEF1A-2 also has this activity then there could be a link with the cytoskeletal component of ALS and a possible explanation for NF-H accumulation in *wst* mice. Alternatively, motor neurons could simply be particularly susceptible to mutations affecting *de novo* protein synthesis because of their high metabolic requirement.

Neuromuscular degeneration

nmd is a spontaneous autosomal recessive mutation in which mice develop a progressive paralysis leading to death within four weeks of age. NF accumulation appears not to have been investigated in these mice. The *nmd* mutation is in the gene encoding immunoglobulin mu binding protein 2 (*Ighmbp2*), a putative general transcriptional activator and DNA helicase [25]. As the gene is ubiquitously expressed and has numerous downstream targets, it is not clear why mutations in this gene should cause a specific neuronal pathology. An interesting aspect of these studies was the identification of a modifier locus on chromosome 13, which enables some *nmd* mice to survive beyond seven months. Intriguingly, it has recently been shown that mutations in the human orthologue of the *nmd* gene, IGHMBP2, are responsible for spinal muscular atrophy with respiratory distress (SMARD) [26]. This suggests that there is a need to be open-minded about classification of mouse models of motor neuron degeneration in terms of ALS and SMA.

Therapeutic implications

Insights from mouse models can clearly lead to therapeutic advances. The identification of new genetic mutations in the mouse that cause motor neuron degeneration can provide new targets for intervention. However, many factors identified in the study of transgenic mice affect the age of onset of the disease rather than its progression. For a disease in which over 80% of cases are sporadic, and in which the genetic lesion is unknown even in most of the familial cases, it will be crucial in the future to identify therapeutic interventions that affect disease progression.

Future directions

Mouse models have provided many valuable insights into both the pathogenesis of ALS and the fundamental biology of motor neurons and neurofilaments. They have also posed many questions. What is the precise role of neurofilaments in the pathogenesis of the disease? It was initially thought that they were pathogenic, but recent evidence supported a protective role, at least for perikaryal accumulations. A number of transgenic animals, including the neurofilament knockout mice, display a marked loss of motor neurons and/or motor axons with either a mild or no clinical phenotype. Does this imply that there is a threshold proportion of motor neuron loss that can be tolerated before clinical features are seen?

The identification of further modifier genes in mice has an obvious relevance to human disease, and could go some way to explain the differences in

This article has been updated since it was first published as part of an online-only supplement to the October 2001 issue of *Trends in Genetics* in association with Mouse Knockout and Mutation Database (MKMD).

age of onset and disease duration, even between members of the same family. A modifier of *SOD1*-transgene-induced pathology has been shown to exist on mouse chromosome 13 (in a region distinct from the *nmd* modifier locus) [27]. Interestingly, the region identified includes the spinal muscular atrophy locus, which could provide another link between the two diseases.

Why do ubiquitously expressed proteins such as SOD1 and IGHMBP2 when mutated affect only motor neurons? It is possible that their sheer size is a factor – the cell volume of a motor neuron is typically 5000 times that of a normal animal cell, placing particular demands on transport mechanisms and metabolic requirements. Motor neurons might be particularly sensitive to insult of any description. However, the fact that expression of mutant SOD1 specifically in neurons does not cause disease casts doubt on these interpretations. Why do mutations in genes with such diverse roles in metabolism, protein synthesis and cell growth all have a similar pathological outcome? Almost invariably, abnormal perikaryal accumulation of neurofilaments is seen. Is this the default reaction of damaged motor neurons, or does it suggest the convergence of different biochemical pathways? In the last few months, a new familial ALS gene with a recessive mode of inheritance has been identified. Mutations in a putative GTPase regulator were found to underly ALS2 [34,35]. This gene contains domains that have homology to RhoGEF. This provides yet another possible link between misregulation of cytoskeletal structure and motor neuron disease. Knockout mice for this gene will undoubtedly provide another valuable tool. As more genes involved in motor neuron degeneration are identified, the key challenge is to identify possible interactions, and common endpoints in the pathogenesis of motor neuron disease.

Acknowledgements
Work in the authors' laboratory is supported by the Scottish Motor Neurone Disease Association. The authors would like to thank S.B. Wharton for helpful comments on the manuscript.

References

1 Robberecht, W. (2000) Genetics of amyotrophic lateral sclerosis. *J. Neurol.* 247 (Suppl. 6), VI/2–VI/6
2 Nicholson, S.J. *et al.* (2000) Mice, the motor system, and human motor neuron pathology. *Mamm. Genome* 11, 1041–1052
3 Raume, A.G. *et al.* (1996) Motor neurons in Cu/Zn superoxide dismutase-deficient mice develop normally but exhibit enhanced cell death after axonal injury. *Nat. Genet.* 13, 43–47
4 Shibata, N. (2001) Transgenic mouse model for familial amyotrophic lateral sclerosis with superoxide dismutase-1 mutation. *Neuropathology* 21, 82–92
5 Klivenyi, P. *et al.* (1999) Neuroprotective effect of creatine in a transgenic animal model of amyotrophic lateral sclerosis. *Nat. Med.* 5, 347–350
6 Pramatarova, A. *et al.* (2001) Neuron-specific expression of mutant superoxide dismutase 1 in transgenic mice does not lead to motor impairment. *J. Neurosci.* 21, 3369–3374
7 Munoz, D.G. *et al.* (1988) Accumulation of phosphorylated neurofilaments in anterior horn motoneurons of amyotrophic lateral sclerosis patients. *J. Neuropathol. Exp. Neurol.* 47, 9–18
8 Zhu, Q. *et al.* (1997) Delayed maturation of regenerating myelinated axons in mice lacking neurofilaments. *Exp. Neurol.* 148, 299–316
9 Elder, G.A. *et al.* (1998) Absence of the mid-sized neurofilament subunit decreases axonal calibers, levels of light neurofilament (NF-L), and neurofilament content. *J. Cell Biol.* 141, 727–739
10 Rao, M.V. (1998) Neurofilament-dependent radial growth of motor axons and axonal organization of neurofilaments does not require the neurofilament heavy subunit (NF-H) or its phosphorylation. *J. Cell Biol.* 143, 171–181
11 Zhu, Q. *et al.* (1998) Disruption of the NF-H gene increases axonal microtubule content and velocity of neurofilament transport: relief of axonopathy resulting from the toxin β,β′-iminodipropionitrile. *J. Cell Biol.* 143, 183–193
12 Elder, G.A. *et al.* (1998) Requirement of heavy neurofilament subunit in the development of axons with large calibers. *J. Cell Biol.* 143, 195–205
13 Côté, F. *et al.* (1993) Progressive neuronopathy in transgenic mice expressing the human neurofilament heavy gene: a mouse model of amyotrophic lateral sclerosis. *Cell* 73, 35–46
14 Marszalek, J.R. *et al.* (1996) Neurofilament subunit NF-H modulates axonal diameter by selectively slowing neurofilament transport. *J. Cell Biol.* 135, 711–724
15 Tu, P.H. *et al.* (1997) Selective degeneration of Purkinje cells with Lewy body-like inclusions in aged NFH/LacZ transgenic mice. *J. Neurosci.* 17, 1064–1074
16 Couillard-Despres, S. *et al.* (1998) Protective effect of neurofilament heavy gene overexpression in motor neuron disease induced by mutant superoxide dismutase. *Proc. Natl. Acad. Sci. U. S. A.* 95, 9626–9630
17 Nguyen, M.D. *et al.* (2001) Deregulation of Cdk5 in a mouse model of ALS: toxicity alleviated by perikaryal neurofilament inclusions. *Neuron* 30, 135–147
18 Nguyen, M.D. *et al.* (2000) Reduction of axonal caliber does not alleviate motor neuron disease caused by mutant superoxide dismutase 1. *Proc. Natl. Acad. Sci. U. S. A.* 97, 12306–12311
19 Oosthuyse, B. *et al.* (2001) Deletion of the hypoxia-response element in the vascular endothelial growth factor promoter causes motor neuron degeneration. *Nat. Genet.* 28, 131–138
20 Chambers, D.M. *et al.* (1998) The lethal mutation of the mouse wasted (*wst*) is a deletion that abolishes expression of a tissue-specific isoform of translation elongation factor-1α, encoded by the *Eef1a2* gene. *Proc. Natl. Acad. Sci. U. S. A.* 95, 4463–4468
21 Lutsep, H.L. and Rodriguez, M. (1998) Ultrastructural, morphometric, and immunocytochemical study of anterior horn cells in mice with 'wasted' mutation. *J. Neuropathol. Exp. Neurol.* 48, 519–533
22 Gangwani, L. *et al.* (1998) Interaction of ZPR1 with translation elongation factor-1α in proliferating cells. *J. Cell Biol.* 143, 1471–1484
23 Gangwani, L. *et al.* (2001) Spinal muscular atrophy disrupts the interaction of ZPR1 with the SMN protein. *Nat. Cell Biol.* 3, 376–383
24 Condeelis, J. (1995) Elongation factor 1α, translation and the cytoskeleton. *Trends Biochem. Sci.* 20, 169–170
25 Cox, G.A. *et al.* (1998) Identification of the mouse neuromuscular degeneration gene and mapping of a second site suppressor allele. *Neuron* 21, 1327–1337
26 Grohmann, K. *et al.* (2001) Mutations in the gene encoding immunoglobulin mu-binding protein 2 cause spinal muscular atrophy with respiratory distress type 1. *Nat. Genet.* 29, 75–77
27 Kunst, C.B. *et al.* (2000) Genetic mapping of a mouse modifier gene that can prevent ALS onset. *Genomics* 70, 181–189
28 Kong, J. and Xu, Z. (2000) Overexpression of neurofilament subunit NF-L and NF-H extends survival of a mouse model for amyotrophic lateral sclerosis. *Neurosci. Lett.* 281, 72–74
29 Williamson, T.L. *et al.* (1998) Absence of neurofilaments reduces the selective vulnerability of motor neurons and slows disease caused by a familial amyotrophic lateral sclerosis-linked superoxide dismutase 1 mutant. *Proc. Natl. Acad. Sci. U. S. A.* 95, 9631–9636
30 Meier, J. *et al.* (1999) Extra neurofilament NF-L subunits rescue motor neuron disease caused by overexpression of the human NF-H gene in mice. *J. Neuropathol. Exp. Neurol.* 58, 1099–1110
31 Xu, Z. *et al.* (1993) Increased expression of neurofilament subunit NF-L produces morphological alterations that resemble the pathology of human motor neuron disease. *Cell* 73, 23–33
32 Beaulieu, J.M. *et al.* (2000) Formation of intermediate filament protein aggregates with disparate effects in two transgenic mouse models lacking the neurofilament light subunit. *J. Neurosci.* 20, 5321–5328
33 Beaulieu, J.M. *et al.* (1999) Late onset death of motor neurons in mice overexpressing wild-type peripherin. *J. Cell Biol.* 147, 531–544
34 Yang, Y. *et al.* (2001) The gene encoding alsin, a protein with three guanine-nucleotide exchange factor domains, is mutated in a form of recessive amyotrophic lateral sclerosis. *Nat. Genet.* 29, 160–165
35 Hadano, S. *et al.* (2001)A gene encoding a putative GTPase regulator is mutated in familial amyotrophic lateral sclerosis 2. *Nat. Genet.* 29, 166–173